



The
University
Of
Sheffield.

THE DRIVERS AND MECHANISMS OF PLUMAGE COLOUR EVOLUTION

Frane Babarović

A thesis submitted in partial fulfilment of the requirements for the degree of
Doctor of Philosophy

The University of Sheffield

Faculty of Science

Ecology and Evolutionary Biology, School of Biosciences

October 2022

ABSTRACT

THE DRIVERS AND MECHANISMS OF PLUMAGE COLOUR EVOLUTION

Frane Babarović

School of Biosciences, The University of Sheffield, 2022

Birds are one of the most colourful groups of animals on the planet. Their colouration has understandably fascinated scientists for decades and this diversity provides opportunities for exploring some fundamental evolutionary questions. In this thesis, by focusing on particular bird groups, I aim to broaden our understanding of the mechanisms and drivers of plumage colour evolution. In the first part of my thesis, I explore behavioural and environmental factors that shape plumage colour evolution in the clade Coraciiformes. I find that, in this clade, the majority of plumage colour variation is explained by variation in environmental light conditions among species, while behavioural traits have limited influence. In the second part of my thesis, I test a previously described hypothesis for an evolutionary pathway between grey and blue plumage colouration. Using phylogenetic models of trait evolution, I find support for this hypothesis, confirming a macroevolutionary pathway towards colour blue from colour grey via colour slate in the clade Thraupidae. Finally, in the last part of my thesis I studied variation in feather nanostructure [specifically the keratin and air matrix (spongy layer) within feathers] to identify structural elements underpinning the described evolutionary transition between grey and blue. In the case of blue colour in Tanagers, I find that it is variation in many elements of the spongy layer that explains colour variation, rather than the presence or absence of any of its elements. Together, the results of this thesis highlight the importance of environmental factors in driving plumage colour evolution, as well as mechanistic changes (and associated developmental constraints) involved in the evolution of novel colour phenotype.

DECLARATION

I confirm that the work done in this thesis is my own. In this paragraph, I will outline the work done by my collaborators that is included in this thesis, alongside my own work.

The entire thesis was conceptualised by myself and my supervisors: Dr Gavin Thomas, Dr Christopher Cooney, and Dr Nicola Nadeau.

Plumage colour data used in the chapter two and three of my theses were generated as part of Project Plumage (www.projectplumage.org), a collaborative project run by Dr Gavin Thomas and Dr Christopher Cooney. I have used the extracted values of plumage colours from the mentioned project, extracted by Dr Christopher Cooney.

The Distinctiveness analysis (3.4.1.) in the chapter three of my thesis was developed in the collaboration with Dr Thomas Guillerme.

Feather samples in the chapter four of my thesis were collected by Dr Johnathan Kennedy at the Zoological Museum, Natural History Museum of Denmark, University of Copenhagen. In chapter four, work at the Diamond facility was split between me, Dr Andrew Parnell and Dr Stephanie Burge. Analysis for the chapter four (Peak and shoulder detection analysis (4.4.2.) One-dimensional correlation analysis (4.4.3.)) were done in collaboration with Dr Stephanie Burge.

The rest of the data collection, analysis, and writing was done by me. In many steps of this thesis, Dr Gavin Thomas, Dr Christopher Cooney, Dr Nicola Nadeau, Dr Thomas Guillerme, Dr Andrew Parnell and Dr Stephanie Burge have provided feedback on my work.

ACKNOWLEDGMENTS

It took an army of me to do this work and produce this thesis. Many people helped, both professionally and privately, during the process of doing this thesis. Thus, in this section, I would like to thank them.

First, I would like to thank my supervisors: Dr Gavin Thomas, Dr Chris Cooney and Dr Nicola Nadeau. You were the best supervision team a PhD student could wish for. Over the years, you allowed me to develop my own ideas and helped me in framing them into a testable hypothesis. I feel you helped me become the person I am today professionally, and I will always be thankful for that. Special thanks to Dr Gavin Thomas whose help and support were crucial for me during the COVID pandemic and in general.

To the past and present members of Macrobird Lab group, thank you for life we lived together in Sheffield, and I am looking forward to seeing our friendship build in the future. My thanks go to Alex, Angela, Jasmine, Jon, Joe, Louie, Thomas, Yichen and Zoë. For many shared memories and supporting me on this PhD path, I would like to thank to Catherine, Emilie, Fay, Lucy and Marion.

Many people came into my life and left a mark on it, academically and personally. Klara, thank you for all the long conversations – about life and colours. Clarissa, forever on my side, thank you endlessly for a beautiful friendship. Thanks to Daniela, who inspired me to be a better academic through her example of always standing up for justice.

Thanks to my friends, who listened, cared, and advised me on many steps of this process. Anastazija, Martina and Nebojsa – my 911, always there when I need, omg. Thank you for everything my friends :*! Zeljka, Marija, Vesna and Katja – thank you for always listening to me and sharing wisdom, academic or skin care. Kruno, Monika and Jakov, for always having my back. To my dear Marin, <3! Huge thanks to my flatmates in Sheffield, who made the house here a real home – to Martin, Max, Pauli and Zeddy.

I would like to thank my family for their support and endless encouragement with my education. To my grandfather Frane, I keep the values you thought me wherever I go and whatever I do. You thought me to always give my best. To my sister, who is the stronghold of my life. Thanks to my mother, who taught me and showed me the beauty of education. I am because you are; you will always inspire me. Thanks to my cousin Tatjana for being there for me when I needed it most. To my aunt Fani, uncle Ivo and Drago, thank you for everything!

I would specifically like to thank my aunt Fani – without you and your support in the last few years, I would not be here today! I dedicate this thesis to you!

Thanks to Lady Gaga, Buffy and Captain Janeway for everything. Finally, thanks to my cat Egon for actively doing nothing.

CONTENTS

Abstract	3
Declaration	4
Acknowledgments	5
Contents	6
List of Figures	9
Chapter 1. General introduction	11
1.1. General overview of the topics of this thesis	11
1.2. Insights into the drivers of colour evolution	12
1.3. Insights into the mechanistic basics of colour evolution	14
1.4. Thesis overview	20
1.5. References	21
Chapter 2. The effects of ecology and behaviour on the evolution of colouration in Coraciiformes	27
2.1. Abstract	27
2.2. Introduction	27
2.3. Materials and methods	30
2.3.1. Specimen selection	30
2.3.2. Plumage Colour	31
2.3.3. Predictor variables	32
2.4. Analysis	33
2.5. Results	34
2.5.1. Coraciiform colour space	34
2.5.2. Sex	35
2.5.3. Multipredictor model results summary	36
2.5.4. Light environment	37
2.5.5. Body size	41
2.5.6. Territoriality	42
2.5.7. Hunting strategy	42

2.5.8. Cooperative breeding	42
2.5.9. Bayesian phylogenetic mixed models	42
2.6. Discussion	43
2.7. Literature cited	45
Chapter 3. Evolutionary dynamics of pigmentary grey and non-iridescent structural blue colouration in Tanagers (family: Thraupidae)	53
3.1. Abstract	53
3.2. Introduction	53
3.3. Materials and methods	55
3.3.1. Data collection	55
3.3.2. Plumage Colour descriptions	55
3.3.3. Plumage Colour measurements	55
3.4. Analysis	56
3.4.1. Distinctiveness analysis	56
3.4.2. Multistate analysis	60
3.5. Results	61
3.5.1. Distinctiveness analysis	61
3.5.2. Multistate	61
3.6. Discussion	65
3.7. References	67
Chapter 4. The mechanistic basis of evolutionary transitions between grey, slate, and blue colour in Tanagers (Thraupidae)	71
4.1. Abstract	71
4.2. Introduction	72
4.3. Materials and methods	75
4.3.1. Feather sampling	75
4.3.2. Reflectance data	75
4.3.3. Small Angle X-ray Scattering (SAXS)	76
4.4. Analysis	77
4.4.1. Principal component analysis	77
4.4.2. Peak and shoulder detection analysis	77

4.4.3. One-dimensional correlation analysis	79
4.4.4. Phylogenetic Generalized Least Squares (PGLS)	81
4.5. Results	83
4.5.1. Grey – slate – blue colour space	83
4.5.2. Description of nanostructural elements of feathers	84
4.5.3. Phylogenetic generalised least square (PGLS) analysis results	87
4.6. Discussion	89
4.7. References	92
Chapter 5. Discussion	97
5.1. General overview of the aims of this thesis	97
5.2. Insights into the drivers of colour evolution	98
5.3. Insights into the mechanistic basics of colour evolution	100
5.4. Further directions	105
5.5. Reflections on my own work and it's context	106
5.6. Final remarks	106
5.7. References	107
Appendix 1	111
Appendix 2	143
Appendix 3	181

LIST OF FIGURES

Figure 0.1. Photos of representative species of two clades I worked on in this thesis.	10
Figure 2.1. A collage showing some of the plumage colour diversity in the Coraciiformes.	30
Figure 2.2. Principal components (PC) of cone catch values (u, s, m, l) for all body patches across all species.	35
Figure 2.3. Multipredictor model results summary.	37
Figure 2.4. Predictors of PC1.	38
Figure 2.5. Predictors of PC2.	39
Figure 2.6. Light environment and territoriality as predictors of brightness.	40
Figure 2.7. Body size, hunting strategy, and parental care as predictors of brightness.	41
Figure 3.1. Overview of plumage colouration across 3 colour categories (blue, slate and grey) in tetrahedral colourspace	57
Figure 3.2. Distinctiveness analysis	59
Figure 3.3. The evolution of blue, slate and grey colour in the plumage of female Tanagers	62
Figure 3.4. The evolution of blue, slate and grey colour in the plumage of male Tanagers.	64
Figure 4.1. Examples of scattering profiles and feathers where the measurements were taken	78
Figure 4.2. Visualization of the colour producing nanostructure and the variables extracted from the One-dimensional correlation analysis that describe its properties	80
Figure 4.3. Overview of colouration of feather samples from Tanagers we used for our research.	84
Figure 4.4. Histogram of the number of feathers (y axis) detected across all the feather samples for each category of nanostructure complexity variable (x axis).	85
Figure 4.5. Multipredictor model results summary.	87
Figure 4.6. Predictors of PC1 for blue-slate-grey colour variation	88
Figure 4.7. Predictors of PC1 for slate colour (a) and blue colour (b, c).	88



Figure 0.1. Photos of representative species of two clades I worked on in this thesis. Top image: Lilac-breasted roller (*Coracias caudatus*) (Kruger National Park; South Africa). Bottom image: Sayaca tanager (*Thraupis sayaca*) (Iberá Wetlands; Argentina). All photos © Daniel J. Field, University of Cambridge. Used with permission.

CHAPTER 1

General introduction

1.1. General overview of the topics of this thesis

Birds are one of the most colourful groups of animals on the planet (Cuthill et al., 2017). To the human eye, their plumage covers almost every colour on Earth. Yet for birds the range of colours detectable is even wider and expands into the UV range (Hunt et al., 1998; Stoddard & Prum, 2011). This is because it is not just birds' plumage colouration that exhibits remarkable complexity but also their visual system. The hues we observe in plumage colouration is detected in birds' brains via stimulation of four cones in their retina, in contrast to three in humans. These four cones have peak sensitivities in the UV, short, medium, and long wavelengths of light respectively (Cuthill, 2006). The other observable component of plumage colouration is its brightness, or how much light across all wavelengths reflects towards the observer. In birds, this characteristic of plumage colouration is detectable by double cones in birds' eyes (Andersson & Prager, 2006; Maia et al., 2016). These phenotypic characteristics, i.e. a complex visual system and diverse plumage colouration, have been fruitful research topics enough to maintain the interest of scientists for many years and still leave many questions unanswered (Cuthill et al., 2017).

One of the central questions in evolutionary biology is trying to explain the diversity of species phenotype, both processes shaping it and the factors producing it (O'Meara et al., 2006; Simpson, 1944; Simpson, 1953). For both, research into plumage colouration can give insight. Plumage colouration plays a critical role in the life of birds, ranging from intraspecific and interspecific signalling, camouflaging to avoid predation risk (Stevens et al., 2017; Troscianko et al., 2016), resistance to bacterial degradation of feathers (Burt et al., 2011, Burt & Ichida, 2004, Goldstein et al., 2004), and thermoregulation (Delhey et al., 2021). Due to many potential drivers, plumage colouration has proven to be an ideal phenotype to study and understand processes shaping phenotypic evolution on a macroevolutionary scale (Cooney et al., 2019; Cooney et al., 2022; Dale et al., 2015; Dunn et al., 2015). From a mechanistic perspective, the diversity of colour-producing mechanisms involved in the production of the avian colouration makes plumage colour and ideal phenotype to study factors influencing phenotypic diversity (Hill & McGraw, 2006). Namely, colour is produced in feathers that have complex internal architecture which is the source of mechanistic diversity of colour production (Prum, 1999; Shawkey & D'Alba, 2017). Diversity in pigments, structures and combinations of both provides much scope for evolutionary drivers to act upon and

ultimately given rise to the plumage colour diversity we see today. Therefore, this thesis aims to tackle both perspectives concerning the evolutionary biology of plumage colouration: first, by studying the drivers of plumage colour evolution in a specific clade of birds (Coraciiformes; Chapter 2) and second, by examining the mechanisms of plumage colour evolution in a case of a specific colour – blue (Chapter 3 and Chapter 4).

1.2. Insights into the drivers of colour evolution

In the case of the drivers of colour evolution, both visual and non-visual functions shape highly complex and multifaceted evolutionary trajectories of plumage colouration. Traditionally, all possible influences are explored under natural or sexual selection frameworks. In birds, natural selection should lead to species being less conspicuous and more camouflaged within the environment, while sexual selection should make them more conspicuous. Due to advances in the quality of the trait datasets (quantifying biotic and abiotic traits in birds) and comparative methods (Garamszegi, 2022; Tobias et al., 2022; Wilman et al., 2014), today, we know much more about drivers of plumage colour evolution. Macroevolutionary approaches that involve detecting correlates of plumage colour variation using phylogenetic methods have provided some of the answers in plumage colour evolution (Cooney et al., 2019; Cooney et al., 2022; Dale et al., 2015; Dunn et al., 2015). For example, Dunn et al. (2015) suggested that both natural and sexual selection can act on plumage colour evolution but may do so on a different axis of plumage colour variation. This research discovered that natural selection may explain the exact colouration that is evolving, while sexual selection will act on an axis of colour differences between the species (Dunn et al., 2015). In contrast, Cooney et al 2019 quantified the convergent evolutionary response of ornamental traits under sexual selection, i.e., towards colour red and yellow plumage colouration in extensive radiation of suboscine passerines (Tyrannidae) (Cooney et al., 2019). Another macroevolutionary research on plumage colouration discovered that male and female plumage colouration is differentially related to morphological (body size), social (cooperative breeding) and life-history variables (migration) (Dale et al., 2015). While some answers have been given throughout the years of research, many important questions remain unanswered.

Plumage colouration participates in many different visual signalling functions that via natural or sexual selection shape plumage colour evolution (Marcondes & Brumfield, 2019, Théry, 2006, Marchetti, 1993). By using colour as a communication trait, birds can participate in mate choice, social signalling in a broader sense, and predator-prey dynamics by achieving crypsis or conspicuousness within the environment. For example, in birds of paradise, a brightly coloured patch is adjacent to super black plumage, making it even more outstanding and visible during

courtship (McCoy et al., 2018). This example shows co-localization of colours on bird plumage for the purpose of greatest exploitation of sensory biases during courtship in the birds of paradise. This effect has been confirmed as a convergent evolutionary trait across 15 bird families (McCoy & Prum, 2019). In 230 species of woodpeckers, a remarkable convergence in plumage patterns has been observed that's explained by strong selection of mimicry between the species as approximated with the geographic overlap (Miller et al., 2019). In this case, an intraspecific social selection has played role in the plumage colour evolution. Finally, the effects of camouflage can help in the avoidance of predators and the acquisition of prey. Some ground-nesting birds actively choose the background that matches their plumage colouration to avoid predators (Troscianko et al., 2016), while many seabirds are cryptic to potential prey with the colouration of their bellies (Bretagnolle, 1993). By using colour in different contexts, birds balance conspicuousness and crypsis in the environment with their plumage colour.

Conspicuousness and crypsis of plumage colour will also depend on the predominant wavelengths of the light in the environment (Endler, 1992). In vegetated habitats, the light environment is the product of the filtration of light through the canopy of the growth coverage above the habitat. By filtration of specific wavelengths of light through different canopy thicknesses, predominant wavelengths of light will differ between different environments. For example, closed habitats with thick growth will be predominantly populated by green wavelengths, woodland habitats (with a more open tree canopy) will have predominantly blue wavelengths, and some spots of sunlight on the forest floor from the patches in the tree canopy will have red wavelengths. Finally, open environments will have all wavelengths of light equally represented. This variation is not only spatial but also temporal, with different balances between predominant wavelengths of light depending on the time of the day and weather, i.e., how cloudy the day is (Endler, 1993). Birds utilise these occurrences in the environment by rendering themselves conspicuous depending on whether their plumage colouration matches the predominant wavelengths of the light in the light environment. This relation has been explored and confirmed in many cases in the bird's plumage (Endler & Thery, 1996, Marchetti, 1993, McNaught & Owens, 2002) . For example, forest-dwelling manakin species chose lekking spots based on matching their plumage colouration with the light gradient in the forest, leading their plumage patches to be more prominent to their potential mates (Heindl & Winkler, 2003). In total, the light environment hypothesis predicts that the conspicuousness or crypsis of certain species in the environment will not depend just on the colour signal emitted in the environment and visual system of the receiver, but also on the light in the environment through which the signals travels between the two. This hypothesis also reveals the complexity of influences

shaping plumage colour evolution and how environmental factors are often related to both interspecific and intraspecific variation in behavioural factors.

The complexity of plumage colour evolution is also built upon the differences in the involvement of the body regions in different signalling functions. The belly patch is an obvious example; it is a large area easily seen by prey if the predator is a hunter. Therefore, matching the background with the belly colouration would improve hunting success. This effect is observed in seabirds (Götmark, 1987, Bretagnolle, 1993). Role of colouration on some other plumage patches have also been confirmed. For example, wing patches (epaulettes) in red-winged blackbirds have a function in maintaining territory (intraspecific) but not mate attraction (Røskoft & Rohwer, 1987). An additional layer of complexity comes from the modality of colouration on each patch. Namely, every patch will have hue, brightness, and saturation, and it has been proven that these different levels of plumage colouration can act for different purposes. For example, in *Phylloscopus* warblers, manipulation of the brightness of the wing patch will influence the individual's territorial performance (Marchetti, 1993, Jabłoński, 1996). Therefore, in two different species and in wing patch of both, different elements of plumage colouration were involved in establishing or maintaining territory. These occurrences add to layers of complexity in studying ecology and the evolution of plumage colouration.

Overall, the evolution of plumage colour will depend on many occurrences: 1. Drivers can range from social and sexual selection to natural selection; 2. These drivers can affect the chromatic (hue and saturation) and achromatic (brightness) variation of plumage colouration; 3. The location of the colour on the bird's body should be considered since birds can use different body parts for different purposes during their intra and interspecific interactions. While tackling these questions and untangling the influences on colour evolution will help us understand why we see the interspecific diversity of colours we see today, it will not help us understand how that diversity is produced mechanistically. To answer these questions, we need to look more closely into the mechanisms of colour production as well as the developmental biology of the feathers.

1.3. Insights into the mechanistic basics of colour evolution

Plumage colouration is not just an exciting phenotype on the surface, it is also "feather deep". Colour is produced and maintained in the feather. A feather is a filamentous appendage protruding from the bird's epidermis. Most of the feather is made of keratin, and once fully grown, a feather is a dead structure. The main parts of the feathers are the central shaft or rachis, with barbs as a primary filament going out from the rachis and barbules as a secondary filament going out perpendicularly

from the barbs (Prum, 1999, Prum & Brush, 2002). Colour production takes place in internal structure of the feather (Prum, 2006, McGraw, 2006). In birds, there are several ways of producing the colours, either by deposition of pigment molecules within the feathers or by the precise arrangement of elements of the feather nanostructure to produce conditions for light refractions or a combination of both (Hill & McGraw, 2006; Prum et al., 1998; Shawkey & D'Alba, 2017). More important for this thesis is the possibility of feathers having biological materials of different refractive indexes in small space, i.e. keratin, air and melanin in barbs and barbules (more in the structural section) (Burg & Parnell, 2018). By having the capacity to harbour pigments within keratin of barbs and barbules and by adjusting the internal anatomy of feathers to light scattering, feathers are an ideal medium for immense colour diversity observed in birds today.

One class of plumage colours are produced by depositing the pigments in the feather barbs and barbules, commonly called pigmentary colours (Hill & McGraw, 2006, Cuthill et al., 2017). Across all pigmentary colours, a common feature is the dependency of colour production on the chemistry of the pigment molecules. Pigment molecules will absorb specific wavelengths of light while others will be reflected towards the observer in the form of colour perceived (McGraw et al., 2005; Saks et al., 2003). The most common pigments in a bird's plumage are carotenoids and melanins. Carotenoids are involved in the production of the red, orange, yellow and pink hues, while melanins are responsible for the production of grey, black, and brown hues (Hill & McGraw, 2006). Some more phylogenetically restricted pigments are psittacofulvine found in parrots (order: Psittaciformes), producing similar colours to carotenoids and turacoverdins found in Turacos (order: Musophagidae), involved in the production of green colour (Hill & McGraw, 2006). Birds harvest carotenoids through their diet, and they have often been taken as an example of the conditional dependence of plumage colouration (Saks et al., 2003, Prum et al., 2014). On the other hand, melanins are endogenously produced and stored in discretely categorised organelles called melanosomes (McGraw, 2006). Melanosomes are places of production, transport and storage of melanins, and they are injected into the growing feathers by melanocytes (McGraw, 2006, Maia et al., 2012, Prum et al., 2009). There are two types of melanins and two types of melanosomes, accordingly. Phaeomelanosomes are responsible for reddish to brown hues production and are stored in the spherical melanosomes. In contrast, eumelanin is stored in the eumelanosomes which are elongated and rod-shaped (McGraw, 2006; Vinther, 2020). Eumelanosomes participate in the production of black and grey, and both melanosome types produce colours by broad range absorption of light (McGraw, 2006). Melanosome shape is discrete, and distinct melanosome types can be found across different melanin-based plumage colourations (Li et al., 2012; Babarović et al., 2019). Black plumage colouration has characteristic thin and elongated melanosomes, while melanosomes from grey

plumage colouration are more prominent and bulkier. Melanosomes can also participate in the production of structural colouration, albeit not with the specificity of their chemistry, but because of their physical properties, i.e. refractive index that is different from keratin and air (Prum, 2006).

Feathers carrying structural colours contain nanoscale arrangements in their internal anatomy that participate in colour production (Prum, 2006). The colour is produced by the refraction of light at the interface between two materials with different refractive indices. Feathers have many combinations of keratin, air, and melanin that facilitates production of a wide range of colour. Depending on the angle dependence of the produced colour after the interaction of the incident light with the nanostructure, structural colours could be iridescent (there is a change in the hue with the change of the viewing angle) or non-iridescent (no change in the hue with the change of the viewing angle) (Prum, 2006; Shawkey & D'Alba, 2017). In iridescent colours, colour change with viewing angle is achieved by the layering of melanosomes within the keratin matrix (Prum, 2006; Burg & Parnell, 2018). This layering facilitates two materials with different refractive indices being adjacent and as the light passes through the two materials it gets refracted on their interface. (Leertouwer et al., 2011; Burg & Parnell, 2018). Experimental results indicate a steady increase in the maximum reflectance of refracted light with increases in the number of melanosomes layers with steady decrease from five layers onwards and plateaus at nine layers (Burg & Parnell, 2018). The further utilisation of differences in the refractive indices of feather materials is achieved by introducing hollow melanosomes filled with air (Prum, 2006; Nordén et al., 2021). Therefore, a second interface between different refractive indices is introduced, i.e. the one between melanin and air alongside melanin and keratin. Furthermore, by varying the shape and size of melanosomes, a great diversity of colour is achieved with this colour-producing mechanism. Iridescent structural colours are located in the barbules of the feathers and have been traditionally explored extensively under the framework of sexual selection (Prum, 2006).

In contrast to iridescent colours, non-iridescent structural colours are produced in the barbs of the feathers and do not change in hue with change in viewing angle (Prum, 2006). The light refraction in these colours is achieved by a keratin and air matrix or "spongy layer" in the medullary cells of feather barbs (Prum et al., 1998; Prum et al., 2009; Saranathan et al., 2012). When looking at the internal architecture of the spongy layer, two conformations can be achieved: "channel type" and "sphere type" (Saranathan et al., 2012). The "channel type" nanostructure consists of long keratin shafts separated by twisted air channels. In contrast, "sphere type" nanostructures consist of air compounds with a spherical shape built by keratin bars of various thicknesses. The effect producing non-iridescent structural colours is coherent scattering (Prum, 2006). Coherent scattering refers to

selective reinforcement of the scattered wavelengths of the light from a certain scattering object that are in the phase. Scattering objects in the feather barb spongy layer are air and keratin organised in one of the two conformations described earlier. Hue produced in this way is predominated by short wavelengths, i.e. UV hue, blue and purple (Bagnara et al., 2007; Burg & Parnell, 2018; Stoddard & Prum, 2011). There are also wavelengths of incident light that do not get scattered by the spongy layer and are absorbed by the melanin layer (packed in melanosomes) placed underneath medullary cells in feather barbs (Prum, 2006). In the case of the absence of this melanin layer, as in the case of amelanotic Steller's Jay, the appearance of the feather is white with slight bluish tinge (Shawkey & Hill, 2006). The last anatomical element in the feather barbs involved in producing non-iridescent structural colours is the unstructured keratin cortex placed above the spongy layer towards the edges of the barbs. Although this layer is not structured, its thickness will affect the chromatic variation, i.e., hues of the colour produced (Fan et al., 2019). In general, it has been shown that it is continuous variation in many elements of the feather barb containing non-iridescent structural colour rather than binary presence or absence of some of its elements is responsible for variation in hue produced (Fan et al., 2019). This could indicate at the considerable potential for selection (both natural and sexual) to act on the many axes of nanostructural variation exhibited in the non-iridescent structural colours.

In order to understand mechanisms of colour evolution fully, their development should also be considered since developmental constraints and evolutionary history can both play a role in the colour evolution (Nordén & Price, 2018). Both types of structural colours are self-assembled in bird feathers during feather development (Prum et al., 2009; Maia et al., 2012). In both cases, the physical consequences of polymer interactions are used to generate energetically undemanding events leading to the final positioning of the anatomical elements (keratin, air and melanosomes) building the nanostructure (Prum, 2006; Burg & Parnell, 2018). In iridescent colours, as mentioned in the previous paragraph, melanosomes are embedded in the keratin matrix and pushed towards the edges of the barbule structure (Nordén et al., 2021). The forces leading them there are depletion-attraction forces (Asakura & Oosawa, 1958). They are formed in a mixture of non-interacting polymers (keratin) and particles (melanosomes) and depend on the size of the particle, the concentration of the particle and the shape of the compartment where the process is taking place (Maia et al., 2012). In non-iridescent structural colours, a repulsion property between two different molecules will favour their unmixing, a process called phase separation (Dufresne et al., 2009; Saranathan et al., 2012). In medullary feather cells, these molecules are air and keratin, and the process depends on the mixture's temperature, composition, and interaction strength between the molecules. Phase separation can proceed through two possible pathways, i.e. nucleation and growth

or spinodal decomposition (Prum et al., 2009). In nucleation and growth, a structure consisting of spherical structures of minority phase is formed, i.e. sphere type porous structure (Jones, 2002). In spinodal decomposition, the structure formed consists of air channels, i.e. channel type nanostructure (Hashimoto et al., 1991). The pathway by which phase separation will proceed will be determined by additional interaction with the remainder of the cytoplasm of the medullary cells where these processes occur. The process of phase separation (in both cases) can proceed limitlessly; it's essential to put a halt to it at the moment when precise sizes of the porous structures are achieved (Prum et al., 2009). This is important because, in structural colours, the colour produced will directly depend on the orientation and sizes of the elements that are their constituents (Prum, 2006; Fan et al., 2019). While phase separation is happening, another irreversible process is taking place – the polymerization of keratin molecules that also participate in the phase separation (Brush, 1983). Therefore, it has been hypothesized that a halt at the appropriate scale will emerge as the outcome of the competition between the rates of phase separation of keratin and air and polymerization of the keratin (Prum et al., 2009). In total, in both structures that produce iridescent colouration and, in the structures, producing non-iridescent colouration, no cellular activity has been observed during the development of these structures, and therefore an energetically active process has been deemed unlikely (Prum, 2006; Burg & Parnell, 2018). Since structural colours are inherently linked to the underlying architectures of the feathers where they are positioned (barbs and barbules), it is important to consider their development to understand colour evolution. For example, besides importance of self-assembly processes we know little about how these processes are initiated and terminated during the development. The reliance on the physical and chemical setting of the feathers themselves are overarching processes guiding feather development, but to fully understand how developmental constraints influence evolution of the feather colouration, a further study into the localization of these processes and their initiation and halt should be researched.

An evolutionary mechanism of transitions between colours should also be considered to understand the plumage colour evolution fully. The mechanistic basis of transitions between colours has been observed previously (Driskell et al., 2010; Doucet et al., 2004; Shawkey et al., 2006). In many cases, a rearrangement of already existing elements of feathers has been employed to produce a new colour phenotype rather than the appearance of an entirely novel structure (Shawkey et al., 2006). This is a process standard in nature and is commonly called evolutionary tinkering (Jacob, 1977; Bockaert & Pin, 1999; Saraste & Castresana, 1994). For example, the transition from matte black to iridescent plumage colouration in grackles and allies (Icteridae) is hypothesized to proceed through the organization of melanosomes scattered in the feather barbules in matte black colour into a thin layer

near the edges of barbules in iridescent colouration (Shawkey et al., 2006). Since the production of colour in structural colours is intimately linked to the underlying nanostructure, a shift in the anatomical component will result in a change in the colour produced. This trend can also be seen in the evolution of black plumage colour in the island species of fairy-wrens, where a significant deposition of melanosomes above and within the colour-producing spongy layer is covering the production of blue colour and the observed colour is finally black. In the next stage of colour evolution, the medullary layer degrades or completely vanishes due to a lack of selective pressure for the perseverance of blue colour (Doucet et al., 2004). In birds' plumage, dependence on the availability of the components present for the colour evolution sometimes extends beyond the feather type where the colour evolution is happening (Nordén & Price, 2018b). In manakins, a hybrid species has been detected with a bright yellow crown patch when neither of the parent species has carotenoid-based colouration in their crowns (Barrera-Guzmán et al., 2018). Upon closer look at the crown feather nanostructures of the hybrid, it has been detected that it has nanostructure, but also deposition of the carotenoids where both contribute to bright yellow colour production. Parental phenotypes of *Lepidothrix vilasboasi* consist of an iridescent crown patch in *Lepidothrix iris* and a white crown in *Lepidothrix nattereri*. It has been proposed that the first produced phenotype after the hybridization is dull grey, but due to selective pressure to maintain a bright crown patch, a sequestering of carotenoids from the belly patch took place to maintain the brightness of the crown patch (Barrera-Guzmán et al., 2018; Nordén & Price, 2018). In total, mechanistic shifts necessary for plumage colour evolution have been detected in several instances (Driskell et al., 2010; Doucet et al., 2004; Shawkey et al., 2006). It seems that evolutionary response to selective pressures on plumage colour evolution typically involve rearrangements of existing feather anatomy or usage of the already existing genetic basis for certain pigments.

Historically, colour-producing nanostructures, both iridescent and non-iridescent, were challenging subjects of colour research because of their development, evolution, and colour production (Maia et al., 2012; Nordén et al., 2021; Prum et al., 1998; Prum, 2006; Prum et al., 2009). Non-iridescent structural colours have been heavily observed in developmental contexts, with promising results describing an energy undemanding and self-guided process of phase separation leading to the arrangement of the colour producing nanostructure (Prum et al., 2009). Colour production has been heavily debated, with Prum et al. (1998) resolving the issue with mechanisms of coherent scattering from the interface of two materials with different refractive indices. Finally, the evolution of non-iridescent structural colours has been comparatively less well studied, and the only examples that we have quantified so far are the evolution of black colour from blue in the island and mainland populations of the fairy-wrens (Doucet et al., 2004; Driskell et al., 2010). Also, in that case, a

mechanism leading to loss of blue, rather than gain, is explained. Therefore, despite the fact of rich history of investigation of non-iridescent structural colours, a knowledge of their evolution is lacking.

1.4. Thesis overview

In this thesis, I examine three core topics of the evolutionary biology of plumage colouration: 1) ecological and behavioural drivers of the interspecific plumage colour diversity (Chapter 2); 2) evolutionary pathway between pigmentary and structural colour (Chapter 3); and 3) mechanistic basis of the evolutionary pathway between the pigmentary and structural colour (Chapter 4). To do this, I used species behavioural and ecological data, plumage colour measurements from digitally calibrated photography, spectroscopy measurements and measurements of nanostructure from scattering experiment to give insight into the mentioned topics.

In the first data chapter (Chapter 2), to give insight into ecological and behavioural drivers of the interspecific plumage colour variation I have focused on the clade Coraciiformes which involves kingfishers (Alcedinidae), the bee-eaters (Meropidae), the rollers (Coraciidae), the motmots (Momotidae), and the todies (Todidae). By quantifying their plumage colour from digitally calibrated images and scoring a broad set of their behavioural and ecological data, I was able to test for the variables correlating plumage colour variation and therefore reveal the drivers of its evolution. Results of this chapter suggest that the main driver of plumage colour evolution is ecological, i.e. light in the environment, while behavioural traits have more limited influence on the colour evolution in this clade.

In the data second chapter (Chapter 3), I tested whether there is an evolutionary relationship between grey and blue plumage with 'slate' being intermediate colour. This hypothesis was built upon the discovery of melanosome shape overlap between pigmentary grey and non-iridescent structural colours as well as the slate colour having "rudimentary spongy layer" (Babarović et al., 2019; Saranathan et al., 2012). Using phylogenetic comparative approaches, I found evidence that blue colour evolves from grey via slate colour across all Tanagers, and that transitions towards blue colour from any other colour than slate were deemed as unlikely. I further showed that blue colour could subsequently evolve further into a range of other colours.

In the third data chapter (Chapter 4), I examined the mechanistic basis of the evolutionary transitions uncovered in the chapter two. The focus of the research was the spongy layer in the medullary cells of the feather barbs, since it's the main structural element responsible for the colour production in the colour blue. For this purpose, I quantified several elements of the spongy layer and found that the elements of the nanostructure responsible for hue variation within each colour

category (i.e. within slate and blue), are not the same as the elements of the nanostructure responsible for the hue variation across colour categories (between grey, slate and blue colours). This indicates the division between developmentally constrained elements of the nanostructure that are responsible for evolution across the grey-slate-blue colour categories and variation in the hue within each category.

In the last chapter of this thesis (Chapter 5), I have discussed the results of each chapter within a broader context of the field as well as several further research ideas that emerged as the next steps in the exploration of the topics I have addressed.

1.5. References

- Andersson, S., & Prager, M. (2006). Quantifying Colors. *Bird Coloration, Vol. 1: Mechanisms and Measurements (Hill GE & McGraw KJ, Eds)*, 41–89.
- Asakura, S., & Oosawa, F. (1958). Interaction between particles suspended in solutions of macromolecules. *Journal of Polymer Science*, 33(126), 183–192.
<https://doi.org/10.1002/pol.1958.1203312618>
- Babarović, F., Puttick, M. N., Zaher, M., Learmonth, E., Gallimore, E.-J., Smithwick, F. M., Mayr, G., & Vinther, J. (2019). Characterization of melanosomes involved in the production of non-iridescent structural feather colours and their detection in the fossil record. *Journal of The Royal Society Interface*, 16(155), 20180921. <https://doi.org/10.1098/rsif.2018.0921>
- Bagnara, J. T., Fernandez, P. J., & Fujii, R. (2007). On the blue coloration of vertebrates. *Pigment Cell Research*, 20(1), 14–26. <https://doi.org/10.1111/j.1600-0749.2006.00360.x>
- Barrera-Guzmán, A. O., Aleixo, A., Shawkey, M. D., & Weir, J. T. (2018). Hybrid speciation leads to novel male secondary sexual ornamentation of an Amazonian bird. *Proceedings of the National Academy of Sciences*, 115(2), E218–E225.
<https://doi.org/10.1073/pnas.1717319115>
- Bockaert, J., & Pin, J. P. (1999). Molecular tinkering of G protein-coupled receptors: An evolutionary success. *The EMBO Journal*, 18(7), 1723–1729. <https://doi.org/10.1093/emboj/18.7.1723>
- Bretagnolle, V. (1993). Adaptive Significance of Seabird Coloration: The Case of Procellariiforms. *The American Naturalist*, 142(1), 141–173.
- Brush, A. H. (1983). Self-assembly of avian ϕ -keratins. *Journal of Protein Chemistry*, 2(1), 63–75.
<https://doi.org/10.1007/BF01025168>
- Burg, S. L., & Parnell, A. J. (2018). Self-assembling structural colour in nature. *Journal of Physics. Condensed Matter: An Institute of Physics Journal*, 30(41), 413001.
<https://doi.org/10.1088/1361-648X/aadc95>

- Burt, E. H., Jr., & Ichida, J. M. (2004). Gloger's Rule, Feather-Degrading Bacteria, and Color Variation Among Song Sparrows. *The Condor*, *106*(3), 681–686.
<https://doi.org/10.1093/condor/106.3.681>
- Burt, E. H., Schroeder, M. R., Smith, L. A., Sroka, J. E., & McGraw, K. J. (2011). Colourful parrot feathers resist bacterial degradation. *Biology Letters*, *7*(2), 214–216.
<https://doi.org/10.1098/rsbl.2010.0716>
- Cooney, C. R., He, Y., Varley, Z. K., Nouri, L. O., Moody, C. J. A., Jardine, M. D., Liker, A., Székely, T., & Thomas, G. H. (2022). Latitudinal gradients in avian colourfulness. *Nature Ecology & Evolution*, *6*(5), Article 5. <https://doi.org/10.1038/s41559-022-01714-1>
- Cooney, C. R., Varley, Z. K., Nouri, L. O., Moody, C. J. A., Jardine, M. D., & Thomas, G. H. (2019). Sexual selection predicts the rate and direction of colour divergence in a large avian radiation. *Nature Communications*, *10*(1), 1773. <https://doi.org/10.1038/s41467-019-09859-7>
- Cuthill, I. C. (2006). Color perception. In *Bird Coloration. Volume 1. Mechanisms and Measurement* (pp. 3–40). Harvard University Press.
- Cuthill, I. C., Allen, W. L., Arbuckle, K., Caspers, B., Chaplin, G., Hauber, M. E., Hill, G. E., Jablonski, N. G., Jiggins, C. D., & Kelber, A. (2017). The biology of color. *Science*, *357*(6350), eaan0221.
- Dale, J., Dey, C. J., Delhey, K., Kempenaers, B., & Valcu, M. (2015). The effects of life history and sexual selection on male and female plumage colouration. *Nature*, *527*(7578), 367–370.
<https://doi.org/10.1038/nature15509>
- Delhey, K., Dale, J., Valcu, M., & Kempenaers, B. (2021). Migratory birds are lighter coloured. *Current Biology*, *31*(23), R1511–R1512. <https://doi.org/10.1016/j.cub.2021.10.048>
- Doucet, S. M., Shawkey, M. D., Rathburn, M. K., Mays, H. L., & Montgomerie, R. (2004). Concordant evolution of plumage colour, feather microstructure and a melanocortin receptor gene between mainland and island populations of a fairy-wren. *Proceedings of the Royal Society of London. Series B: Biological Sciences*, *271*(1549), 1663–1670.
<https://doi.org/10.1098/rspb.2004.2779>
- Driskell, A. C., Prum, R. O., & Pruett-Jones, S. (2010). The evolution of black plumage from blue in Australian fairy-wrens (Maluridae): Genetic and structural evidence. *Journal of Avian Biology*, *41*(5). <https://onlinelibrary.wiley.com/doi/full/10.1111/j.1600-048X.2009.04823.x>
- Dufresne, E. R., Noh, H., Saranathan, V., Mochrie, S. G. J., Cao, H., & Prum, R. O. (2009). Self-assembly of amorphous biophotonic nanostructures by phase separation. *Soft Matter*, *5*(9), 1792–1795. <https://doi.org/10.1039/B902775K>

- Dunn, P. O., Armenta, J. K., & Whittingham, L. A. (2015). Natural and sexual selection act on different axes of variation in avian plumage color. *Science Advances*, *1*(2), e1400155. <https://doi.org/10.1126/sciadv.1400155>
- Endler, J. A. (1992). Signals, Signal Conditions, and the Direction of Evolution. *The American Naturalist*, *139*, S125–S153.
- Endler, J. A. (1993). The Color of Light in Forests and Its Implications. *Ecological Monographs*, *63*(1), 1–27. <https://doi.org/10.2307/2937121>
- Endler, J. A., & Thery, M. (1996). Interacting Effects of Lek Placement, Display Behavior, Ambient Light, and Color Patterns in Three Neotropical Forest-Dwelling Birds. *The American Naturalist*, *148*(3), 421–452.
- Fan, M., D'alba, L., Shawkey, M. D., Peters, A., & Delhey, K. (2019). Multiple components of feather microstructure contribute to structural plumage colour diversity in fairy-wrens. *Biological Journal of the Linnean Society*, *128*(3), 550–568. <https://doi.org/10.1093/biolinnean/blz114>
- Garamszegi, L. Z. (2022). *Modern Phylogenetic Comparative Methods and Their Application in Evolutionary Biology*. Springer. <https://link.springer.com/book/10.1007/978-3-662-43550-2>
- Goldstein, G., Flory, K., Browne, B., Majid, S., Ichida, J., & Burt, E. (2004). Bacterial Degradation of Black and White Feathers. *The Auk*, *121*, 656–659. <https://doi.org/10.1093/auk/121.3.656>
- Götmark, F. (1987). White underparts in gulls function as hunting camouflage. *Animal Behaviour*, *35*, 1786–1792. [https://doi.org/10.1016/S0003-3472\(87\)80071-4](https://doi.org/10.1016/S0003-3472(87)80071-4)
- Hashimoto, T., Takenaka, M., & Jinnai, H. (1991). Scattering studies of self-assembling processes of polymer blends in spinodal decomposition. *Journal of Applied Crystallography*, *24*(5), 457–466. <https://doi.org/10.1107/S0021889891000444>
- Heindl, M., & Winkler, H. (2003). Vertical lek placement of forest-dwelling manakin species (Aves, Pipridae) is associated with vertical gradients of ambient light: Ambient light and vertical lek placement in manakins. *Biological Journal of the Linnean Society*, *80*, 647–658. <https://doi.org/10.1111/j.1095-8312.2003.00264.x>
- Hill, Geoffrey E. & McGraw, Kevin J. (2006). *Bird Coloration, Volume 1: Mechanisms and Measurements*. Harvard University Press. <https://www.hup.harvard.edu/catalog.php?isbn=9780674018938>
- Hunt, S., Bennett, A. T. D., Cuthill, I. C., & Griffiths, R. (1998). Blue tits are ultraviolet tits. *Proceedings of the Royal Society of London. Series B: Biological Sciences*, *265*(1395), 451–455. <https://doi.org/10.1098/rspb.1998.0316>
- Jabłoński, P. (1996). Dark Habitats and Bright Birds: Warblers May Use Wing Patches to Flush Prey. *Oikos*, *75*(2), 350–352. JSTOR. <https://doi.org/10.2307/3546264>

- Jacob, F. (1977). Evolution and Tinkering. *Science*, 196(4295), 1161–1166.
<https://doi.org/10.1126/science.860134>
- Jones, R. A. L. (2002). Soft Condensed Matter. *European Journal of Physics*, 23(6), 652–652.
<https://doi.org/10.1088/0143-0807/23/6/703>
- Leertouwer, H. L., Wilts, B. D., & Stavenga, D. G. (2011). Refractive index and dispersion of butterfly chitin and bird keratin measured by polarizing interference microscopy. *Optics Express*, 19(24), 24061–24066. <https://doi.org/10.1364/OE.19.024061>
- Li, Q., Gao, K.-Q., Meng, Q., Clarke, J. A., Shawkey, M. D., D’Alba, L., Pei, R., Ellison, M., Norell, M. A., & Vinther, J. (2012). Reconstruction of Microraptor and the Evolution of Iridescent Plumage. *Science*, 335(6073), 1215–1219. <https://doi.org/10.1126/science.1213780>
- Maia, R., Macedo, R. H. F., & Shawkey, M. D. (2012). Nanostructural self-assembly of iridescent feather barbules through depletion attraction of melanosomes during keratinization. *Journal of The Royal Society Interface*, 9(69), 734–743. <https://doi.org/10.1098/rsif.2011.0456>
- Maia, R., Rubenstein, D. R., & Shawkey, M. D. (2016). Selection, constraint, and the evolution of coloration in African starlings. *Evolution*, 70(5), 1064–1079.
<https://doi.org/10.1111/evo.12912>
- Marchetti, K. (1993). Dark habitats and bright birds illustrate the role of the environment in species divergence. *Nature*, 362(6416), 149–152. <https://doi.org/10.1038/362149a0>
- Marcondes, R. S., & Brumfield, R. T. (2019). Fifty shades of brown: Macroevolution of plumage brightness in the Furnariida, a large clade of drab Neotropical passerines. *Evolution*, 73(4), 704–719. <https://doi.org/10.1111/evo.13707>
- McCoy, D. E., Feo, T., Harvey, T. A., & Prum, R. O. (2018). Structural absorption by barbule microstructures of super black bird of paradise feathers. *Nature Communications*, 9(1), 1–8.
<https://doi.org/10.1038/s41467-017-02088-w>
- McCoy, D. E., & Prum, R. O. (2019). Convergent evolution of super black plumage near bright color in 15 bird families. *Journal of Experimental Biology*, 222(18), jeb208140.
<https://doi.org/10.1242/jeb.208140>
- McGraw, K. J. (2006). Mechanics of melanin-based coloration. *Bird Coloration*, 1, 243–294. Harvard University Press.
- McGraw, K., Safran, R., & Wakamatsu, K. (2005). How feather colour reflects its melanin content. *Functional Ecology*, 19, 816. <https://doi.org/10.1111/j.1365-2435.2005.01032.x>
- McNaught, M. K., & Owens, I. P. F. (2002). Interspecific variation in plumage colour among birds: Species recognition or light environment? *Journal of Evolutionary Biology*, 15(4), 505–514.
<https://doi.org/10.1046/j.1420-9101.2002.00431.x>

- Miller, E. T., Leighton, G. M., Freeman, B. G., Lees, A. C., & Ligon, R. A. (2019). Ecological and geographical overlap drive plumage evolution and mimicry in woodpeckers. *Nature Communications*, *10*(1), Article 1. <https://doi.org/10.1038/s41467-019-09721-w>
- Nordén, K. K., Eliason, C. M., & Stoddard, M. C. (2021). Evolution of brilliant iridescent feather nanostructures. *ELife*, *10*, e71179. <https://doi.org/10.7554/eLife.71179>
- Nordén, K. K., & Price, T. D. (2018). Historical Contingency and Developmental Constraints in Avian Coloration. *Trends in Ecology & Evolution*, *33*(8), 574–576. <https://doi.org/10.1016/j.tree.2018.05.003>
- O’Meara, B. C., Ané, C., Sanderson, M. J., & Wainwright, P. C. (2006). Testing for Different Rates of Continuous Trait Evolution Using Likelihood. *Evolution*, *60*(5), 922–933. <https://doi.org/10.1111/j.0014-3820.2006.tb01171.x>
- Prum, R. O. (1999). Development and evolutionary origin of feathers. *Journal of Experimental Zoology*, *285*(4), 291–306. [https://doi.org/10.1002/\(SICI\)1097-010X\(19991215\)285:4<291::AID-JEZ1>3.0.CO;2-9](https://doi.org/10.1002/(SICI)1097-010X(19991215)285:4<291::AID-JEZ1>3.0.CO;2-9)
- Prum, R. O., & Brush, A. H. (2002). The evolutionary origin and diversification of feathers. *The Quarterly Review of Biology*, *77*(3), 261–295. <https://doi.org/10.1086/341993>
- Prum, R. O., Dufresne, E. R., Quinn, T., & Waters, K. (2009). Development of colour-producing β -keratin nanostructures in avian feather barbs. *Journal of The Royal Society Interface*, *6*(suppl_2), S253–S265. <https://doi.org/10.1098/rsif.2008.0466.focus>
- Prum, R. O., LaFountain, A. M., Berg, C. J., Tauber, M. J., & Frank, H. A. (2014). Mechanism of carotenoid coloration in the brightly colored plumages of broadbills (Eurylaimidae). *Journal of Comparative Physiology B*, *184*(5), 651–672. <https://doi.org/10.1007/s00360-014-0816-1>
- Prum, R. O., Torres, R. H., Williamson, S., & Dyck, J. (1998). Coherent light scattering by blue feather barbs. *Nature*, *396*(6706), 28–29. <https://doi.org/10.1038/23838>
- Prum. (2006). Anatomy, physics, and evolution of avian structural colors; *Bird Coloration*, *1*; pp. 295–353; Harvard University Press.
- Røskaft, E., & Rohwer, S. (1987). An experimental study of the function of the red epaulettes and the black body colour of male red-winged blackbirds. *Animal Behaviour*, *35*(4), 1070–1077. [https://doi.org/10.1016/S0003-3472\(87\)80164-1](https://doi.org/10.1016/S0003-3472(87)80164-1)
- Saks, L., McGraw, K., & Hörak, P. (2003). How Feather Colour Reflects Its Carotenoid Content. *Functional Ecology*, *17*, 555–561. <https://doi.org/10.1046/j.1365-2435.2003.00765.x>
- Saranathan, V., Forster, J. D., Noh, H., Liew, S.-F., Mochrie, S. G. J., Cao, H., Dufresne, E. R., & Prum, R. O. (2012). Structure and optical function of amorphous photonic nanostructures from avian feather barbs: A comparative small angle X-ray scattering (SAXS) analysis of 230 bird

- species. *Journal of The Royal Society Interface*, 9(75), 2563–2580.
<https://doi.org/10.1098/rsif.2012.0191>
- Saraste, M., & Castresana, J. (1994). Cytochrome oxidase evolved by tinkering with denitrification enzymes. *FEBS Letters*, 341(1), 1–4. [https://doi.org/10.1016/0014-5793\(94\)80228-9](https://doi.org/10.1016/0014-5793(94)80228-9)
- Shawkey, M. D., & D’Alba, L. (2017). Interactions between colour-producing mechanisms and their effects on the integumentary colour palette. *Philosophical Transactions of the Royal Society B: Biological Sciences*, 372(1724), 20160536. <https://doi.org/10.1098/rstb.2016.0536>
- Shawkey, M. D., Hauber, M. E., Estep, L. K., & Hill, G. E. (2006). Evolutionary transitions and mechanisms of matte and iridescent plumage coloration in grackles and allies (Icteridae). *Journal of The Royal Society Interface*, 3(11), 777–786.
<https://doi.org/10.1098/rsif.2006.0131>
- Simpson, G. G. (1944). *Tempo and mode in evolution*. (Vol. 3). Columbia University Press.
<https://onlinelibrary.wiley.com/doi/abs/10.1002/ajpa.1330030215>
- Simpson, G. G. (1953). The Major Features of Evolution. In *The Major Features of Evolution*. Columbia University Press. <https://doi.org/10.7312/simp93764>
- Stevens, M., Troscianko, J., Wilson-Aggarwal, J. K., & Spottiswoode, C. N. (2017). Improvement of individual camouflage through background choice in ground-nesting birds. *Nature Ecology & Evolution*, 1(9), 1325–1333. <https://doi.org/10.1038/s41559-017-0256-x>
- Stoddard, M. C., & Prum, R. O. (2011). How colorful are birds? Evolution of the avian plumage color gamut. *Behavioral Ecology*, 22(5), 1042–1052. <https://doi.org/10.1093/beheco/arr088>
- Théry, M. (2006). *Effect of light environment on color communication in birds*. *Bird Coloration*, 1; pp. 148 - 173; Harvard University Press.
- Tobias, J. A., Sheard, C., Pigot, A. L., Devenish, A. J., Yang, J., Sayol, F., Neate-Clegg, M. H., Alioravainen, N., Weeks, T. L., & Barber, R. A. (2022). AVONET: Morphological, ecological and geographical data for all birds. *Ecology Letters*, 25(3), 581–597.
- Troscianko, J., Wilson-Aggarwal, J., Stevens, M., & Spottiswoode, C. N. (2016). Camouflage predicts survival in ground-nesting birds. *Scientific Reports*, 6(1), Article 1.
<https://doi.org/10.1038/srep19966>
- Vinther, J. (2020). Reconstructing Vertebrate Paleocolor. *Annual Review of Earth and Planetary Sciences*, 48(1), 345–375. <https://doi.org/10.1146/annurev-earth-073019-045641>
- Wilman, H., Belmaker, J., Simpson, J., Rosa, C. de la, Rivadeneira, M. M., & Jetz, W. (2014). EltonTraits 1.0: Species-level foraging attributes of the world’s birds and mammals. *Ecology*, 95(7), 2027–2027. <https://doi.org/10.1890/13-1917.1>

CHAPTER 2

The effects of ecology and behaviour on the evolution of colouration in Coraciiformes

2.1. Abstract

What drives the evolution of plumage colour in birds? Bird colour is likely to be under both natural and sexual selection where natural selection may favour evolution towards crypsis or camouflage whereas sexual selection may favour evolution towards conspicuousness. The responses to selection are predicted to relate to species' ecology, behaviour, and life history. Key hypotheses have focused on habitat and light environment, breeding strategy, territoriality, and hunting behaviour. We tested these potential causes of colour variation in the Coraciiformes, a colourful clade of non-passerine birds, using phylogenetic comparative methods and data on chromatic and achromatic properties of plumage colouration measured from museum specimens. We found that correlates of colour evolution in Coraciiformes vary across body regions and depend on the focal colour property (chromatic or achromatic properties of plumage colouration). While the light environment showed widespread effects on colouration in multiple body regions for both colour properties, selection pressures related to behavioural characteristics had more spatially localized effects (e.g. territoriality on achromatic properties of wing feathers and hunting strategy on chromatic properties of belly feathers). Our results reveal both general patterns that may hold across other bird clades and more nuanced effects of selection that are likely to be mediated through the visual ecology of the signaller and receiver and the behavioural characteristics of Coraciiform species.

2.2. Introduction

Birds are one of the most colourful groups of animals on the planet (Cuthill et al., 2017; Hill & McGraw, 2006; Stoddard & Prum, 2011). The range of avian vision and the avian colour gamut spans the entire human-visible light spectrum and extends into the ultraviolet (UV) spectrum (Bennett & Cuthill, 1994; Hunt et al., 1998). This variation in colouration has many functions in the life of birds, from attracting a mate (conspicuousness) to camouflage from predators (crypsis). Conspicuousness has been broadly attributed to sexual and social selection, while concealment (camouflage and crypsis) is often attributed to natural selection for predator avoidance or for successfully catching prey (Ruiz-Rodríguez et al., 2013; Troscianko et al., 2016). The evolution of bird plumage colouration

is therefore multifaceted, with many environmental, ecological, behavioural and life history traits potentially interacting to drive evolutionary divergence in colour (Dale et al., 2015; Dunn et al., 2015). The detectability of a plumage patch (or body part) is the combination of chromatic [hue (the dominant wavelength of light) and saturation (the colour intensity)] and achromatic (relative brightness) properties of the signal itself, the visual system of the receiver, and the light environment in which the signal is transmitted (Bennett & Cuthill, 1994; Cuthill et al., 2017; Stoddard & Prum, 2011, Endler, 1992, Stoddard & Prum, 2008). Variation in selection pressures may lead to different responses in chromatic and achromatic colour properties, particularly across different parts of the birds body (e.g. McNaught & Owens, 2002, Gomez & Théry, 2004, Andersson & Prager, 2006).

How and why each of these components evolve has been tackled previously, but our understanding of how they evolve in response to different selection pressures on different body parts remains unresolved (Delhey, 2020; Dunn et al., 2015; Gomez & Théry, 2004; Maia et al., 2016; Marcondes & Brumfield, 2019; McNaught & Owens, 2002; Shultz & Burns, 2013,). Various ecological, behavioural and life history traits have been proposed to influence colour evolution (Dale et al., 2015; Dunn et al., 2015). First, relative conspicuousness or crypsis may be contingent on the light environment (the light environment hypothesis; Endler, 1992, 1993; Endler & Thery, 1996; Espmark et al., 2000; Marchetti, 1993). Under this hypothesis, signal detectability is affected by aspects of the signalling environment, such as light intensity, canopy thickness, time of day, and the amount of cloud cover in the sky (Endler, 1993). Second, several studies argue that body size can restrict colour evolution (Cooney et al., 2022; Endler, 1992; Galván et al., 2013; Hagman & Forsman, 2003; Iqic et al., 2018; Winebarger et al., 2018). The sensory and ecological constraints hypothesis predicts that body size determines detectability of the animal in the habitat and mediates its predation risk. Specifically, being large is expected to reduce predation risk and therefore facilitate increased signal intensity, whereas being small is expected to increase predation risk and therefore constrain signalling capacity (regardless of its chromatic variance) (Dale et al., 2015; Hagman & Forsman, 2003; Hossie et al., 2015). Second, hunting strategy is predicted to influence colour evolution. For example, if hunting success is increased with more cryptic colouration that reduces detectability by prey (Bretagnolle, 1993; Götmark, 1987; Tate et al., 2016). Third, the establishment or maintenance of a territory has been suggested to affect colour evolution and its distribution on the body (Røskaft & Rohwer, 1987). Among other behavioural traits, presence or absence of cooperative breeding could mediate intersexual and intrasexual contact leading to the evolution of conspicuous colouration in both males and females for signalling purposes (Rubenstein & Lovette, 2009).

The opposing effects of selection for crypsis or conspicuousness on colouration may also be reflected in colour variation across the birds' body (Doucet et al., 2007; Gomez & Théry, 2007;

Marcondes & Brumfield, 2019; Shultz & Burns, 2017). Because of variation in the extent to which body regions are exposed to predators, prey, or conspecific competitors, different body parts are likely to experience different levels of selection for crypsis relative to conspicuousness. For example, countershading is a common way for animals to achieve concealment within the environment that involves gradual shading of the entire body from darker to lighter across dorsal to ventral body parts (Allen et al., 2012; Edmunds & Dewhirst, 1994; Rowland et al., 2007). In contrast, front-facing body regions that can be directed at the potential signal receiver are commonly used in intraspecific communication (Andersson & Amundsen, 1997; Keyser & Hill, 2000; Pryke & Griffith, 2007; Stein & Uy, 2006). Overall, ventral body parts are thought to be under stronger selection for conspicuousness than dorsal body parts which are easily seen by predators, while ventral body parts are often concealed from the predators view, making evolution of their colouration less constrained, at least in birds (Marcondes & Brumfield, 2019; Shultz & Burns, 2017). Together, this suggests that understanding the evolution of avian colouration requires consideration of effects of its proximate drivers on each body part separately.

To explore key factors influencing the evolution of plumage colouration, we focused on the non-passerine order Coraciiformes (bee-eaters, ground rollers, rollers, todies, motmots and kingfishers). Coraciiform species (Fig. 2.1) have diverse plumage colouration including pigmentary and structural colours, live in a range of different environments, show variable levels of territoriality, variability in the presence or absence of cooperative breeding (but with near uniform social monogamy), and different types of hunting strategy (Eliason et al., 2019; Fry et al., 1992; Stavenga et al., 2011). This diversity makes them an ideal study system for addressing the significance of life history traits on the evolution of colouration, as well as disentangling the interaction between light environment and plumage colour and how it affects conspicuousness and concealment. We measured plumage colouration from digital images of museum specimens and quantified several proxies for factors that could play a key role in the evolution of colouration including sex, body size, hunting strategy, habitat light environment, territoriality, and social mating system. This information allows us to (i) disentangle different possible biotic and abiotic factors affecting the evolution of Coraciiform colouration, and (ii) test how chromatic and achromatic properties of plumage colouration have evolved in response to these variables and whether they have evolved for the same or different purposes.



Figure 2.1. A collage showing some of the plumage colour diversity in the Coraciiformes. a) Forest kingfisher (*Todiramphus macleayii*), Alcedinidae; b) Common kingfisher (*Alcedo atthis*), Alcedinidae; c) White-fronted bee-eater (*Merops bullockoides*), Meropidae; d) Red-bearded bee-eater (*Nyctyornis amictus*), Meropidae; e) European roller (*Coracias garrulus*), Coraciidae; f) Lilac-breasted roller (*Coracias caudatus*), Coraciidae; g) Broad-billed tody (*Todus subulatus*), Todidae; h) Narrow-billed tody (*Todus angustirostris*), Todidae. All photos © Daniel J. Field, University of Cambridge. Used with permission.

2.3. Materials and methods:

2.3.1. Specimen selection:

To collect data on plumage colouration, we used study skins of 135 species of Coraciiformes (families Meropidae, Brachypteraciidae, Coraciidae, Todidae, Momotidae, Alcedinidae) from the bird collections of the Natural History Museum at Tring, UK. We aimed to sample three male and three female study skins per species. For most patches (patches are distinct body regions, more details further down in 2.3.2. section: Plumage colour), we had 135 species sampled, except for tail (134) and tail underside (122) due to these patches being obscured in some specimens (Appendix 1: Table S1). The number of species in subsequent analysis depends on the availability of museum specimens and data from the literature on predictor variables traits. We included a total of 117 species for males for every patch other than tail (116 species) and tail underside (113 species), and 114 species

for females for every patch but tail underside (110). Across all analysis this ranges from ~75% to ~80% of the entire order when compared to the 146 species in the phylogeny of Jetz et al., (2012; Appendix 1: Table S1.).

2.3.2. Plumage Colour:

Calibrated digital images of study skins were taken using methods described in Cooney et al. (2019) and were used to quantify both chromatic (hue and saturation) and achromatic (brightness) components of colour. Briefly, a Nikon D7000 digital single-lens reflex camera with two filters (permitting human visible and UV wavelengths) was used for imaging of study skins and each bird specimen was photographed six times: from three different angles (dorsal, lateral, ventral) and with each filter. For full details regarding the technical specificity of camera, lens filters and illumination, see Cooney et al. (2019).

Digital images were then linearized and converted to .TIFF files using DCRAW (Coffin, 2016). Each linearized photo was normalized by comparison of pixel values of five grey standards with known reflectance, as suggested by Troscianko & Stevens (2015). On each image, a series of polygons were drawn in IMAGEJ (Rueden et al., 2017) using custom scripts to demark 11 body regions for colour measurement. The selected body regions were: crown, nape, mantle, rump, tail, wing coverts, wing primaries and secondaries, throat, breast, belly, and tail underside. By measuring the colour of these 11 regions, thorough coverage of whole-plumage colour variability was achieved (Maia et al., 2016). For each of these polygons, RGB values were extracted for both the human-visible and UV range.

To convert mean RGB values to avian colourspace values we used a method developed by Troscianko and Stevens (2015) to generate mapping functions that convert RGB colour values into cone-catch values adjusted to avian colour vision (see Cooney et al. 2019 for full details). We based our analysis on UVS avian visual system since genomic sequencing of the UV/violet SWS1 cone opsin gene indicated presence of amino acid residues signifying UV sensitivity in Coraciiformes (Ödeen & Håstad, 2013). Mapping functions were used to convert RGB values for each patch on each specimen into raw cone catch values. We then calculated average patch values (separately for each sex) as a species-level measure for each body patch. These values were then projected into avian tetrahedral colourspace, using methods from Stoddard & Prum (2008) implemented in the R package pavo (Maia et al., 2019). This method generated relative cone stimulation values (ultraviolet cone – u, short-wavelength cone – s, medium-wavelength cone – m, long-wavelength cone - l) that were used in subsequent analyses.

In addition to chromatic variation, we also quantified achromatic colour variation as the stimulation values of double cones, with higher values indicating a brighter patch (Maia et al., 2016). The full dataset is provided in Additional table 1 (<https://figshare.com/s/1110fce894e65a69c329>).

2.3.3. Predictor variables

We compiled data on sex, light environment, body size, territoriality, hunting strategy, and cooperative breeding (Appendix 1: Table S3.).

(i) Sex of each specimen was recorded from specimen labels during the collection of calibrated digital images.

(ii) Body size data were taken from the EltonTraits database (Wilman et al., 2014).

(iii) We quantified light environment using habitat preference as a proxy. Data on habitat preferences were collected from Fry et al. (1992). First, we assigned each species to one of three habitat types: forest, woodland, and open. Categories represent major light environment types that differ according to the dominant canopy geometry (Endler, 1992, Fig. 3.). The “forest shade” light environment occurs when the light is filtered through the thick forest canopy, and this can be further divided into canopy and understorey light conditions. These two differ in the distance from the tree top and thus the resulting filtered wavelengths. The tree canopy is rich in blue and UV light (peak wavelength ~470 nm) while the understorey is predominately rich in green light (peak wavelength ~550 nm), generating a light gradient from the canopy to the ground (Endler, 1993). The forest shade category includes forest understory, dense undergrowth and shrubby habitats, but excludes the tree canopy which we instead class as “woodland shade”. “Woodland shade” is dominated by bluish or blue-grey light with peak wavelength ~470 nm and is similar to light conditions in tree canopies (see above). These conditions are produced when light coming from the sky is filtered through a discontinuous canopy with large gaps. The “woodland shade” light environment has a spatially uniform distribution of bluish light and is found in habitats including woodlands, sparsely aggregated shrubs and, as mentioned, upper forest canopy and forest edge habitats. Finally, “open” light environments lack any canopy coverage and refer to light conditions found in habitats including riversides, open plains and grasslands. In “open” light environments, all wavelengths come directly from the sky without filtration through the canopy, and light intensity is more evenly distributed all wavelengths, albeit with a distinct peak in blue part of the spectrum (below ~470 nm) (Théry, 2006). Species were assigned to a single light environment category based on their habitat preferences, with forest-dwelling species divided into either “forest shade” or

“woodland shade” category depending on whether birds predominantly live in the understorey or upper levels of the forest, respectively (Endler, 1992, 1993; Gomez & Théry, 2004; Marchetti, 1993).

(iv) Data on hunting strategies were collected from the *Birds of the World* and a monogram on Coraciiformes (Billerman et al., 2022; Fry et al., 1992). We assigned each species in our dataset to one of the following hunting strategies: aerial catcher, ground dweller, ground catcher and water diver. The hunting strategy provides a proxy for which body part is most exposed to potential prey during hunting. For example, fish catching-behaviour that involves underwater diving, has been shown to be related to the evolution of belly colouration in seabirds (Bretagnolle, 1993; Götmark, 1987). We assigned species to one of the following hunting strategies: water diver (which submerge under the water), ground dweller (digging in the soil for worms, following ant trails, lifting leaves for insects), aerial catcher (perching on a branch and flying above and ahead to catch prey in the air) and ground catchers (species that perch on a tree and fly down to the ground to catch food low in the understorey or on the ground).

(v) Territoriality was assigned for each species using descriptions in Fry et al. (1992). Territoriality was coded as the presence or absence of both intraspecific and/or interspecific aggressive behaviours. For example, *Tanysiptera danae*, the Brown-headed Paradise Kingfisher, shows intraspecific territoriality (“strongly territorial, three or four birds chasing each other from branch to branch”), whereas *Dacelo gaudichaud*, the Rufous-bellied Kingfisher shows both intra and interspecific territoriality (“they are strongly territorial, chasing their own species and being aggressive towards some others”).

(vi) Cooperative breeding was coded for each species in our dataset based on a larger dataset of the modes of parental care of birds (Cockburn, 2006). We coded for the presence and absence of pair breeding and cooperative breeding. Each species was assigned to one of these two categories.

2.4. Analysis

Relative cone-catch values (u , s , m , l) represent the relative stimulation of four avian colour cones and together describe avian tetrahedral colourspace, a sensory equivalent of morphospace where the distance between two colours is comparable to their similarity (Stoddard & Prum, 2008). We estimated both chromatic properties of colour (hue and saturation) via cone catch values and reduced the dimensionality of the colourspace using Principal Component Analysis (PCA; Jolliffe, 2002) applied to the entire database, covering colour values for all measured colour patches. Our measurement of colour does not allow us to separate hue and saturation. Instead, the principal components that we use (PC1 and PC2) capture both elements of chromatic variation.

To assess sex differences in colouration, we compared colour variables between sexes using phylogenetic reduced major axis regression (phylorMA) as implemented in the function `phyl.RMA` (“lambda” method) in the `phytools` R-package (Revell, 2012), with values for males as x-variable and values for females as y-variable.

To test hypotheses regarding the predictors of colour variation we used Phylogenetic Generalized Least Squares (PGLS) regression (Grafen & Hamilton, 1989) as implemented in the R package `caper` (Orme et al., 2018). Using multipredictor models, we tested the influence of the predictor variables (light environment, body size, hunting strategy, territoriality, and parental care) separately for PC1, PC2 and achromatic variation and for each body patch. We analysed data for each sex separately. To provide a phylogenetic framework for our analyses, we used molecular phylogenies for Coraciiformes available from `birdtree.org` (Jetz et al., 2012). We downloaded 1000 random trees and extracted the maximum clade credibility tree in R using `maxCladeCred` function from `phangorn` package (Schliep, 2011).

Finally, we tested for the predictability of colour between different patches and sexes with Bayesian phylogenetic mixed models in the R package `MCMCglmm` (Hadfield, 2010). We ran models with PC1, PC2, and the achromatic property of plumage colour as dependent variables with sex, patch and their interaction as predictors. We used a flat prior and ran for each model for 220000 iterations, sampled every 20 iterations with the first 20 000 iterations taken as a burnin and removed.

2.5. Results

2.5.1. Coraciiform colour space

The first two principal components explained 96.27% of the variance in raw cone-catch values (u , s , m , l) (PC1 90.21% and PC2 16.07%) and were used in further analysis to describe chromatic variation (Appendix 1: Table S2). Lower values on PC1 indicated greater stimulation of m and l cones (green and red colouration), while higher values of PC1 indicated greater stimulation of s and u cones (blue and UV colouration). Lower PC2 values indicated stimulation of the m cone (green colouration) while higher PC2 values indicated stimulation of the l cone (red colouration) (Fig. 2.2.). The relationship between raw cone catch values and PC scores are shown in Appendix 1: Figures S10-S12.

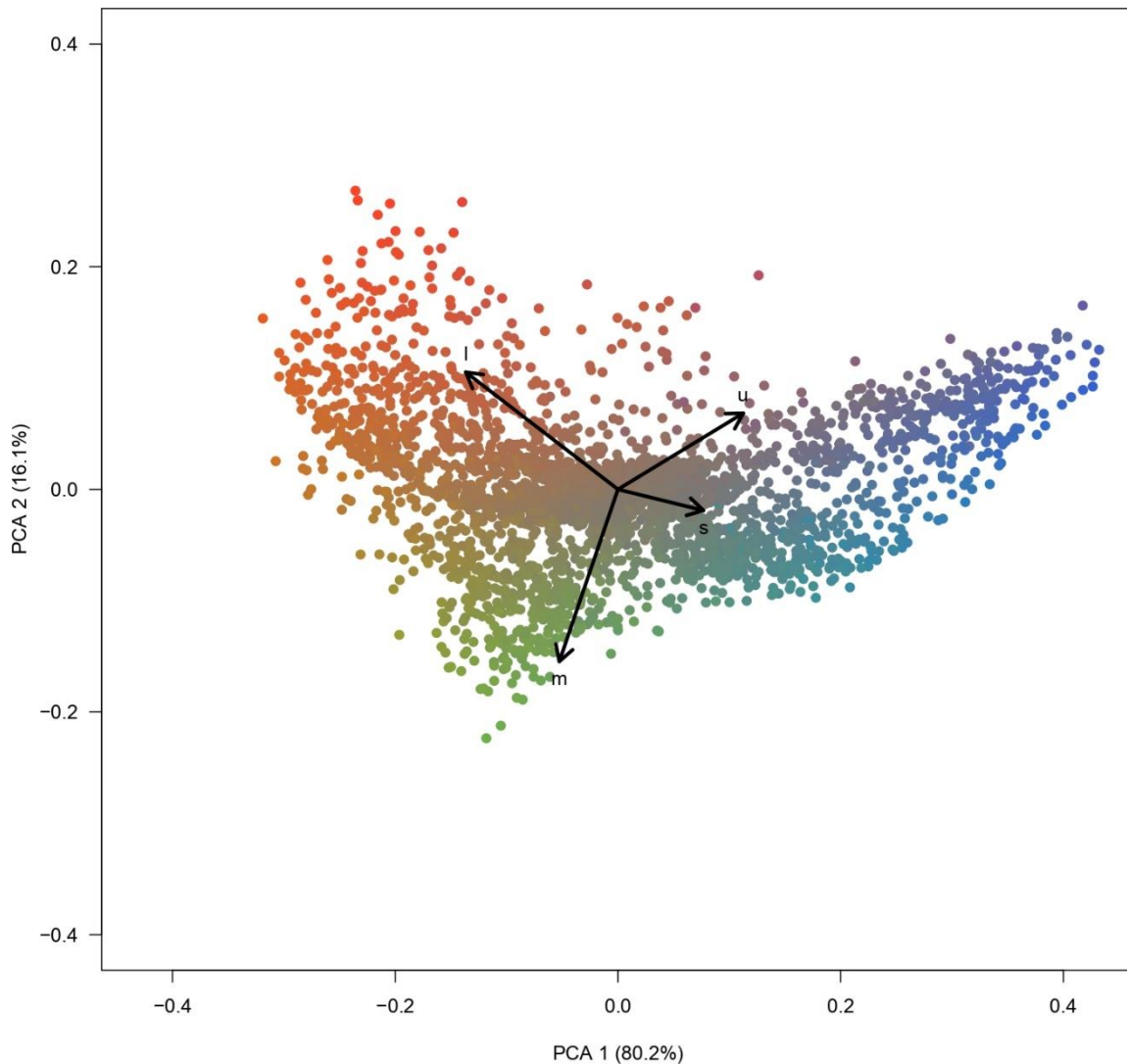


Figure 2.2. Principal components (PC) of cone catch values (u, s, m, l) for all body patches across all species. Each point in the plot represents one of 11 body patches for one species, with point colour providing an indication of patch colour in the visible spectrum. PC1 explains 80.2 % of the variation of colour scores. Higher PC1 value indicates a tendency toward blue and UV colour, while lower PC1 scores indicates a tendency toward red and green colour. PC2 explains 16.1% of variation in colour. Higher PC2 values are ascribed to red hues, while lower PC2 scores are indicative of green and blue hues.

2.5.2. Sex

Colour variation (PC1, PC2, achromatic) between the sexes was analysed with phylORMA regression (Appendix 1: Table S4), with slopes and intercepts that differ significantly from one and zero respectively indicating differences in colouration between the sexes (plots shown in Appendix 1:

Figure S7-S9). In total, significant differences in plumage colouration between the sexes were detected in four body patches for achromatic variation, one body patch for PC1, and seven body patches for PC2. Regression of female against male PC1 values showed slopes significantly different from one for crown (Appendix 1: Table S4.1). For crown, slope values of <1 suggest that male plumage has more blue-UV reflectance than female plumage but that this difference decreases as PC1 values increases. Analysis of the relationship between male and female PC2 values revealed significant between-sex variation for crown, nape, wing coverts, wing primaries and secondaries, throat, breast, and belly (Appendix 1: Table S4.12-S4.13, S4.17-S4.21). Slope values significantly <1 and negative intercepts for crown, nape, wing coverts, and belly indicated that males are generally redder in these patches than females, but that the difference reduces as PC2 values increase. A slope value significantly <1 and a positive intercept for wing primaries and secondaries and throat indicated that males become redder than females as PC2 value increases. Comparison of achromatic variation between the sexes revealed a slope significantly <1 and a positive intercept in wing coverts, wing primaries and secondaries, and tail. For these patches, this suggests that as species become brighter, males tend to be relatively more bright than females (Appendix 1: Table S4.27-S4.29). For the nape patch, however, a slope <1 and a negative intercept indicate that males tend to be brighter than females, but that this difference reduces as achromatic intensity increases (Appendix 1: Table S4.24). Overall, this suggests that there are significant differences between the sexes in colour variation for some body patches.

2.5.3. Multipredictor model results summary

We present an overview of our results here and in Figure 2.3, followed by key results in relation to each predictor variable in turn below and in Figures 2.4–2.7. We report full details (p -values, parameter estimates and R^2 values) in Appendix 1: Table S5 and Appendix 1: Figure S1-S6.

In total, light environment showed a significant association with colour variables in ten body patches for PC1 (four in males and six in females) (Fig. 2.3, a-b), five body patches for PC2 (three in males and two in females) (Fig. 2.3, c-d), and thirteen body patches for achromatic property (six in males and seven in females) (Fig. 2.3, e-f). In nine instances, colour variables were correlated with body size, including one patch for PC1, three patches with PC2 (one in males and two in females) (Fig. 2.3, c-d) and five patches with achromatic property (one in males and four in females) (Fig. 2.3, e-f). Territoriality correlated with PC1 in one body patch (only in females) (Fig. 2.3, b) and with achromatic variation in four body patches (two in males and two in females) (Fig. 2.3, e-f). Hunting strategy had a significant effect in two body patches with PC1 (one in males and two in females) (Fig. 2.3, a-b), two patches with PC2 (both in males) (Fig. 2.3, c), and one patch with achromatic variation

(only in males) (Fig. 2.3, e). Cooperative breeding is associated with achromatic variation in one body patch (in males) only (Fig. 2.3, e). Overall, the explanatory power (R^2) was greater for models describing achromatic variation in colour across species than for either principal component (PC1 and PC2) describing chromatic variation (Appendix 1: Table S5).

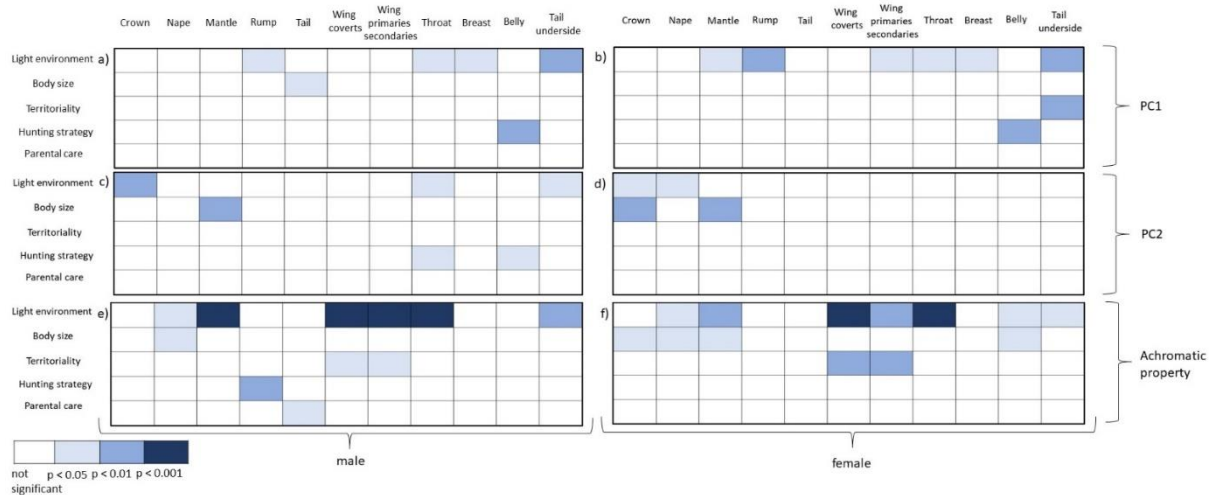


Figure 2.3. Multipredictor model results summary. Panels a-b represent results for PC1, panels c-d represent results for PC2 and panels e-f represent results for brightness. Panels on left hand side represent results for males and panels on right hand side represent results for females. Predictor variables are represented as rows with their names indicated further left. Body patches are represented as a column with each one represented on top of the column. White squares are non-significant results, light blue squares represent $p < 0.05$ level of significance, darker blue represent $p < 0.01$ level of significance and dark blue represent $p < 0.001$ level of significance.

2.5.4. Light environment

We found lower values on PC1 among forest species and higher PC1 values for woodland and open environment species for several patches, namely the mantle and wing primaries/secondaries in females, and the rump, throat, breast and tail underside in both females and males. This suggests a tendency towards reds and greens in forest light environments and UV-blues in open and woodland shade light environments (Fig. 2.4, a-f).

We found that the crown (males and females), nape (females) and throat (males) have higher PC2 scores for forest species, while open and woodland shade species show lower and comparable values indicating a tendency towards reddish plumage colour in forest species and greens and UV-blues in woodland and open environment species. For PC2 tail underside scores, forest and woodland environment species have higher and similar values when compared to open species. (Fig. 2.4, a-d).

Values for achromatic (brightness) variation are higher in open light environments (for both males and females) for the nape, mantle, wing coverts, wing primaries/secondaries and tail underside (Fig. 2.6, a-d, g). For male and female throat patches, species living in forest light environments have lower average achromatic scores compared to woodland and open light environment species (Fig. 2.5, e), while for female belly patches, species living in forest light environments have higher average achromatic scores (Fig. 2.6, f).

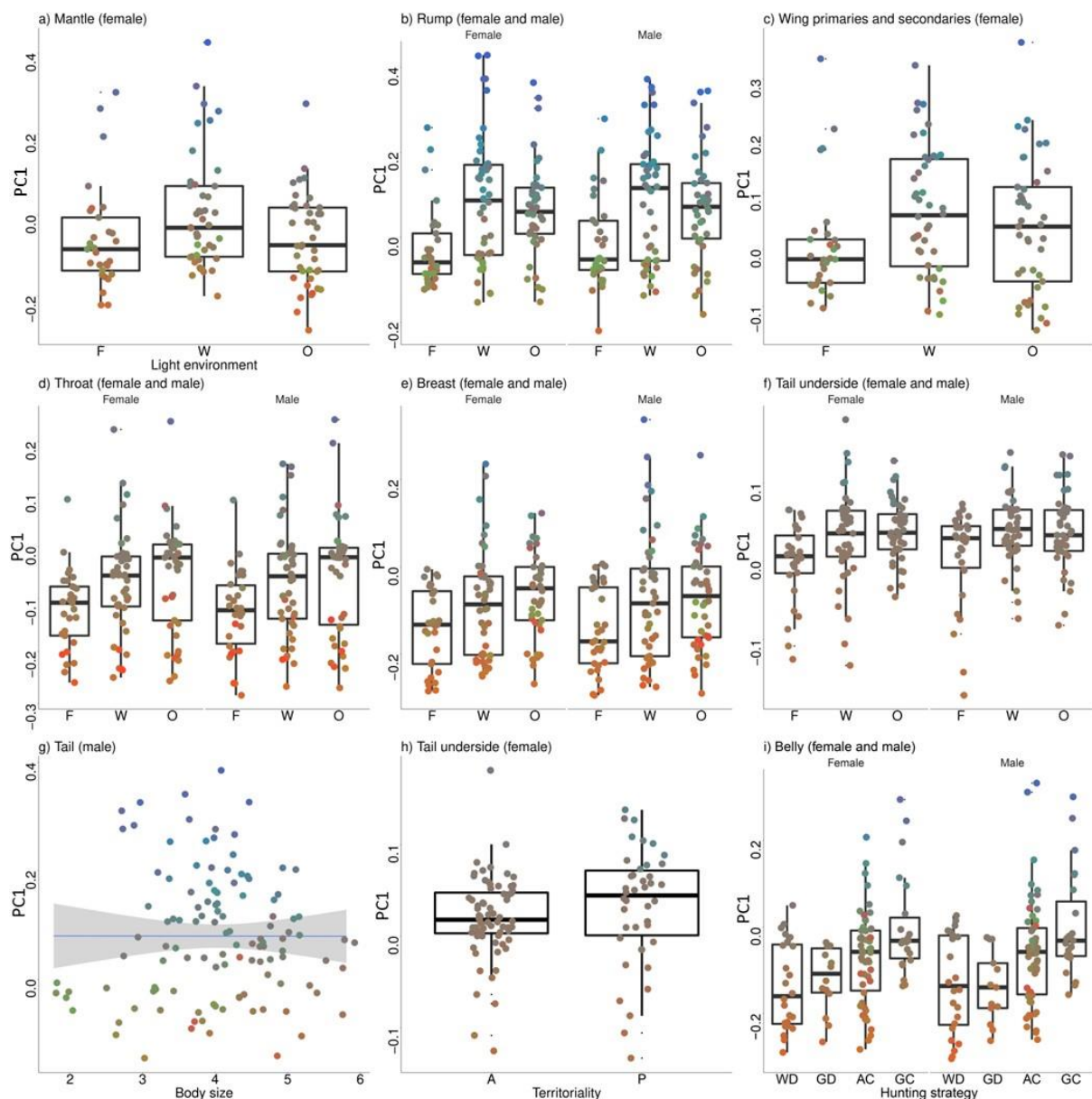


Figure 2.4. Predictors of PC1. Only body patches for which at least one independent variable indicated significant result are shown. Within each panel, each point represents a species, and the colour of each point represents the approximate reflectance of that body patch in visible spectrum. Data represented across all panels is raw data, i.e. not controlled for phylogeny. In the title of each panel, a patch and for which sex a significance has been detected is indicated. Panels a-f represent

variation in PC1 across different light environment categories. (x-axis on each panel for light environment variable have abbreviations for light environment categories that represent following: F – forest, W – woodland, and O – open.) Panel g shows the relationship between PC1 and body size. Panel h shows the relationship between PC1 and territoriality. (x-axis on each panel for territoriality variable have abbreviations for territoriality categories that represent following: A – absent, and P - present.) Panel i shows the relationship between PC1 and hunting strategy. (x-axis on each panel for hunting strategy variable have abbreviations for hunting strategy categories that represent following: GD – ground dweller, WD – water diver, AC – aerial catcher, and GC – ground catcher.)

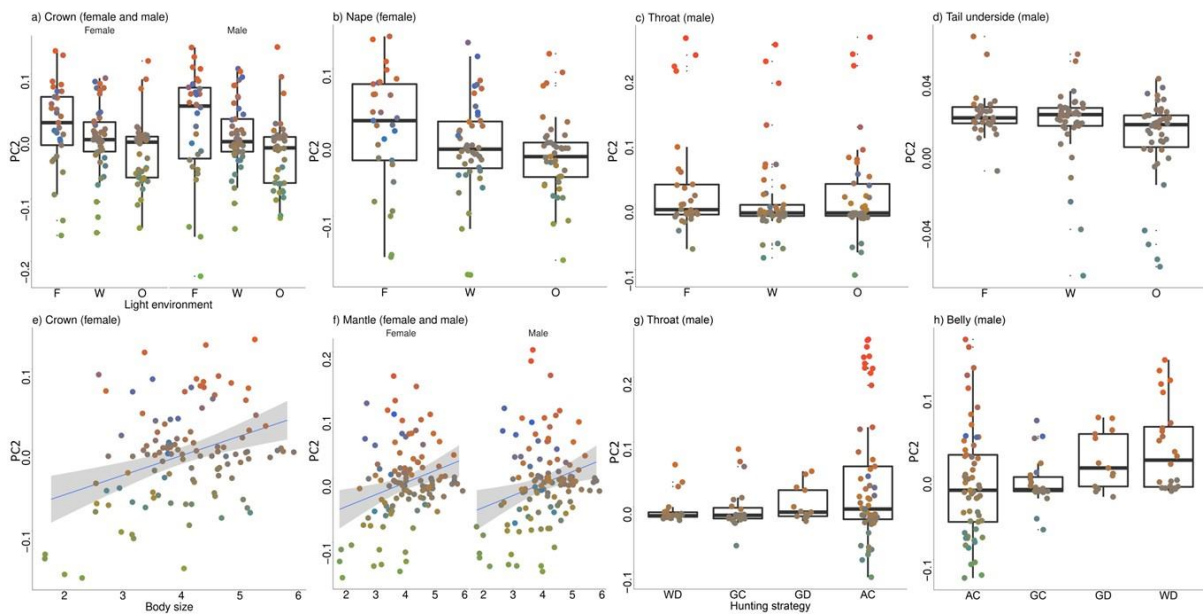


Figure 2.5. Predictors of PC2. Only body patches for which at least one independent variable indicated significant result are shown. Within each panel, each point represents a species, and the colour of each point represents the approximate reflectance of that body patch in visible spectrum. Data represented across all panels is raw data, i.e. not controlled for phylogeny. In the title of each panel, a patch and for which sex a significance has been detected is indicated. Panels a-d represent variation of PC2 values across different light environment categories. (x-axis on each panel for light environment variable have abbreviations for light environment categories that represent following: F – forest, W – woodland, and O – open.) Panels e-f show relation of PC2 with body size. Panel g-h represents association of PC2 values with different hunting strategies. (x-axis on each panel for hunting strategy variable have abbreviations for hunting strategy categories that represent following: GD – ground dweller, WD – water diver, AC – aerial catcher, and GC – ground catcher.)

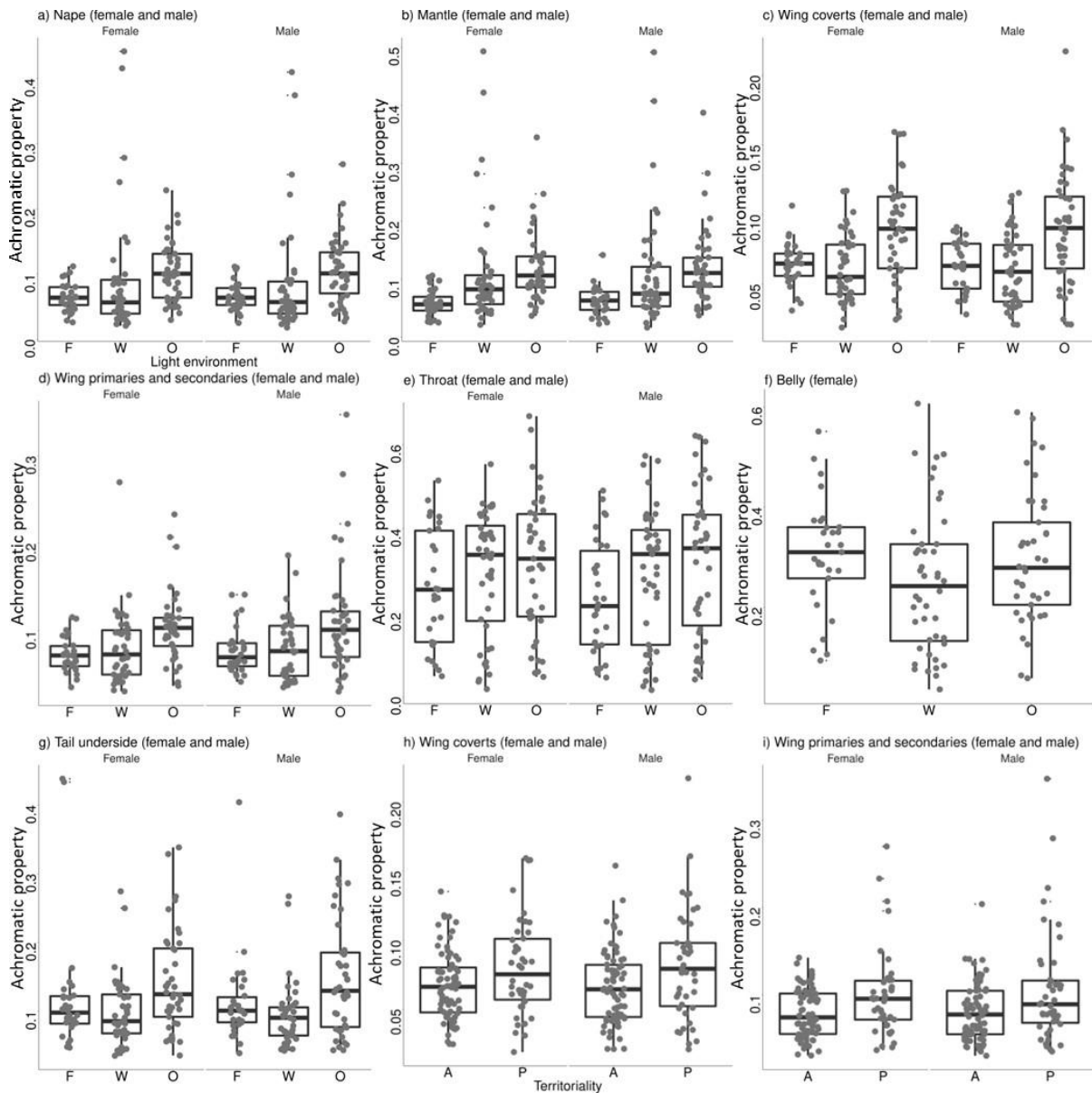


Figure 2.6. Light environment and territoriality as predictors of brightness. Only body patches for which at least one independent variable indicated significant result are shown. Within each panel, each point represents a species. In the title of each panel, a patch and for which sex a significance has been detected is indicated. Data represented across all panels is raw data, i.e. not controlled for phylogeny. Panels a-g represent variation in brightness across different light environment categories. (x-axis on each panel for light environment variable have abbreviations for light environment categories that represent following: F – forest, W – woodland, and O – open.) Panels h-i show relationship between brightness and territoriality. (x-axis on each panel for territoriality variable have abbreviations for territoriality categories that represent following: A – absent, and P - present.)

2.5.5. Body size

For PC1, tail of larger bodied males is weakly associated with the blue part of the colour spectrum (Fig. 2.5, g). Larger bodied species are also associated with higher PC2 values for the crown (females) and mantle (males and females) indicating a shift towards the red part of the colour spectrum (Fig. 2.5, e-f). We also found that larger size was correlated with brighter plumage for the crown and mantle in females, and nape in both males and females (Fig. 7, a-c). For the belly patch (in females), larger body size is associated with reduced achromatic values (Fig. 2.5, d).

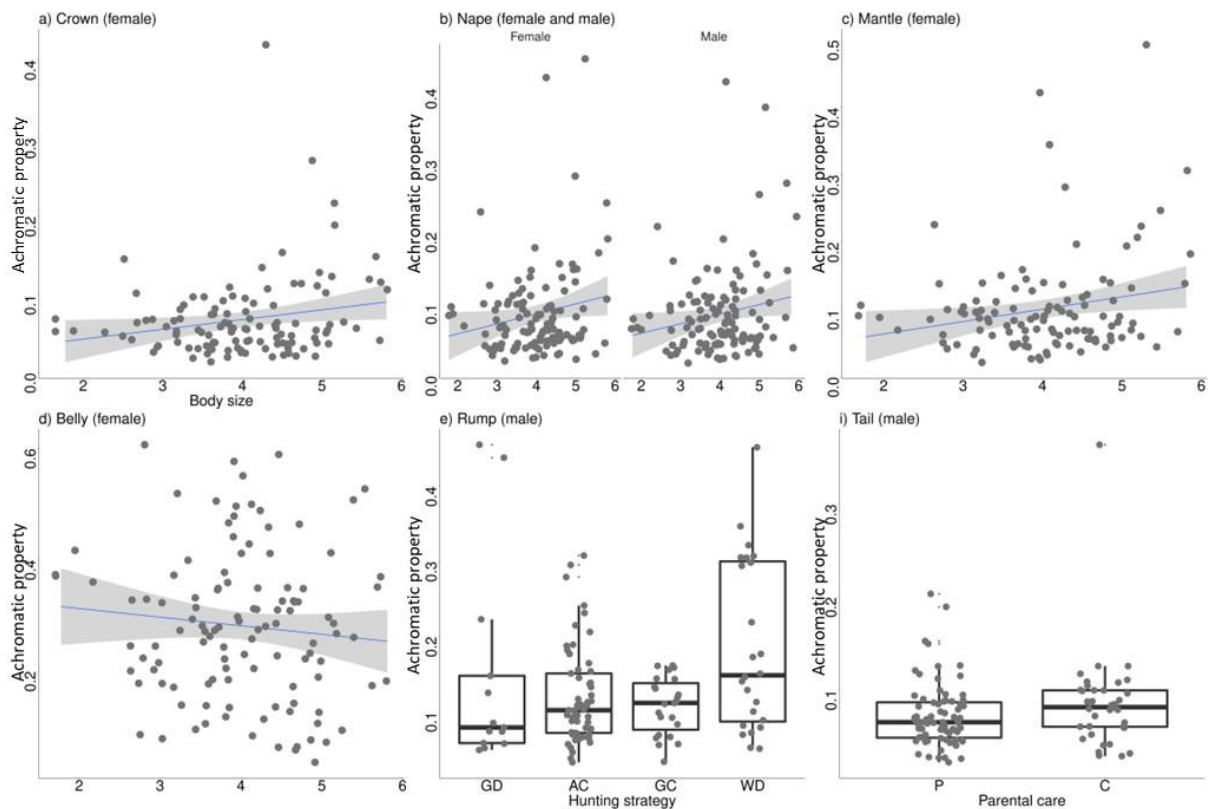


Figure 2.7. Body size, hunting strategy, and parental care as predictors of brightness. Only body patches for which at least one independent variable indicated significant result are shown. Within each panel, each point represents a species. In the title of each panel, a patch and for which sex a significance has been detected is indicated. Data represented across all panels is raw data, i.e. not controlled for phylogeny. Panels a-d show relation of brightness with body size. Panel e shows relationship between brightness and hunting strategy. (x-axis on each panel for hunting strategy variable have abbreviations for hunting strategy categories that represent following: GD – ground dweller, AC – aerial catcher, GC – ground catcher and WD – water diver.) Panel i shows relationship between brightness and parental care. (x-axis on each panel for parental care variable have abbreviations for parental care categories that represent following: C – cooperative breeding, and P – pair breeding.)

2.5.6. Territoriality

Territorial species have higher PC1 values for tail underside in females, indicating a tendency towards increased UV-blue colouration compared to non-territorial species (Fig. 2.4, h). Territorial species also have higher achromatic values on wing coverts and wing primaries/secondaries in both males and females when compared to non-territorial species (Fig. 2.6, h-i).

2.5.7. Hunting strategy

We found significant associations between PC1 values and hunting strategy for the belly in both males and females (Fig. 2.4, i). For the belly patch, ground dwelling and water diving species have the lowest (and similar) values, aerial catching species have higher values and ground catching species have the highest values. This reflects ground dwelling and water diving species having a tendency towards duller brownish plumage, aerial catching species a tendency towards UV-blues, while ground catching species tending towards green colouration.

For the belly patch (only in males) mean values on PC2 across hunting strategies are lowest and similar for aerial catching species and ground catching species, and increases for ground dwelling species, and have the highest mean values among water diving species (Fig. 2.5, h). This indicates a tendency towards green for aerial and ground catching species, while ground dwelling and water diving species tend more towards brown and duller colours in general. For the throat patch (only in males), we found opposing trend than for the belly patch with aerial catching species having the highest values and ground dwelling, ground catching and water diving species having lower values for PC2 (Fig. 2.5, g).

Males of water diving species have the highest average achromatic values for rumps, followed by ground catching species and aerial catching species, while ground dwelling species have the lowest mean values (Fig. 7, e).

2.5.8. Cooperative breeding

In cooperative breeders, males have higher average achromatic values for tails than pair breeding species (Fig. 7, i). The same effect was not detected for females, where both cooperative breeders and pair breeders exhibit no difference in achromatic values in the tail.

2.5.9. Bayesian phylogenetic mixed models

Analyses with MCMCglmm confirm that colour varies greatly among patches but not, on average, between the sexes (Appendix 1: Table S6 and Appendix 1: Figure S13.).

2.6. Discussion

Our results show that among multiple ecological and behavioural indices, light environment is the dominant correlate of plumage colour in the order Coraciiformes. Importantly, however, there is nuanced variation dependent on the specific property of colour variation (chromatic or achromatic) and the location of the colour on the bird's body. In particular, we found consistent effects of light environment on both chromatic and achromatic properties of plumage colour across multiple body regions. Other variables capturing variation in Coraciiform life history indicated more idiosyncratic effects on colouration and only for subsets of body patches. We also find some divergence in colouration between the sexes, particularly in patches associated with signalling (e.g. ventral body regions), with males having more UV-blue for certain body patches but more red reflectance for other body patches. Achromatic variation between the sexes is also significant for certain body patches and, together, this could be indicative of the influence of sexual selection. Overall, these results may indicate both the generality of light environment as a consistent predictor of colouration but also more nuanced roles for other selection pressures.

Whether colours appear conspicuous or cryptic will depend on the environment they are found in. Conspicuousness is achieved by utilising colours that overlap in peak wavelength with the predominant wavelengths of the light environment and that do not overlap with the colour of the background (Endler, 1992). In contrast, cryptic plumage colours should not overlap with the predominant light wavelength and should match the background colour (Endler, 1992). The prevailing wavelengths of light in woodland are blue (peak wavelength ~ 470 nm, Endler, 1992, Fig. 3.), which overlaps with our observed tendency towards increased UV-blue reflectance among woodland species (Fig. 2.4, a-f), consistent with selection for conspicuousness and a possible role of UV as a signal (Gomez & Théry, 2004). Species that live in open light environments also showed a tendency towards UV-blue reflectance, which is predicted to have a signalling function in these localities. However, when compared to the effect of the same colour in woodlands, it is likely to be less optimal for achieving conspicuousness. Forest shade produces light environments that peak at ~ 550 nm (green) with small spots of direct sunlight rich in longer wavelengths appearing yellow-orange, against a green background (Endler, 1990, Fig. 3.; Théry, 2006). Therefore, our observed red and green plumage patches in forest shade could locally achieve both conspicuousness and crypsis. Our result differed slightly for PC2 with a trend toward more green plumage in woodland and open environments when compared to PC1 (Fig. 2.5, a-d). In woodlands, green would indicate a mismatch with the predominant light in the environment (blue), and therefore lesser potential for conspicuousness. In open light environments, green is amongst a set of possible colours that could theoretically achieve conspicuousness (alongside blue, grey, yellow-green and red plumage colours),

but less so than in a green-dominated light environment (e.g. forest shade with no gaps) (Endler, 1990, 1992). Forest species have similar results for particular plumage patches with PC2 as with PC1, i.e. redder plumage patches. Taken together, our results suggest that selection for signalling purposes plays an important role in shaping chromatic colour variation in Coraciiformes, with a tendency towards the evolution of colours that are likely to be highly conspicuous within particular light environments (e.g. UV-blue in woodland).

Our results in relation to light environment also highlight potentially different explanations for the chromatic and achromatic properties of plumage colouration (Endler, 1992, 1993; Marcondes & Brumfield, 2019). Several studies indicate a general trend for matching achromatic attributes of plumage colour to the environment to facilitate crypsis (Dunn et al., 2015; Gomez & Théry, 2004; Maia et al., 2016; McNaught & Owens, 2002; Shultz & Burns, 2013). In contrast, Marchetti (1993) inferred conspicuousness because of increased achromatic brightness in closed light environments in *Phylloscopus* warblers. Our results show increased brightness of plumage in lighter (i.e. open) environments relative to darker (forest and woodland) environments in most cases. Thus, in Coraciiformes this suggests selection for crypsis rather than conspicuousness in terms of achromatic colour properties, at least for the nape, mantle, wing coverts, wing primaries and secondaries and tail underside (Fig. 2.6, a - d, g). Our results therefore suggest that variation in chromatic properties of plumage colouration is associated with increasing conspicuousness, whereas variation in achromatic property of plumage colouration is associated with reducing conspicuousness. This could indicate a compromise between intraspecific signalling and avoidance of detection by predators (Endler, 1992). This is similar to the private channel hypothesis which suggests that due to visual system variation across the animal kingdom, certain animals can use particular colours for signalling purposes while also avoiding detection from predators or prey (Endler, 1992; Håstad et al., 2005; Stevens & Cuthill, 2007).

In contrast to light environment, we found localised and variable effects of life history and behaviour. We recognize that our analytical approach might suffer from multiple comparisons issue due to large number of analyses and while the results for light environment are consistent and widespread across our analyses, we are more cautious in individually interpreting other, often patch and predictor specific, results. Nonetheless, some results are tentatively interesting. For example, hunting strategy was associated with chromatic variation for the ventral body parts (throat and belly) and with achromatic variation (but only in the rump). This is consistent with previous research suggesting that successful hunting in birds is associated with ventral body parts that are camouflaged against their natural background (Bretagnolle, 1993; Götmark, 1987; Johnson & Brush, 1972; Preston, 1980). Our results suggest that the belly would be camouflaged to some extent

against the likely background, potentially aiding hunting success in this group that contains many aerial hunters. We also found that territorial species have higher achromatic values for wings (coverts, primaries, and secondaries) than non-territorial species, in both males and females (Fig. 2.6, h-i). Wing colour is important for establishing and maintaining territories in warblers (Marchetti, 1993; Marchetti & Price, 1997) and our results are consistent with the prediction that territorial species are showier (lighter/brighter) than non-territorial species (Røskoft & Rohwer, 1987; Peek, 1972; Marchetti & Price, 1997). We also found that body size affects both achromatic and chromatic properties of plumage colouration on some patches, but the results make generalisation difficult. Body size is related to animals' detectability within the environment, with bigger animals theoretically achieving greater signal to background noise ratio for the receiver because of the greater signal intensity. The increase of achromatic values in the crown and nape with body size could improve their signalling capacity (Endler, 1992) (Fig. 2.7, a-c). However, the reduced achromatic values for the belly patch could be related to the hunting strategy and need for lesser visibility from the prey (Fig. 2.7, d) (Bretagnolle, 1993; Götmark, 1987). We found a link to cooperative breeding only to tail colouration in males (Fig. 2.7, i).

Taken together, our results suggest that colour evolution in Coraciiformes is dominated by light environment and the contrasting need for both crypsis and conspicuousness. Properties of plumage colouration, i.e. chromatic and achromatic variance, showed differential response to light environment, with achromatic properties indicating camouflage with adjacent environment and chromatic properties conspicuousness. However, while selection imposed by the light environment may drive evolution of colouration on most body regions, some regions do not follow this pattern and are more strongly affected by other factors. These include the belly patch that varies with hunting strategy, and the wings that vary with territorial defence. Our results are in line with the interpretation that the evolution of avian colouration is shaped by a set of interacting general ecological selection pressures and clade specific, idiosyncratic, life history traits.

2.7. Literature cited

Literature cited

- Allen, W. L., Baddeley, R., Cuthill, I. C., Scott-Samuel, N. E., Sherratt, A. E. T. N., & Day, E. T. (2012). A Quantitative Test of the Predicted Relationship between Countershading and Lighting Environment. *The American Naturalist*, 180(6), 762–776. <https://doi.org/10.1086/668011>
- Andersson, S., & Amundsen, T. (1997). Ultraviolet colour vision and ornamentation in bluethroats. *Proceedings of the Royal Society B: Biological Sciences*, 264(1388), 1587–1591. <https://doi.org/10.1098/rspb.1997.0221>

- Andersson, S., & Prager, M. (2006). Quantifying Colors. In Hill, G.E. & McGraw, K.J. (Editors) *Bird Coloration*. Vol. 1: Mechanisms and Measurements. 295–353. Cambridge, MA: Harvard University Press
- Bennett, A. T. D., & Cuthill, I. C. (1994). Ultraviolet vision in birds: What is its function? *Vision Research*, 34(11), 1471–1478. [https://doi.org/10.1016/0042-6989\(94\)90149-X](https://doi.org/10.1016/0042-6989(94)90149-X)
- Billerman, S. M., Keeney, B. K., Rodewald, P. G., & Schulenberg, T. S. (Editors) (2022). *Birds of the World*. Cornell Laboratory of Ornithology, Ithaca, NY, USA. <https://birdsoftheworld.org/bow/home>
- Bretagnolle, V. (1993). Adaptive Significance of Seabird Coloration: The Case of Procellariiforms. *The American Naturalist*, 142(1), 141–173.
- Cockburn, A. (2006). Prevalence of different modes of parental care in birds. *Proceedings of the Royal Society B: Biological Sciences*, 273(1592), 1375–1383. <https://doi.org/10.1098/rspb.2005.3458>
- Coffin, D. (2016) DCRAW V. 9.27. <https://www.cybercom.net/~dcoffin/dcraw/>.
- Cooney, C. R., He, Y., Varley, Z. K., Nouri, L. O., Moody, C. J. A., Jardine, M. D., Liker, A., Székely, T., & Thomas, G. H. (2022). Latitudinal gradients in avian colourfulness. *Nature Ecology & Evolution*, 6(5), 622–629. <https://doi.org/10.1038/s41559-022-01714-1>
- Cooney, C. R., Varley, Z. K., Nouri, L. O., Moody, C. J. A., Jardine, M. D., & Thomas, G. H. (2019). Sexual selection predicts the rate and direction of colour divergence in a large avian radiation. *Nature Communications*, 10(1), 1773. <https://doi.org/10.1038/s41467-019-09859-7>
- Cuthill, I. C., Allen, W. L., Arbuckle, K., Caspers, B., Chaplin, G., Hauber, M. E., Hill, G. E., Jablonski, N. G., Jiggins, C. D., Kelber, A., Mappes, J., Marshall, J., Merrill, R., Osorio, D., Prum, R., Roberts, N. W., Roulin, A., Rowland, H. M., Sherratt, T. N., Skelhorn, J., Speed, M. P., Stevens, M., Stoddard, M. C., Stuart-Fox, D., Talas, L., Caro, T. (2017). The biology of color. *Science*, 357(6350). <https://doi.org/10.1126/science.aan0221>
- Dale, J., Dey, C. J., Delhey, K., Kempenaers, B., & Valcu, M. (2015). The effects of life history and sexual selection on male and female plumage colouration. *Nature*, 527(7578), 367–370. <https://doi.org/10.1038/nature15509>

- Delhey, K. (2020). Revealing the colourful side of birds: spatial distribution of conspicuous plumage colours on the body of Australian birds. *J Avian Biol*, 51:. <https://doi.org/10.1111/jav.02222>
- Doucet, S. M., Mennill, D. J., Hill, G. E., & Théry, S. editors: A. T. D. B. and M. (2007). The Evolution of Signal Design in Manakin Plumage Ornaments. *The American Naturalist*, 169(S1), S62–S80. <https://doi.org/10.1086/510162>
- Dunn, P. O., Armenta, J. K., & Whittingham, L. A. (2015). Natural and sexual selection act on different axes of variation in avian plumage color. *Science Advances*, 1(2), e1400155. <https://doi.org/10.1126/sciadv.1400155>
- Edmunds, M., & Dewhirst, R. A. (1994). The survival value of countershading with wild birds as predators. *Biological Journal of the Linnean Society*, 51(4), 447–452. <https://doi.org/10.1006/bijl.1994.1034>
- Eliason, C. M., Andersen, M. J., & Hackett, S. J. (2019). Using Historical Biogeography Models to Study Color Pattern Evolution. *Systematic Biology*, 68(5), 755–766. <https://doi.org/10.1093/sysbio/syz012>
- Endler, J. A. (1990). On the measurement and classification of colour in studies of animal colour patterns. *Biological Journal of the Linnean Society*, 41(4), 315–352. <https://doi.org/10.1111/j.1095-8312.1990.tb00839.x>
- Endler, J. A. (1992). Signals, Signal Conditions, and the Direction of Evolution. *The American Naturalist*, 139, S125–S153.
- Endler, J. A. (1993). The Color of Light in Forests and Its Implications. *Ecological Monographs*, 63(1), 1–27. <https://doi.org/10.2307/2937121>
- Endler, J. A., & Thery, M. (1996). Interacting Effects of Lek Placement, Display Behavior, Ambient Light, and Color Patterns in Three Neotropical Forest-Dwelling Birds. *The American Naturalist*, 148(3), 421–452.
- Espmark, Y., Amundsen, T., & Rosenqvist, G. (2000). *Animal Signals: Signalling and Signal Design in Animal Communication*. Tapir Academic Press.
- Fry, H., Fry, K., & Harris, A. (1992). *Kingfishers, Bee-eaters and Rollers: A Handbook*. Helm Field Guides Series.

- Galván, I., Negro, J. J., Rodríguez, A., & Carrascal, L. M. (2013). On Showy Dwarfs and Sober Giants: Body Size as a Constraint for the Evolution of Bird Plumage Colouration. *Acta Ornithologica*, 48(1), 65–80. <https://doi.org/10.3161/000164513X670007>
- Gomez, D., & Théry, M. (2004). Influence of ambient light on the evolution of colour signals: Comparative analysis of a Neotropical rainforest bird community. *Ecology Letters*, 7(4), 279–284. <https://doi.org/10.1111/j.1461-0248.2004.00584.x>
- Gomez, D., & Théry, M. (2007). Simultaneous Crypsis and Conspicuousness in Color Patterns: Comparative Analysis of a Neotropical Rainforest Bird Community. *The American Naturalist*, 169(S1), S42–S61. <https://doi.org/10.1086/510138>
- Götmark, F. (1987). White underparts in gulls function as hunting camouflage. *Animal Behaviour*, 35, 1786–1792. [https://doi.org/10.1016/S0003-3472\(87\)80071-4](https://doi.org/10.1016/S0003-3472(87)80071-4)
- Grafen, A., & Hamilton, W. D. (1989). The phylogenetic regression. *Philosophical Transactions of the Royal Society of London. B, Biological Sciences*, 326(1233), 119–157. <https://doi.org/10.1098/rstb.1989.0106>
- Hadfield, J. D. (2010). MCMC Methods for Multi-Response Generalized Linear Mixed Models: The MCMCglmm R Package. *Journal of Statistical Software*, 33(2), 1–22.
- Hagman, M., & Forsman, A. (2003). Correlated evolution of conspicuous coloration and body size in poison frogs (Dendrobatidae). *Evolution*, 57(12), 2904–2910. <https://doi.org/10.1554/03-357>
- Håstad, O., Victorsson, J., & Ödeen, A. (2005). Differences in color vision make passerines less conspicuous in the eyes of their predators. *Proceedings of the National Academy of Sciences*, 102(18), 6391–6394. <https://doi.org/10.1073/pnas.0409228102>
- Hill, G. E., & McGraw, K. J. (2006). *Bird Coloration, Volume 1: Mechanisms and Measurements*. Harvard University Press. <https://www.hup.harvard.edu/catalog.php?isbn=9780674018938>
- Hossie, T. J., Skelhorn, J., Breinholt, J. W., Kawahara, A. Y., & Sherratt, T. N. (2015). Body size affects the evolution of eyespots in caterpillars. *Proceedings of the National Academy of Sciences*, 112(21), 6664–6669. <https://doi.org/10.1073/pnas.1415121112>
- Hunt, S., Bennett, A. T. D., Cuthill, I. C., & Griffiths, R. (1998). Blue tits are ultraviolet tits. *Proceedings of the Royal Society of London. Series B: Biological Sciences*, 265(1395), 451–455. <https://doi.org/10.1098/rspb.1998.0316>

- Igic, B., D'Alba, L., & Shawkey, M. D. (2018). Fifty shades of white: How white feather brightness differs among species. *The Science of Nature*, 105(3), 18. <https://doi.org/10.1007/s00114-018-1543-3>
- Jetz, W., Thomas, G. H., Joy, J. B., Hartmann, K., & Mooers, A. O. (2012). The global diversity of birds in space and time. *Nature*, 491(7424), 444–448. <https://doi.org/10.1038/nature11631>
- Johnson, N. K., & Brush, A. H. (1972). Analysis of Polymorphism in the Sooty-capped Bush Tanager. *Systematic Biology*, 21(3), 245–262. <https://doi.org/10.1093/sysbio/21.3.245>
- Jolliffe, I. T. (2002). *Principal Component Analysis* (2nd ed.). Springer-Verlag. <https://doi.org/10.1007/b98835>
- Keyser, A. J., & Hill, G. E. (2000). Structurally based plumage coloration is an honest signal of quality in male blue grosbeaks. *Behavioral Ecology*, 11(2), 202–209. <https://doi.org/10.1093/beheco/11.2.202>
- Maia, R., Gruson, H., Endler, J. A., & White, T. E. (2019). pavo 2: New tools for the spectral and spatial analysis of colour in R. *Methods in Ecology and Evolution*, 10(7), 1097–1107. <https://doi.org/10.1111/2041-210X.13174>
- Maia, R., Rubenstein, D. R., & Shawkey, M. D. (2016). Selection, constraint, and the evolution of coloration in African starlings. *Evolution*, 70(5), 1064–1079. <https://doi.org/10.1111/evo.12912>
- Marchetti, K. (1993). Dark habitats and bright birds illustrate the role of the environment in species divergence. *Nature*, 362(6416), 149–152. <https://doi.org/10.1038/362149a0>
- Marchetti, K., and T. Price. (1997). The adaptive significance of colour patterns in the Old World leaf warblers, genus *Phylloscopus*. *Oikos* 79:410–412.
- Marcondes, R. S., & Brumfield, R. T. (2019). Fifty shades of brown: Macroevolution of plumage brightness in the Furnariida, a large clade of drab Neotropical passerines. *Evolution*, 73(4), 704–719. <https://doi.org/10.1111/evo.13707>
- McNaught, M. K., & Owens, I. P. F. (2002). Interspecific variation in plumage colour among birds: Species recognition or light environment? *Journal of Evolutionary Biology*, 15(4), 505–514. <https://doi.org/10.1046/j.1420-9101.2002.00431.x>

- Ödeen, A., & Håstad, O. (2013). The phylogenetic distribution of ultraviolet sensitivity in birds. *BMC Evolutionary Biology*, 13(1), 36. <https://doi.org/10.1186/1471-2148-13-36>
- Orme, D., Freckleton, R. P., Thomas, G. H., Petzoldt, T., Fritz, S. A., & Isaac, N. (2013). CAPER: Comparative analyses of phylogenetics and evolution in R. *Methods in Ecology and Evolution*, 3, 145–151.
- Peek, F. W. (1972) An experimental study of the territorial function of vocal and visual display in the male red-winged blackbird (*Agelaius phoeniceus*). *Animal Behaviour*, 20, 1, 112-118, [https://doi.org/10.1016/S0003-3472\(72\)80180-5](https://doi.org/10.1016/S0003-3472(72)80180-5).
- Preston, C. R. (1980). Differential Perch Site Selection by Color Morphs of the Red-Tailed Hawk (*Buteo jamaicensis*). *The Auk*, 97(4), 782–789.
- Pryke, S. R., & Griffith, S. C. (2007). The relative role of male vs. Female mate choice in maintaining assortative pairing among discrete colour morphs. *Journal of Evolutionary Biology*, 20(4), 1512–1521. <https://doi.org/10.1111/j.1420-9101.2007.01332.x>
- Revell, L. J. (2012). phytools: An R package for phylogenetic comparative biology (and other things). *Methods in Ecology and Evolution* 3(2), 217–223.
- Røskaft, E., & Rohwer, S. (1987). An experimental study of the function of the red epaulettes and the black body colour of male red-winged blackbirds. *Animal Behaviour*, 35(4), 1070–1077. [https://doi.org/10.1016/S0003-3472\(87\)80164-1](https://doi.org/10.1016/S0003-3472(87)80164-1)
- Rowland, H. M., Speed, M. P., Ruxton, G. D., Edmunds, M., Stevens, M., & Harvey, Ian. F. (2007). Countershading enhances cryptic protection: An experiment with wild birds and artificial prey. *Animal Behaviour*, 74(5), 1249–1258. <https://doi.org/10.1016/j.anbehav.2007.01.030>
- Rubenstein, D. R., & Lovette, I. J. (2009). Reproductive skew and selection on female ornamentation in social species. *Nature*, 462, 786–789. <https://doi.org/10.1038/nature08614>
- Rueden, C. T., Schindelin, J., Hiner, M. C., DeZonia, B. E., Walter, A. E., Arena, E. T., & Eliceiri, K. W. (2017). ImageJ2: ImageJ for the next generation of scientific image data. *BMC Bioinformatics*, 18(1), 529. <https://doi.org/10.1186/s12859-017-1934-z>
- Ruiz-Rodríguez, M., Aviles, J. M., Cuervo, J. J., Parejo, D., Ruano, F., Zamora-Muñoz, C., Sergio, F., López-Jiménez, L., Tanferna, A., Martín-Vivaldi, M. (2013). Does avian conspicuous colouration increase or reduce predation risk? *Oecologia* 173:83–93.

- Schliep, K. P. (2011). phangorn: Phylogenetic analysis in R. *Bioinformatics*, 27(4), 592–593. <https://doi.org/10.1093/bioinformatics/btq706>
- Shultz, A. J., & Burns, K. J. (2013). Plumage evolution in relation to light environment in a novel clade of Neotropical tanagers. *Molecular Phylogenetics and Evolution*, 66(1), 112–125. <https://doi.org/10.1016/j.ympev.2012.09.011>
- Shultz, A. J., & Burns, K. J. (2017). The role of sexual and natural selection in shaping patterns of sexual dichromatism in the largest family of songbirds (Aves: Thraupidae). *Evolution*, 71(4), 1061–1074. <https://doi.org/10.1111/evo.13196>
- Stavenga, D. G., Tinbergen, J., Leertouwer, H. L., & Wilts, B. D. (2011). Kingfisher feathers – colouration by pigments, spongy nanostructures and thin films. *Journal of Experimental Biology*, 214(23), 3960–3967. <https://doi.org/10.1242/jeb.062620>
- Stein, A. C., & Uy, J. A. C. (2006). Unidirectional introgression of a sexually selected trait across an avian hybrid zone: a role for female choice? *Evolution*, 60(7), 1476–1485. <https://doi.org/10.1554/05-575.1>
- Stevens, M., & Cuthill, I. C. (2007). Hidden Messages: Are Ultraviolet Signals a Special Channel in Avian Communication? *BioScience*, 57(6), 501–507. <https://doi.org/10.1641/B570607>
- Stoddard, M. C., & Prum, R. O. (2008). Evolution of Avian Plumage Color in a Tetrahedral Color Space: A Phylogenetic Analysis of New World Buntings. *The American Naturalist*, 171(6), 755–776. <https://doi.org/10.1086/587526>
- Stoddard, M. C., & Prum, R. O. (2011). How colorful are birds? Evolution of the avian plumage color gamut. *Behavioral Ecology*, 22(5), 1042–1052. <https://doi.org/10.1093/beheco/arr088>
- Tate, G.J., Bishop, J.M. and Amar, A. (2016). Differential foraging success across a light level spectrum explains the maintenance and spatial structure of colour morphs in a polymorphic bird. *Ecology Letters*, 19: 679–686. <https://doi.org/10.1111/ele.12606>
- Théry, M. (2006). Effect of light environment on color communication in birds. In Hill, G.E. & McGraw, K.J. (eds) *Bird Coloration. Vol. 1: Mechanisms and Measurements*. 295–353. Cambridge, MA: Harvard University Press
- Troscianko, J., & Stevens, M. (2015). Image calibration and analysis toolbox – a free software suite for objectively measuring reflectance, colour and pattern. *Methods in Ecology and Evolution*, 6(11), 1320–1331. <https://doi.org/10.1111/2041-210X.12439>

- Troscianko, J., Wilson-Aggarwal, J., Stevens, M. & Spottiswoode, C. N. (2016). Camouflage predicts survival in ground-nesting birds. *Scientific Reports* 6, 19966
- Wilman, H., Belmaker, J., Simpson, J., Rosa, C. de la, Rivadeneira, M. M., & Jetz, W. (2014). EltonTraits 1.0: Species-level foraging attributes of the world's birds and mammals. *Ecology*, 95(7), 2027–2027. <https://doi.org/10.1890/13-1917.1>
- Winebarger, M. M., Pugh, M. W., Gangloff, M. M., Osbourn, M. S., & Siefferman, L. (2018). Body Size Is Positively Correlated With Conspicuous Coloration in Ambystoma Salamanders, but Negatively Correlated With Conspicuous Coloration in Plethodon Salamanders. *Frontiers in Ecology and Evolution*, 6. <https://doi.org/10.3389/fevo.2018.00143>

CHAPTER 3

Evolutionary dynamics of pigmentary grey and non-iridescent structural blue colouration in Tanagers (family: Thraupidae)

3.1. Abstract

Birds are one of the most colourful animal groups in the world and there are multiple ways by which they achieve this feature. Mechanisms of colour production range from pigmentary (pigment deposition) to structural (nanostructural arrangements), or the combination of both. Despite the huge *breadth* of colour gamut, the basic components of feathers are shared across all of them (keratin, air and presence of pigments in accordance with the colour produced). It has been shown that in some instances, colour evolution between pigmentary and structural colours can proceed by rearrangement of the nano-structural elements of feathers. Here, we investigated evolutionary transitions between pigmentary grey and non-iridescent structural blue. We focus on the Thraupidae (tanagers and allies) that display a variety of blues and greys including a potential transition state that we refer to as slate. We used digitally calibrated images of birds to quantify colour and determine the distinctiveness of slate colour in colourspace. Following, we identify the most likely pathway for the evolution of the colour blue: from grey via slate colour. Our research reveals a new pathway in the evolution of blue colour.

3.2. Introduction:

The array of colours in a bird's plumage are produced either by pigment deposition in their plumage (pigmentary colours), precisely arranged structural elements of feathers (structural colours) or as a combination of both (Hill & McGraw, 2006; Shawkey & D'Alba, 2017). In melanin-based pigmentary colour, the pigment melanin is produced, transported, and stored in organelles called melanosomes (D'Alba & Shawkey, 2019). Melanin based colouration includes black, brown, and grey hues with each one having a characteristic melanosome shape (Babarović et al., 2019; Li et al., 2010). In structural colours, precisely arranged elements of feather nanostructure are responsible for colour production (Hill & McGraw, 2006). Non-iridescent structural colours in birds are produced by a keratin and air matrix (spongy layer) placed within the feather barb (Hill & McGraw, 2006; Prum et al., 1998; Shawkey & Hill, 2006). A melanosomes layer beneath the colour producing nanostructure

is essential in colour production by absorption of all backscattered light (Shawkey & Hill, 2006). Non-iridescent structural colours encompass blue, violet and ultraviolet (UV) hues (Saranathan et al., 2012; Shawkey & D'Alba, 2017).

Evolutionary transitions between pigmentary and structural colours in birds' plumage have been described previously (Doucet et al., 2004; Driskell et al., 2010; Shawkey et al., 2006). Due to the similarity of elements involved in the production of each colour, i.e. keratin, melanin and air gaps, it has been proposed that evolutionary transitions happen through rearrangements of feather nanostructure (Prum, 2006). This hypothesis has been demonstrated in the case of the transition between matte black and iridescent colouration in grackles and allies (Icteridae), where light-scattering melanosomes are organized in an ordered layer on the edges of the barbules (Shawkey et al., 2006). Other structural similarities between certain pigmentary and structural colours exist that indicate their potential transitions. For example, the black plumage of some fairy wrens has been found to have a spongy layer indicative of non-iridescent structural colours, but with additional melanosomes incorporated into the feather barb. These additional melanosomes prevent colour production by the spongy layer, leading to a black colour (Doucet et al., 2004; Driskell et al. 2010).

Recently, it has been suggested that non-iridescent structural blue colours evolve via a transition from grey, based on the similarity in the structural components of the feather (Babarović et al., 2019). The investigation of melanosome shape showed an overlap between those involved in grey colour production and melanosomes placed underneath the colour producing nanostructures in non-iridescent structural colour. The mechanistic shift needed for this colour evolution would involve the rearrangement of melanosomes from grey colouration around the central feather shaft and subsequent development of the spongy layer. The potential mechanism for this transition is also supported by evidence from research into the colour producing spongy layer in feather barbs (Saranathan et al., 2012). A broad analysis of non-iridescent structural colours across different bird clades indicated that a colour category broadly defined as blue-grey (or slate) possesses "rudimentary or weakly nanostructured" feathers (Saranathan et al., 2012). This indicates that this colour state has a poorly developed spongy layer and could potentially be a transition between grey and non-iridescent structural blue colour (which has the spongy layer fully developed) in bird's plumage.

To explore the evolutionary dynamics and potential transition between pigmentary grey colour and the non-iridescent structural blue colour, we focused on the passerine family Thraupidae, the tanagers. Thraupidae have diverse plumage including pigmentary grey, non-iridescent structural blue as well as a wide range of slate (blue-grey) colours. This diversity of colour distribution across

the phylogeny makes them an ideal study system for addressing the origins and potential dynamics that lead to the proliferation of blue colours among birds. We collected data from handbook descriptions of bird colouration as well as using quantitative measure of colour (cone catch values) from digital images of birds from museum specimens. We tested: 1) whether slate is an intermediate colour state between pigmentary grey and non-iridescent structural blue using visual modelling in avian colourspace, and 2) whether an evolutionary pathway to non-iridescent structural blue in Tanagers started with grey and proceeded through slate.

3.3. Materials and methods:

3.3.1. Data collection:

We collected plumage colouration data from written descriptions of the plumage colour from *Birds of the World* (Billerman, et al. 2022) and from digitally calibrated images of study skins from the bird collection from Natural History Museum at Tring.

3.3.2. Plumage Colour descriptions:

We classified colour in ten patches (crown, nape, mantle, rump, throat, breast, belly, tail, wing coverts and wing primaries/secondaries) for both males and females for 174 species based on verbal descriptions from the Identification paragraph in the *Birds of the World* (Appendix 2: Table S1). Using these descriptions, we coded each plumage patch as blue, slate and grey (Appendix 2: Table S1). Due to human induced bias in recognising each colour, we verified the verbal description of colour from both the available images and video recordings from *Birds of the World* (Billerman, et al. 2022). Full colour descriptions and the subsequent assigned colour categories are reported in the Additional table 2. (Males scoring) and Additional table 3. (Females scoring) (<https://figshare.com/s/1110fce894e65a69c329>). In the Appendix 2 (Table S1) is the abbreviated version of these tables with only plumage patches that have either grey, slate or blue reported.

3.3.3. Plumage Colour measurements:

To quantify chromatic variation of colour (hue and saturation), calibrated digital images of study skins from Cooney et al. (2022) were used and colour was quantified from them. Briefly, each bird species was photographed six times: from dorsal, lateral, and ventral angle and with two filters (one permitting UV wavelengths and human visible wavelengths). An average of three male and three female study skins were photographed per species. For all imaging, a Nikon D7000 digital single-lens reflex camera was used (for details of all technical specificity, see Cooney et al. (2019)).

Next, all digital images were linearized and converted to .TIFF files (Coffin, D., 2016). The images were normalized by reference to grey standards with known reflectance (Troscianko & Stevens, 2015). Plumage colouration was measured for seven selected body regions: crown, nape, mantle, rump, throat, breast, and belly. On these regions a predominance of a single colour is more likely than in other plumage patches. On every photo, polygons used to mark plumage patches with a custom IMAGE J script and RGB values were extracted for both the human-visible and UV range (Rueden et al., 2017).

Finally, by using already available tools in the IMAGE J Calibration and Analysis Toolbox (version 1.22), mapping functions were applied using methods described in Troscianko and Stevens (2015) to convert all RGB values to raw cone-catch values (u, s, m, l) adjusted to avian colour vision. We used u, s, m and l values for further analysis because they account for avian spectral sensitivities to ultraviolet (u), shortwave (s), mediumwave (m), and longwave (l) light (Stoddard & Prum, 2011). For each sex, average patch values were calculated across all specimens as a species-level measurements.

3.4. Analysis

3.4.1. Distinctiveness analysis

The extracted data from digital images were filtered for only those plumage patches that scored either blue, slate or grey in our written description dataset and for seven plumage patches (crown, nape, mantle, rump, throat, breast and belly) (Appendix 2: Table S1). We focused on these seven patches because the marked regions on the digital image data for other patches typically included only a small proportion of the focal colour resulting in patch colour measurements that would provide inconsistent and unreliable measures of the presence of grey, slate, and blue. These values were then visualised in an avian tetrahedral colourspace, using methods from Stoddard & Prum (2008) implemented in the R package pavo (Maia et al., 2019; R Core Team, 2021) (Fig. 3.1, a, b, c). In tetrahedral colourspace every data point is represented by four values (ultraviolet cone – u, short-wavelength cone – s, medium-wavelength cone – m, long-wavelength cone - l) that are equivalent to how much each colour stimulates each cone in the bird's retina.

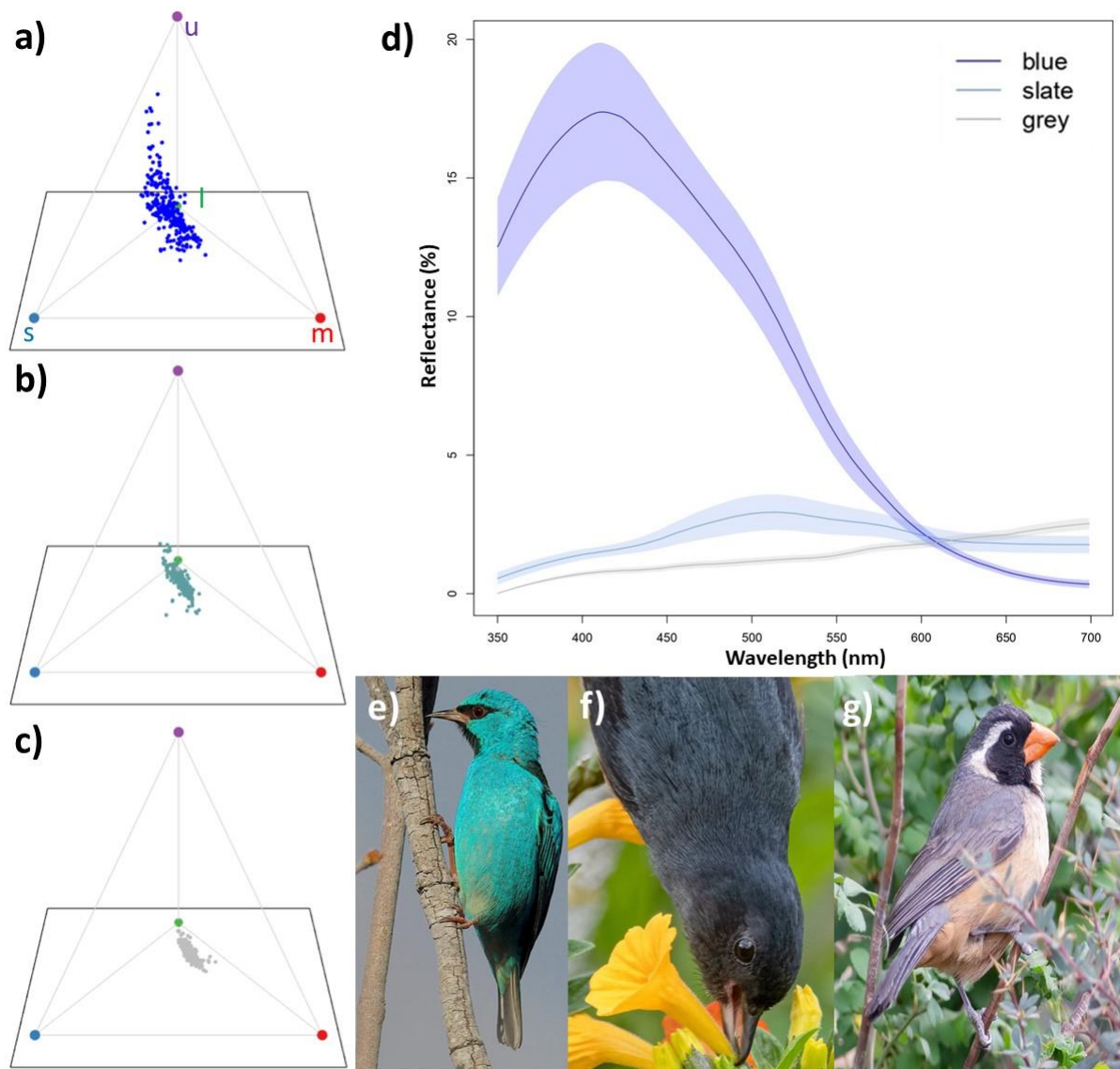


Figure 3.1. Overview of plumage colouration across three colour categories (blue, slate and grey) in tetrahedral colour space. Panel a) is a tetrahedral colour space with examples of blue data points, with panel e) (Blue dacnis; *Dacnis cayana*) an example of blue plumage colouration in living birds. Panel b) is tetrahedral colour space with examples of slate data points, with panel f) (Slaty flowerpiercer; *Diglossa plumbea*) being an example of slate plumage colouration in living birds. Panel g) is a tetrahedral colour space with examples of grey data points, with panel i) (Black-and-rufous warbling finch; *Poospiza nigrorufus*) an example of grey plumage colouration in living birds. Panel d) represents the average reflectance data of blue, slate and grey plumage patches (as indicated on the legend within the panel) with an average value shown with a line and standard error as the shaded area around the average for each colour. The data for panel d) are taken from

Chapter 4 (section 4.3.2. Reflectance data with species listed in details in Appendix 3: Table S1.). All photos © Daniel J. Field, University of Cambridge. Used with permission.

First, we tested for how different the blue, slate and grey colour categories are and whether the proposed intermediate colour category, i.e. slate, could be considered distinct from either blue or grey or both in avian colour space. For this purpose, we calculated the orthogonal projection of every data point onto the vector constructed in the colourspace. We constructed a vector through the colourspace that goes from one side of the tetrahedral colourspace (cone catch values: $u = 0, s = 1/3, m = 1/3, l = 1/3$) to its opposite side, i.e., u cone (cone catch values: $s = 0, u = 1, m = 0, l = 0$). The vector \bar{B} is defined with two sets of coordinates:

$$\bar{B} = \begin{bmatrix} 0 & 1 \\ 1/3 & 0 \\ 1/3 & 0 \\ 1/3 & 0 \end{bmatrix}$$

Since most of the data points have strong reflectance in the u part of the spectrum, the vector is constructed to capture the orientation of our data within the colourspace. Every data point in the colourspace, defined by the four coordinates that correspond to four cone catch values (u, s, m, l), can be represented as the vector itself:

$$\bar{A} = \begin{bmatrix} u \\ s \\ m \\ l \end{bmatrix}$$

Projection is a linear transformation of any data point in the morphospace (in our case, tetrahedral colourspace), defined by four coordinates (in our case: u, s, m and l values) by orthogonal projection of that data point to a vector defined by two sets of coordinates. In the following step, an orthogonal projection of the data point \bar{A} to a vector \bar{B} is calculated by:

$$\bar{A1} = \frac{\bar{A} \cdot \bar{B}}{\|\bar{B}\|}$$

With $\|\bar{B}\|$ being the norm (lengths) of the \bar{B} . The norm was calculated for every data point in our dataset, and we named them projection values and used them for further analysis. (Fig. 3.2, a; Appendix 2: Table S1, projection values). After the data point in the colourspace is orthogonally projected on the predefined vector, the distance from the vector's origin to the new point is calculated and called projection value.

We used the projection values to calculate the Bhattacharyya coefficient which quantified the overlap between the distributions of projection values between two colour categories, i.e. blue – slate, grey – slate and blue – grey. Higher value of Bhattacharyya coefficient will indicate greater overlap between two distributions and therefore lesser distinctiveness. The calculation of both the projection values and the Bhattacharyya coefficient were performed using the R package *dispRity* (Guillerme, 2018).

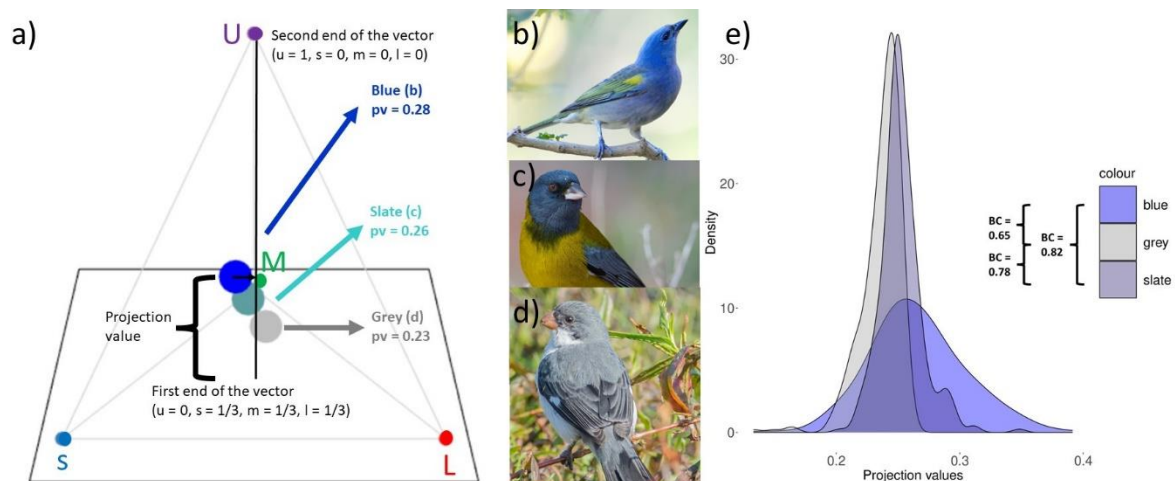


Figure 3.2. Distinctiveness analysis. Panel a) shows tetrahedral colourspace with the examples of grey, slate and blue data points. On an example of blue data point, a calculation of the projection value is shown. Blue, slate and grey data points are from the crown patch: blue is from Golden chevroned tanager (*Thraupis ornata*) (panel b), slate is from the Grey-hooded siera finch (*Phygilus gayi*) (panel c) and in grey is for White-bellied Seedeater (*Sporophila leucoptera*) (panel d). A vector is constructed throughout the colourspace that goes from one side of the tetrahedral colourspace (cone catch values: $u = 0, s = 1/3, m = 1/3, l = 1/3$, “first end of the vector” on the figure) to its opposite side, i.e., u cone (cone catch values: $s = 0, u = 1, m = 0, l = 0$; “second end of the vector” on the figure). On the example of the blue data point, we showed how is the projection value calculated, i.e. once data point is projected on the vector how far away that new data point is from the vector’s 0 end (“first end of the vector” on the figure). Near every data point, a projection value for that data point is indicated. Panel e) shows distribution of the grey, slate and blue data points with the Bhattacharyya coefficient (BC) indicated for each colour pair on the right-hand side. All photos © Daniel J. Field, University of Cambridge. Used with permission.

3.4.2. Multistate analysis

To test for the evolutionary sequence from grey through slate to blue (grey → slate → blue) we used Reverse Jump Multistate model in BayesTraits (Currie & Meade, 2014; Pagel et al., 2004). This analysis allows testing a range of models with all possible combinations of transitions among character states (all possible pathways are illustrated in an Appendix 2., Fig. S1.) The model that is best fit to our data is visited during the analysis most frequently. For our evolutionary hypothesis, this would translate to pathway that leads from any colour to grey, grey to slate, and slate to blue being more visited in comparison to any other model or have higher transition rates than the rest of parameters in our model. We used molecular phylogenies for Tanagers available from birdtree.org (Jetz et al., 2012) with 1000 random trees downloaded. From a previously collected dataset of presence and absence of blue, slate and grey colour in Tanagers, we developed a new database used for the RJ MCMC Multistate analysis (Appendix 2: Table S2; Table S3). We coded each species in our dataset for presence/absence of each colour category such that the colour is treated as present if the bird has it on at least one body patch (crown, nape, mantle, rump, throat, breast, belly, tail, wing coverts and wing primaries/secondaries). Therefore, 0 is coded absence of the colour of interest, 1 for presence of grey colour, 2 for presence of slate colour (also if slate co-occurs with grey colour in the same bird species: two species in both males and females) and 3 for presence of blue colour (also if blue co-occurs with grey in the same species: four cases in males and nine cases in females; or slate in the same species: five species in males and four species in females). This coding scheme implicitly assumes that if a species has the ability to produce the subsequent colour in the proposed evolutionary pathway, it also can produce the preceding colour in the evolutionary pathway. A separate dataset was made for males and females (Appendix 2: Table S2; Table S3) which were analysed separately due to notable differences in the plumage colouration. We repeated the same analysis for males and females, but without species that exhibit co-occurrence of two colours of our interest (Appendix 2: Table S2; Table S3, in both dataset, species marked with red have double scoring and were not included in the second analysis). By excluding these species we avoid the assumption of a specific evolutionary pathway. We report the results of the latter analysis, that are qualitatively similar to the main analysis, in the Appendix 2 (Table S6; Table S7). For each analysis we applied Reverse Jump (RJ) MCMC which considers all possible models of evolution with proportionally visiting the best fitting one. Models were run for 220000000 iterations with Burnin 2000000 and exponential prior of value 10. Each analysis was run 3 times to confirm the consistency in our results.

3.5. Results

3.5.1. Distinctiveness analysis

First, we plotted grey, slate and blue colour categories in tetrahedral colourspace (Fig. 3.1, a, d, g). Our measure of the overlap between probability distributions (Battacharayya coefficient, BC) of the projection values for grey, blue and slate colour indicated that the categories are neither distinct nor completely overlapping (BC for slate and blue = 0.82, BC for slate and grey = 0.78, and BC for grey and blue = 0.65) (Fig. 3.2, e). A Battacharayya coefficient greater than 0.95 would indicate overlap and less than 0.05 would indicate distinctiveness (Guillerme & Cooper, 2016). These results can be interpreted as evidence that grey and blue are opposite ends of continuum in which slate is an intermediate state.

3.5.2. Multistate

Our RJ MCMC Multistate analyses revealed that a pathway from any other colour to grey through slate leading to blue is present. While other evolutionary transitions among the coded characters are possible in both males and females, no other pathways led towards blue colour.

In females, the 95% credible set consists of only one model (Fig. 3.3, b). The model suggests that transition from any other colour to slate (q02), any other colour to blue (q03), grey to blue (q13), blue to grey (q31) and blue to slate (q32) are very unlikely to happen. This is indicated by low percentage of models that estimate these transition rates to not be zero (0.01% -3.32%) (Fig. 3.3, d). On the other hand, transition from any other colour to grey and vice versa (q01, q10), grey to slate and vice versa (q12 and q21), slate to any other colour (q20), slate to blue (q23) and blue to any other colour (q30) are likely to happen. These parameters are estimated as non-zero in a very high percentage of all models (99.4% - 100%) (Fig. 3.3, d). All the transitions that do happen have the same mean values of 0.06 indicating that when the transitions do happen, their average rate is equal (Fig. 3.3, c). Full results are reported in the Appendix 2: Tale S5. Results without double scoring species are reported in the Appendix 2: Table S7.

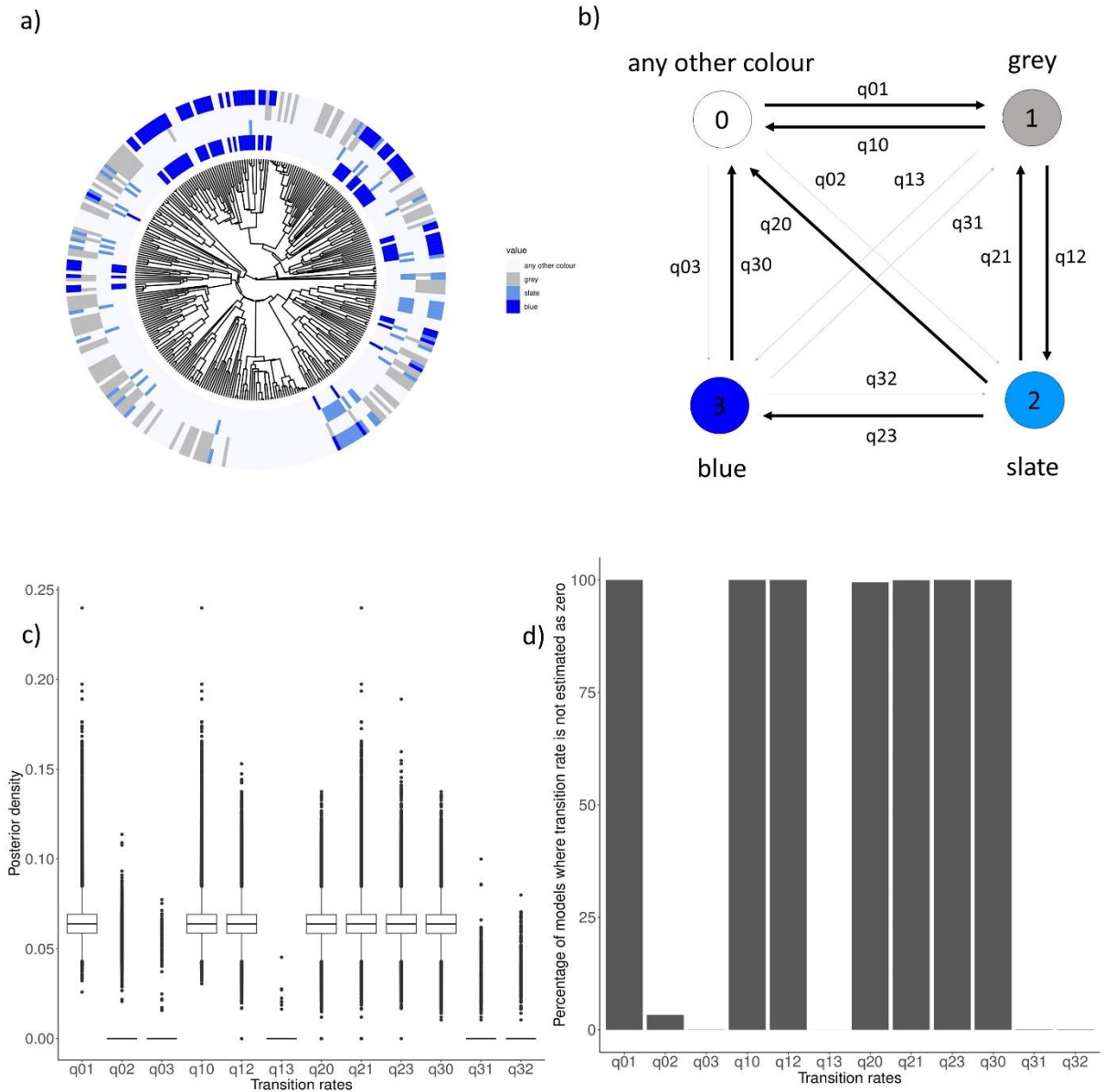


Figure 3.3. The evolution of blue, slate and grey colour in the plumage of female Tanagers. Panel a shows the phylogeny of 319 Tanagers species with the plotting of blue, slate and grey on tips of the phylogeny. The first circle indicates the presence of blue colour, the second circle indicates the presence of slate colour, the third circle indicates the presence of grey colour and the fourth circle represents the coding of colours used for the analysis. The presence of colour in the plumage of species is indicated with the presence of the bar, while the lack of it is represented with the lack of it for each circle. Panel b shows schematics of the evolutionary pathway between coded colour states. Transition rates that are present are represented with thicker lines, while those that are not detected are represented with thinner lines. Panel c shows posterior densities of the transition rates from the RJ Multistate model. Panel d shows the percentage of models from 220 000 000 iterations where transition rates are not estimated as zero. A high percentage indicates that the transition is

happening (q01, q10, q12, q20, q21, q23, q30). A low percentage indicates that the transitions are not happening (q02, q03, q13, q31, q32). Transition rates on panels c and d indicate the following transition rates: q01 is any other colour to grey, q02 is any other colour to slate, q03 is any other colour to blue, q10 is grey to any other colour, q12 is grey to slate, q13 is grey to blue, q20 is slate to any other colour, q21 is slate to grey, q23 is slate to blue, q30 is blue to any other colour, q31 is blue to grey, q32 is blue to slate.

In males, the 95% credible set of all models visited during the analysis consists of three possible models. Below we focus on the most frequently visited model (144,398 times out of 218,000) (Fig. 3.4, b). In this model, transitions from any other colour to blue (q03), grey to blue (q13), blue to grey (q31) and blue to slate (q32) are very unlikely to happen. This is indicated by low percentage of models that include these transitions at a non-zero rate (0.1% - 1.9%) (Fig. 3.4, d). Contrary to that, transitions from any other colour to grey (and reverse) (q01, q10), grey to slate (and reverse) (q12, q21), slate to blue (q23) and blue to any other colour (q30), are frequently estimated to be non-zero (99.999 – 100%) indicating that they are likely to happen (Fig. 3.4, d). In between these two extremes, both the gain of slate from any other colour and vice versa (q02, q20) occur in an intermediate percentage of models at a non-zero rate (93.45% and 70.45% respectfully) (Fig. 3.4, d). This would indicate that these transitions occur, but are not as likely as those with a very low percentage of models that estimate them to be zero. The most favoured model sets all non-zero transition rates to be equal with a rate of 0.4 transitions per lineage per million years (Fig. 3.4, c). The other two models in the 96% credible set are visited less frequently (57,610 and 8,357 times respectively). They differ from the most visited model only in two parameters: in the second most visited model the parameter q20 = 0 whereas in the third most visited model q02 = 0. These parameters relate to transitions between any other colour and slate. The presence or absence of these specific transitions does not qualitatively alter our main conclusions on the most likely pathways in grey-slate-blue colour space. Full results are reported in the Appendix 2: Table S4. Results without double scoring species are reported in the Appendix 2: Table S6.

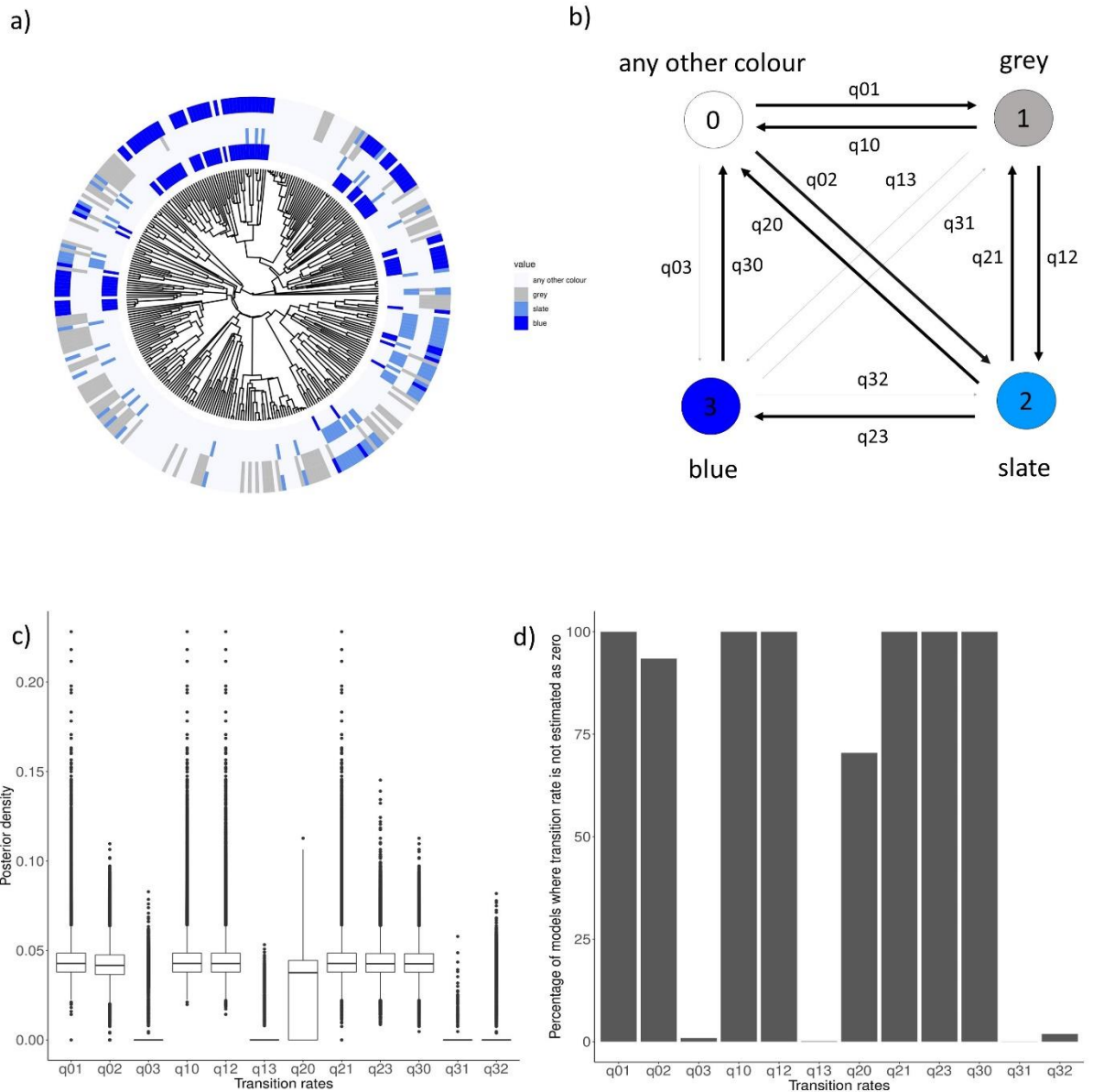


Figure 3.4. The evolution of blue, slate and grey colour in the plumage of male Tanagers. Panel a shows the phylogeny of 319 Tanagers species with the plotting of blue, slate and grey on tips of the phylogeny. The first circle represent the blue colour, the second circle represents slate colour, the third circle represents the grey colour and the fourth circle represents the coding of colours used for the analysis. The presence of colour in the plumage of species is indicated with the presence of the bar, while the lack of it is represented with the lack of it for each circle. Panel b shows schematics of the evolutionary pathway between coded colour states. Transition rates that are present are represented with thicker lines, while those that are not detected are represented with thinner lines. Panel c shows posterior densities of the transition rates from the RJ Multistate model. Panel d shows the percentage of models from 220 000 000 iterations where transition rates are not estimated as zero. A high percentage indicates that the transition is happening ($q_{01}, q_{10}, q_{12}, q_{20}, q_{21}, q_{23}$,

q30). A low percentage indicates that the transitions are not happening (q02, q03, q13, q31, q32). Transition rates on panels c and d indicate the following transition rates: q01 is any other colour to grey, q02 is any other colour to slate, q03 is any other colour to blue, q10 is grey to any other colour, q12 is grey to slate, q13 is grey to blue, q20 is slate to any other colour, q21 is slate to grey, q23 is slate to blue, q30 is blue to any other colour, q31 is blue to grey, q32 is blue to slate.

Multistate analysis also allows us to estimate ancestral state in the basal node of the entire clade for the categorical variables that we use for the analysis (i.e. any other colour, grey, slate, and blue). The model output provides a probability estimate of each state in the basal node of the Tanagers. In males, the highest probability of the ancestral estimate for the basal node is for the slate colour ($P(\text{slate}) = 0.587$), the lower and equivalent probability is for the grey colour, and any other category colour ($P(\text{grey}) = 0.175$, $P(\text{any other colour}) = 0.188$) and the lowest probability is for the blue colour ($P(\text{blue}) = 0.05$). In females, the highest probability of the ancestral estimate for the basal node is slate colour ($P(\text{slate}) = 0.49$), followed by grey colour ($P(\text{grey}) = 0.37$), while blue and any other colour category has the lowest and similar probabilities ($P(\text{blue}) = 0.07$ and $P(\text{any other colour}) = 0.06$). The full results are reported in Additional table 5.; (<https://figshare.com/s/1110fce894e65a69c329>).

3.6. Discussion

Our results showed that slate colour is an intermediate colour with blue colour on one and grey on the other side of the area occupied by these three colours in the tetrahedral colourspace of Tanager plumage colouration. Furthermore, analysis of all possible evolutionary pathways between grey, slate and blue indicated that the most likely pathway for the evolution of the blue colour is the route from grey colour and through the slate colour. Blue colour can equally likely evolve to other parts of the colourspace and we propose white and black colour as the most likely candidates of this transition. Interestingly, slate colour could have an independent evolutionary origin in males suggesting that discovered evolutionary pathway towards blue colour might be rare and hard to achieve.

Due to the fourth cone in their retina, birds' colour vision is extended into the UV part of the light spectrum, making analysis of plumage colouration within the tetrahedral colourspace a crucial part of the framework for understanding colour evolution (Endler & Mielke Jr, 2005; Stoddard & Prum, 2008). We confirm that, as expected, slate is part of a continuum in tetrahedral colourspace between grey and blue. While grey and blue are distinct from one another, the slate colour category overlaps with both grey and blue colour equally (Fig. 3.2, e) suggesting that slate colour shares

properties both of grey colour and blue colour. To what extent the observed overlap in tetrahedral colourspace translates to overlap in the nanostructures of these colours is yet to be seen, but some general assumptions based on what we know about these nanostructures can be made. Slate colour was previously described to be weakly nanostructured, implying that the feather barbs have at least a partially developed medullary spongy layer that would produce what seems to be blue wavelengths in this colour (Saranathan et al., 2012). Since thickness of the medullary layer is important for hue variance in non-iridescent structural colours (Fan et al., 2019), it might be that observed the hue of slate is due to the lack of the sufficient thickness of rudimentary medullary spongy layer. Alternatively, we suggest that melanin deposition masks the blue colour produced by the medullary layer nanostructure as this effect has previously been observed in the case of blue colour (Doucet et al., 2004). In the case of slate, melanosomes characteristic of grey colour could be involved in this process (Babarović et al., 2019).

We tested the macroevolutionary origins and dynamics of non-iridescent structural colours in Tanagers. Our results revealed that the most common pathway for the evolution of blue colour in Tanagers is from slate colour (Fig. 3.3, b; Fig. 3.4, b). Any other evolutionary pathway to non-iridescent structural blue is highly unlikely (Fig. 3.3, b; Fig. 3.4, b). Evolution from pigmentary to structural colour has been recorded previously and explained as a process of evolutionary tinkering (Shawkey et al., 2006). This process would involve the evolution of a new phenotype by rearrangements of elements of an already existing phenotype (Bockaert & Pin, 1999, 1999). In the case of the evolution from pigmentary grey to non-iridescent structural colour blue this would involve a two-stage process: 1) arrangement of melanosomes in a layer next to the central shaft, and 2) development of a keratin and air nanostructure in medullary cells of the feather barbs responsible to produce the colour. Due to the lack of information of the internal anatomy of slate feather barbs, the precise sequence and extent of these processes remains to be tested. The existence of the intermediary stage is vital for the emergence of the blue colouration since direct pathways from “any other colour” to blue have not been detected in our analysis (Fig. 3.3, b; Fig. 3.4, b). Nevertheless, the requirement for an intermediary stage indicates that the process of evolution of blue colour via this route is likely hard to achieve and rare.

Interestingly, slate colour is the most likely ancestral state estimate for the plumage colour out of the colours we have investigated. This could further indicate the dynamics of the evolutionary processes we observe in this analysis. Namely, while slate is the most likely ancestral state, and we know that transitions between slate and grey are bi-directional and common, we suggest that these transitions happened early in the evolutionary history of this clade. This also suggests that the

evolutionary sequence we observe is not hierarchical for grey and slate colours, while blue can evolve only from slate colour. The observed outcome could depend on the ecological and behavioural characteristics of the species having these colours in the modern clade and the hypothesized ancestral species to modern Tanagers.

The transition from blue to “any other colour” has also been detected within our plumage colour evolution model (Fig. 3.3, b; Fig. 3.4, b). Transitions from blue colour to other colours have been detected previously in birds’ plumage. For example, in swallow tanager (*Tarsina viridis*) white belly feathers have a slight blue-green wash on the tips of the distant barbs (Bazzano et al., 2021). Production of that colour was assigned to the keratin and air matrix which was like that of blue feathers. The rest of the plumage of swallow tanager is green-blue produced by the keratin and air nanostructure in medullary cells of feather barbs with an underlying melanosome layer. This common nanostructural component might indicate a potential evolutionary transition between white colour and non-iridescent structural colours. Furthermore, the black plumage of two island subspecies of the White-winged fairywren *Malurus leucopterus* (*M. l. leucopterus* and *M. l. edouardi*) has been confirmed by genetic and nanostructural analysis to have evolved from blue plumage colouration of mainland subspecies *M. l. leuconotus* (Doucet et al., 2004). The black plumage of the two island subspecies has a rudimentary spongy layer embedded with melanosomes that cloud blue colour production resulting in black. These examples are consistent with our finding that blue can evolve into multiple other colours.

The existence of the intermediary stage could also indicate that slate colour could have a separate ecological or signalling purpose within a bird’s plumage colouration which made it a stable phenotype. Due to the lack of information on the nanostructural basis of slate colour, it is impossible to predict from which colour this transition might happen. Both blue and grey colour have predictions of their signalling capacities in their adjacent light environments. While blue colour achieves increased conspicuousness in woodland light environment, grey colour does the same in the open light environment. It would be interesting to test experimentally the signalling capacity of slate colour in the different light environments and whether slate colour contains trade-off between signalling properties of blue and grey colour.

3.7. References

Babarović, F., Puttick, M. N., Zaher, M., Learmonth, E., Gallimore, E.-J., Smithwick, F. M., Mayr, G., & Vinther, J. (2019). Characterization of melanosomes involved in the production of non-

- iridescent structural feather colours and their detection in the fossil record. *Journal of The Royal Society Interface*, 16(155), 20180921. <https://doi.org/10.1098/rsif.2018.0921>
- Bazzano, L. T., Mendicino, L. R., Inchaussandague, M. E., Skigin, D. C., García, N. C., Tubaro, P. L., & Barreira, A. S. (2021). Mechanisms involved in the production of differently colored feathers in the structurally colored swallow tanager (*Tersina viridis*; Aves: Thraupidae). *Journal of Experimental Zoology Part B: Molecular and Developmental Evolution*, 336(5), 404–416. <https://doi.org/10.1002/jez.b.23043>
- Billerman, S. M., Keeney B. K., Rodewal P. G., and Schulenberg T. S. (2022). *Birds of the World*. Cornell Laboratory of Ornithology, Ithaca, NY, USA. <https://birdsoftheworld.org/bow/home>
- Bockaert, J., & Pin, J. P. (1999). Molecular tinkering of G protein-coupled receptors: An evolutionary success. *The EMBO Journal*, 18(7), 1723–1729. <https://doi.org/10.1093/emboj/18.7.1723>
- Coffin, D. (2016). *DCRAW V. 9.27*. <https://www.cybercom.net/~dcoffin/dcrawl/>
- Cooney, C. R., He, Y., Varley, Z. K., Nouri, L. O., Moody, C. J. A., Jardine, M. D., Liker, A., Székely, T., & Thomas, G. H. (2022). Latitudinal gradients in avian colourfulness. *Nature Ecology & Evolution*, 6(5), Article 5. <https://doi.org/10.1038/s41559-022-01714-1>
- Cooney, C. R., Varley, Z. K., Nouri, L. O., Moody, C. J. A., Jardine, M. D., & Thomas, G. H. (2019). Sexual selection predicts the rate and direction of colour divergence in a large avian radiation. *Nature Communications*, 10(1), 1773. <https://doi.org/10.1038/s41467-019-09859-7>
- Currie T.E. & Meade A. (2014). Keeping Yourself Updated: Bayesian Approaches in Phylogenetic Comparative Methods with a Focus on Markov Chain Models of Discrete Character Evolution. In *Modern Phylogenetic Comparative Methods and Their Application in Evolutionary Biology* (pp. 263–286). Springer.
- D’Alba, L., & Shawkey, M. D. (2019). Melanosomes: Biogenesis, Properties, and Evolution of an Ancient Organelle. *Physiological Reviews*, 99(1), 1–19. <https://doi.org/10.1152/physrev.00059.2017>
- Doucet, S. M., Shawkey, M. D., Rathburn, M. K., Mays, H. L., & Montgomerie, R. (2004). Concordant evolution of plumage colour, feather microstructure and a melanocortin receptor gene between mainland and island populations of a fairy-wren. *Proceedings of the Royal Society of London. Series B: Biological Sciences*, 271(1549), 1663–1670. <https://doi.org/10.1098/rspb.2004.2779>
- Driskell, A. C., Prum, R. O., & Pruett-Jones, S. (2010). The evolution of black plumage from blue in Australian fairy-wrens (Maluridae): Genetic and structural evidence. *Journal of Avian Biology*, 41(5). <https://onlinelibrary.wiley.com/doi/full/10.1111/j.1600-048X.2009.04823.x>

- Endler, J. A., & Mielke Jr, P. W. (2005). Comparing entire colour patterns as birds see them. *Biological Journal of the Linnean Society*, 86(4), 405–431. <https://doi.org/10.1111/j.1095-8312.2005.00540.x>
- Fan, M., D'alba, L., Shawkey, M. D., Peters, A., & Delhey, K. (2019). Multiple components of feather microstructure contribute to structural plumage colour diversity in fairy-wrens. *Biological Journal of the Linnean Society*, 128(3), 550–568. <https://doi.org/10.1093/biolinnean/blz114>
- Guillerme, T. (2018). dispRity: A modular R package for measuring disparity. *Methods in Ecology and Evolution*, 9(7), 1755–1763. <https://doi.org/10.1111/2041-210X.13022>
- Guillerme, T., & Cooper, N. (2016). Effects of missing data on topological inference using a Total Evidence approach. *Molecular Phylogenetics and Evolution*, 94, 146–158. <https://doi.org/10.1016/j.ympev.2015.08.023>
- Hill, & McGraw, second. (2006). *Bird Coloration, Volume 1: Mechanisms and Measurements*. Harvard University Press. <https://www.hup.harvard.edu/catalog.php?isbn=9780674018938>
- Jetz, W., Thomas, G. H., Joy, J. B., Hartmann, K., & Mooers, A. O. (2012). The global diversity of birds in space and time. *Nature*, 491(7424), 444–448. <https://doi.org/10.1038/nature11631>
- Li, Q., Gao, K.-Q., Vinther, J., Shawkey, M. D., Clarke, J. A., D'Alba, L., Meng, Q., Briggs, D. E. G., & Prum, R. O. (2010). Plumage Color Patterns of an Extinct Dinosaur. *Science*, 327(5971), 1369–1372. <https://doi.org/10.1126/science.1186290>
- Maia, R., Gruson, H., Endler, J. A., & White, T. E. (2019). pavo 2: New tools for the spectral and spatial analysis of colour in r. *Methods in Ecology and Evolution*, 10(7), 1097–1107. <https://doi.org/10.1111/2041-210X.13174>
- Pagel, M., Meade, A., & Barker, D. (2004). Bayesian Estimation of Ancestral Character States on Phylogenies. *Systematic Biology*, 53(5), 673–684. <https://doi.org/10.1080/10635150490522232>
- Prum, R. O., Torres, R. H., Williamson, S., & Dyck, J. (1998). Coherent light scattering by blue feather barbs. *Nature*, 396(6706), 28–29. <https://doi.org/10.1038/23838>
- Prum, R. O. (2006). *Anatomy, physics, and evolution of avian structural colors* (Vol. 1, pp. 295–353). Harvard University Press.
- R Core Team. (2021). *R: A language and environment for statistical computing*. R Foundation for Statistical Computing, Vienna, Austria. <https://www.r-project.org/>
- Rueden, C. T., Schindelin, J., Hiner, M. C., DeZonia, B. E., Walter, A. E., Arena, E. T., & Eliceiri, K. W. (2017). ImageJ2: ImageJ for the next generation of scientific image data. *BMC Bioinformatics*, 18(1), 529. <https://doi.org/10.1186/s12859-017-1934-z>

- Saranathan, V., Forster, J. D., Noh, H., Liew, S.-F., Mochrie, S. G. J., Cao, H., Dufresne, E. R., & Prum, R. O. (2012). Structure and optical function of amorphous photonic nanostructures from avian feather barbs: A comparative small angle X-ray scattering (SAXS) analysis of 230 bird species. *Journal of The Royal Society Interface*, *9*(75), 2563–2580.
<https://doi.org/10.1098/rsif.2012.0191>
- Shawkey, M. D., & D’Alba, L. (2017). Interactions between colour-producing mechanisms and their effects on the integumentary colour palette. *Philosophical Transactions of the Royal Society B: Biological Sciences*, *372*(1724), 20160536. <https://doi.org/10.1098/rstb.2016.0536>
- Shawkey, M. D., Hauber, M. E., Estep, L. K., & Hill, G. E. (2006). Evolutionary transitions and mechanisms of matte and iridescent plumage coloration in grackles and allies (Icteridae). *Journal of The Royal Society Interface*, *3*(11), 777–786.
<https://doi.org/10.1098/rsif.2006.0131>
- Shawkey, M. D., & Hill, G. E. (2006). Significance of a basal melanin layer to production of non-iridescent structural plumage color: Evidence from an amelanotic Steller’s jay (*Cyanocitta stelleri*). *Journal of Experimental Biology*, *209*(7), 1245–1250.
<https://doi.org/10.1242/jeb.02115>
- Stoddard, M. C., & Prum, R. O. (2008). Evolution of Avian Plumage Color in a Tetrahedral Color Space: A Phylogenetic Analysis of New World Buntings. *The American Naturalist*, *171*(6), 755–776. <https://doi.org/10.1086/587526>
- Stoddard, M. C., & Prum, R. O. (2011). How colorful are birds? Evolution of the avian plumage color gamut. *Behavioral Ecology*, *22*(5), 1042–1052. <https://doi.org/10.1093/beheco/arr088>
- Troscianko, J., & Stevens, M. (2015). Image calibration and analysis toolbox – a free software suite for objectively measuring reflectance, colour and pattern. *Methods in Ecology and Evolution*, *6*(11), 1320–1331. <https://doi.org/10.1111/2041-210X.12439>

CHAPTER 4

The mechanistic basis of evolutionary transitions between grey, slate, and blue colour in Tanagers (Thraupidae)

4.1 Abstract

Both pigmentary and structural colours share many common elements of their feather anatomy, i.e. keratin, air and melanin packed in the melanosomes, despite utilizing different mechanisms of the colour production. This means that evolutionary transitions between pigmentary and structural colours can be achieved through a simple adjustment of these elements. Recently, an evolutionary hypothesis for the transition between pigmentary grey, through slate and finally to structural blue colour has been proposed and confirmed in the clade Tanagers on a macroevolutionary level (chapter three of this thesis). Here, we investigate mechanistic basis of this evolutionary pathway. By using SAXS (small-angle X-ray scattering) we have quantified important elements of spongy layer in medullary cells that is crucial for colour production by coherent scattering of light wavelengths. We have quantified five elements of the spongy layer: nanostructure complexity, average hard block thickness, average soft block thickness, filling fraction and I_0 value (Table 4.1.). We report that across different categories of feather colour, i.e. blue, slate and grey, nanostructure complexity, filling fraction and I_0 value explained variation in the chromatic component of the colour (between the three colour categories). Chromatic variation within the colour category was explained by filling fraction in the case of slate colour and by nanostructure complexity and average hard block thickness in the case of blue colour. We propose that variation in different elements or combination of elements of the spongy nanostructure has been utilised in feather colour evolution, both within and between colour categories, to overcome developmental constraints imposed by self-assembly processes.

4.2. Introduction

Birds are one of the most colourful groups of animals (Cuthill et al., 2017). The mechanisms by which they achieve their full colour gamut range from structural to pigmentary as well as the combination of both (Shawkey & D'Alba, 2017; Stoddard & Prum, 2011). The breadth of the plumage colour spectrum relies on the internal architecture of feathers (either variation in feather nanostructure and/or pigment composition) in both types of colour producing mechanisms (Prum, 2006; McGraw, 2006). Therefore, to understand the evolution of plumage colouration, it is critical to study the elements of feather nanostructure that participate in colour production (Maia et al., 2013).

Pigmentary colours are produced by selective absorption and reflection of certain wavelengths of light from the pigments deposited in feathers and the colour produced will depend on the chemical composition of the pigments themselves (McGraw, 2006). The most common pigments in birds' plumage are melanins (brown, grey and black colour) and carotenoids. In melanin-based plumage colouration, melanin is stored within melanosomes, which are organelles that produce, transport and store melanin pigment (Marks & Seabra, 2001; D'Alba & Shawkey, 2019). It has been shown that different melanosome shapes are characteristic of different melanin-based plumage colouration (Babarović et al., 2019; Li et al., 2010; Nordén et al., 2019). For example, grey plumage colouration has characteristic melanosomes that are larger than any other melanosomes in pigmentary melanin colouration (Babarović et al., 2019; Li et al., 2010). The concentration of melanosomes is also important for melanin-based pigmentary colours with increasing concentration contributing to darker colours (Field et al., 2013).

In structural colour, the colour is produced by coherent scattering of light as it interacts with the interface of nanoscale structures within the feathers, normally biopolymer (chitin and beta-keratin) and air that possess different refractive indices (Burg & Parnell, 2018; Prum, 2006). In iridescent structural colours in feathers, the colour producing nanostructure consists of a periodical arrangement of melanosomes embedded in keratin on the periphery of the feather barbules (Prum, 2006). Colours produced in this way are angle dependent (changing hue with the changing viewing angle) (Kinoshita et al., 2008; Nordén et al., 2021). In contrast, non-iridescent structural colours in feathers, are independent of viewing angle, and are often purple, blue and UV in hue (Prum, 2006; Fan et al., 2019). In these instances, the colours are produced by coherent scattering of light by the nanoscale arrangement of keratin and air in the medullary cells of feather barbs. A keratin matrix is placed above this nanostructure (towards the edge of the feather barbs) while a layer of melanosomes is located below it (i.e. towards the central shaft of feather barbs) (Fan et al., 2019; Prum, 2006; Shawkey et al., 2003; Shawkey & Hill, 2006). In addition, characteristics of the

melanosomes (size and shape) are also correlated with structural colours (Babarović et al., 2019; Li et al., 2010). For example, melanosomes found in non-iridescent structural colours are bigger than in most other colour categories and they overlap in shape with melanosomes characteristic for grey pigmentary colour (Babarović et al., 2019).

In non-iridescent structural colour production, keratin and air are structured in the medullary cells and this can be ordered in two possible ways to produce coherent scattering and ultimately colour production (Prum, 2006; Saranathan et al., 2012). Sphere type nanostructure consists of numerous spherical air cavities uniform in their length scale and interconnected by small air passages that are embedded in the keratin matrix. Channel type nanostructure consists of elongated and often rotated air channels embedded in a keratin matrix that creates keratin bars around them. In both nanostructure architectures, there is a periodicity between the two different refractive indices, with a length scale on the order of the wavelength of visible light which produces coherent scattering (Prum, 2006; Prum et al., 2009; Saranathan et al., 2012). In this type of scattering, colour is produced as a sum of the interactions among scattered waves (Prum et al., 1998). Variation in the physical parameters of the nanostructure, as well of the other components of the barb (the thickness of the keratin matrix as well as melanosomes layer), will influence the hue of the produced colour. Namely, uniformity of the diameter of keratin rods strongly predicts spectral saturation while chromatic variation is related to the spatial frequency and thickness of the spongy layer, the ratio of the amount of spongy layer to melanin and the thickness of keratin layer above the spongy layer (Fan et al., 2019; Shawkey et al. 2003). Therefore, colour variation in non-iridescent structural colours is not produced by absence or presence of any of these structural elements, but rather by the difference in their properties.

Despite the differences in colour production mechanisms, feathers exhibiting melanin-based pigmentary colours and structural colours in many cases have similar building materials, i.e. keratin and melanin packed in melanosomes (McGraw, 2006; Prum, 2006; Shawkey & D'Alba, 2017). This similarity in structural components has led to the hypothesis that evolutionary transitions between pigmentary and structural colours in birds' plumage can proceed through structural rearrangement of already pre-existing elements within the feathers, rather than evolution of a completely novel phenotype (Prum, 2006, Shawkey et al., 2006). This is referred to as 'evolutionary tinkering' to reflect the idea that modifications of an existing phenotype can lead to a novel phenotype (Bockaert & Pin, 1999; Jacob, 1977; Saraste & Castresana, 1994). This type of evolutionary transition has already been detected in birds' plumage (Shawkey et al., 2006; Driskell et al., 2010; Doucet et al., 2004). For example, evolutionary transitions between matte black plumage and iridescent plumage

colouration in grackles and allies depend on rearrangement of melanosomes (Shawkey et al., 2006). In feathers with matte black plumage, melanosomes are scattered evenly around barbules while in iridescent feathers melanosomes are arranged in layers near the edges of the barbules (Shawkey et al., 2006). This ordering of melanosomes creates interfaces with beta keratin and is responsible for coherent scattering and therefore colour production.

Recently, it has been proposed that grey (a pigmentary colour) and blue (a non-iridescent structural colour) are evolutionarily linked (Babarović et al., 2019). For a phylogenetically wide range of feathers, an investigation of the shape of the melanosomes placed underneath the spongy layer revealed that they overlap in shape with the melanosomes characteristic of grey pigmentary feathers (Babarović et al., 2019). Furthermore, rudimentary spongy nanostructure, whose colouration has been described as slate (grey-blue or blue-grey), was proposed to be an intermediary link between pigmentary grey and structural blue colour (Saranathan et al., 2012). Finally, in the chapter three of this thesis, a macroevolutionary transition between these colours has been confirmed in the Tanager clade (Aves: Thraupidae). In Tanagers, transitions between grey and slate were found to be common, but blue colour was found to evolve only from the slate colour. Nevertheless, a mechanical basis of these evolutionary transitions has not been tackled previously. Specifically, we do not know what structural elements of the spongy structure in feather barbs are changing to enable this transition.

Here, we investigated the nanostructural characteristics of elements of the medullary (or spongy) layer in blue, slate and grey feathers, i.e. air and keratin matrices, in Tanagers (Aves: Thraupidae). Our research is focused on the chromatic variation of the colour, i.e. hue and brightness, across blue, slate and grey colour categories. The Tanagers are large radiation of birds with a primarily Neotropical distribution and a diverse array of plumage colours including many species with blue, slate, and grey plumage colour. We used small angle x-ray scattering (SAXS) to assess several nanostructural elements of grey, slate and blue feathers in Tanagers to understand: i) what structural elements are responsible for the colour differences between these three colour categories? and ii) what structural elements account for colour variance within slate and blue colour categories?

4.3. Materials and methods

4.3.1. Feather sampling

We sampled feathers at the Zoological Museum, Natural History Museum of Denmark, University of Copenhagen. We sampled 10 species for grey feathers, 16 species for slate feathers and 11 species for blue feathers. Across all species, we sampled from following patches: wing covert, breast, nape, rump, throat, and mantle. We aimed at sampling one feather from three different bird skins from the same plumage patch. In total, 117 feather samples were collected (30 grey feathers, 48 slate and 33 blue feathers). (Full report on sampling details are in Appendix 3: Table S1). Feather sampling was designed to ensure coverage of a wide range of the grey, slate and blue colour gamut and was informed by analysis of colour categorization from written descriptions of plumage colouration from Birds of the World and digitally calibrated images of plumage colours in Tanagers (Babarovic, chapter three: Distinctiveness analysis) (Billerman et al., 2022).

4.3.2. Reflectance data

The reflectance of each collected feather was measured using an Ocean Optics USB2000+ spectrometer with UV transmissive fibre optic cable. A Y-shaped cable was connected to the light source, spectrometer and a third opening was mounted to the sample. The light source used was A DT-MINI-2-GS (Ocean Optics) Deuterium Tungsten Halogen UV-Vis-NIR light source with wavelength range from 215-2500 nm. The probe was placed 5 mm from the feather sample at 90 degrees to produce a small spot of light (~ 1 mm in diameter). To maximise the reflectance signal as much as possible, we populated the ~1 mm light spot with as many distal and coloured contour feather barbs as possible (~3 barbs). The measurements were acquired with the Spectra Suite (Ocean Optics) software with an integration time of 300 ns, 3 scans to average and 3 nm boxcar width. The collected reflectance spectra were then normalized by dividing the results by the spectra collected from a white standard (a Polytetrafluoroethylene (PTFE) diffuse white standard (Labsphere)) measured under the same instrumental conditions.

Spectral data were further analysed in R using the package “pavo” (version 2.7.1) (Maia et al., 2019; R Core Team, 2021). Spectra were first individually smoothed and then averaged on a species level (measurements from three feathers were averaged) with “Procspec” and “aggspec” functions, respectively. Next, we estimated the chromatic properties (hue and saturation) of the measured spectra by estimating avian cone catch values (u , s , m , l) associated with each spectrum using the “vismodel” function. The UVS avian visual system was used as the visual model since genomic

sequencing of the UV/violet SWS1 cone opsin gene indicated the presence of amino acid residues signifying UV sensitivity in Tanagers (Ödeen & Håstad, 2013).

4.3.3. Small Angle X-ray Scattering (SAXS)

SAXS data for the spongy layer in the medullary cells of the feather barbs were collected at the Diamond Light Source (UK) with the beamline I22. Historically, the internal structure of feathers has been investigated using different microscopy techniques, with Transmission Electron Microscopy (TEM) yielding most detailed results. Limitations, however, do exist with the TEM approach. Namely, artificial shrinkage of the samples during the sample preparation as well as time-consuming sample preparation. In contrast, SAXS requires no sample prep, beyond mounting the sample in the path of the beam. This allowed us to analyse 10s of intact feathers in a short period of time (Saranathan et al., 2012; Janas et al., 2020; Parnell et al., 2015).

SAXS was performed on the samples mounted over 3mm apertures on an aluminium sample plate perpendicular to the direction of the x-rays. Scattering of the photons occurs at interfaces in the biological material, here the electron density contrast produces a diffraction pattern that is detected by a 2-D detector. In the case of colour producing nanostructures in feather barbs, the diffraction pattern will take a circular form due to the isotropic nature of the structure. The data is reduced to a 1D scattering pattern by radially integrating the 2D detector image with I (intensity) on the y -axis and q (scattering vector) on the x -axis. Bright rings in the diffraction pattern will correspond to a peak in the 1D scattering profile. In samples which lack colour-producing nanostructure in the feather barb, the scattering plot will be featureless with no peaks detected (Saranathan et al., 2012; Prum et al., 1998). At Diamond, an x-ray wavelength of 1.2 Å (10 keV) was used with a rectangular shaped microfocus beam (20 µm x 20 µm) and a Pilatus P3-2M 2D detector placed at the 9.575 m from the sample. This setup allowed a length scale of 620 nm as an upper resolution.

We aimed to scan the same regions of the feather using SAXS as were measured for the spectrometer measurements. For each barb scanned (117 in total), either 121 or 49 individual 2D SAXS images were collected (frames) using a raster scan. For each measured frame a scattering profile with intensity (I) as a function of q (scattering wavevector $q=4\pi\sin\theta/\lambda$) was extracted with the DAWN software (Filik et al., 2017). Following this, for each feather, we calculated the sum value in intensity (I) for each scattering profile and selected the top 3 scattering profiles with the highest summed scattering intensities. This resulted in a total of 351 scattering profiles, i.e. three for each of the 117 feathers which were carried forward for 1) peak and shoulder detection analysis and 2) One-dimensional correlation function analysis (CORFUNC) (Strobl & Schneider, 1980). The analysis was

implemented in the custom python code, written by Dr Adam Washington, and modified for the purpose of this research by Dr Stephanie Burge.

4.4. Analysis

4.4.1. Principal component analysis

We transformed the reflectance spectra measurements into cone catch values (u , s , m and l) which estimate the chromatic properties of colour (hue and saturation), as birds see them (Stoddard & Prum, 2008). Cone catch values describe a point in the colourspace, a morphospace adjusted to ultraviolet-sensitive avian visual system (Ödeen & Håstad, 2013; Stoddard & Prum, 2008). Furthermore, we used Principal Component Analysis (PCA; Jolliffe, 2002) to reduce the dimensionality of the colourspace. Therefore, the principal components capture both elements of the chromatic variation (hue and saturation) of the measured colour.

4.4.2. Peak and shoulder detection analysis

Every SAXS profile of a feather containing nanostructure will contain 1) shoulders, 2) peaks or 3) both (explained further down) (Saranathan et al., 2012). If the nanostructure responsible for the structural colour is absent, the scattering intensity will decrease with increasing q (spatial frequency of variation in electron density) with no detectable features (Fig. 4.1, a). In the scattering patterns, a shoulder without any peaks represents a feather with a rudimentary spongy layer in the medullary cells of the feather barbs, this is a structure organized enough to produce coherent scattering and therefore structural colour, but not sufficiently monodisperse to generate a sharp peak (Fig. 4.1, b). In contrast, a peak in the scattering pattern represents a feather where the medullary cells in the feather barbs have short-range periodicity in the spongy layer and a more uniform length scale distribution resulting in a more well-defined scattering feature (Fig. 4.1, c). Furthermore, additional peaks and/or shoulders detected after the first peak demonstrates a long-range periodicity in the nanostructure not present in a nanostructure with just one peak/shoulder (Fig. 4.1, c-d). The number of higher order features corresponds to the number of elements following peak or a shoulder (more than one scattering feature) (Fig. 4.1, c-d). Any scattering pattern with just one peak or one peak and additional shoulders represents channel-type spongy layer (Fig. 4.1, c) while patterns with additional peaks after the first peak is representative of sphere-type nanostructure in the spongy layer (Fig. 4.1, d).

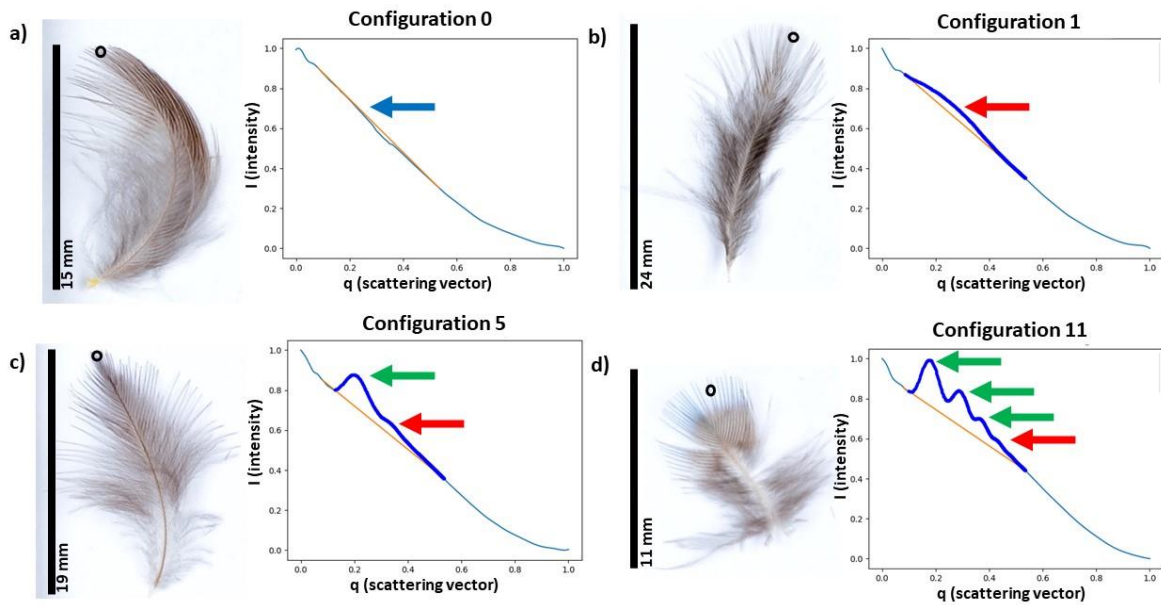


Figure 4.1. Examples of scattering profiles and feathers where the measurements were taken. On each panel first image represents the feather and second an accompanying scattering profile. For each panel, the SAXS measurement is taken on the spot marked with the black circle on the feather. Features describing nanostructure components in each scattering panel are marked with arrows: blue arrow represents lack of the scattering feature, red arrow represents shoulder, and green arrow represents peak. The figure is a visual representation of Table 4.2, and the classification of combinations of features is explained in the table. Scattering profiles of other possible configurations are represented in the Appendix 3: Figure S1. Panel (a) represents configuration 0, with a lack of any structural components. Feather where this scattering plot was obtained is from is the mantle of Double-collared seedeater (*Sporophila caerulescens*). Panel (b) represents configuration 1, with a one shoulder detected and is typical for the rudimentary form of the spongy nanostructure in the medullary feather cells. Feather where this scattering plot was obtained is from is the rump of Black-throated flowerpiercer (*Diglossa brunneiventris*). Panel (c) represents configuration 5, with a one peak and one shoulder detected and is typical for the channel-type spongy layer. Feather where this scattering plot was obtained is from is the rump of Masked flowerpiercer (*Diglossa cyanea*). Panel (d) represents configuration 11, with three peaks and one shoulder detected and is typical for the sphere-type spongy layer. Feather where this scattering plot was obtained is from is the breast of Blue dacnis (*Dacnis cayana*).

To detect and classify these features in the 351 scattering patterns, we developed code in Python to detect peaks and shoulders. Peaks were defined as a point where the derivative of the 1D curve was equal to 0 and the second derivative was negative (Stewart, 2005). In each instance that a peak was detected, a Gaussian curve was fitted to the local peak which returned the peak intensity (I_0), the

peak position (q_m), and the standard deviation or “width” (σ) of the peak (Additional table 4.; <https://figshare.com/s/1110fce894e65a69c329>) (Stewart, 2005). For shoulder detection, we used the “Kneedle” approach which searches for a point of maximum curvature in the function defined as a peak in a calculated detection function based on the sum of the vertical and perpendicular distance between the function and a straight line (Satopaa et al., 2011). When the algorithm detects a shoulder is it is characterized by a (l_o , q_m) value indicating this point of maximum curvature (Table S4.). The max l_o value of the first feature detected in the scattering plots where nanostructure is present is proportional to the thickness of the spongy layer in the medullary cell. The q_m position corresponds to the dominate lengthscale or spacing within the nanostructure calculated in as $2\pi/q_m$. We used l_o for the further analysis by choosing the value of the l_o for each species of the highest average values across 3 feathers (Appendix: Table S3.)

Examining our results, the possible scattering patterns across all the feathers had a limited number of peak and shoulder configurations. A scoring system for the scattering patterns was used to classify and sort these configurations as follows: i) peak is scored as 3, ii) shoulder after the peak is scored as 2, and iii) just a shoulder is scored as 1. The highest scoring nanostructure is 13 with three peaks and two shoulders (Fig. 4.1, d), while the lowest is zero with no nanostructure detected (Fig. 4.1, a). We termed this variable “nanostructure complexity” and used it for further analysis. Nanostructure complexity indicates a length-scale of periodicity with higher values indicating nanostructures with a longer range periodicity than smaller values. Due to our scoring system, some configurations are not possible, i.e. nanostructure scoring of 4, 7, 9 and 12. The scoring system, all possible configurations, and their meanings are reported in the Table 1 and Appendix 1: Figure S1. The representative of the main configuration and the feathers from which the measurements were taken are illustrated in the Fig. 4.1. The scores are reported in Appendix 3: Table S4. For species level score of the nanostructure, a highest score of the nanostructure among 9 frames from 3 feathers was taken (Additional table 4.; <https://figshare.com/s/1110fce894e65a69c329>).

4.4.3. One-dimensional correlation analysis

To extract length scale values of the nanostructure elements in the medullary cells spongy layer from the SAXS scattering profiles we used a one-dimensional correlation analysis known as CORFUNC (Strobl & Schneider, 1980). The foundation of this analysis is a Fourier transform of the 1-dimensional scattering profiles with the assumption that the system is a two-phase system of different electron densities. In our case this is keratin and air. The analysis involves extrapolating the low- q scattering data to a zero by fitting it to a Guinier curve and extrapolating the high- q scattering data to infinity using a Porod curve (Strobl & Schneider, 1980). The experimental data together with

the extrapolated data across the new q range (from zero to infinity) is then Fourier transformed and returns the real space correlation function for the feather specimen. Finally, a linear fit together with the position of the first minimum and first maximum of the correlation function is used to extract the length scales of elements of the medullary cells spongy layer based on a two-phase assumption.

Therefore, for further analysis, we have extracted the following values: 1. Average hard block thickness – a value of the average thickness of the keratin bar in the sample, 2. Average soft block thickness – a value of the average thickness of the air bubble (in sphere type nanostructure) or air channel (in channel type nanostructure) embedded in the keratin. 3. Long period – a distance between the midpoint of one keratin bar and the nearest neighbouring keratin bar. Long period is used to calculate average soft block thickness by subtracting average hard block thickness from it and to calculate filling fraction. 4. Filling fraction - is calculated by dividing average hard block thickness by long period. It is a value indicating the percent material in the region containing the nanostructure. All four of the variables extracted from the correlation analysis were averaged for each species (Appendix 3: Table S3.). The representation of the 3-D nanostructure and visual depiction of the variables is represented in the Fig. 4.2.

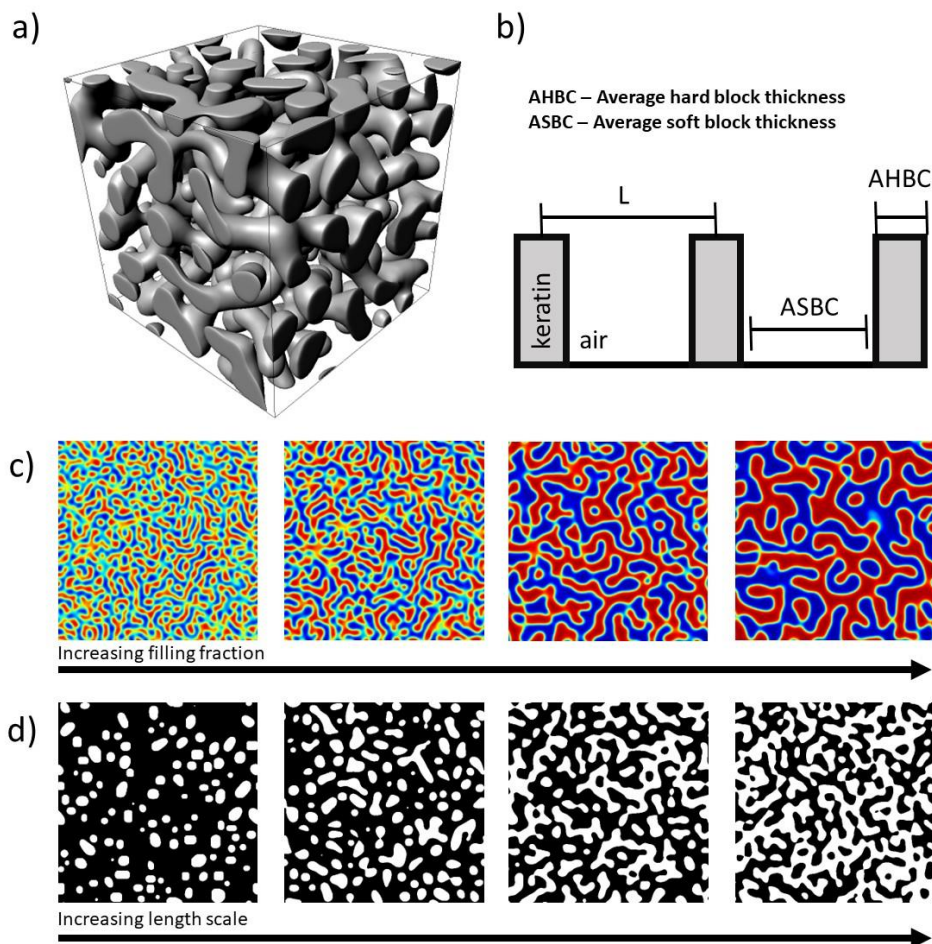


Figure 4.2. Visualization of the colour producing nanostructure and the variables extracted from the one-dimensional correlation analysis that describe its properties. Panel (a) shows a render of the channel-type nanostructure involved in the production of the colour blue. Keratin is shaded grey and unshaded area represents air. Panel (b) shows a 2-D representation of the 3-D keratin air and channel nanostructure. On the image, L stands for the long period, i.e. length between two keratin bars; ASBC is an average hard block thickness (keratin); ASBC is an average soft block thickness (air). Panel (c) is a representation of the filling fraction variable where red is the keratin and blue is the air. The length scales of the elements of the nanostructure do not change across the panels, but the percentage of the material filling the observed area does. Panel (d) is a representation of the increase in the length scale of the elements of the nanostructure. Black areas are keratin and white areas are air. Across the panels, an average length scale of these elements is increasing.

4.4.4. Phylogenetic Generalized Least Squares (PGLS)

We used Phylogenetic Generalized Least Squares (PGLS) for the three analyses described below (Grafen & Hamilton, 1989) as implemented in the R package caper (Orme et al., 2013). In all cases we used molecular phylogenies of Tanagers available from birdtree.org (Jetz et al., 2012), as a phylogenetic framework. We downloaded 1000 random trees and extracted the maximum clade credibility tree in R using the maxCladeCred function from the phangorn package (Schliep, 2011).

In the first analysis to test which variables predict colour variation across blue, slate and grey colour, we used a multipredictor model with PC1 (approximating chromatic variation of the feathers, i.e. hue and saturation) of all three colours as a response variable and variables approximating nanostructure as a predictor variable (nanostructure complexity, average soft block thickness, average hard block thickness, filling fraction, and I_0 (first scattering feature), summarized in Table 4.1. Since PC1 represents measurement of chromatic variation across all colour categories, with this analysis we will investigate which variables approximating nanostructure are important for the evolution of grey – slate – blue transition.

Variable	Calculation	Description	Analysis
Nanostructure complexity	For each peak and shoulder detected in the scattering patterns, a scoring system is employed and finally, all the scores are added to give a value of nanostructure complexity. (Scoring system is: i) peak is scored as 3, ii) shoulder after the peak is scored as 2, iii) just a shoulder is scored as 1, and iv) lack of any peaks and shoulders is scored as 0)	A value indicating a number of higher order features, i.e. features of the nanostructure showing periodicity on a level of a certain range. The nanostructure complexity goes from 0 (nanostructure is not detected) to 13 (nanostructure with the highest order features is present).	Peak and shoulder detection analysis
Long period	Calculated directly from the CORFUNC analysis as the location of the first maximum or 2x the location of the first minimum	A distance between the midpoint of one keratin bar and the neighbouring keratin bar.	One-dimensional correlation analysis
Average soft block thickness	Calculated by subtracting average hard block thickness from long period.	A value of the average thickness of the air bubble (in sphere type nanostructure) or air channel (in channel type nanostructure) embedded in the keratin.	One-dimensional correlation analysis
Average hard block thickness	Calculated directly from the CORFUNC analysis as the intersection of a linear fit to the initial decent with the tangent line to the first minimum	A value of the average thickness of the keratin bar in the sample.	One-dimensional correlation analysis
Filling fraction	Calculated by dividing average hard block thickness by long period.	A value indicating the percent material in the region containing the nanostructure	One-dimensional correlation analysis
l_0	Max l_0 value of the first feature detected (peak or shoulder) in the scattering plots where nanostructure is present	Value is proportional to the thickness of the spongy layer in the medullary cell	Peak and shoulder detection analysis

Table 4.1. Variables extracted from the Peak and shoulder detection analysis and One-dimensional correlation analysis of the Small-angle X-ray scattering experiment. For each variable (first column), a description of how the variable is calculated (second column), what part of the nanostructure it quantifies (third column) and which analysis is used to obtain the variable (fourth column) is listed.

Next, we used a multipredictor model in PGLS to test which elements of the nanostructure influences variation in the chromatic component of the colour within blue (second analysis) and slate colour category (third analysis) separately. For this analysis, we used variables approximating nanostructure as a predictor variable (nanostructure, average soft block thickness, average hard block thickness, filling fraction and I_0), and PC1 of a specific colour category as a response variable (i.e. PC1 of only blue colour and PC1 of only slate colour). With this analysis we wanted to explore what variables are affecting variation in individual colour and therefore are important for the evolution of hue and saturation (as approximated by PC1) within each colour category.

4.5. Results

4.5.1. Grey – slate – blue colour space

The first two principal components explained 97.5% of the variance in the raw cone-catch values: u, s, m, l of the measured feathers (Appendix 3: Table S2; Fig. 4.3, a-c) with PC1 explaining 79.1 % and PC2 explaining 18.2% of the variance respectively (Appendix 3: Table S4). Raw cone-catch values are obtained by transforming reflectance data measured by spectrometer (as outlined in the section 4.3.2. Reflectance data). Since PC1 explained a high percentage of the variance in the raw cone-catch value data, we decided to use PC1 as a variable explaining chromatic variation of colour in further analysis. PC1 is one variable representing both hue and saturation (chromatic variation) of a certain feather. Lower values of PC1 indicated greater stimulation of s and u cones (blue and UV colouration), while higher values of PC1 indicated greater stimulation of m and l cones (red and green colouration). PC1 therefore aligns well with a grey – slate – blue transition with grey colour data associated with the highest PC1 values, slate colour data in the middle, and blue colour associated with the lowest PC1 values (Fig. 4.3, d).

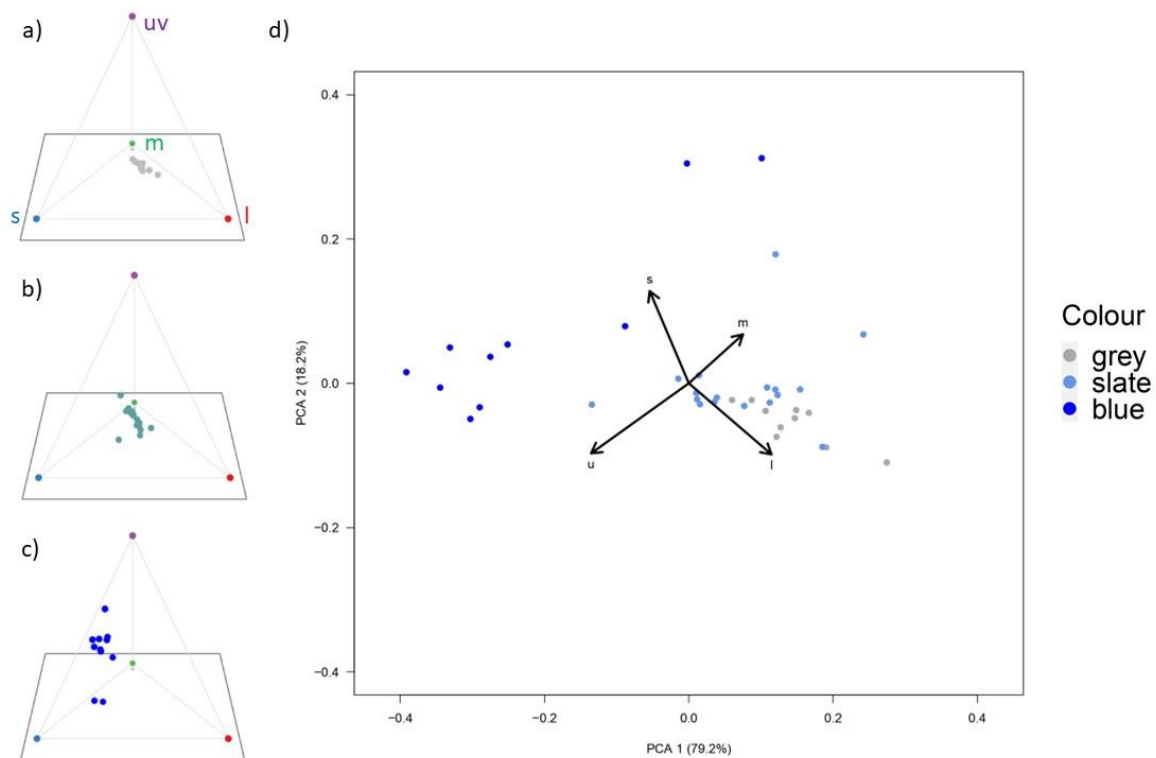


Figure 4.3. Panels a-c show the datapoints in avian tetrahedral colourspace for grey (a), slate (b) and blue (c) colour. The cone catch values describe every point in these 3 panels (u, s, m and l). Panel d shows principal components (PC) of cone catch values for all the feathers across all species. Each point in the plot represents one of the 38 feather samples measurements with point colour indicating which colour category a measurement belongs to (blue, slate or grey). PC1 explains the variation of colour scores. A higher PC1 value indicates a tendency toward m and l cone stimulations (grey colour in our case), while lower PC1 scores indicate a tendency towards blue and UV colour (blue in our case). Slate colour data points are roughly positioned between the data points for blue and grey colours.

4.5.2. Description of nanostructural elements of feathers

We analysed all scattering profiles with the python code to detect peaks and shoulders. We divided the scattering profiles into categories according to the level of nanostructure detected and named that variable nanostructure complexity. The nanostructure complexity ranges from 0 (nanostructure is not detected) to 13 (nanostructure with the highest order features is present). Scores of 4, 7, 9 and 12 are not possible. The entire list of feathers and their scoring systems is in Additional table 4. (<https://figshare.com/s/1110fce894e65a69c329>), while a summary is presented in Fig. 4.4 and Appendix 3: Table 1.

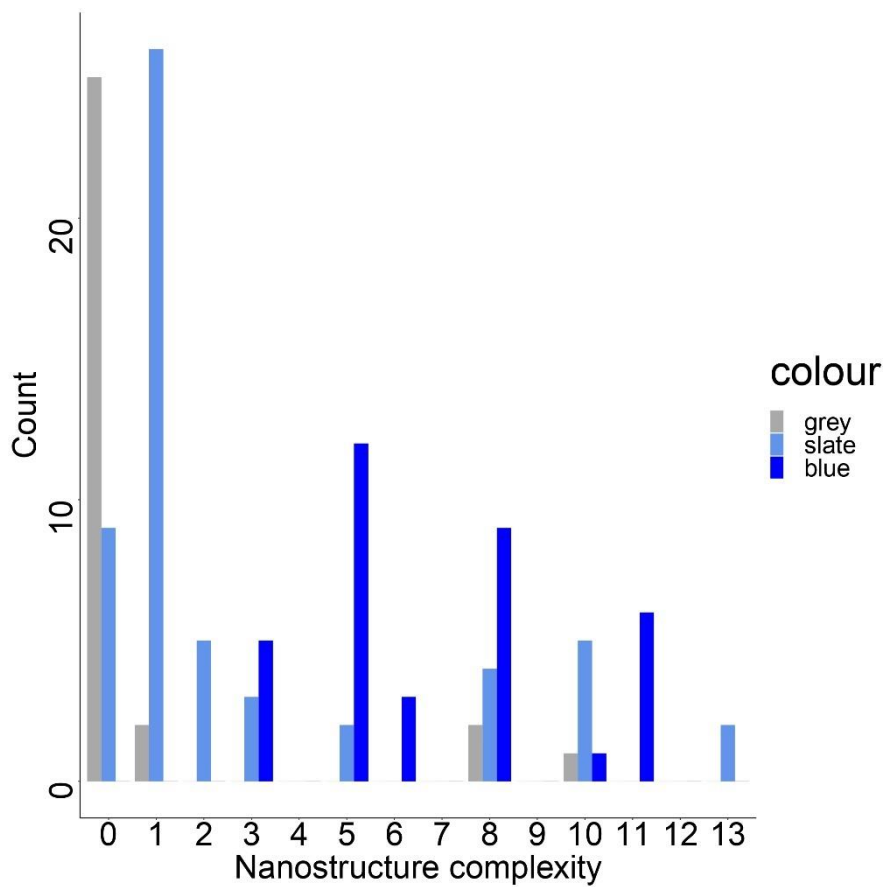


Figure 4.4. Histogram of the number of feathers (y axis) detected across all the feather samples for each category of nanostructure complexity variable (x axis). In short, every species was sampled with 3 feathers, and we analysed 3 frames per each feather, making 117 feathers in total with 351 frames. Here, a feather was counted in certain nanostructure complexity category if at least one of the frames was detected belonging to that category. Feathers that did not have all three frames belonging to a same category are: *Chlorophanes spiza* (605), *Anisognathus igiventris* (608), *Pipraeidea melanoto* (612, 614), *Thraupis episcopus* (538), *Diglossa sittoides* (574), *Diglossa caerulescens* (577, 579), *Conirostrum cinerum* (590). In the brackets, a feather number as indicated in the Additional table 4 (<https://figshare.com/s/1110fce894e65a69c329>).

Nanostructure complexity	Elements detected	Biological meaning	Grey colour	Slate colour	Blue colour
0	0 peaks, 0 shoulders	No Nanostructure	25 feathers from 9 species	8 feathers from 4 species	0 feathers
1	0 peaks, 1 shoulder	Rudimentary nanostructure	2 feathers from 1 species	26 feathers from 13 species	0 feathers
2	0 peaks, 2 shoulders		0 feathers	5 feathers from 2 species	
3	1 peak	Channel-type nanostructure	0 feathers	3 feathers from 1 species	5 feathers from 2 species
4	Not possible				
5	1 peak, 1 shoulder		0 feathers	2 feathers from 1 species	12 feathers from 5 species
6	2 peaks	Sphere-type nanostructure	0 feathers	0 feathers	3 feathers from 2 species
7	Not possible		0 feathers	0 feathers	
8	2 peaks, 1 shoulder		2 feathers from 1 species	4 feathers from 3 species	9 feathers from 4 species
9	Not possible				
10	2 peaks, 2 shoulders		1 feather from 1 species	5 feathers from 3 species	1 feather from 1 species
11	3 peaks, 1 shoulder		0 feathers	0 feathers	6 feathers from 2 species
12	Not possible				
13	3 peaks, 2 shoulders	0 feathers	2 feathers from 1 species	0 feathers	

Table 4.2. Overview of the nanostructure complexity variable. The first column lists all the possible values of the variable. Column two shows absence (first row) and presence (the rest of the rows) and the count of structural elements for each score of the nanostructure complexity. Values of the nanostructure complexity are calculated by addition of the scores associated with each structural elements detected for each category. Scoring system is as follows: i) peak is scored as 3, ii) shoulder after the peak is scored as 2, and iii) just a shoulder is scored as 1. Column three shows the biological meaning of every score of nanostructure complexity. In short, score 0 indicates no nanostructure detected, scores 1 – 2 indicate rudimentary nanostructure, scores 3 – 5 show channel-type nanostructure and finally, scores 6 – 13 indicate sphere-type nanostructure. Columns four, five and six show the number of feathers and species where each nanostructure complexity score was detected across grey, slate and blue colour category.

4.5.3. Phylogenetic generalised least square (PGLS) analysis results

The overview of the results is presented in the Fig. 4.5. Fig. 4.6-4.7 represent the effects of variables that showed significant correlation with colour variables. The full details of the analysis (p -values, parameter estimates and R^2 values) are reported in the Appendix 3: Table S4.

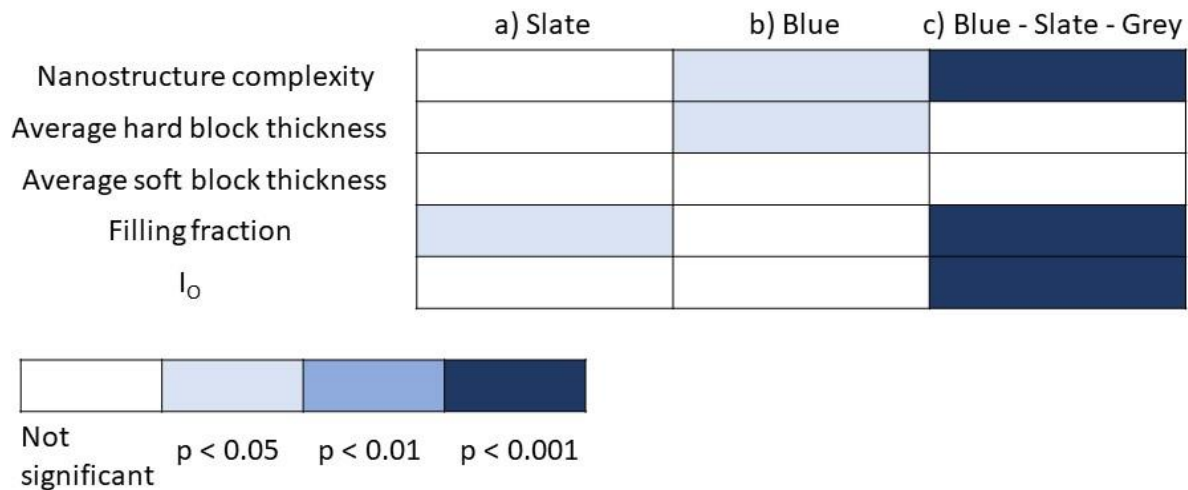


Figure 4.5. Multipredictor model results summary. All three panels represent values of PC1, with the panel a representing value only for slate colour, panel b only for the blue colour, and panel c representing combined values for grey, slate, and blue colour. Predictor variables are represented as rows with their names indicated further left. The colour of the squares represents the significance of the results, as indicated by the figure legend in the bottom left corner.

In the first analysis (Fig. 4.5, c), we used multipredictor PGLS analysis to assess which feather nanostructure variables correlated with the variation in the chromatic component of colour between colour categories as approximated by PC1. Nanostructure complexity ($p = 0.0008953$; slope = $2.9624e-02$ (+/- $7.9681e-03$)), filling fraction ($p = 4.45E-08$; slope = $-2.9664e+00$ (+/- $4.8490e-01$)) and I_0 ($p = 0.0005619$; slope = $-1.9381e-06$ (+/- $5.0592e-07$)) showed significant association with the variation of the PC1 variable (Fig. 4.6, a–c). PC1 declines with increasing nanostructure complexity, filling fraction, and I_0 .

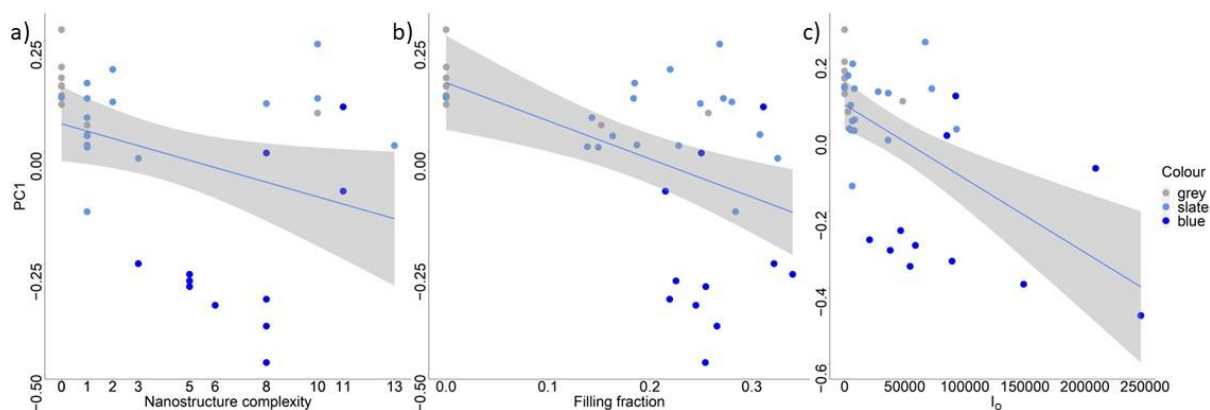


Figure 4.6. Predictors of PC1 for blue-slate-grey colour variation: a) nanostructure complexity, b) filling fraction, and c) I_0 . Within each panel, each point represents a species, and the colour of each point represents the colour category a measurement belongs to.

In the following analysis, we analysed slate and blue colour separately (i.e. in the analysis of slate colour, we analysed PC1 for only slate colour and in the analysis of blue colour, we analysed PC1 values for only blue colour as a response variable) (Fig. 4.5, a-b). For the slate colour analysis (Fig. 4.5, a; Fig. 4.7, a), only filling fraction ($p = 0.01399$, slope = $-1.3408e+00$ ($\pm 4.8115e-01$)) had a significant relationship with variation in PC1 (Fig. 4.7, a; Appendix 3: Table S4, a). For a decrease in the value of PC1, there was an increase in the filling fraction value. For the blue colour analysis (Fig. 4.5, b), nanostructure complexity ($p = 0.02315$; slope = $4.0498e-02$ ($\pm 1.6217e-02$)) and average hard block thickness ($p = 0.01042$; slope = $4.7362e-03$ ($\pm 3.3676e-03$)) had a significant association with variation in PC1 (Fig. 4.7, b – c; Appendix 3: Table S4, b). For an increase in the value of PC1, an increase in values of nanostructure complexity and average hard block thickness was detected.

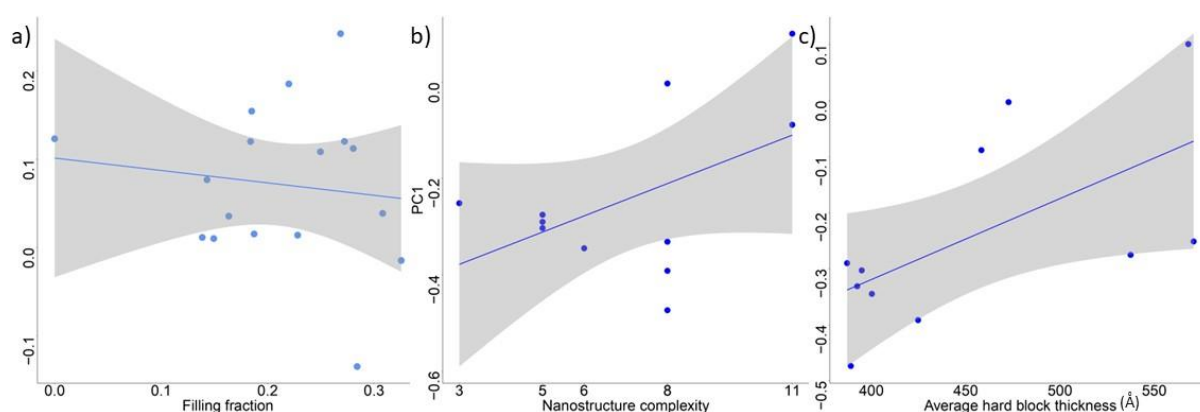


Figure 4.7. Predictors of PC1 for slate colour (a) and blue colour (b, c). Within each panel, each point represents a species. The predictor of slate colour PC1 variation is filling fraction (a), while predictors for PC1 of blue colour are nanostructure complexity (b) and average hard block thickness (c).

Overall, explanatory power (R^2) was greatest for model explaining variation in blue colour, followed by all three colours combined (blue-slate-grey) and finally model involving only slate colour had the lowest explanatory power (Appendix 3: Table S4).

4.6. Discussion

We analysed the spongy structure of medullary keratinocytes in feather barbs from three broad colour groups (blue, slate and grey) to assess the mechanisms underpinning colour evolution from pigmentary grey to structural blue as well as variation within colour classes along this continuum. To do this we first quantified the absence or presence of nanostructure and classified the level of nanostructure present. We then quantified length scales and properties of the colour producing nanostructure, i.e. average hard block thickness, average soft block thickness, filling fraction and l_o .

Correlates of variation in chromatic component of colour encompassing all three colour categories included nanostructure complexity, filling fraction and l_o , while average hard block thickness and average soft block thickness showed no significant association. This indicates that it is the ratio of keratin to air that is more important than variation in keratin thickness for colour variation. However, patterns across the colours do not translate to within-colour categories correlates, i.e. those for blue and slate colour individually. PC1 values for blue colour were correlated with nanostructure level and average hard block thickness, while slate colour PC1 showed correlation with the filling fraction. This pattern shows that while multiple components of variability in medullary cells spongy layer are needed for evolutionary transitions between blue, slate and grey occur, a more limited number of variables account for the variation in chromatic component of colour within the colour categories themselves.

Evolutionary transitions from pigmentary to structural colour have previously been detected in birds' plumage (Shawkey et al., 2006; Driskell et al., 2010; Doucet et al., 2004). Our results indicate that for the transition from pigmentary grey towards structural blue colour, multiple variables describing spongy layer are important. l_o (thickness of the spongy layer), filling fraction and degree of order (nanostructure complexity) all increase as colour tends towards blue (PC1 decreases). Separately, for both blue and slate colour, the l_o (thickness of the spongy layer) does not show a correlation with PC1. This could indicate that there might be a critical length scale of the nanostructure that is important for the evolutionary transition from grey to blue to happen. Increasing thickness of the spongy layer (correlated with the increase in l_o) will result in greater reflectance across the short-wavelength range, i.e. blue and UV (Fan et al., 2019). Filling fraction is a measure of what volume fraction is occupied or filled by the biopolymer (keratin). To produce white colour in some species of

beetles, it has been proposed that a filling fraction of 31 – 34 % is responsible for the colour production, while simulated results indicate a theoretical maximum reflectance from a spongy nanostructure at 25% (Burg et al., 2019). This is observed in our results as well, i.e. increase in filling fraction from 0 (for *Sporophila caerulescens* grey feather) through 0.1386 (13.86% for *Catemina analis* slate rump feather) to 0.34012 (34.012% for *Diglossa cayana* blue rump feather) is observed with decreasing PC1 (moving towards blue colour in the colour space). This result further confirms nanostructural resemblance in spongy structure between blue and white colour in bird's feathers as previously observed in amelanotic Steller's jay (*Cyanocitta stelleri*) and in swallow tanager (*Tersina viridis*) (Bazzano et al., 2021; Shawkey & Hill, 2006). In both cases, white and blue feathers have similar peak in reflectance in blue part of the spectrum, but the pronunciation of the peak in blue feathers is due to the underlying melanin layer which is lacking in white feathers. Finally, the value of nanostructural complexity showed an increase with decreasing PC1 values, and this could indicate that blue colour is associated with structural uniformity and increased order of the nanostructures. Overall, changes in many variables explaining spongy barb nanostructure have proven to be important for the evolution of grey-slate-blue continuum in the colour space.

Previous research into changes in nanostructural parameters between different hues of non-iridescent structural colour revealed that variation in many nanostructural elements, rather than a change in single parameter, is responsible for observed colour diversity (Fan et al., 2019). These parameters involve the thickness of the outer layer of keratin (above colour producing nanostructure), spatial frequency and thickness of the keratin and air matrix, as well as the amount of melanin beneath the colour producing nanostructure. Our results are focused only on the blue colour and show that two main components for colour production are nanostructure complexity and hard block thickness (Fig. 4.5, b; Fig. 4.7, b-c). The increase in PC1 follows increasing hard block thickness indicating that thicker keratin bars in either channel or sphere type spongy layer would shift away from blue and UV cone stimulations. Increases in the level of nanostructure also follow the same trend. Surprisingly, we did not find a thickness of the spongy layer as a correlate of PC1 of the colour blue as opposed to the previous research (Fan et al., 2019). This could be explained by the absence of other structural colours from our dataset, namely purple. Thicker spongy layer would increase reflectance in the short wavelengths (Fan et al., 2019), meaning that the spongy structure length scale could be correlated if we had a broader range of structural colours within our dataset. Nevertheless, this variable proved to be important for the transition into blue colour from slate (as showed by our results).

In previous research on the nanostructure of slate colour it has been identified that this colour category is characterised by more rudimentary and highly disordered versions of the channel and sphere type nanostructures that are found in the blue feathers (Saranathan et al., 2012). Nevertheless, it seems that these feathers still have nanostructure ordered enough to produce colour by coherent scattering. The only variable that correlates with PC1 for slate colour is filling fraction where higher values of filling fraction are associated with lower values of PC1 for slate colour. Within slate colour category, higher values of filling fraction correlate with the lower PC1 values showing more inclinations toward colour blue (i.e. blue and UV cone stimulation). As explained previously, filling fraction is the value that indicates the filling of the volume of the crystalline structure with its constituent elements, i.e. keratin in our case. Increasing filling fraction has been shown to be important in evolution of colour blue (this research) while it is not important for a hue variation within blue colour category. A limitation of our research is not knowing the location of melanosomes within the feathers. It is known from literature that coherent scattering that produces blue colour can be masked by melanin deposition and in that case the feather is black (Doucet et al., 2004; Driskell et al., 2010). Whether this rudimentary spongy layer detected in the slate feathers has a melanosome deposition above it that participate in the colour production by interfering with the colour produced from the spongy layer is yet to be seen. Nevertheless, the fact that variation in PC1 for slate colour correlates with filling fraction indicates that the spongy layer is ordered enough to participate in colour production (giving the slight blue of the slate colour).

Our results suggest that the parameters of spongy structure that influence colour variation between colour categories (blue-slate-grey) differ from parameters that influence colour variation within colour categories (blue and slate). Structural colours are intrinsically linked to their underlying nanostructure (Prum, 2006). It has been shown that small changes in their nanostructures will lead to a change in the colour produced and, therefore, the signal emitted in the environment (Fan et al., 2019; Saranathan et al., 2012). Development of the spongy structure is proceeding without active cellular processes, i.e. by phase separation of the mixture of keratin and air in the medullary cells (Prum et al., 2009). These self-guided processes could theoretically lead to complete unmixing of the solution and loss of nanostructure arrangement necessary for colour production (Jones, 2002; Prum et al., 2009). It is still debated what causes halts in the phase separation during feather growth (and colour production), but it is known that these physical processes are deterministic, and there is little opportunity for a variation in the outcome of the development once the process is initiated (Jones, 2002; Prum et al., 2009). Our results indicate that the inherent issue with the phase separation (its deterministic nature) and control over the variation in hue within and between colour categories could be overcome by varying different elements (slate colour results) or combinations of elements

(blue-slate-grey and blue colour results) of spongy structure in medullary cells. The variation in multiple elements of the nanostructure rather than binary presence/absence scheme for productions of different hues has been already confirmed for non-iridescent structural colours (Fan et al., 2019). It seems that similar processes are involved in their evolution and here we propose that this is a natural consequence of utilizing basic physical processes during feather development.

4.7. References

- Babarović, F., Puttick, M. N., Zaher, M., Learmonth, E., Gallimore, E.-J., Smithwick, F. M., Mayr, G., & Vinther, J. (2019). Characterization of melanosomes involved in the production of non-iridescent structural feather colours and their detection in the fossil record. *Journal of The Royal Society Interface*, *16*(155), 20180921. <https://doi.org/10.1098/rsif.2018.0921>
- Bazzano, L. T., Mendicino, L. R., Inchaussandague, M. E., Skigin, D. C., García, N. C., Tubaro, P. L., & Barreira, A. S. (2021). Mechanisms involved in the production of differently colored feathers in the structurally colored swallow tanager (*Tersina viridis*; Aves: Thraupidae). *Journal of Experimental Zoology Part B: Molecular and Developmental Evolution*, *336*(5), 404–416. <https://doi.org/10.1002/jez.b.23043>
- Billerman, S. M., Keeney, B. K., Rodewal, P. G., and Schulenberg, T. S. (2022). *Birds of the World*. Cornell Laboratory of Ornithology, Ithaca, NY, USA. <https://birdsoftheworld.org/bow/home>
- Bockaert, J., & Pin, J. P. (1999). Molecular tinkering of G protein-coupled receptors: An evolutionary success. *The EMBO Journal*, *18*(7), 1723–1729. <https://doi.org/10.1093/emboj/18.7.1723>
- Burg, S. L., & Parnell, A. J. (2018). Self-assembling structural colour in nature. *Journal of Physics. Condensed Matter: An Institute of Physics Journal*, *30*(41), 413001. <https://doi.org/10.1088/1361-648X/aadc95>
- Burg, S. L., Washington, A., Coles, D. M., Bianco, A., McLoughlin, D., Mykhaylyk, O. O., Villanova, J., Dennison, A. J. C., Hill, C. J., Vukusic, P., Doak, S., Martin, S. J., Hutchings, M., Parnell, S. R., Vasilev, C., Clarke, N., Ryan, A. J., Furnass, W., Croucher, M., ... Parnell, A. J. (2019). Liquid–liquid phase separation morphologies in ultra-white beetle scales and a synthetic equivalent. *Communications Chemistry*, *2*(1), Article 1. <https://doi.org/10.1038/s42004-019-0202-8>
- Cuthill, I. C., Allen, W. L., Arbuckle, K., Caspers, B., Chaplin, G., Hauber, M. E., Hill, G. E., Jablonski, N. G., Jiggins, C. D., & Kelber, A. (2017). The biology of color. *Science*, *357*(6350), eaan0221.
- D’Alba, L., & Shawkey, M. D. (2019). Melanosomes: Biogenesis, Properties, and Evolution of an Ancient Organelle. *Physiological Reviews*, *99*(1), 1–19. <https://doi.org/10.1152/physrev.00059.2017>
- Doucet, S. M., Shawkey, M. D., Rathburn, M. K., Mays, H. L., & Montgomerie, R. (2004). Concordant evolution of plumage colour, feather microstructure and a melanocortin receptor gene

- between mainland and island populations of a fairy-wren. *Proceedings of the Royal Society of London. Series B: Biological Sciences*, 271(1549), 1663–1670.
<https://doi.org/10.1098/rspb.2004.2779>
- Driskell, A. C., Prum R. O., & Pruett-Jones, S. (2010). The evolution of black plumage from blue in Australian fairy-wrens (Maluridae): Genetic and structural evidence. *Journal of Avian Biology*, 41(5). <https://onlinelibrary.wiley.com/doi/full/10.1111/j.1600-048X.2009.04823.x>
- Fan, M., D'alba, L., Shawkey, M. D., Peters, A., & Delhey, K. (2019). Multiple components of feather microstructure contribute to structural plumage colour diversity in fairy-wrens. *Biological Journal of the Linnean Society*, 128(3), 550–568. <https://doi.org/10.1093/biolinnean/blz114>
- Field, D. J., D'Alba, L., Vinther, J., Webb, S. M., Gearty, W., & Shawkey, M. D. (2013). Melanin Concentration Gradients in Modern and Fossil Feathers. *PLOS ONE*, 8(3), e59451.
<https://doi.org/10.1371/journal.pone.0059451>
- Filik, J., Ashton, A. W., Chang, P. C. Y., Chater, P. A., Day, S. J., Drakopoulos, M., Gerring, M. W., Hart, M. L., Magdysyuk, O. V., Michalik, S., Smith, A., Tang, C. C., Terrill, N. J., Wharmby, M. T., & Wilhelm, H. (2017). Processing two-dimensional X-ray diffraction and small-angle scattering data in DAWN 2. *Journal of Applied Crystallography*, 50(Pt 3), 959–966.
<https://doi.org/10.1107/S1600576717004708>
- Grafen, A., & Hamilton, W. D. (1989). The phylogenetic regression. *Philosophical Transactions of the Royal Society of London. B, Biological Sciences*, 326(1233), 119–157.
<https://doi.org/10.1098/rstb.1989.0106>
- Jacob, F. (1977). Evolution and Tinkering. *Science*, 196(4295), 1161–1166.
<https://doi.org/10.1126/science.860134>
- Janas, K., Łatkiewicz, A., Parnell, A., Lutyk, D., Barczyk, J., Shawkey, M. D., Gustafsson, L., Cichoń, M., & Drobnik, S. M. (2020). Differential effects of early growth conditions on colour-producing nanostructures revealed through small angle X-ray scattering and electron microscopy. *Journal of Experimental Biology*, 223(18), jeb228387. <https://doi.org/10.1242/jeb.228387>
- Jetz, W., Thomas, G. H., Joy, J. B., Hartmann, K., & Mooers, A. O. (2012). The global diversity of birds in space and time. *Nature*, 491(7424), 444–448. <https://doi.org/10.1038/nature11631>
- Jolliffe, I. T. (2002). *Principal Component Analysis* (2nd ed.). Springer-Verlag.
<https://doi.org/10.1007/b98835>
- Jones, R. A. L. (2002). Soft Condensed Matter. *European Journal of Physics*, 23(6), 652–652.
<https://doi.org/10.1088/0143-0807/23/6/703>
- Kinoshita, S., Yoshioka, S., & Miyazaki, J. (2008). Physics of structural colors. *Reports on Progress in Physics*, 71(7), 076401. <https://doi.org/10.1088/0034-4885/71/7/076401>

- Li, Q., Gao, K.-Q., Vinther, J., Shawkey, M. D., Clarke, J. A., D'Alba, L., Meng, Q., Briggs, D. E. G., & Prum, R. O. (2010). Plumage Color Patterns of an Extinct Dinosaur. *Science*, *327*(5971), 1369–1372. <https://doi.org/10.1126/science.1186290>
- Maia, R., Gruson, H., Endler, J. A., & White, T. E. (2019). pavo 2: New tools for the spectral and spatial analysis of colour in R. *Methods in Ecology and Evolution*, *10*(7), 1097–1107. <https://doi.org/10.1111/2041-210X.13174>
- Maia, R., Rubenstein, D. R., & Shawkey, M. D. (2013). Key ornamental innovations facilitate diversification in an avian radiation. *Proceedings of the National Academy of Sciences*, *110*(26), 10687–10692. <https://doi.org/10.1073/pnas.1220784110>
- Marks, M. S., & Seabra, M. C. (2001). The melanosome: Membrane dynamics in black and white. *Nature Reviews Molecular Cell Biology*, *2*(10), Article 10. <https://doi.org/10.1038/35096009>
- McGraw, K. J. (2006a). Carotenoid-Based Coloration. *Bird Coloration, Volume 1: Mechanisms and Measurements*, *1*, 177.
- McGraw, K. J. (2006b). Mechanics of melanin-based coloration. *Bird Coloration*, *1*, 243–294.
- Nordén, K. K., Eliason, C. M., & Stoddard, M. C. (2021). Evolution of brilliant iridescent feather nanostructures. *eLife*, *10*, e711179. <https://doi.org/10.7554/eLife.71179>
- Nordén, K. K., Faber, J. W., Babarović, F., Stubbs, T. L., Selly, T., Schiffbauer, J. D., Peharec Štefanić, P., Mayr, G., Smithwick, F. M., & Vinther, J. (2019). Melanosome diversity and convergence in the evolution of iridescent avian feathers—Implications for paleocolor reconstruction. *Evolution*, *73*(1), 15–27.
- Ödeen, A., & Håstad, O. (2013). The phylogenetic distribution of ultraviolet sensitivity in birds. *BMC Evolutionary Biology*, *13*(1), 36. <https://doi.org/10.1186/1471-2148-13-36>
- Orme, D., Freckleton, R. P., Thomas, G. H., Petzoldt, T., Fritz, S. A., & Isaac, N. (2013). CAPER: Comparative analyses of phylogenetics and evolution in R. *Methods in Ecology and Evolution*, *3*, 145–151.
- Parnell, A., Washington, A., Mykhaylyk, O., Hill, C., Bianco, A., Burg, S., Dennison, A., Snape, M., Cadby, A., Smith, A., Prévost, S., Whittaker, D., Jones, R., Patrick, J., Fairclough, P., & Parker, A. (2015). Spatially modulated structural colour in bird feathers. *Scientific Reports*, *5*. <https://doi.org/10.1038/srep18317>
- Prum, R. O. (2006). *Anatomy, physics, and evolution of avian structural colors* (Vol. 1, pp. 295–353). Harvard University Press.
- Prum, R. O., Dufresne, E. R., Quinn, T., & Waters, K. (2009). Development of colour-producing β -keratin nanostructures in avian feather barbs. *Journal of The Royal Society Interface*, *6*(suppl_2), S253–S265. <https://doi.org/10.1098/rsif.2008.0466.focus>

- Prum, R. O., Torres, R. H., Williamson, S., & Dyck, J. (1998). Coherent light scattering by blue feather barbs. *Nature*, *396*(6706), 28–29. <https://doi.org/10.1038/23838>
- R Core Team. (2021). *R: A language and environment for statistical computing*. R Foundation for Statistical Computing, Vienna, Austria. <https://www.r-project.org/>
- Saranathan, V., Forster, J. D., Noh, H., Liew, S.-F., Mochrie, S. G. J., Cao, H., Dufresne, E. R., & Prum, R. O. (2012). Structure and optical function of amorphous photonic nanostructures from avian feather barbs: A comparative small angle X-ray scattering (SAXS) analysis of 230 bird species. *Journal of The Royal Society Interface*, *9*(75), 2563–2580. <https://doi.org/10.1098/rsif.2012.0191>
- Saraste, M., & Castresana, J. (1994). Cytochrome oxidase evolved by tinkering with denitrification enzymes. *FEBS Letters*, *341*(1), 1–4. [https://doi.org/10.1016/0014-5793\(94\)80228-9](https://doi.org/10.1016/0014-5793(94)80228-9)
- Schliep, K. P. (2011). phangorn: Phylogenetic analysis in R. *Bioinformatics*, *27*(4), 592–593. <https://doi.org/10.1093/bioinformatics/btq706>
- Shawkey, M. D., & D’Alba, L. (2017). Interactions between colour-producing mechanisms and their effects on the integumentary colour palette. *Philosophical Transactions of the Royal Society B: Biological Sciences*, *372*(1724), 20160536. <https://doi.org/10.1098/rstb.2016.0536>
- Shawkey, M. D., Estes, A. M., Siefferman, L. M., & Hill, G. E. (2003). Nanostructure predicts intraspecific variation in ultraviolet-blue plumage colour. *Proceedings of the Royal Society B: Biological Sciences*, *270*(1523), 1455–1460. <https://doi.org/10.1098/rspb.2003.2390>
- Shawkey, M. D., Hauber, M. E., Estep, L. K., & Hill, G. E. (2006). Evolutionary transitions and mechanisms of matte and iridescent plumage coloration in grackles and allies (Icteridae). *Journal of The Royal Society Interface*, *3*(11), 777–786. <https://doi.org/10.1098/rsif.2006.0131>
- Shawkey, M. D., & Hill, G. E. (2006). Significance of a basal melanin layer to production of non-iridescent structural plumage color: Evidence from an amelanotic Steller’s jay (*Cyanocitta stelleri*). *Journal of Experimental Biology*, *209*(7), 1245–1250. <https://doi.org/10.1242/jeb.02115>
- Stewart, J. (2005). *Multivariable Calculus: Concepts and Contexts*. Brooks/Cole.
- Stoddard, M. C., & Prum, R. O. (2008). Evolution of Avian Plumage Color in a Tetrahedral Color Space: A Phylogenetic Analysis of New World Buntings. *The American Naturalist*, *171*(6), 755–776. <https://doi.org/10.1086/587526>
- Stoddard, M. C., & Prum, R. O. (2011). How colorful are birds? Evolution of the avian plumage color gamut. *Behavioral Ecology*, *22*(5), 1042–1052. <https://doi.org/10.1093/beheco/arr088>

Strobl, G. R., & Schneider, M. (1980). Direct evaluation of the electron density correlation function of partially crystalline polymers. *Journal of Polymer Science: Polymer Physics Edition*, *18*(6), 1343–1359. <https://doi.org/10.1002/pol.1980.180180614>

CHAPTER 5

Discussion

5.1. General overview of the aims of this thesis

In this thesis I aimed to cast new light on our understanding of the evolutionary patterns and mechanisms that drive the diversity of plumage colour in birds. I did this by asking two clade-specific questions. In the first part of the thesis, I asked, “What shapes plumage colouration in the clade Coraciiformes?”. I placed this chapter within the broader context of investigating drivers of plumage colouration, or simply – “why?” plumage colour evolves. In the second and third parts of the thesis, I asked, “Did blue colour evolve from grey colour via an intermediate colour (slate) in the clade Thraupidae?”. This question aimed to tackle the evolutionary pathway and mechanisms by which plumage colour evolves, or simply – “how?” plumage colour evolves.

Answers to “why?” and “how?” questions in my thesis rely on idiosyncrasy, i.e. detailed work on a single clade, and they both benefit and suffer from it. The second chapter of this thesis gave a detailed account of the plumage colour evolution in Coraciiformes and all the answers reached in this chapter are applicable for Coraciiformes and come from the specificities of their ecology and behaviour. Nevertheless, I think the patterns observed could be translated to other bird species to some extent. For example, I suspect that a white and brown (beige) belly is a convergent trait in birds that hunt prey that's "below them" – i.e. water diving and ground-dwelling hunting strategies. More importantly, my research brought up front the importance of light in the environment on the plumage colour evolution. Accounts of previous correlations of plumage colour with the light environment have been tested and confirmed. However, my research brought it directly into a collision with other variables explaining colour variation. Therefore, in relation to the "why?" question in this field, I feel the biggest contribution to knowledge from my thesis is the conclusion that light environment influences the evolution of colouration across most plumage patches, whereas behavioural variables affect a limited set of plumage patches. Second, the question of "how?" was addressed in the case of the evolution of the blue colour in the clade Thraupidae and across two chapters. The transition towards blue colour was confirmed from the slate colour, which, in turn, could have evolved from grey colour in the clade Thraupidae. Therefore, I detected a new evolutionary pathway among colour categories in this thesis. The mechanistic basis of the evolution of the colour blue tells us that occurrence and then modulation of the elements of the spongy structure is vital for this evolutionary transition. The bigger picture for the evolutionary biology of

plumage colouration seen unfolding in this thesis is the detection of one more evolutionary pathway that depends on already existing elements within the feathers, i.e. novel phenotype evolves based on what is "on hand" in the feather and therefore developmental constraint plays an important role for plumage colour evolution. I firmly believe that focus on specific clade allowed me to discover this specific evolutionary pathway and that this pathway could be detected in other clades as well. The overarching conclusion of using what's "on hand" in plumage colour evolution leads us to speculation that in other clades some other evolutionary pathways towards colour blue could be detected based on the evolutionary history and developmental constraints of those clades. I further discuss one potential pathway in the later section of the Discussion.

5.2. Insights into the drivers of colour evolution

In chapter two, I wanted to explore further the ecological and behavioural drivers of the interspecific plumage colour variation. This aim was addressed in the colourful clade Coraciiformes with macroevolutionary approach: by quantifying several traits across species in this clade and correlating them with the colour measurements. The traits quantified were: 1. the light in the environment where species live (Fry et al., 2010); 2. body size (Wilman et al., 2014); 3. presence or absence of territoriality (Fry et al., 2010); 4. modes of hunting (Fry et al., 2010); and 5. forms of parental care (Cockburn, 2006). Plumage colour was quantified for males and females and across 11 body patches separately for chromatic (hue and saturation) and achromatic (brightness) properties of plumage colouration. The analysis involved testing for the correlates of both components of plumage colouration in males and females and for each plumage patch separately. The results indicated a strong and consistent influence of light environment on plumage colour evolution, while behavioural and life history traits had more limited effects. The general trend indicates a stronger influence of environment rather than behavioural traits on plumage colour evolution in the Coraciiformes.

Although light environment was the dominant predictor, several more subtle and idiosyncratic results emerged that indicate that different selection pressures are dominant on different body regions. For example, while the belly patch showed no effect of the light environment in males, it correlated with hunting strategy. This could indicate that specific patches overcome a general trend and take on separate evolutionary trajectories because of the importance of that patch for a specific function in the lives of birds. In the lives of Coraciiformes, bellies play an essential function as the first patch a potential prey observes when hunting fish (as well as ground catching). Their belly patches are mostly brownish in colour and therefore, they can blend in with the low growth near rivers where they perch while hunting and make themselves less visible to the potential prey. Some patches respond with both colour variables (chromatic and achromatic) to the same evolutionary

driver. For example, the rump patch is correlated to the light environment with both variation in hue (on PC1) and variation in the achromatic component of the colour. Patches also responded to different selection pressures with different colour variables. For example, for the rump patch, the light environment influenced the chromatic component of the colour while for the hunting strategy, light environment was related to brightness. Overall, my results showed multiple ways that plumage colouration, in general, could evolve in response to a range of behavioural and ecological drivers. In total, my second chapter shows that when investigating drivers of plumage colour evolution, it is essential to investigate the colouration of each plumage patch separately, for both chromatic and achromatic variation of the colouration and assess the relative importance of multiple factors simultaneously.

The results of chapter two allowed me to speculate about the potential conspicuousness or crypsis of plumage patches when compared between different light environments. Taken together, these results suggest that increasing conspicuousness is achieved via changes in hue while reducing conspicuousness is associated with changes in brightness. This could be linked to a compromise between intraspecific signalling and avoidance of detection by predators (Endler, 1992). This is similar to the private channel hypothesis that suggest that due to the different properties of visual systems across the animal kingdom, certain animals can use some colours for signalling purposes while avoiding detection from predators or prey (Endler, 1992; Håstad et al., 2005; Cuthill, 2007). Common colours within plumage of Coraciiformes tend to be blue to UV in hue (Babarović et al., 2019; Eliason et al., 2019). Our results indicate that in Coraciiformes this part of colour space may often be associated with conspicuousness (for example, PC1 hue variation in woodlands). While variation in brightness could be perceived by both the predators and potential prey, perception of non-iridescent structural colours (blue, purple, violet) and UV part of the spectrum is limited for many predators of these birds (reptiles, mammals and some other birds) (Cuthill, 1994; Harvey, 1998). Therefore, with green to blue and UV hue variation, certain body patches could be conspicuous through a “private channel” for interspecies communication purposes, and at the same time concealed from predators regarding brightness. This indicates even finer division of signalling strategies in bird plumage colouration according to specific intraspecific and interspecific communicational needs.

There are some exciting perspectives that I think the focus of the field should turn to in the future to further understand the plumage colour evolution in greater detail. For every behavioural variable I scored across all Coraciiformes in the chapter two, there was a research correlating plumage colour with a behavioural trait on a single species level (in the same or different clade). For example, wing

patches (epaulettes) in red-winged blackbirds have a function in maintaining territory (intraspecific) (Røskaft & Rohwer, 1987). Based on the significances discovered in these instances, I scored the variables across the entire clade. To broaden the scope of macroevolutionary research of plumage colouration a further study from behavioural ecology of plumage colouration should be done that would then inform choices of variables that could potentially be correlates of colour variation. For example, a recent discovery showed that white plumage under the full-moon conditions in the Barn Owl (*Tyto alba*) triggers longer freezing time in the prey and therefore makes them better predators (San-Jose et al., 2019). It would be challenging to score this behavioural response to plumage colour and environment and test for this correlation on the broader phylogenetic level. Nevertheless, this is the “back-and-forth” relationship between the research in behavioural ecology of the colour and the macroevolution that should be tackled more in the future to further explore plumage colour evolution. Furthermore, I focused on colour but variation in plumage patterns are also important for crypsis and conspicuousness (Curantz & Manceau, 2021; Hidalgo et al., 2022). While colour is only one aspect of each patch, many patches also have patterning consisting of multiple colours. Quantifying the pattern colouration is challenging but should be considered in macroevolutionary research. The distribution of colour is relevant to the light environment hypothesis. Specifically, the light environment hypothesis predicts that an adjacent colour should not overlap in the predominant wavelengths of light for maximal conspicuousness achieved (Endler, 1992). At the same time, the bigger of the two patches should also match in colouration with the light environment. This hypothesis indicates the intra-patch complexity and integration of the colour signal across patches that could arise during plumage colour evolution. Quantifying these aspects of plumage colouration could prove to be hard to achieve, but these aspects of plumage colouration could also be an exciting new avenue of exploration (Gluckman & Cardoso, 2010).

5.3. Insights into the mechanistic basics of colour evolution

While chapter two of my thesis explored the drivers of plumage colour evolution using Coraciiformes as a study system, chapters three and four were dedicated to exploring the discovery of the pathway and mechanisms of evolution of blue colour in birds' plumage. The hypothesis for these two chapters stated that blue colour evolves from grey colour with the slate colour as an intermediate state. This hypothesis was built upon previous research showing that: 1. pigmentary grey and non-iridescent structural colour share a similar melanosome shape (Babarović et al., 2019), and 2. Slate colour and blue colour have a similar nanostructural basis for colour production, i.e. a spongy layer in the medullary cells. However, in slate colour, this nanostructure was previously described as

“rudimentary”, indicating that it is like the nanostructure found in the non-iridescent structural colour but not fully developed (Saranathan et al., 2012).

In chapter three, I explored the evolution of these three colour categories at the macroevolutionary level. My results indicated that on a macroevolutionary level in the clade Thraupidae, blue colouration evolves from slate colouration, which in turn evolves from grey colouration, consistent with the nanostructure hypothesis outlined above. Notably, the only transition pathway leading towards the colour blue is from the colour slate. In addition to this core result, I also found that transitions from blue colour to “any other colour” occur often. Also, slate colouration could have an independent evolutionary pathway from the grey colour, i.e. from the category of “any other colour”. In total, these results showed that the evolutionary pathway towards colour blue is not straightforward and that intermediary stage, i.e. slate colour, is necessary.

In chapter four, I explored the mechanistic basis for the proposed evolutionary pathway from grey through slate colour to blue. To do this, I focused on the spongy layer in the medullary cells of the feather barbs, which is responsible for the coherent light scattering in non-iridescent structural colours and, ultimately, for colour production (Prum, 2006). I assessed the measurements of some aspects of the nanostructure with small-angle X-ray scattering (SAXS) (Saranathan et al., 2012). The analysis was once again a comparative phylogenetic analysis with the investigation of the correlates of the colour variance across grey, slate and blue colours as well as for slate and blue colours separately. My analyses revealed that the complexity of the spongy nanostructure, filling fraction and thickness of the spongy layer in general (as approximated by the I_0 parameter) are essential for the evolutionary transition between colour categories. However, my results also indicate that different elements or combinations are responsible for hue variation within and between colour categories. Namely, nanostructure complexity, combined with average hard block thickness, is responsible for hue variation among blue colours, while filling fraction is responsible for hue variation among slate colours.

This discovery should be put into a broader context of the development of colour-producing nanostructures. In all the explored cases so far, these processes are deemed to be low energy and without active cellular processes. After the feather has died, the elements of the nanostructure in the non-iridescent structural colours are self-assembled based on physical and chemical settings of the feather cells (Prum, 2006; Prum et al., 2009; Shawkey & Hill, 2006). Significantly, these processes depend on the chemical and physical characteristics of the materials building the feathers, i.e. keratin, air and pigments (melanin in the cases we have explored). In the case of non-iridescent structural colours, the development of the spongy nanostructure is a process guided by phase-

separation of keratin and air. This process needs to have a halting mechanism at a certain point otherwise, the two phases would separate entirely. A vivid image of this one can get in the kitchen after mixing of water and oil, which would inevitably separate in the two phases across a certain time. This makes it a problem if a separate colour category depend on the same developmental regime, which is the case for blue and slate colour. Colour production in both colour categories depend partly to the spongy nanostructure which develops by phase separation of keratin and air. More so since structural colours are inherently linked to their underlying nanostructure and slight changes in the nanostructure would influence hue production and ultimately, the signal emitted in the environment (Fan et al., 2019). In both cases of the colour evolution, we are investigating hue variation, but on a different scale. In the first analysis, I investigated colour variation between grey, slate and blue colour categories, while in the second and third analysis, I restricted the analysis only to blue and slate colour. This approach revealed differences in the nanostructural elements responsible for each colour variation. I suggested that because both of these colours will depend on the outcome of phase separation (between keratin and air) and that process has inevitable fate – separation of the two phases – evolutionary response to the demand of separating colour variation within and between colour categories was the separation of colour mechanisms. Therefore, one set of the variation of nanostructure parameters is responsible for the colour variation within blue colour category and they are different from the set of parameters responsible for the colour variation within slate colour category. Finally, the transition between grey, slate and blue colour categories requires variability in the third set of nanostructural parameters.

Previous research on the evolution of nanostructure in birds' feathers highlighted the importance of evolutionary tinkering – the evolution of a novel phenotype that is the product of the rearrangement of the already existing phenotype (Doucet et al., 2004; Shawkey et al., 2006). My research confirms that the evolution of structural blue from pigmentary grey is a two-stage process and I suggest that both stages proceed through the similar process of rearrangement of already existing elements of the feathers. In the first stage of this evolutionary pathway, a transition from grey to slate colour occurs. The appearance of the spongy nanostructure is responsible for the evolutionary transition from grey colour towards the slate colour with my results showing a step change in nanostructural complexity associated with slate. Therefore, the appearance of the spongy layer is the critical driver in this stage of the evolution of this pathway. The spongy layer consists of the air and keratin, and hollow medullary cells in the feathers are an adaptive response across all bird's feathers (Vogel, 2013). The hollowness of the medullary cells allows for the feathers' greater integrity for the same keratin material volume (Niklas, 1992; Vogel, 2013). Therefore, the transition from grey to slate colour by the appearance of the spongy layer also involves the reorganization of already existing

elements, i.e. keratin and air. Evolution towards blue colour is associated with these two elements becoming increasingly organized. Going from slate to blue spongy layer goes through three adjustments: 1. increases in the thickness, 2. increase in the filling fraction (percentage of the investigated space is populated more with the nanostructure), 3. and there is an increase in the nanostructure complexity (features of the nanostructure showing periodicity on a level of a certain range). These results add to the narrative that in the evolution of plumage colouration the potential for evolution of novel colour pathways is developmentally constrained (Nordén & Price, 2018; Stoddard & Prum, 2011). In many studies of plumage colour evolution on the nanostructural level, it has been shown that novel phenotypes evolve either through rearrangement of already existing elements within the feather or by sequestering genetic mechanisms for pigment production that are already present and expressed in other body regions (Barrera-Guzmán et al., 2018; Doucet et al., 2004; Driskell et al., 2010; Shawkey et al., 2006). The grey-slate-blue evolutionary pathway follows the same evolutionary explanation: evolution from grey through slate to blue colour is a process of rearrangement of already existing elements of the feathers that proceeds through regulation of each step via adjustments in the elements of the spongy layer.

A certain limitation of the chapter four should be put forward, i.e. there is a lack of knowledge about melanosomes localization and movement during the detected evolutionary pathway between grey, slate and blue colour. Despite the fact of being a structural colour, blue colour has a underlying melanosomes layer that is important for the colour production since it absorbs all backscattered white light not refracted from the spongy layer (Shawkey & Hill, 2006). Without this melanosome layer, a colour produced from these feathers is white with a slight blue tint. Grey is a pigmentary colour and melanosomes in this colour are scattered around the barb nanostructure. Looking at the beginning (grey colour and melanosomes scattered all around barb) and end point of this evolutionary transition (blue colour and melanosomes concentrated in the bottom layer of the barb) it seems reasonable that this transition was also accompanied by melanosomes shifts. Other research indicates that melanosome deposition can mask production of the structural colour if melanosomes are placed above the spongy layer – as has been shown in the case of the evolution of black colour from blue in fairy wrens (Doucet et al., 2004; Driskell et al., 2010). From my research the conclusion about placement of melanosomes during evolutionary processes cannot be drawn and therefore variables such as melanosome concentration, distance of melanosomes from barb edges, thickness of melanosome layer cannot be used as a variable for explaining colour variation in the colours I have investigated. Whether melanosomes get pushed first to the bottom of barb as the evolution proceeds or the transgression proceeds stepwise with the development of the spongy layer is yet to be tested.

The results of my thesis propose a further question in the topic of evolution of the colour blue: that is, the evolutionary link between blue colour and the colour white. Several times in the literature, this evolutionary link has been suggested, but it was never tested. In a study of amelanotic Steller's jay feathers, a lack of the underlying melanosomes has been linked to the appearance of the white colour in these feathers (Shawkey & Hill, 2006). In the white feathers of amelanotic Steller's jay (*Cyanocitta stelleri*), a spongy nanostructure has been detected and the colour measured by the spectrometer comes completely from the colour produced by the spongy layer without interference of the melanosomes. These feathers have a broad reflectance curve (typical of white colour) with a slight blue peak, but the blue colour has been termed as "washed-out". Namely, in blue feathers (i.e. those containing basal melanosome layer), a reflectance curve has a distinct bell-shaped blue curve with a well pronounced peak. An investigation of the within-species variation in the feather nanostructure in the Swallow tanager (*Tersina viridis*) revealed that the white feather colour has a nanostructure capable of producing blue colour but it's washed out (Bazzano et al., 2021). In our analysis, a filling fraction (occupancy of the analysed space of the nanostructure with the keratin material) in the blue feathers matches with the filling fraction from white beetles' scales (Burg et al., 2019). The variation of filling fraction has also been a primary driver of hue variance within the slate colour category. Therefore, if any of the feathers in the slate and blue colour category "lost" melanosomes, their colour would be white. These speculations could easily be tested for by involving white colour as a category both in the analysis of the chapter three and the chapter four. By doing this, we could shed a light on the pathway discovered that leads from colour blue to "any other colour category" in the analysis of the chapter three. As stated in this paragraph, a nanostructural mechanism for this to happen would be a simple loss of the underlying melanosome layer as going from blue feathers to white feathers. Interestingly, a transition in the reverse way, from "any other colour" (and therefore, potentially white) to blue has not been shown in the results of the chapter three. This could lead to speculation that gain of all the elements of the feather nanostructure needed for the production of the colour blue is not easy to achieve and therefore, evolution via intermediate colour state (slate) is still the most likely way.

An attention in this thesis has been given to the colour blue and especially in the chapters two and three where: 1. evolutionary pathway (chapter two) and 2. mechanisms of the transitions (chapter three) in the evolution of the colour blue have been tackled. This calls for some clarification of the category of the colour blue used in this thesis. Hues of the colour blue are only a fraction of colours produced by coherent scattering from the spongy layer in medullary cells of feather barbs, i.e. with non-iridescent structural colours. Other colours include purple, UV colours and, in combination with carotenoids – green colour. The argument for the colour blue is two-fold. First, in habitats, the

colour blue has a unique relationship with light in the environment, with conspicuousness achieved heavily in the woodlands and not prominently in a deep forest light environment. This would separate it from green or purple hues regarding visual perception and achievement of conspicuousness and crypsis within the environment (Endler, 1992; Endler, 1993b). Second, recently, it has been shown that melanosomes participating in the colour production of purple non-iridescent structural colours are predominantly phaeomelanosomes, and not eumelanosomes (Fan et al., 2019; Peters et al., 2013). This could indicate separate developmental and evolutionary mechanisms leading to blue compared to other non-iridescent structural colours, for example purple. Nevertheless, in this thesis, the attempts to answer certain questions about transitions towards structural colours and mechanistic basis of the evolution of the structural colours in general were tackled by investigation of blue colour in specific. It remains to be seen whether evolutionary mechanisms and favouring factors for other non-iridescent structural colours are the same.

5.4. Further directions

In a seminal paper on the plumage colour evolution – "How colourful are birds? Evolution of the avian plumage color gamut", authors propose two hypotheses for the constraints on plumage colouration (Stoddard & Prum, 2011). Namely, they address them as the "blue rose" hypothesis and the "nosebleed section" hypothesis. According to the "blue rose" hypothesis, a certain colour is challenging to produce due to the developmental constraints with the existing colour-producing mechanisms. In the "nosebleed section" hypothesis, a particular colour is rare in birds' plumage due to natural and sexual selection rendering their signalling function unfavourable in the environment. Specific results of my thesis could inform the development of an examination on how to answer these two questions in the case of the blue colour in birds' plumage. I suggest that macroevolutionary inquiry into the correlation between instances of the colour blue in birds' plumage with 1) forest coverage and 2) temperature ranges across the globe would give us insight into which of the two hypotheses could play a role in the evolution of blue colouration across all bird species. First: forest coverage; In chapter two, the results of the light environment hypothesis showed a consistent correlation between the colour blue and woodland light environment in the clade Coraciiformes. Colour blue in those light environments would exhibit increased conspicuousness due to the overlap of predominant wavelengths in the environment with the predominant colour of the bird's plumage. Therefore, by correlating forest coverage across the world with the blue colour in plumage, we could test if the constraint for the blue plumage colouration is the signalling one. Second: temperature range; in chapter four of my thesis, I showed that the spongy layer is essential in the evolution of the colour blue. In turn, the stability of the

mixture (air and keratin) during the development of the spongy layer in the medullary cells will depend on the temperature surrounding the developing nanostructure (Prum et al., 2009). There is a possibility of the existence of a constraint that could impose a limitation in the development of the colour blue ("blue rose" hypothesis), i.e. temperature. Therefore, by correlating temperature ranges worldwide with the blue colour in plumage, we could test if the constraint for the blue plumage colouration is a developmental one ("blue rose" hypothesis). Taken together, these two correlates with the blue plumage colouration could help us understand both why and how the blue colour in a bird's plumage has evolved.

5.5. Reflections on my work and it's context

Many aspects of this thesis depended on the museum collection (Natural History Museum at Tring, UK and Zoological Museum, Natural History Museum of Denmark, University of Copenhagen). I would like to acknowledge the colonial legacies of these collections. During my PhD, I was part of a broader initiative at the School of Biosciences that aimed at putting biological work in a decolonial context. We developed a guideline considering the critical observation of this occurrences. The overview of the work and useful resources can be found here: <https://sites.google.com/sheffield.ac.uk/contextualising-eeb-curriculum/home?authuser=0>. Inspired by my experiences in the academia, I co-supervised a master's thesis project that looked at the colonial legacy of the teaching collection at the Alfred Denny Museum at our department (work was done by Rebecca Ford). The audio guide that summarizes this work can be accessed here: <https://drive.google.com/drive/folders/1OC7UMsqTU9Y1S8dQxj-eff7BnEa3vNH3>.

5.6. Final remarks

As a reader, I ask you to draw a large circle in front of you with a pen and then put a dot the size of the pen tip on the circumference. Now halve that dot in your mind - imagine the entire big circle is the field of plumage colour evolution and that dot is how I imagine my thesis has contributed to the field. A little, but more importantly, through trials and errors and half of that dot of new knowledge, I explored and thought about most of that circle. Plumage colour evolution is the field that will forever be interesting to researchers because of the almost immeasurable complexity of the biological system displayed in front of us. More importantly, it changes with technological innovations and trends revealed in other research areas across all natural sciences. In a sense, research on plumage colour evolution is a mirrorball spinning in a room of all natural sciences and reflecting methodologies and theories from all of them to answer the questions it addresses. My endeavour in this field started from palaeontology to proceed in macroevolution and ended up in

physics, so far. Besides the scientific journey, it was also a personal emotional journey. I wish that the beginning sentences from Maggie Nelsons' book *Bluets* be one of the last sentences of my thesis, and I wish you to take them with you, reader. It goes like this, and it perfectly addresses my last 4 (and a bit) years of life: "Suppose I were to begin by saying that I had fallen in love with a colour. Suppose I were to speak this as though it were a confession; suppose I shredded my napkin as we spoke. It began slowly. An appreciation, an affinity. Then, one day, it became more serious. Then (looking into an empty teacup, its bottom stained with thin brown excrement coiled into the shape of a sea horse) it became somehow personal." The topics I am dealing with in this thesis followed this similar pathway and became, on many occasions, extremely personal; by submitting this thesis, I am making part of my personal fascinations a public one, and I hope that I managed to spark your interest as well.

5.7. References

- Babarović, F., Puttick, M. N., Zaher, M., Learmonth, E., Gallimore, E.-J., Smithwick, F. M., Mayr, G., & Vinther, J. (2019). Characterization of melanosomes involved in the production of non-iridescent structural feather colours and their detection in the fossil record. *Journal of The Royal Society Interface*, *16*(155), 20180921. <https://doi.org/10.1098/rsif.2018.0921>
- Barrera-Guzmán, A. O., Aleixo, A., Shawkey, M. D., & Weir, J. T. (2018). Hybrid speciation leads to novel male secondary sexual ornamentation of an Amazonian bird. *Proceedings of the National Academy of Sciences*, *115*(2), E218–E225. <https://doi.org/10.1073/pnas.1717319115>
- Bazzano, L. T., Mendicino, L. R., Inchaussandague, M. E., Skigin, D. C., García, N. C., Tubaro, P. L., & Barreira, A. S. (2021). Mechanisms involved in the production of differently colored feathers in the structurally colored swallow tanager (*Tersina viridis*; Aves: Thraupidae). *Journal of Experimental Zoology Part B: Molecular and Developmental Evolution*, *336*(5), 404–416. <https://doi.org/10.1002/jez.b.23043>
- Bennett, A. T. D., & Cuthill, I. C. (1994). Ultraviolet vision in birds: What is its function? *Vision Research*, *34*(11), 1471–1478. [https://doi.org/10.1016/0042-6989\(94\)90149-X](https://doi.org/10.1016/0042-6989(94)90149-X)
- Burg, S. L., Washington, A., Coles, D. M., Bianco, A., McLoughlin, D., Mykhaylyk, O. O., Villanova, J., Dennison, A. J. C., Hill, C. J., Vukusic, P., Doak, S., Martin, S. J., Hutchings, M., Parnell, S. R., Vasilev, C., Clarke, N., Ryan, A. J., Furnass, W., Croucher, M., ... Parnell, A. J. (2019). Liquid–liquid phase separation morphologies in ultra-white beetle scales and a synthetic equivalent. *Communications Chemistry*, *2*(1), Article 1. <https://doi.org/10.1038/s42004-019-0202-8>

- Cockburn, A. (2006). Prevalence of different modes of parental care in birds. *Proceedings of the Royal Society B: Biological Sciences*, 273(1592), 1375–1383.
<https://doi.org/10.1098/rspb.2005.3458>
- Curantz, C., & Manceau, M. (2021). Trends and variation in vertebrate patterns as outcomes of self-organization. *Current Opinion in Genetics & Development*, 69, 147–153.
<https://doi.org/10.1016/j.gde.2021.05.001>
- Doucet, S. M., Shawkey, M. D., Rathburn, M. K., Mays, H. L., & Montgomerie, R. (2004). Concordant evolution of plumage colour, feather microstructure and a melanocortin receptor gene between mainland and island populations of a fairy-wren. *Proceedings of the Royal Society of London. Series B: Biological Sciences*, 271(1549), 1663–1670.
<https://doi.org/10.1098/rspb.2004.2779>
- Driskell, A. C., Prum, R. O., & Pruett-Jones, S. (2010). The evolution of black plumage from blue in Australian fairy-wrens (Maluridae): Genetic and structural evidence. *Journal of Avian Biology*, 41(5). <https://onlinelibrary.wiley.com/doi/full/10.1111/j.1600-048X.2009.04823.x>
- Eliason, C. M., Andersen, M. J., & Hackett, S. J. (2019). Using Historical Biogeography Models to Study Color Pattern Evolution. *Systematic Biology*, 68(5), 755–766.
<https://doi.org/10.1093/sysbio/syz012>
- Endler, J. A. (1990). On the measurement and classification of colour in studies of animal colour patterns. *Biological Journal of the Linnean Society*, 41(4), 315–352.
<https://doi.org/10.1111/j.1095-8312.1990.tb00839.x>
- Endler, J. A. (1992). Signals, Signal Conditions, and the Direction of Evolution. *The American Naturalist*, 139, S125–S153.
- Fan, M., D'alba, L., Shawkey, M. D., Peters, A., & Delhey, K. (2019). Multiple components of feather microstructure contribute to structural plumage colour diversity in fairy-wrens. *Biological Journal of the Linnean Society*, 128(3), 550–568. <https://doi.org/10.1093/biolinnean/blz114>
- Fry, H., Fry, K., & Harris, A. (2010). *Kingfishers, Bee-eaters and Rollers*. Bloomsbury Publishing.
<https://www.nhbs.com/kingfishers-bee-eaters-and-rollers-book>
- Gluckman, T.-L., & Cardoso, G. C. (2010). The dual function of barred plumage in birds: Camouflage and communication. *Journal of Evolutionary Biology*, 23(11), 2501–2506.
<https://doi.org/10.1111/j.1420-9101.2010.02109.x>
- Guilford, T., & Harvey, P. H. (1998). The purple patch. *Nature*, 392(6679), 867–869.
<https://doi.org/10.1038/31813>

- Håstad, O., Victorsson, J., & Ödeen, A. (2005). Differences in color vision make passerines less conspicuous in the eyes of their predators. *Proceedings of the National Academy of Sciences*, *102*(18), 6391–6394. <https://doi.org/10.1073/pnas.0409228102>
- Hidalgo, M., Curantz, C., Quenech'Du, N., Neguer, J., Beck, S., Mohammad, A., & Manceau, M. (2022). A conserved molecular template underlies color pattern diversity in estrildid finches. *Science Advances*, *8*(35), eabm5800. <https://doi.org/10.1126/sciadv.abm5800>
- Niklas, K. J. (1992). *Plant biomechanics: An engineering approach to plant form and function*. University of Chicago Press. <https://ecommons.cornell.edu/handle/1813/28577>
- Nordén, K. K., & Price, T. D. (2018). Historical Contingency and Developmental Constraints in Avian Coloration. *Trends in Ecology & Evolution*, *33*(8), 574–576. <https://doi.org/10.1016/j.tree.2018.05.003>
- Prum, R. O., Dufresne, E. R., Quinn, T., & Waters, K. (2009). Development of colour-producing β -keratin nanostructures in avian feather barbs. *Journal of The Royal Society Interface*, *6*(suppl_2), S253–S265. <https://doi.org/10.1098/rsif.2008.0466.focus>
- Prum. (2006). *Anatomy, physics, and evolution of avian structural colors* (Vol. 1, pp. 295–353). Harvard University Press.
- Røskoft, E., & Rohwer, S. (1987). An experimental study of the function of the red epaulettes and the black body colour of male red-winged blackbirds. *Animal Behaviour*, *35*(4), 1070–1077. [https://doi.org/10.1016/S0003-3472\(87\)80164-1](https://doi.org/10.1016/S0003-3472(87)80164-1)
- San-Jose, L. M., Séchaud, R., Schalcher, K., Judes, C., Questiaux, A., Oliveira-Xavier, A., Gémard, C., Almasi, B., Bézières, P., Kelber, A., Amar, A., & Roulin, A. (2019). Differential fitness effects of moonlight on plumage colour morphs in barn owls. *Nature Ecology & Evolution*, *3*(9), Article 9. <https://doi.org/10.1038/s41559-019-0967-2>
- Saranathan, V., Forster, J. D., Noh, H., Liew, S.-F., Mochrie, S. G. J., Cao, H., Dufresne, E. R., & Prum, R. O. (2012). Structure and optical function of amorphous photonic nanostructures from avian feather barbs: A comparative small angle X-ray scattering (SAXS) analysis of 230 bird species. *Journal of The Royal Society Interface*, *9*(75), 2563–2580. <https://doi.org/10.1098/rsif.2012.0191>
- Shawkey, M. D., Hauber, M. E., Estep, L. K., & Hill, G. E. (2006). Evolutionary transitions and mechanisms of matte and iridescent plumage coloration in grackles and allies (Icteridae). *Journal of The Royal Society Interface*, *3*(11), 777–786. <https://doi.org/10.1098/rsif.2006.0131>
- Shawkey, M. D., & Hill, G. E. (2006). Significance of a basal melanin layer to production of non-iridescent structural plumage color: Evidence from an amelanotic Steller's jay (*Cyanocitta*

- stelleri). *Journal of Experimental Biology*, 209(7), 1245–1250.
<https://doi.org/10.1242/jeb.02115>
- Stevens, M., Cuthill, I. C. (2007). Hidden Messages: Are Ultraviolet Signals a Special Channel in Avian Communication?, *BioScience*, Volume 57, Issue 6, June 2007, Pages 501–507, <https://doi.org/10.1641/B570607>
- Stoddard, M. C., & Prum, R. O. (2011). How colorful are birds? Evolution of the avian plumage color gamut. *Behavioral Ecology*, 22(5), 1042–1052. <https://doi.org/10.1093/beheco/arr088>
- Vogel, S. (2013). *Comparative Biomechanics*. Princeton University Press.
<https://press.princeton.edu/books/hardcover/9780691155661/comparative-biomechanics>
- Wilman, H., Belmaker, J., Simpson, J., Rosa, C. de la, Rivadeneira, M. M., & Jetz, W. (2014). EltonTraits 1.0: Species-level foraging attributes of the world’s birds and mammals. *Ecology*, 95(7), 2027–2027. <https://doi.org/10.1890/13-1917.1>

APPENDIX 1

Supplementary materials and methods for Chapter 2: The effects of ecology and behaviour on the evolution of colouration in Coraciiformes

Table S1: Number of species used for each analysis. Reasoning explained in the main text, Material and Methods section, specimen selection paragraph.

		phylo.RMA			PGLS + ANOVA	
		PC1	PC2	Brightness	m	f
1	Crown	135	135	135	117	114
2	Nape	135	135	135	117	114
3	Mantle	135	135	135	117	114
4	Rump	135	135	135	117	114
5	Tail	134	134	134	116	114
6	Wing coverts	135	135	135	117	114
7	Wing primaries secondaries	135	135	135	117	114
8	Throat	135	135	135	117	114
9	Breast	135	135	135	117	114
10	Belly	135	135	135	117	114
11	Tail underside	122	122	122	113	110

Table S2: Results of Principal component analysis. We have reported Standard deviation, Proportion of Variance, Cumulative Proportion.

Results of PCA				
Importance of components:				
	PC1	PC2	PC3	PC4
Standard deviation	0.1438	0.064	0.03099	2.83E-10
Proportion of Variance	0.8021	0.160	0.03723	0.00E+00
Cumulative Proportion	0.8021	0.962	1	1.00E+00
Rotation (n x k) = (4 x 4):				
	PC1	PC2	PC3	PC4
u	0.562540	0.341	0.562789	0.5
s	0.383979	0.094	0.770432	0.5
m	0.263309	0.772	0.288406	0.5
l	0.683210	0.526	0.080763	0.5

Table S3: List of Coraciiformes species used for this research with the coding of their ecological and behavioral traits. Coded traits for each species are: light environment, hunting strategy, territoriality, parental care and body size. Information for each of these categories were extracted from the literature as explained in the Material and methods section of the main text, Predictor variables subsection.

Sciname	Size	Light environment	Parental care	Territoriality	Hunting strategy
<i>Actenoides bougainvillei</i>	188	forest	pair	0	NA
<i>Actenoides concretus</i>	73.47	forest	pair	0	ground dweller
<i>Actenoides hombroni</i>	117	forest	pair	0	ground dweller
<i>Actenoides lindsayi</i>	92.84	forest	pair	0	ground dweller
<i>Actenoides monachus</i>	106	forest	pair	0	ground dweller
<i>Actenoides princeps</i>	105	forest	pair	0	NA
<i>Alcedo argentata</i>	17.84	woodland	pair	0	water diver
<i>Alcedo atthis</i>	31.09	woodland	pair	1	water diver
<i>Alcedo azurea</i>	34.9	woodland	pair	NA	water diver
<i>Alcedo coerulescens</i>	27.59	open	pair	0	water diver
<i>Alcedo cristata</i>	15.7	open	pair	1	water diver
<i>Alcedo cyanopectus</i>	21.5	woodland	pair	0	water diver
<i>Alcedo euryzona</i>	43.08	woodland	pair	0	water diver
<i>Alcedo hercules</i>	27.59	woodland	pair	0	water diver
<i>Alcedo leucogaster</i>	14.5	woodland	pair	0	water diver
<i>Alcedo meninting</i>	20.42	woodland	pair	0	water diver
<i>Alcedo pusilla</i>	13.3	woodland	pair	NA	water diver
<i>Alcedo quadribrachys</i>	34.9	woodland	pair	1	water diver
<i>Alcedo semitorquata</i>	47.32	woodland	pair	0	water diver
<i>Alcedo vintsioides</i>	17.9	open	pair	NA	water diver
<i>Alcedo websteri</i>	60.97	woodland	pair	NA	water diver
<i>Aspatha gularis</i>	62.7	forest	pair	0	aerial catcher
<i>Atelornis crossleyi</i>	79	forest	pair	1	ground dweller
<i>Atelornis pittoides</i>	91.5	forest	pair	1	ground dweller
<i>Baryphthengus martii</i>	165.02	forest	pair	0	ground catcher
<i>Baryphthengus ruficapillus</i>	141.65	forest	pair	0	ground dweller
<i>Brachypteracias leptosomus</i>	185	forest	pair	1	aerial catcher
<i>Brachypteracias squamiger</i>	155	forest	pair	NA	ground dweller
<i>Caridonax fulgidus</i>	171.81	forest	pair	1	NA
<i>Ceryle rudis</i>	84.37	open	cooperative	1	water diver
<i>Ceyx erithaca</i>	17.79	woodland	pair	1	ground catcher
<i>Ceyx fallax</i>	18	forest	pair	0	NA
<i>Ceyx lecontei</i>	9.5	woodland	pair	NA	ground catcher
<i>Ceyx lepidus</i>	21.32	forest	pair	0	aerial catcher
<i>Ceyx madagascariensis</i>	17.7	woodland	pair	NA	ground catcher
<i>Ceyx melanurus</i>	22.8	forest	pair	0	NA
<i>Ceyx pictus</i>	12.72	woodland	pair	NA	aerial catcher

<i>Ceyx rufidorsa</i>	17.79	woodland	pair	0	NA
<i>Chloroceryle aenea</i>	13.75	woodland	pair	0	aerial catcher
<i>Chloroceryle amazona</i>	126.38	open	pair	0	water diver
<i>Chloroceryle americana</i>	33.73	open	pair	0	water diver
<i>Chloroceryle inda</i>	52.1	woodland	pair	0	water diver
<i>Cittura cyanotis</i>	147.02	forest	pair	0	ground catcher
<i>Clytoceyx rex</i>	242	woodland	pair	0	ground dweller
<i>Coracias abyssinicus</i>	102	open	pair	1	aerial catcher
<i>Coracias benghalensis</i>	157.46	open	pair	1	aerial catcher
<i>Coracias caudatus</i>	110	open	pair	1	ground catcher
<i>Coracias cyanogaster</i>	142	woodland	cooperative	1	ground catcher
<i>Coracias garrulus</i>	146	open	pair	1	aerial catcher
<i>Coracias naevia</i>	168	open	pair	NA	ground catcher
<i>Coracias spatulatus</i>	90.36	woodland	pair	1	ground catcher
<i>Coracias temminckii</i>	153.67	woodland	pair	0	ground catcher
<i>Dacelo gaudichaud</i>	143	woodland	pair	1	aerial catcher
<i>Dacelo leachii</i>	307.98	open	cooperative	1	aerial catcher
<i>Dacelo novaeguineae</i>	333.8	woodland	cooperative	1	ground catcher
<i>Dacelo tyro</i>	145.9	woodland	cooperative	0	aerial catcher
<i>Electron carinatum</i>	64.9	forest	pair	1	aerial catcher
<i>Electron platyrhynchum</i>	73	forest	pair	0	aerial catcher
<i>Eumomota superciliosa</i>	62.5	woodland	pair	0	aerial catcher
<i>Eurystomus azureus</i>	122.76	open	pair	0	aerial catcher
<i>Eurystomus glaucurus</i>	110	open	pair	1	aerial catcher
<i>Eurystomus gularis</i>	96.29	woodland	pair	1	aerial catcher
<i>Eurystomus orientalis</i>	143.02	open	pair	1	aerial catcher
<i>Halcyon albiventris</i>	65.1	woodland	pair	1	ground catcher
<i>Halcyon badia</i>	57.9	forest	pair	0	aerial catcher
<i>Halcyon chelicuti</i>	43.24	open	cooperative	1	ground catcher
<i>Halcyon coromanda</i>	77.5	forest	pair	1	water diver
<i>Halcyon cyanoventris</i>	93	open	pair	0	ground catcher
<i>Halcyon leucocephala</i>	41.8	open	pair	1	aerial catcher
<i>Halcyon malimbica</i>	91.8	woodland	pair	1	ground catcher
<i>Halcyon pileata</i>	83.99	open	pair	0	aerial catcher
<i>Halcyon senegalensis</i>	73.44	open	pair	1	ground catcher
<i>Halcyon senegaloides</i>	61.8	woodland	pair	1	ground catcher
<i>Halcyon smyrnensis</i>	91.4	woodland	pair	1	water diver
<i>Hylomanes momotula</i>	29.3	forest	pair	0	aerial catcher
<i>Lacedo pulchella</i>	47.27	forest	pair	1	aerial catcher
<i>Megaceryle alcyon</i>	148	open	pair	1	water diver
<i>Megaceryle lugubris</i>	270.99	open	pair	1	water diver
<i>Megaceryle maxima</i>	325	open	pair	0	water diver
<i>Megaceryle torquata</i>	317	open	pair	0	water diver
<i>Melidora macrorrhina</i>	97	forest	pair	1	ground dweller
<i>Meropogon forsteni</i>	55	woodland	cooperative	0	aerial catcher
<i>Merops albicollis</i>	25.9	open	cooperative	0	aerial catcher

<i>Merops apiaster</i>	56.6	open	cooperative	0	aerial catcher
<i>Merops boehmi</i>	16.6	woodland	pair	0	aerial catcher
<i>Merops breweri</i>	49.74	woodland	cooperative	0	aerial catcher
<i>Merops bullockoides</i>	34.8	open	cooperative	1	aerial catcher
<i>Merops bullocki</i>	23.1	open	cooperative	1	aerial catcher
<i>Merops gularis</i>	27.3	woodland	cooperative	0	aerial catcher
<i>Merops hirundineus</i>	21.7	open	cooperative	0	aerial catcher
<i>Merops leschenaulti</i>	27.2	open	cooperative	0	aerial catcher
<i>Merops malimbicus</i>	50.37	open	cooperative	0	aerial catcher
<i>Merops muelleri</i>	22.5	woodland	cooperative	0	aerial catcher
<i>Merops nubicoides</i>	42.4	open	cooperative	0	aerial catcher
<i>Merops nubicus</i>	42.4	open	cooperative	0	aerial catcher
<i>Merops oreobates</i>	23.96	woodland	cooperative	0	aerial catcher
<i>Merops orientalis</i>	14.8	open	cooperative	1	aerial catcher
<i>Merops ornatus</i>	29.5	open	cooperative	1	aerial catcher
<i>Merops persicus</i>	49.3	open	cooperative	1	aerial catcher
<i>Merops philippinus</i>	34	open	cooperative	0	aerial catcher
<i>Merops pusillus</i>	15.1	open	cooperative	0	aerial catcher
<i>Merops revoilii</i>	12.9	open	pair	0	aerial catcher
<i>Merops superciliosus</i>	38.5	woodland	cooperative	0	aerial catcher
<i>Merops variegatus</i>	22.5	open	pair	1	aerial catcher
<i>Merops viridis</i>	34.8	woodland	cooperative	0	aerial catcher
<i>Momotus aequatorialis</i>	158	woodland	NA	0	ground dweller
<i>Momotus mexicanus</i>	75.7	woodland	pair	0	aerial catcher
<i>Momotus momota</i>	114.96	woodland	pair	0	aerial catcher
<i>Nyctyornis amictus</i>	71.89	forest	pair	0	aerial catcher
<i>Nyctyornis athertoni</i>	84.23	woodland	pair	0	aerial catcher
<i>Pelargopsis amauroptera</i>	162	open	pair	0	water diver
<i>Pelargopsis capensis</i>	178.68	woodland	pair	1	water diver
<i>Pelargopsis melanorhyncha</i>	193.26	woodland	pair	0	water diver
<i>Syma megarhyncha</i>	40	forest	pair	0	aerial catcher
<i>Syma torotoro</i>	37.7	forest	pair	1	ground catcher
<i>Tanysiptera carolinae</i>	50.15	woodland	pair	0	NA
<i>Tanysiptera danae</i>	43.48	forest	pair	1	NA
<i>Tanysiptera ellioti</i>	50.15	forest	pair	0	ground dweller
<i>Tanysiptera galatea</i>	50	forest	pair	0	ground dweller
<i>Tanysiptera hydrocharis</i>	50.15	forest	pair	0	ground dweller
<i>Tanysiptera nympha</i>	57	forest	pair	0	ground dweller
<i>Tanysiptera riedelii</i>	65	forest	pair	0	NA
<i>Tanysiptera sylvia</i>	49.6	forest	cooperative	0	ground dweller
<i>Todiramphus australasia</i>	65.45	forest	pair	0	aerial catcher
<i>Todiramphus chloris</i>	66.09	open	pair	1	ground catcher
<i>Todiramphus cinnamominus</i>	62.2	woodland	cooperative	0	NA
<i>Todiramphus diops</i>	47.37	open	cooperative	0	NA
<i>Todiramphus farquhari</i>	38.8	woodland	pair	0	aerial catcher
<i>Todiramphus funebris</i>	105.79	woodland	pair	0	ground catcher

<i>Todiramphus gambieri</i>	34.98	woodland	cooperative	0	NA
<i>Todiramphus godeffroyi</i>	63.35	woodland	cooperative	0	aerial catcher
<i>Todiramphus lazuli</i>	65.45	woodland	cooperative	0	NA
<i>Todiramphus leucopygius</i>	47.92	woodland	pair	0	ground catcher
<i>Todiramphus macleayii</i>	37.3	woodland	cooperative	1	ground catcher
<i>Todiramphus nigrocyaneus</i>	54.2	woodland	cooperative	0	ground catcher
<i>Todiramphus pyrrhopygius</i>	51.7	open	pair	0	ground catcher
<i>Todiramphus recurvirostris</i>	52.96	open	NA	0	ground catcher
<i>Todiramphus sanctus</i>	52.96	open	pair	1	ground catcher
<i>Todiramphus saurophaga</i>	126	open	pair	NA	ground catcher
<i>Todiramphus tutus</i>	42.32	woodland	cooperative	0	aerial catcher
<i>Todiramphus veneratus</i>	65.45	woodland	pair	0	ground catcher
<i>Todiramphus winchelli</i>	67.39	woodland	cooperative	0	ground catcher
<i>Todus angustirostris</i>	7.5	forest	cooperative	0	aerial catcher
<i>Todus mexicanus</i>	5.9	forest	cooperative	0	aerial catcher
<i>Todus multicolor</i>	5.9	woodland	cooperative	0	aerial catcher
<i>Todus subulatus</i>	8.7	forest	cooperative	0	aerial catcher
<i>Todus todus</i>	6.4	woodland	cooperative	0	aerial catcher
<i>Uratelornis chimaera</i>	226	woodland	pair	0	NA

Table S4. Results of phylogenetic reduced major axis regression (phylo.RMA) analysis of PC1 (1 – 11), PC2 and achromatic property values for males and females. The analysis was done for each body patch and then for PC1, PC2 and achromatic property of plumage colour. R2 and p-values are reported.

	1) Crown	2) Nape	3) Mantle	4) Rump	5) Tail	6) Wing covert	7) Wing primaries secondaries	8) Throat	9) Breast	10) Belly	11) Tail underside
Intercept	-0.013	-0.006	-0.003	0.005	-0.007	-0.007	-0.009	0.003	0.005	-0.001	-0.004
x	0.899	0.971	0.963	1.025	1.059	0.950	0.954	0.982	0.984	0.952	1.053
lambda	0.071	0.190	0.354	0.331	0.276	0.460	0.345	0.385	0.425	0.254	0.691
log(L)	260.47 3	239.96 4	270.23 9	264.72 4	288.55 7	303.152	310.302	404.31 2	302.82 1	370.60 8	465.831
r ²	0.809	0.830	0.765	0.781	0.777	0.823	0.693	0.828	0.731	0.884	0.428

T	2.795	0.814	0.888	0.609	1.389	1.403	0.981	0.511	0.358	1.676	0.746
df	96.701	95.982	98.202	97.657	97.061	96.226	100.762	96.049	99.393	94.240	100.855
P	0.006	0.417	0.377	0.544	0.168	0.164	0.329	0.610	0.721	0.097	0.458

	12) Crown	13) Nape	14) Mantle	15) Rump	16) Tail	17) Wing coverts	18) Wing primariesNsec ondaries	19) Throat	20) Breast	21) Belly	22) Tail underside
Intercept	-0.001	-0.006	-0.002	0.006	0.003	-0.003	0.000	0.006	-0.004	-0.001	-0.001
x	0.909	0.943	0.940	1.014	0.972	0.884	0.896	0.845	0.878	0.908	1.062
lambda	0.193	0.282	0.141	0.519	0.375	0.370	0.492	0.802	0.158	0.004	0.375
log(L)	479.294	487.400	498.630	484.370	491.425	504.206	529.011	538.097	487.217	553.927	733.208
r2	0.844	0.890	0.873	0.742	0.727	0.881	0.821	0.865	0.832	0.871	0.791
T	2.801	2.040	1.983	0.314	0.624	4.126	2.982	5.271	3.666	3.082	1.432
df	95.521	94.052	94.596	99.008	98.805	94.329	96.281	94.852	95.928	94.656	88.004
P	0.006	0.044	0.050	0.754	0.534	0.000	0.004	0.000	0.000	0.003	0.156

	23) Crown	24) Nape	25) Mantle	26) Rump	27) Tail	28) Wing coverts	29) Wing primaries secondaries	30) Throat	31) Breast	32) Belly	33) Tail underside
Intercept	-0.005	-0.007	0.000	0.008	0.018	0.008	0.015	0.003	-0.007	-0.001	0.000
x	1.018	1.075	0.991	0.911	0.740	0.920	0.808	1.007	1.037	1.009	0.962
lambda	0.023	0.000	0.059	0.059	0.000	0.345	0.384	0.645	0.511	0.321	0.227
log(L)	517.994	519.78 7	405.879	346.43 9	518.84 8	678.119	569.188	314.961	295.71 5	294.4 18	411.422
r ²	0.891	0.949	0.750	0.485	0.677	0.795	0.689	0.802	0.668	0.820	0.839
T	0.611	3.714	0.208	1.497	6.089	2.134	4.413	0.178	0.720	0.237	1.069
df	94.000	92.199	98.720	109.03 8	100.61 4	97.166	100.936	96.940	101.71 4	96.34 2	86.540
p	0.543	0.000	0.836	0.137	0.000	0.035	0.000	0.859	0.473	0.813	0.288

Table S5. Results of Phylogenetic generalized least square (PGLS) used to test the influence of predictor variables (light environment, body size, hunting strategy, territoriality, and parental care) separately for PC1, PC2 and achromatic property of plumage colour and for each body patch. Intercept estimates, standard error and p-values are reported.

	1) Crown (PC1 male)		2) Nape (PC1 male)		3) Mantle (PC1 male)	
	Estimate (+/- SE)	P [anova]	Estimate (+/- SE)	P [anova]	Estimate (+/- SE)	P [anova]
Intercept	-0.010343 (+/- 0.124236)		0.0368426 (+/- 0.1434900)		0.03266262 (+/- 0.11037371)	
LE [open]	0.023141 (+/- 0.041891)	0.1593	-0.0020348 (+/- 0.0466115)	0.06255	0.00605022 (+/- 0.03468974)	0.07762
LE [woodland]	0.067371 (+/- 0.038135)		0.0639499 (+/- 0.0424174)		0.04469185 (+/- 0.03156135)	
Body size	0.005231 (+/- 0.023503)	0.8863	-0.0088143 (+/- 0.0267616)	0.55663	-0.02510650 (+/- 0.02032583)	0.26068
Territoriality	-0.011355 (+/- 0.025872)	0.3906	-0.0037491 (+/- 0.0286220)	0.64779	-0.00014162 (+/- 0.02119588)	0.99637
Strategy [ground catcher]	-0.046947 (+/- 0.039468)	0.1191	-0.0393844 (+/- 0.0439934)	0.3198	0.01893655 (+/- 0.03280765)	0.63236
Strategy [ground dweller]	0.072366 (+/- 0.053835)		0.0741595 (+/- 0.0606180)		0.06142436 (+/- 0.04562953)	
Strategy [water diver]	-0.085424 (+/- 0.052321)		-0.0645440 (+/- 0.0585493)		0.01368993 (+/- 0.04374644)	
Parental care [pair]	-0.066904 (+/- 0.034445)	0.0547	-0.0713602 (+/- 0.0383431)	0.06545	-0.03227148 (+/- 0.02855992)	0.261
Multiple R2	0.1166		0.1093		0.08098	
Adjusted R2	0.05117		0.04336		0.0129	
Lambda	0.746		0.781		0.809	

	4) Rump (PC1 male)		5) Tail (PC1 male)		6) Wing coverts (PC1 male)	
	Estimate (+/- SE)	P [anova]	Estimate (+/- SE)	P [anova]	Estimate (+/- SE)	P [anova]
Intercept	0.0905893 (+/- 0.0892876)		0.1186803 (+/- 0.0824727)		0.14031328 (+/- 0.11320663)	
LE [open]	0.0652571 (+/- 0.0358140)	0.03284	0.0297157 (+/- 0.0307945)	0.08867	-0.01770113 (+/- 0.03258898)	0.25987
LE [woodland]	0.0475057 (+/- 0.0327259)		0.0590519 (+/- 0.0281134)		0.01158353 (+/- 0.02964016)	
Body size	-0.0246917 (+/- 0.0180234)	0.10518	-0.0270005 (+/- 0.0162305)	0.03541 *	-0.02864059 (+/- 0.02015610)	0.10347
Territoriality	0.0032111 (+/- 0.0227077)	0.74737	-0.0072417 (+/- 0.0193359)	0.60121	-0.00021555 (+/- 0.01968382)	0.98861
Strategy [ground catcher]	0.0132858 (+/- 0.0335942)	0.53695	-0.0179641 (+/- 0.0289211)	0.45766	0.00300550 (+/- 0.03107904)	0.8146
Strategy [ground dweller]	-0.0486257 (+/- 0.0440928)		-0.0275436 (+/- 0.0384931)		-0.01477763 (+/- 0.04436933)	
Strategy [water diver]	-0.0150233 (+/- 0.0428029)		-0.0598259 (+/- 0.0377874)		-0.02435978 (+/- 0.04134673)	
Parental care [pair]	-0.0245901 (+/- 0.0294436)	0.40547	0.0124245 (+/- 0.0253165)	0.6246	-0.05097208 (+/- 0.02698077)	0.06155
Multiple R2	0.1053		0.1056		0.08428	
Adjusted R2	0.03903		0.03871		0.01645	
Lambda	0.542		0.632		0.871	

	7) Wing primaries secondaries (PC1 male)		8) Throat (PC1 male)		9) Breast (PC1 male)	
	Estimate (+/- SE)	P [anova]	Estimate (+/- SE)	P [anova]	Estimate (+/- SE)	P [anova]
Intercept	0.05808174 (+/- 0.08964472)		-0.1821994 (+/- 0.0678155)		-0.0945837 (+/- 0.0755598)	
LE [open]	0.06397747 (+/- 0.03093709)	0.05561	0.0588288 (+/- 0.0296963)	0.02161 *	0.0526700 (+/- 0.0376472)	0.02504 *
LE [woodland]	0.06448191 (+/- 0.02817117)		0.0551267 (+/- 0.0272415)		0.0611907 (+/- 0.0348672)	

Body size	-0.01310875 0.01710863)	(+/-)	0.239 22	0.0175379 0.0141516)	(+/-)	0.3380 5	0.0008635 0.0166318)	(+/-)	0.7576 5
Territoriality	-0.00076596 0.01917656)	(+/-)	0.841 69	0.0068770 0.0190614)	(+/-)	0.6817 5	-0.0059317 0.0246111)	(+/-)	0.9670 5
Strategy [ground catcher]	-0.02150208 0.02912202)	(+/-)	0.537 04	-0.0050242 0.0278201)	(+/-)	0.4070 4	0.0435372 0.0352090)	(+/-)	0.0888 4
Strategy [ground dweller]	-0.01590596 0.03948447)	(+/-)		-0.0445092 0.0360468)	(+/-)		-0.0404899 0.0451794)	(+/-)	
Strategy [water diver]	-0.05206820 0.03847720)	(+/-)		-0.0461946 0.0343564)	(+/-)		-0.0490928 0.0410736)	(+/-)	
Parental care [pair]	-0.02308086 0.02543664)	(+/-)	0.366 22	0.0167399 0.0243748)	(+/-)	0.4937	-0.0167259 0.0307343)	(+/-)	0.5874 2
<i>Multiple R2</i>	0.08773			0.1033			0.1199		
<i>Adjusted R2</i>	0.02016			0.03688			0.05473		
<i>Lambda</i>	0.722			0.424			0.251		

	10) Belly (PC1 male)		11) Tail underside (PC1 male)	
	Estimate (+/- SE)	P [anova]	Estimate (+/- SE)	P [anova]
Intercept	-0.0470289 (+/- 0.0736081)		-0.0139418 (+/- 0.0501061)	
LE [open]	0.0309675 (+/- 0.0350969)	0.255134	0.0388365 (+/- 0.0137321)	0.001497 **
LE [woodland]	0.0060229 (+/- 0.0323786)		0.0491576 (+/- 0.0125795)	
Body size	0.0090901 (+/- 0.0158957)	0.920762	0.0047609 (+/- 0.0089198)	0.763255
Territoriality	-0.0431426 (+/- 0.0227963)	0.15757	-0.0032184 (+/- 0.0082986)	0.421251
Strategy [ground catcher]	0.0864817 (+/- 0.0328440)	0.004043 **	-0.0153688 (+/- 0.0131041)	0.498733
Strategy [ground dweller]	-0.0315177 (+/- 0.0422270)		0.0088834 (+/- 0.0189662)	
Strategy [water diver]	-0.0332168 (+/- 0.0391185)		-0.0180617 (+/- 0.0181382)	
Parental care [pair]	-0.0415155 (+/- 0.0287155)	0.151142	0.0006593 (+/- 0.0113502)	0.953791
<i>Multiple R2</i>	0.1626		0.1404	
<i>Adjusted R2</i>	0.1006		0.07432	
<i>Lambda</i>	0.309		0.895	

	12) Crown (PC2 male)			13) Nape (PC2 male)			14) Mantle (PC2 male)		
	Estimate (+/- SE)	P [anova]		Estimate (+/- SE)	P [anova]		Estimate (+/- SE)	P [anova]	
Intercept	-0.0435050 0.0459850)	(+/-)		-0.0048523 0.0561150)	(+/-)		-0.0672806 0.0297160)	(+/-)	
LE [open]	-0.0638506 0.018939)	(+/-)	0.0043 27	-0.0559654 0.0216564)	(+/-)	0.0698 4	-0.0025387 0.0185969)	(+/-)	0.3070 25
LE [woodland]	-0.0317906 0.0173239)	(+/-)		-0.0382899 0.0197649)	(+/-)		-0.0232191 0.0181326)	(+/-)	
Body size	0.0144548 0.0093747)	(+/-)	0.0539 58	0.0086176 0.0111660)	(+/-)	0.2647 9	0.0143356 0.0075768)	(+/-)	0.0069 77
Territoriality	-0.0045562 0.0120539)	(+/-)	0.8725 79	-0.0145853 0.0136545)	(+/-)	0.4014 5	-0.0074146 0.0129413)	(+/-)	0.6786 42
Strategy [ground catcher]	0.0191948 0.0177584)	(+/-)	0.4112 57	0.0139488 0.0203278)	(+/-)	0.4355 1	0.0192326 0.0169037)	(+/-)	0.2707 96
Strategy [ground dweller]	-0.0012992 0.0232062)	(+/-)		-0.0064151 0.0268717)	(+/-)		0.0107406 0.0229621)	(+/-)	
Strategy [water diver]	0.0333081 0.0224299)	(+/-)		0.0426243 0.0262008)	(+/-)		0.0266562 0.0173897)	(+/-)	
Parental care [pair]	0.0089613 0.0155660)	(+/-)	0.5660 19	-0.0127558 0.0178081)	(+/-)	0.4753 6	0.0072477 0.0150642)	(+/-)	0.6314 04
<i>Multiple R2</i>	0.1463			0.09003			0.1171		
<i>Adjusted R2</i>	0.08306			0.02263			0.05171		
<i>Lambda</i>	0.507			0.592			0		

	15) Rump (PC2 male)		16) Tail (PC2 male)		17) Wing coverts (PC2 male)	
	Estimate (+/- SE)	P [anova]	Estimate (+/- SE)	P [anova]	Estimate (+/- SE)	P [anova]
Intercept	-0.07086896 (+/- 0.04035142)		-0.0465466 (+/- 0.0386847)		-0.0459198 (+/- 0.0519546)	
LE [open]	0.01870448 (+/- 0.01608084)	0.6844	-0.0116227 (+/- 0.0169444)	0.7977	-0.0147970 (+/- 0.0217159)	0.6759
LE [woodland]	0.01305597 (+/- 0.01469099)		-0.0162781 (+/- 0.0155609)		-0.0085830 (+/- 0.0198755)	
Body size	0.00204408 (+/- 0.00812561)	0.5094	0.0066301 (+/- 0.0080868)	0.253	0.0052963 (+/- 0.0106506)	0.3401
Territoriality	-0.00382736 (+/- 0.01018654)	0.6983	-0.0033563 (+/- 0.0108894)	0.852	-0.0142840 (+/- 0.0138493)	0.415
Strategy [ground catcher]	0.01397880 (+/- 0.01508574)	0.2338	0.0106669 (+/- 0.0158747)	0.4859	0.0360301 (+/- 0.0203569)	0.1403
Strategy [ground dweller]	0.03740571 (+/- 0.01982275)		0.0102786 (+/- 0.0205671)		0.0378588 (+/- 0.0265419)	
Strategy [water diver]	0.02072850 (+/- 0.01926015)		0.0323489 (+/- 0.0196812)		0.0511085 (+/- 0.0255807)	
Parental care [pair]	0.00068408 (+/- 0.01322118)	0.9588	-0.0107096 (+/- 0.0139078)	0.443	-0.0221816 (+/- 0.0178434)	0.2165
Multiple R2	0.05003		0.04345		0.0809	
Adjusted R2	-0.02034		-0.02807		0.01282	
Lambda	0.551		0.422		0.487	

	18) Wing primaries secondaries (PC2 male)		19) Throat (PC2 male)		20) Breast (PC2 male)	
	Estimate (+/- SE)	P [anova]	Estimate (+/- SE)	P [anova]	Estimate (+/- SE)	P [anova]
Intercept	-0.0071202 (+/- 0.0514018)		0.0395109 (+/- 0.0827760)		-0.0043994 (+/- 0.0317822)	
LE [open]	-0.0051221 (+/- 0.0186455)	0.7261	-0.0171773 (+/- 0.0122629)	0.01724 *	-0.0030264 (+/- 0.0198900)	0.82144
LE [woodland]	-0.0130754 (+/- 0.0169922)		-0.0289204 (+/- 0.0110363)		-0.0125059 (+/- 0.0193934)	
Body size	-0.0059245 (+/- 0.0099952)	0.8347	0.0078048 (+/- 0.0124505)	0.18649	0.0055243 (+/- 0.0081037)	0.42673
Territoriality	-0.0084465 (+/- 0.0116472)	0.5017	-0.0059775 (+/- 0.0060884)	0.83571	-0.0208240 (+/- 0.0138411)	0.10253
Strategy [ground catcher]	0.0018887 (+/- 0.0175254)	0.439	0.0325792 (+/- 0.0142502)	0.03531 *	0.0007745 (+/- 0.0180790)	0.09164
Strategy [ground dweller]	0.0189060 (+/- 0.0234759)		0.0178296 (+/- 0.0269448)		0.0158610 (+/- 0.0245587)	
Strategy [water diver]	0.0347975 (+/- 0.0229400)		0.0347617 (+/- 0.0144475)		0.0393703 (+/- 0.0185988)	
Parental care [pair]	-0.0114015 (+/- 0.0153316)	0.4587	-0.0134349 (+/- 0.0137115)	0.32936	0.0024858 (+/- 0.0161116)	0.87767
Multiple R2	0.03933		0.1569		0.0877	
Adjusted R2	-0.03183		0.09446		0.02012	
Lambda	0.667		1		0	

	21) Belly (PC2 male)		22) Tail underside (PC2 male)	
	Estimate (+/- SE)	P [anova]	Estimate (+/- SE)	P [anova]
Intercept	-0.0321287 (+/- 0.0265854)		0.0050962 (+/- 0.0159839)	
LE [open]	0.0019185 (+/- 0.0166377)	0.24427	-0.0149363 (+/- 0.0052634)	0.01617 *
LE [woodland]	0.0188119 (+/- 0.0162224)		-0.0071893 (+/- 0.0048202)	
Body size	0.0048308 (+/- 0.0067786)	0.25354	0.0024075 (+/- 0.0030535)	2.80E-01
Territoriality	-0.0058999 (+/- 0.0115779)	0.43444	-0.0063028 (+/- 0.0032716)	1.10E-01

Strategy [ground catcher]	-0.0053237 (+/- 0.0151229)	0.02379 *	0.0047706 (+/- 0.0049569)	0.2251
Strategy [ground dweller]	0.0284896 (+/- 0.0205430)		-0.0109829 (+/- 0.0067811)	
Strategy [water diver]	0.0351929 (+/- 0.0155577)		0.0048814 (+/- 0.0067882)	
Parental care [pair]	0.0018184 (+/- 0.0134772)	0.89292	0.0055941 (+/- 0.0043197)	0.19818
Multiple R2	0.1194		0.1508	
Adjusted R2	0.05417		0.08546	
Lambda	0		0.756	

	23) Crown (Achromatic property male)		24) Nape (Achromatic property male)		25) Mantle (Achromatic property male)	
	Estimate (+/- SE)	P [anova]	Estimate (+/- SE)	P [anova]	Estimate (+/- SE)	P [anova]
Intercept	0.0273841 (+/- 0.0232048)		0.0242207 (+/- 0.0282315)		0.0119774 (+/- 0.0394977)	
LE [open]	0.0081801 (+/- 0.0145221)	0.11883	0.0206683 (+/- 0.0176679)	0.02178	0.0421943 (+/- 0.0220244)	0.000749
LE [woodland]	0.0039800 (+/- 0.0141595)		0.0054648 (+/- 0.0172268)		0.0312699 (+/- 0.0207059)	
Body size	0.0120636 (+/- 0.0059166)	0.07018	0.0167916 (+/- 0.0071983)	0.04717	0.0155245 (+/- 0.0092038)	0.170431
Territoriality	0.0166246 (+/- 0.0101057)	0.08892	0.0128503 (+/- 0.0122948)	0.26454	0.0260711 (+/- 0.0146907)	0.067997
Strategy [ground catcher]	-0.0022198 (+/- 0.0131998)	0.27467	0.0036991 (+/- 0.0160592)	0.32997	-0.0121920 (+/- 0.0205286)	0.356055
Strategy [ground dweller]	-0.0243082 (+/- 0.0179308)		-0.0238971 (+/- 0.0218150)		-0.0454953 (+/- 0.0264644)	
Strategy [water diver]	-0.0122309 (+/- 0.0135793)		-0.0104858 (+/- 0.0165210)		-0.0053522 (+/- 0.0225839)	
Parental care [pair]	-0.0136094 (+/- 0.0117634)	0.24985	-0.0227647 (+/- 0.0143116)	0.11461	-0.0200953 (+/- 0.0178647)	0.263142
Multiple R2	0.1284		0.1511		0.1894	
Adjusted R2	0.06382		0.08818		0.1294	
Lambda	0		0		0.116	

	26) Rump (Achromatic property male)		27) Tail (Achromatic property male)		28) Wing coverts (Achromatic property male)	
	Estimate (+/- SE)	P [anova]	Estimate (+/- SE)	P [anova]	Estimate (+/- SE)	P [anova]
Intercept	0.09385417 (+/- 0.06142567)		0.1034824 (+/- 0.0191691)		0.03957460 (+/- 0.02280543)	
LE [open]	0.00157472 (+/- 0.02617384)	0.88009	0.0088044 (+/- 0.0119527)	0.18706	0.02408429 (+/- 0.00886884)	4.792e-06 ***
LE [woodland]	0.00265652 (+/- 0.02397678)		-0.0096632 (+/- 0.0116751)		0.00091095 (+/- 0.00809603)	
Body size	0.00540537 (+/- 0.01268448)	0.32639	-0.0050794 (+/- 0.0049006)	0.16934	0.00725893 (+/- 0.00455080)	0.181988
Territoriality	0.00068202 (+/- 0.01673716)	0.97009	-0.0068127 (+/- 0.0083230)	0.24369	0.01947407 (+/- 0.00559816)	0.001477 **
Strategy [ground catcher]	-0.01785682 (+/- 0.02452921)	0.01007	0.0059299 (+/- 0.0108651)	0.06051	-0.02208751 (+/- 0.00832359)	0.064034
Strategy [ground dweller]	0.03672868 (+/- 0.03189412)		0.0393144 (+/- 0.0147621)		-0.01356624 (+/- 0.01098677)	
Strategy [water diver]	0.08967119 (+/- 0.03060944)		0.0217312 (+/- 0.0112851)		-0.00636326 (+/- 0.01070505)	
Parental care [pair]	-0.03945328 (+/- 0.02149825)	0.06923	-0.0197925 (+/- 0.0096958)	0.04368	-0.00654123 (+/- 0.00729269)	0.371737
Multiple R2	0.1324		0.1472		0.3087	
Adjusted R2	0.06815		0.08347		0.2575	
Lambda	0.461		0		0.582	

	29) Wing primaries secondaries (Achromatic property male)		30) Throat (Achromatic property male)		31) Breast (Achromatic property male)	
	Estimate (+/- SE)	P [anova]	Estimate (+/- SE)	P [anova]	Estimate (+/- SE)	P [anova]
Intercept	0.0808116 (+/- 0.0394818)		0.2166934 (+/- 0.1123958)		0.2490859 (+/- 0.0944937)	
LE [open]	0.0418790 (+/- 0.0139391)	0.0009382 ***	0.1257470 (+/- 0.0366790)	0.0009233 ***	0.0481197 (+/- 0.0338039)	0.2532
LE [woodland]	0.0167712 (+/- 0.0126971)		0.0644169 (+/- 0.0333799)		0.0282766 (+/- 0.0307986)	
Body size	-0.0051154 (+/- 0.0075999)	0.3193557	-0.0197904 (+/- 0.0209993)	0.333981	-0.0224431 (+/- 0.0182793)	0.1206
Territoriality	0.0230546 (+/- 0.0086709)	0.0123182 *	0.0189131 (+/- 0.0225388)	0.426578	0.0231108 (+/- 0.0210710)	0.2877
Strategy [ground catcher]	-0.0090939 (+/- 0.0131116)	0.7955263	-0.0248721 (+/- 0.0346103)	0.838445	-0.0099839 (+/- 0.0317849)	0.7714
Strategy [ground dweller]	-0.0034896 (+/- 0.0176766)		-0.0135764 (+/- 0.0476284)		-0.0223628 (+/- 0.0427156)	
Strategy [water diver]	-0.0162217 (+/- 0.0172560)		0.0116475 (+/- 0.0460439)		-0.0378543 (+/- 0.0417256)	
Parental care [pair]	0.0025376 (+/- 0.0114609)	0.8251888	0.0077833 (+/- 0.0301702)	0.796912	-0.0130448 (+/- 0.0277948)	0.6398
Multiple R2	0.1783		0.1388		0.06668	
Adjusted R2	0.1174		0.07503		-0.002454	
Lambda	0.697		0.777		0.683	

	32) Belly (Achromatic property male)		33) Tail underside (Achromatic property male)	
	Estimate (+/- SE)	P [anova]	Estimate (+/- SE)	P [anova]
Intercept	0.3820028 (+/- 0.0870095)		0.0654970 (+/- 0.0480834)	
LE [open]	0.0191164 (+/- 0.0412746)	0.07746	0.0196467 (+/- 0.0209071)	0.00113 **
LE [woodland]	-0.0493470 (+/- 0.0380623)		-0.0311452 (+/- 0.0192914)	
Body size	-0.0326141 (+/- 0.0187493)	0.08563	0.0165256 (+/- 0.0101949)	0.11185
Territoriality	0.0143519 (+/- 0.0267893)	0.46424	0.0091622 (+/- 0.0135357)	0.48554
Strategy [ground catcher]	0.0478482 (+/- 0.0386277)	0.66577	-0.0037262 (+/- 0.0195982)	0.98961
Strategy [ground dweller]	0.0093057 (+/- 0.0496792)		-0.0066612 (+/- 0.0253670)	
Strategy [water diver]	0.0176931 (+/- 0.0461145)		0.0025725 (+/- 0.0247049)	
Parental care [pair]	-0.0212478 (+/- 0.0337779)	0.53065	-0.0131891 (+/- 0.0171669)	0.44406
Multiple R2	0.0906		0.1494	
Adjusted R2	0.02324		0.08396	
Lambda	0.316		0.408	

	34) Crown (PC1 female)		35) Nape (PC1 female)		36) Mantle (PC1 female)	
	Estimate (+/- SE)	P [anova]	Estimate (+/- SE)	P [anova]	Estimate (+/- SE)	P [anova]
Intercept	-0.0079372 (+/- 0.1040191)		-0.07499248 (+/- 0.12319704)		-0.0082632 (+/- 0.0967293)	
LE [open]	0.0086268 (+/- 0.0373970)	0.2556	0.02635005 (+/- 0.04376040)	0.06169	0.0115820 (+/- 0.0329593)	0.04457
LE [woodland]	0.0418800 (+/- 0.0338864)		0.07936183 (+/- 0.03964999)		0.0500593 (+/- 0.0298604)	
Body size	-0.0011823 (+/- 0.0200159)	0.7842	0.00608792 (+/- 0.02360291)	0.87025	-0.0186025 (+/- 0.0182520)	0.49309
Territoriality	-0.0235915 (+/- 0.0241322)	0.222	-0.01734488 (+/- 0.02819884)	0.4251	0.0090732 (+/- 0.0211338)	0.55851
Strategy [ground catcher]	-0.0180077 (+/- 0.0338773)	0.3662	0.00024662 (+/- 0.03964033)	0.34035	0.0268673 (+/- 0.0298585)	0.40249

Strategy [ground dweller]	0.0571955 (+/- 0.0463072)		0.08531473 (+/- 0.05438077)		0.0648980 (+/- 0.0414940)	
Strategy [water diver]	-0.0475013 (+/- 0.0453827)		-0.04179918 (+/- 0.05326075)		0.0424163 (+/- 0.0404723)	
Parental care [pair]	-0.0402990 (+/- 0.0309507)	0.1958	-0.03687056 (+/- 0.03622308)	0.31108	-0.0395253 (+/- 0.0272990)	0.15063
Multiple R2	0.08094		0.09339		0.1047	
Adjusted R2	0.01091		0.02432		0.0365	
Lambda	0.684		0.698		0.742	

	37) Rump (PC1 female)			38) Tail (PC1 female)			39) Wing coverts (PC1 female)		
	Estimate (+/- SE)	P [anova]		Estimate (+/- SE)	P [anova]		Estimate (+/- SE)	P [anova]	
Intercept	0.0098458 (+/- 0.0901642)			0.1399253 (+/- 0.0850906)			0.0885276 (+/- 0.1098588)		
LE [open]	0.1063591 (+/- 0.0381762)	0.006625		0.0185949 (+/- 0.0329946)	0.17629		0.0119126 (+/- 0.0348112)	0.1236	
LE [woodland]	0.0901149 (+/- 0.0346934)			0.0416801 (+/- 0.0299213)			0.0416609 (+/- 0.0315430)		
Body size	-0.0162766 (+/- 0.0183866)	0.311665		-0.0269855 (+/- 0.0168211)	0.08728		-0.0242279 (+/- 0.0201728)	0.2295	
Territoriality	-0.0190495 (+/- 0.0250430)	0.440889		-0.0301118 (+/- 0.0214680)	0.16398		-0.0091748 (+/- 0.0221304)	0.7283	
Strategy [ground catcher]	-0.0019282 (+/- 0.0346370)	0.972725		0.0079714 (+/- 0.0299064)	0.96382		0.0059625 (+/- 0.0315800)	0.9927	
Strategy [ground dweller]	-0.0187912 (+/- 0.0454272)			0.0036291 (+/- 0.0400307)			0.0019152 (+/- 0.0449507)		
Strategy [water diver]	-0.0154105 (+/- 0.0438504)			-0.0118480 (+/- 0.0391711)			0.0010284 (+/- 0.0432218)		
Parental care [pair]	0.0144259 (+/- 0.0314598)	0.647505		-0.0071164 (+/- 0.0272712)	0.79464		-0.0371248 (+/- 0.0288886)	0.2016	
Multiple R2	0.1071			0.07749			0.06743		
Adjusted R2	0.03911			0.007201			-0.003622		
Lambda	0.474			0.592			0.809		

	40) Wing primaries secondaries (PC1 female)			41) Throat (PC1 female)			42) Breast (PC1 female)		
	Estimate (+/- SE)	P [anova]		Estimate (+/- SE)	P [anova]		Estimate (+/- SE)	P [anova]	
Intercept	-0.0364881 (+/- 0.0799681)			-0.2232991 (+/- 0.0622170)			-0.1149416 (+/- 0.0755396)		
LE [open]	0.0713343 (+/- 0.0316197)	0.01851*		0.0572916 (+/- 0.0277320)	0.01631*		0.0539350 (+/- 0.0330918)	0.02694*	
LE [woodland]	0.0758108 (+/- 0.0286844)			0.0498817 (+/- 0.0252526)			0.0359933 (+/- 0.0301106)		
Body size	0.0030147 (+/- 0.0159177)	0.94828		0.0258531 (+/- 0.0129242)	0.06782		0.0068123 (+/- 0.0155933)	0.73166	
Territoriality	-0.0150905 (+/- 0.0206136)	0.42573		-0.0019673 (+/- 0.0182654)	0.98694		-0.0308577 (+/- 0.0217671)	0.33334	
Strategy [ground catcher]	-0.0032431 (+/- 0.0286661)	0.76171		0.0087747 (+/- 0.0251760)	0.5037		0.0664326 (+/- 0.0300358)	0.05432	
Strategy [ground dweller]	-0.0138351 (+/- 0.0381822)			-0.0302826 (+/- 0.0326999)			-0.0318104 (+/- 0.0391326)		
Strategy [water diver]	-0.0390855 (+/- 0.0372900)			-0.0329162 (+/- 0.0311346)			-0.0032747 (+/- 0.0374500)		
Parental care [pair]	0.0093120 (+/- 0.0261219)	0.72219		0.0178359 (+/- 0.0227901)	0.43562		-0.0174700 (+/- 0.0272225)	0.52243	
Multiple R2	0.08874			0.1246			0.1382		
Adjusted R2	0.01931			0.05788			0.0725		
Lambda	0.567			0.403			0.427		

	43) Belly (PC1 female)		44) Tail underside (PC1 female)	
	Estimate (+/- SE)	P [anova]	Estimate (+/- SE)	P [anova]
Intercept	-0.02685984 (+/- 0.06712942)		0.0305029 (+/- 0.0468390)	
LE [open]	0.01168772 (+/- 0.03250179)	0.56013	0.0381136 (+/- 0.0140208)	0.007197 **
LE [woodland]	-0.00873561 (+/- 0.02973969)		0.0369180 (+/- 0.0128347)	
Body size	-0.00093953 (+/- 0.01438750)	0.86436	-0.0011114 (+/- 0.0083870)	0.80307
Territoriality	-0.01018559 (+/- 0.02152738)	0.8986	-0.0193082 (+/- 0.0085073)	0.015609 *
Strategy [ground catcher]	0.09646971 (+/- 0.02953243)	0.00258 **	0.0055090 (+/- 0.0123317)	0.44604
Strategy [ground dweller]	-0.00301566 (+/- 0.03790438)		0.0101849 (+/- 0.0182491)	
Strategy [water diver]	-0.01346880 (+/- 0.03498659)		-0.0216189 (+/- 0.0185170)	
Parental care [pair]	-0.03761446 (+/- 0.02654685)	0.15947	-0.0157498 (+/- 0.0112427)	0.164309
Multiple R2	0.1492		0.173	
Adjusted R2	0.08434		0.1075	
Lambda	0.288		0.875	

	45) Crown (PC2 female)		46) Nape (PC2 female)		47) Mantle (PC2 female)	
	Estimate (+/- SE)	P [anova]	Estimate (+/- SE)	P [anova]	Estimate (+/- SE)	P [anova]
Intercept	-1.7067 (+/- 0.090827)		-0.0329888 (+/- 0.0520968)		-0.0652141 (+/- 0.0293619)	
LE [open]	-0.05263173 (+/- 0.01736706)	0.031259	-0.0611967 (+/- 0.0194657)	0.03664	-0.0061056 (+/- 0.0183033)	0.249196
LE [woodland]	-0.02877024 (+/- 0.01581462)		-0.0477567 (+/- 0.0176439)		-0.0212078 (+/- 0.0175389)	
Body size	0.01839570 (+/- 0.00809201)	0.008762	0.0119559 (+/- 0.0101642)	0.11346	0.0135309 (+/- 0.0072305)	0.005272
Territoriality	0.00040179 (+/- 0.01143894)	0.80932	-0.0017228 (+/- 0.0126158)	0.85044	-0.0024191 (+/- 0.0124214)	0.951537
Strategy [ground catcher]	0.01420024 (+/- 0.01576649)	0.402898	0.0153916 (+/- 0.0176379)	0.2504	0.0144985 (+/- 0.0162906)	0.373245
Strategy [ground dweller]	-0.01067975 (+/- 0.02047710)		-0.0209325 (+/- 0.0238441)		0.0110354 (+/- 0.0215255)	
Strategy [water diver]	0.02581525 (+/- 0.01949488)		0.0377600 (+/- 0.0233776)		0.0198612 (+/- 0.0163928)	
Parental care [pair]	0.01250494 (+/- 0.01427197)	0.382927	0.0031109 (+/- 0.0161010)	0.84717	0.0120403 (+/- 0.0144933)	0.408
Multiple R2	0.1469		0.1148		0.1234	
Adjusted R2	0.08191		0.04732		0.05662	
Lambda	0.402		0.638		0	

	48) Rump (PC2 female)		49) Tail (PC2 female)		50) Wing coverts (PC2 female)	
	Estimate (+/- SE)	P [anova]	Estimate (+/- SE)	P [anova]	Estimate (+/- SE)	P [anova]
Intercept	-0.0759056 (+/- 0.0396871)		-0.06462753 (+/- 0.03509956)		-0.0445032 (+/- 0.0479644)	
LE [open]	0.0231630 (+/- 0.0176838)	0.3468	-0.00342326 (+/- 0.01658399)	0.70669	-0.0193658 (+/- 0.0205249)	0.6057
LE [woodland]	0.0186236 (+/- 0.0161025)		-0.01031547 (+/- 0.01514929)		-0.0107729 (+/- 0.0186591)	
Body size	0.0034874 (+/- 0.0082431)	0.4339	0.01080639 (+/- 0.00745156)	0.08946	0.0070167 (+/- 0.0098181)	0.3094
Territoriality	-0.0029277 (+/- 0.0116470)	0.7832	-0.00236469 (+/- 0.01096716)	0.84085	-0.0148788 (+/- 0.0134758)	0.4172

Strategy [ground catcher]	0.0043148 0.0160539)	(+/-)	0.571 3	0.00248460 0.01506530)	(+/-)	0.722 11	0.0317783 0.0186243)	(+/-)	0.3566
Strategy [ground dweller]	0.0151610 0.0208528)	(+/-)		0.00522739 0.01939416)	(+/-)		0.0122255 0.0243740)	(+/-)	
Strategy [water diver]	0.0228005 0.0198566)	(+/-)		0.01979656 0.01808716)	(+/-)		0.0296545 0.0234696)	(+/-)	
Parental care [pair]	0.0091665 0.0145328)	(+/-)	0.529 6	0.00010526 0.01357296)	(+/-)	0.993 83	-0.0140944 0.0169054)	(+/-)	0.4063
<i>Multiple R2</i>	0.04758			0.04552			0.05982		
<i>Adjusted R2</i>	-0.02498			-0.02721			-0.01181		
<i>Lambda</i>	0.403			0.322			0.46		

	51) Wing primaries secondaries (PC2 female)			52) Throat (PC2 female)			53) Breast (PC2 female)		
	Estimate (+/- SE)	P [anova]		Estimate (+/- SE)	P [anova]		Estimate (+/- SE)	P [anova]	
Intercept	-2.1233e-02 4.6342e-02)	(+/-)		0.05533171 0.06611455)	(+/-)		0.0043553 0.0299826)	(+/-)	
LE [open]	-1.3423e-02 1.7184e-02)	(+/-)	0.590 1	-0.01753920 0.01308593)	(+/-)	0.234 7	-0.0143077 0.0186903)	(+/-)	0.46
LE [woodland]	-1.4662e-02 1.5574e-02)	(+/-)		-0.02594428 0.01186560)	(+/-)		-0.0109194 0.0179097)	(+/-)	
Body size	-7.0796e-04 9.0169e-03)	(+/-)	0.741 1	0.00525414 0.01042672)	(+/-)	0.280 5	0.0019219 0.0073834)	(+/-)	0.6229
Territoriality	-1.4738e-02 1.1127e-02)	(+/-)	0.208 8	-0.01211689 0.00849376)	(+/-)	0.429 1	-0.0058505 0.0126840)	(+/-)	0.5567
Strategy [ground catcher]	1.5203e-03 1.5569e-02)	(+/-)	0.448 5	0.02114780 0.01330167)	(+/-)	0.270 9	-0.0031930 0.0166350)	(+/-)	0.3678
Strategy [ground dweller]	7.4667e-03 2.1092e-02)	(+/-)		0.00030626 0.02227813)	(+/-)		0.0096610 0.0219806)	(+/-)	
Strategy [water diver]	3.1876e-02 2.0682e-02)	(+/-)		0.02542629 0.01634195)	(+/-)		0.0214364 0.0167393)	(+/-)	
Parental care [pair]	4.8563e-05 1.4215e-02)	(+/-)	0.997 3	-0.00967929 0.01231019)	(+/-)	0.433 5	0.0062872 0.0147997)	(+/-)	0.6718
<i>Multiple R2</i>	0.04927			0.08163			0.05001		
<i>Adjusted R2</i>	-0.02316			0.01166			-0.02237		
<i>Lambda</i>	0.648			0.983			0		

	54) Belly (PC2 female)		55) Tail underside (PC2 female)	
	Estimate (+/- SE)	P [anova]	Estimate (+/- SE)	P [anova]
Intercept	-0.0383617 (+/- 0.0253966)		-0.0053770 (+/- 0.0152708)	
LE [open]	0.0072959 (+/- 0.0158315)	0.19734	-0.0103237 (+/- 0.0060865)	0.17255
LE [woodland]	0.0209298 (+/- 0.0151703)		-0.0033075 (+/- 0.0055954)	
Body size	0.0061488 (+/- 0.0062541)	0.22314	0.0028717 (+/- 0.0030436)	0.2727
Territoriality	-0.0102050 (+/- 0.0107439)	0.23212	-0.0018400 (+/- 0.0038810)	0.70798
Strategy [ground catcher]	-0.0051201 (+/- 0.0140905)	0.06265	0.0013629 (+/- 0.0054012)	0.61455
Strategy [ground dweller]	0.0153675 (+/- 0.0186185)		-0.0077669 (+/- 0.0072934)	
Strategy [water diver]	0.0287659 (+/- 0.0141789)		0.0041337 (+/- 0.0074127)	
Parental care [pair]	0.0035558 (+/- 0.0125360)	0.77724	0.0082896 (+/- 0.0049092)	0.09439
<i>Multiple R2</i>	0.1166		0.08675	
<i>Adjusted R2</i>	0.04928		0.01441	
<i>Lambda</i>	0		0.575	

	56) Crown (Achromatic property female)		57) Nape (Achromatic property female)		58) Mantle (Achromatic property female)	
	Estimate (+/- SE)	P [anova]	Estimate (+/- SE)	P [anova]	Estimate (+/- SE)	P [anova]
Intercept	0.0087080 (+/- 0.0259384)		0.0181590 (+/- 0.0315313)		-0.0026035 (+/- 0.0351894)	
LE [open]	0.0098447 (+/- 0.0161692)	0.12207	0.0183697 (+/- 0.0196557)	0.04706	0.0371970 (+/- 0.0219360)	0.001639
LE [woodland]	0.0126050 (+/- 0.0154940)		0.0109071 (+/- 0.0188348)		0.0307404 (+/- 0.0210199)	
Body size	0.0157945 (+/- 0.0063875)	0.02378	0.0192894 (+/- 0.0077648)	0.04196	0.0206877 (+/- 0.0086656)	0.013315
Territoriality	0.0069795 (+/- 0.0109731)	0.46554	0.0051414 (+/- 0.0133392)	0.64687	0.0041241 (+/- 0.0148867)	0.614792
Strategy [ground catcher]	0.0048171 (+/- 0.0143912)	0.59581	0.0023830 (+/- 0.0174942)	0.41779	0.0127191 (+/- 0.0195238)	0.37824
Strategy [ground dweller]	-0.0164484 (+/- 0.0190157)		-0.0272750 (+/- 0.0231159)		-0.0379419 (+/- 0.0257977)	
Strategy [water diver]	-0.0038464 (+/- 0.0144814)		-0.0076148 (+/- 0.0176039)		0.0070922 (+/- 0.0196462)	
Parental care [pair]	-0.0184383 (+/- 0.0128035)	0.15281	-0.0245522 (+/- 0.0155642)	0.11769	-0.0081180 (+/- 0.0173698)	0.641208
<i>Multiple R2</i>	0.1181		0.1329		0.1834	
<i>Adjusted R2</i>	0.05091		0.06684		0.1211	
<i>Lambda</i>	0		0		0	

	59) Rump (Achromatic property female)		60) Tail (Achromatic property female)		61) Wing coverts (Achromatic property female)	
	Estimate (+/- SE)	P [anova]	Estimate (+/- SE)	P [anova]	Estimate (+/- SE)	P [anova]
Intercept	0.1384857 (+/- 0.0462151)		0.1118266 (+/- 0.0247048)		0.0510171 (+/- 0.0199051)	
LE [open]	0.0149405 (+/- 0.0288091)	0.53049	0.0056683 (+/- 0.0154002)	0.3187	0.0204103 (+/- 0.0083607)	1.345e-05***
LE [woodland]	0.0309418 (+/- 0.0276060)		-0.0073671 (+/- 0.0147571)		-0.0010858 (+/- 0.0075960)	
Body size	-0.0035992 (+/- 0.0113807)	0.62608	-0.0098508 (+/- 0.0060837)	0.148	0.0046900 (+/- 0.0040476)	2.41E-01
Territoriality	0.0070691 (+/- 0.0195511)	0.94185	-0.0048272 (+/- 0.0104512)	0.4701	0.0160002 (+/- 0.0054808)	0.007152**
Strategy [ground catcher]	-0.0100720 (+/- 0.0256411)	0.051	-0.0022452 (+/- 0.0137067)	0.1034	-0.0155078 (+/- 0.0075849)	0.154862
Strategy [ground dweller]	0.0676199 (+/- 0.0338808)		0.0362506 (+/- 0.0181113)		-0.0042126 (+/- 0.0099643)	
Strategy [water diver]	0.0549076 (+/- 0.0258019)		0.0169841 (+/- 0.0137927)		0.0042214 (+/- 0.0096354)	
Parental care [pair]	-0.0393521 (+/- 0.0228122)	0.08746	0.0015344 (+/- 0.0121945)	0.9001	-0.0075709 (+/- 0.0068923)	0.274515
<i>Multiple R2</i>	0.1065		0.09722		0.2783	
<i>Adjusted R2</i>	0.03848		0.02843		0.2233	
<i>Lambda</i>	0		0		0.485	

	62) Wing primaries secondaries (Achromatic property female)		63) Throat (Achromatic property female)		64) Breast (Achromatic property female)	
	Estimate (+/- SE)	P [anova]	Estimate (+/- SE)	P [anova]	Estimate (+/- SE)	P [anova]
Intercept	0.0700820 (+/- 0.0279152)		0.1927083 (+/- 0.1089691)		0.2417871 (+/- 0.0796045)	
LE [open]	0.0287561 (+/- 0.0113479)	0.001056**	0.0815107 (+/- 0.0365836)	0.01298*	0.0452751 (+/- 0.0349696)	0.1614

LE [woodland]	0.0130438 0.0103007)	(+/-		0.0299049 0.0331440)	(+/-		0.0095285 0.0318229)	(+/-	
Body size	-0.0022983 0.0056111)	(+/-	0.735615	-0.0102464 0.0204489)	(+/-	0.6228 8	-0.0119630 0.0164489)	(+/-	0.378 1
Territoriality	0.0228268 0.0074174)	(+/-	0.002229 **	0.0182799 0.0234160)	(+/-	0.3874 2	-0.0028251 0.0230072)	(+/-	0.935 1
Strategy [ground catcher]	-0.0031318 0.0102910)	(+/-	0.947075	-0.0054688 0.0331461)	(+/-	0.8110 7	0.0236620 0.0317413)	(+/-	0.775 6
Strategy [ground dweller]	-0.0034491 0.0136171)	(+/-		-0.0379058 0.0462827)	(+/-		-0.0091306 0.0413335)	(+/-	
Strategy [water diver]	0.0047601 0.0132482)	(+/-		0.0189319 0.0450447)	(+/-		-0.0020637 0.0395252)	(+/-	
Parental care [pair]	-0.0017487 0.0093667)	(+/-	0.852261	0.0177049 0.0303091)	(+/-	0.5603 8	-0.0467341 0.0287628)	(+/-	0.107 2
<i>Multiple R2</i>	0.1922			0.09759			0.07284		
<i>Adjusted R2</i>	0.1307			0.02884			0.002199		
<i>Lambda</i>	0.53			0.757			0.423		

	65) Belly (Achromatic property female)		66) Tail underside (Achromatic property female)	
	Estimate (+/- SE)	P [anova]	Estimate (+/- SE)	P [anova]
Intercept	0.420971 (+/- 0.077818)		0.0395485 (+/- 0.0536739)	
LE [open]	0.010704 (+/- 0.039632)	0.04435 *	0.0148047 (+/- 0.0231737)	0.02063 *
LE [woodland]	-0.063255 (+/- 0.036419)		-0.0222465 (+/- 0.0213564)	
Body size	-0.036289 (+/- 0.017028)	0.04681 *	0.0184725 (+/- 0.0110109)	0.08301
Territoriality	0.013270 (+/- 0.026331)	0.41891	0.0183834 (+/- 0.0149503)	0.22276
Strategy [ground catcher]	0.066814 (+/- 0.036023)	0.35648	-0.0023604 (+/- 0.0206575)	0.99226
Strategy [ground dweller]	0.029137 (+/- 0.046021)		0.0076738 (+/- 0.0273657)	
Strategy [water diver]	0.048379 (+/- 0.041445)		0.0011816 (+/- 0.0270747)	
Parental care [pair]	-0.047903 (+/- 0.032216)	0.14004	-0.0104120 (+/- 0.0187105)	0.57911
<i>Multiple R2</i>	0.1366		0.1144	
<i>Adjusted R2</i>	0.07079		0.04423	
<i>Lambda</i>	0.221		0.457	

Table 6. Results of MCMCglmm analysis.

PC1				
Iterations = 20001:219981				
Thinning interval = 20				
Sample size = 10000				
DIC: -4511.278				
G-structure: ~Sciname				
	post.mean	l-95% CI	u-95% CI	eff.samp
Sciname	0.025	0.017	0.034	10429.000
R-structure: ~units				
	post.mean	l-95% CI	u-95% CI	eff.samp
units	0.009	0.009	0.010	10680.000
Location effects: PC1 ~ sex * patch				
	post.mean	l-95% CI	u-95% CI	eff.samp

				p	pMC MC
(Intercept)	-0.103	-0.236	0.032	10202.000	0.136
sexM	0.006	-0.019	0.030	8240.000	0.612
patchbreast	-0.014	-0.039	0.011	10000.000	0.272
patchcrown	0.065	0.041	0.090	10000.000	<1e-04
patchmantle	0.043	0.018	0.068	10000.000	<1e-04
patchnape	0.067	0.041	0.091	10000.000	<1e-04
patchrump	0.128	0.101	0.152	10472.000	<1e-04
patchtail	0.144	0.119	0.169	10000.000	<1e-04
patchtail.underside	0.104	0.079	0.130	10000.000	<1e-04
patchthroat	-0.001	-0.024	0.025	10671.000	0.952
patchwing.coverts	0.098	0.074	0.123	10000.000	<1e-04
patchwing primaries.secondaries	0.119	0.095	0.146	8525.000	<1e-04
sexM:patchbreast	-0.005	-0.040	0.031	10000.000	0.809
sexM:patchcrown	0.006	-0.029	0.041	10000.000	0.740
sexM:patchmantle	0.000	-0.035	0.035	10000.000	0.973
sexM:patchnape	0.005	-0.030	0.040	10000.000	0.799
sexM:patchrump	-0.004	-0.038	0.033	10000.000	0.833
sexM:patchtail	0.007	-0.027	0.043	10000.000	0.700
sexM:patchtail.underside	0.001	-0.035	0.037	10000.000	0.941
sexM:patchthroat	-0.006	-0.040	0.031	10376.000	0.744
sexM:patchwing.coverts	0.006	-0.0282758 0.715	0.0410562 10000	0.0410562 10000	10000.000 0.715
sexM:patchwing primaries.secondaries	0.008	-0.027	0.044	8868.000	0.657

PC2					
Iterations = 20001:219981					
Thinning interval = 20					
Sample size = 10000					
DIC: -7870.129					
G-structure: ~Sciname					
	post.mean	l-95% CI	u-95% CI	eff.samp	
Sciname	0.009	0.006	0.012	9422.000	
R-structure: ~units					
	post.mean	l-95% CI	u-95% CI	eff.samp	
units	0.002	0.002	0.003	10000.000	
Location effects: PC2 ~ sex * patch					
	post.mean	l-95% CI	u-95% CI	eff.samp	pMCMC
(Intercept)	-0.001	-0.082	0.080	10000.000	0.988

sexM	0.002	-0.011	0.014	10000.000	0.765
patchbreast	0.007	-0.006	0.020	10000.000	0.272
patchcrown	-0.009	-0.023	0.004	10000.000	0.170
patchmantle	-0.008	-0.021	0.005	10000.000	0.221
patchnape	-0.007	-0.021	0.006	10000.000	0.276
patchrump	-0.031	-0.044	-0.018	10000.000	0.000
patchtail	-0.017	-0.029	-0.003	9999.000	0.012
patchtail.underside	0.009	-0.004	0.023	10000.000	0.155
patchthroat	0.009	-0.003	0.023	10000.000	0.157
patchwing.coverts	-0.019	-0.032	-0.005	10000.000	0.004
patchwing.primarys.secondarys	-0.022	-0.035	-0.009	10000.000	0.001
sexM:patchbreast	0.005	-0.012	0.024	10000.000	0.601
sexM:patchcrown	0.001	-0.018	0.018	10000.000	0.948
sexM:patchmantle	-0.002	-0.020	0.016	10000.000	0.794
sexM:patchnape	0.002	-0.016	0.021	10000.000	0.794
sexM:patchrump	-0.009	-0.027	0.009	10000.000	0.351
sexM:patchtail	-0.007	-0.025	0.011	10000.000	0.457
sexM:patchtail.underside	0.000	-0.018	0.018	9861.000	0.984
sexM:patchthroat	0.004	-0.015	0.021	10000.000	0.706
sexM:patchwing.coverts	-0.004	-0.022	0.014	10000.000	0.629
sexM:patchwing.primarys.secondarys	-0.005	-0.024	0.012	11568.000	0.563

Brightness					
Iterations = 20001:219981					
Thinning interval = 20					
Sample size = 10000					
DIC: -5668.46					
G-structure: ~Sciname					
	post.mean	I-95% CI	u-95% CI	eff.samp	
Sciname	0.012	0.008	0.017	10000.000	
R-structure: ~units					
	post.mean	I-95% CI	u-95% CI	eff.samp	
units	0.006	0.006	0.006	10552.000	
Location effects: lum ~ sex * patch					
	post.mean	I-95% CI	u-95% CI	eff.samp	pMCMC
(Intercept)	0.257	0.160	0.350	9597.000	<1e-04
sexM	-0.004	-0.024	0.015	10000.000	0.663
patchbreast	-0.063	-0.082	-0.042	10000.000	<1e-04
patchcrown	-0.213	-0.233	-0.193	10000.000	<1e-04
patchmantle	-0.180	-0.200	-0.159	10000.000	<1e-04
patchnape	-0.195	-0.214	-0.174	10000.000	<1e-04
patchrump	-0.147	-0.167	-0.127	10000.000	<1e-04

patchtail	-0.203	-0.223	-0.183	10000.00 0	<1e-04
patchtail.underside	-0.161	-0.180	-0.141	9321.000	<1e-04
patchthroat	0.013	-0.007	0.033	10000.00 0	0.212
patchwing.coverts	-0.209	-0.229	-0.189	9463.000	<1e-04
patchwing primaries.secondaries	-0.195	-0.215	-0.175	10000.00 0	<1e-04
sexM:patchbreast	-0.004	-0.033	0.023	9628.000	0.777
sexM:patchcrown	0.010	-0.018	0.038	10000.00 0	0.474
sexM:patchmantle	0.007	-0.022	0.034	10000.00 0	0.645
sexM:patchnape	0.007	-0.020	0.036	10000.00 0	0.628
sexM:patchrump	0.007	-0.020	0.036	10000.00 0	0.606
sexM:patchtail	0.005	-0.023	0.033	10000.00 0	0.723
sexM:patchtail.underside	0.006	-0.023	0.035	10000.00 0	0.660
sexM:patchthroat	0.001	-0.026	0.029	10000.00 0	0.936
sexM:patchwing.coverts	0.007	-0.023	0.034	10000.00 0	0.623
sexM:patchwing primaries.secondaries	0.011	-0.017577	0.039799	10000 0.463	0.463

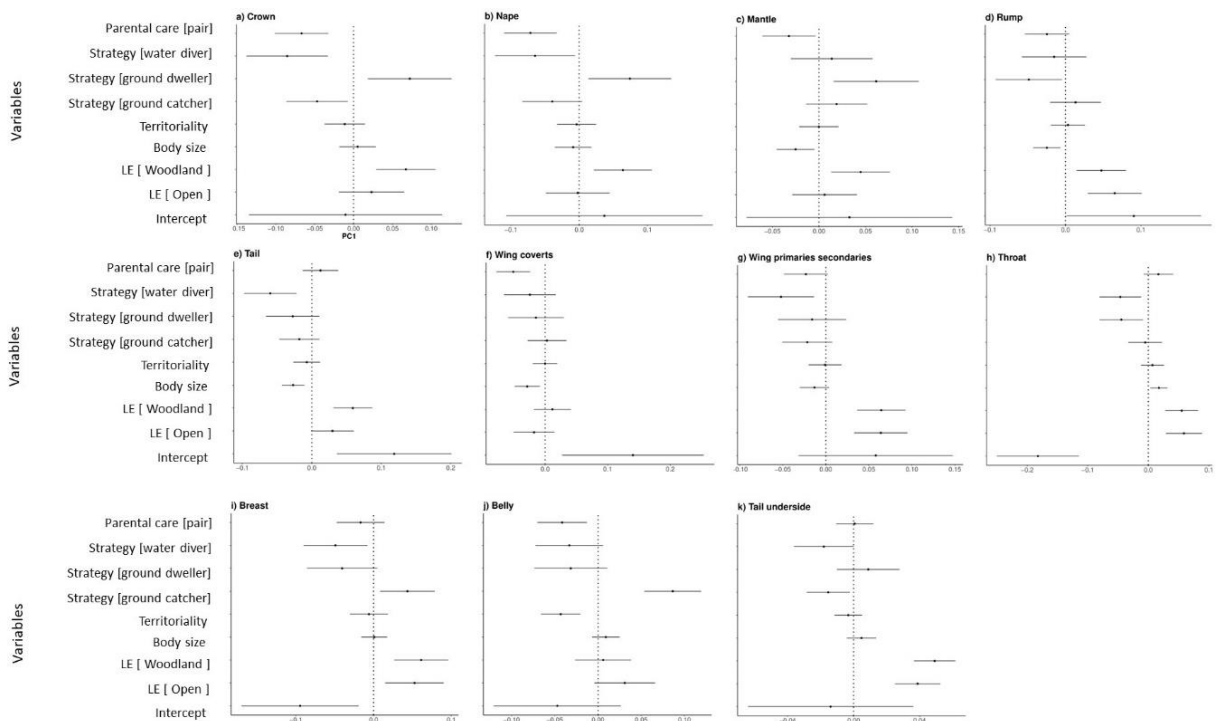


Figure S1. Predictors of PC1 part of the chromatic colour variation of males in Coraciiformes. Every plot within the figure represents different body part: a) crown, b) nape, c) mantle, d) rump, e) tail, f) wing coverts, g) wing primaries and secondaries, h) throat, i) breast, j) belly, k) tail underside. Variables that we tested are indicated on the y-axis of the most left plot in each row. PC1 values are indicated on the x-axis of each plot separately. Within each plot, points indicate values of intercept estimate of regression of each variable and lines indicate their standard error. Within each plot variables with a significant effect do not cross the vertical line that indicates zero.

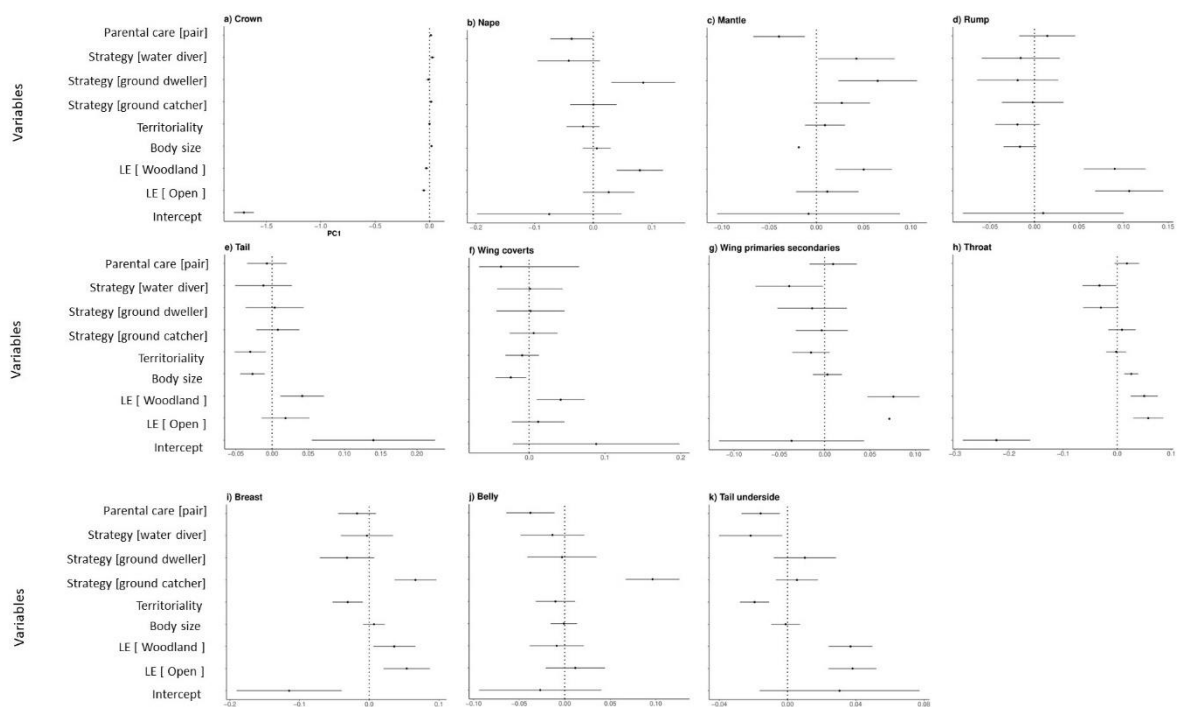


Figure S2. Predictors of PC1 part of the chromatic colour variation of females in Coraciiformes. Every plot within the figure represents different body part: a) crown, b) nape, c) mantle, d) rump, e) tail, f) wing coverts, g) wing primaries and secondaries, h) throat, i) breast, j) belly, k) tail underside. Variables that we tested are indicated on the y-axis of the most left plot in each row. PC1 values are indicated on the x-axis of each plot separately. Within each plot, points indicate values of intercept estimate of regression of each variable and lines indicate their standard error. Within each plot variables with a significant effect do not cross the vertical line that indicates zero.

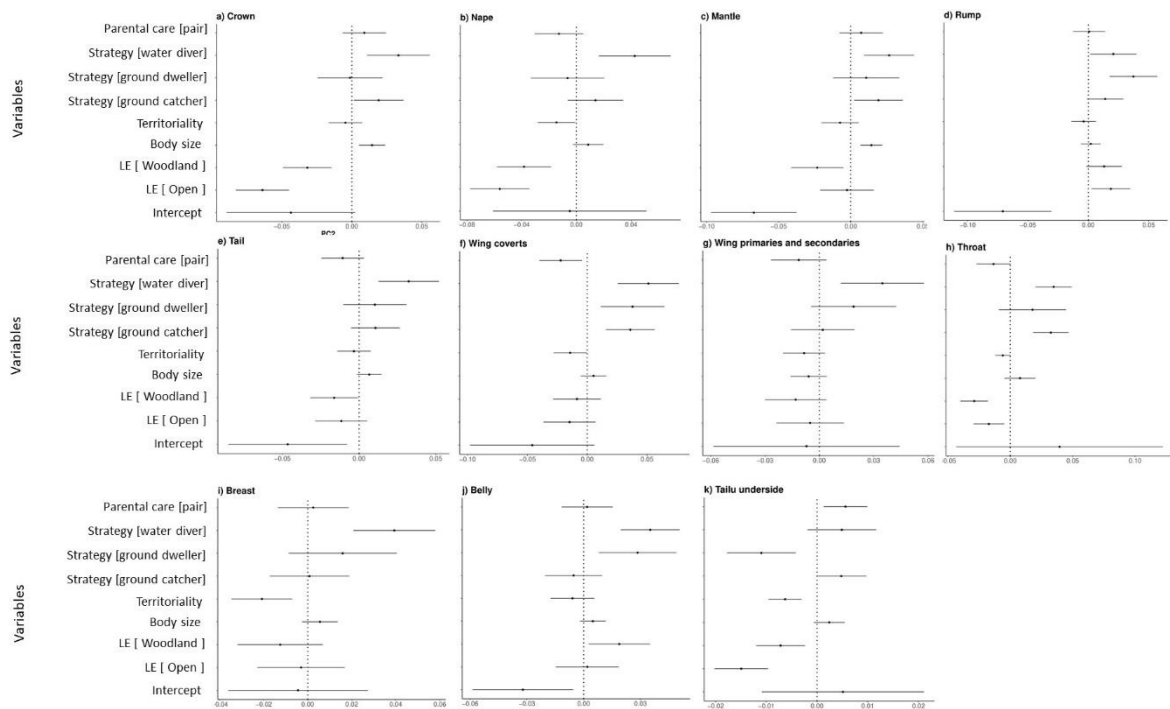


Figure S3. Predictors of PC2 part of the chromatic colour variation in Coraciiformes. Every plot within the figure represents different body part: a) crown, b) nape, c) mantle, d) rump, e) tail, f) wing coverts, g) wing primaries and secondaries, h) throat, i) breast, j) belly, k) tail underside. Variables that we tested are indicated on the y-axis of the most left plot in each row. PC1 values are indicated on the x-axis of each plot separately. Within each plot, points indicate values of intercept estimate of regression of each variable and lines indicate their standard error. Within each plot variables with a significant effect do not cross the vertical line that indicates zero.

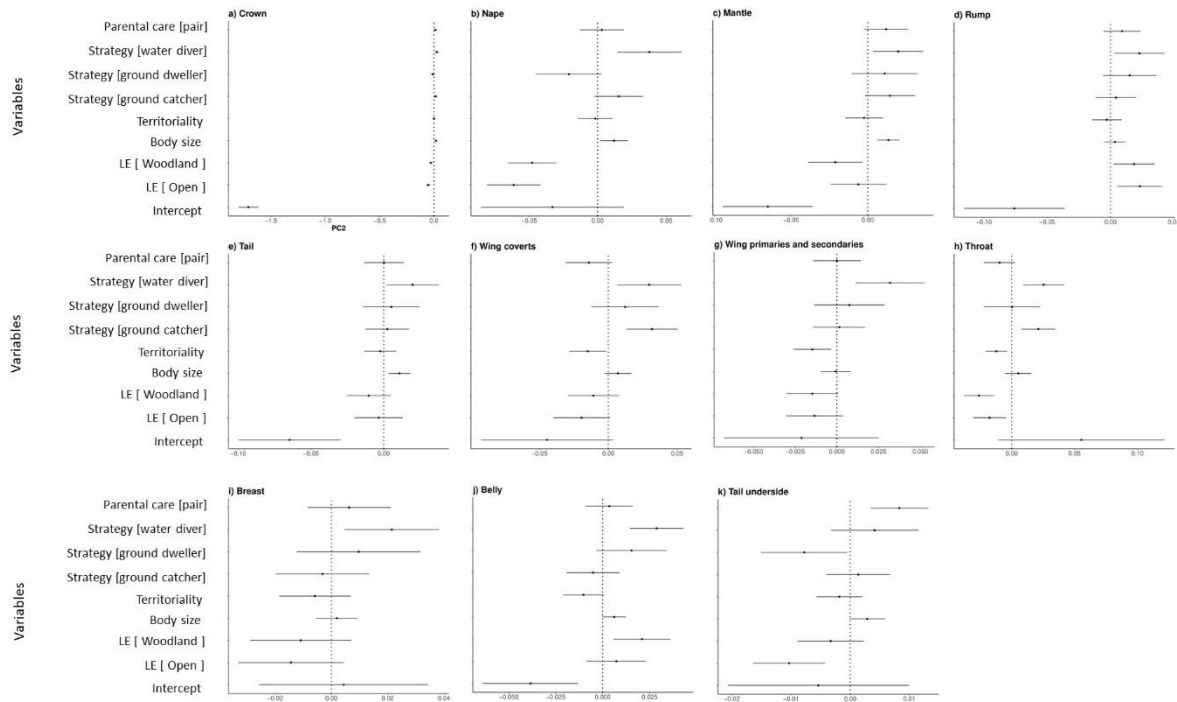


Figure S4. Predictors of PC2 part of the chromatic colour variation in Coraciiformes. Every plot within the figure represents different body part: a) crown, b) nape, c) mantle, d) rump, e) tail, f) wing coverts, g) wing primaries and secondaries, h) throat, i) breast, j) belly, k) tail underside. Variables that we tested are indicated on the y-axis of the most left plot in each row. PC1 values are indicated on the x-axis of each plot separately. Within each plot, points indicate values of intercept estimate of regression of each variable and lines indicate their standard error. Within each plot variables with a significant effect do not cross the vertical line that indicates zero.

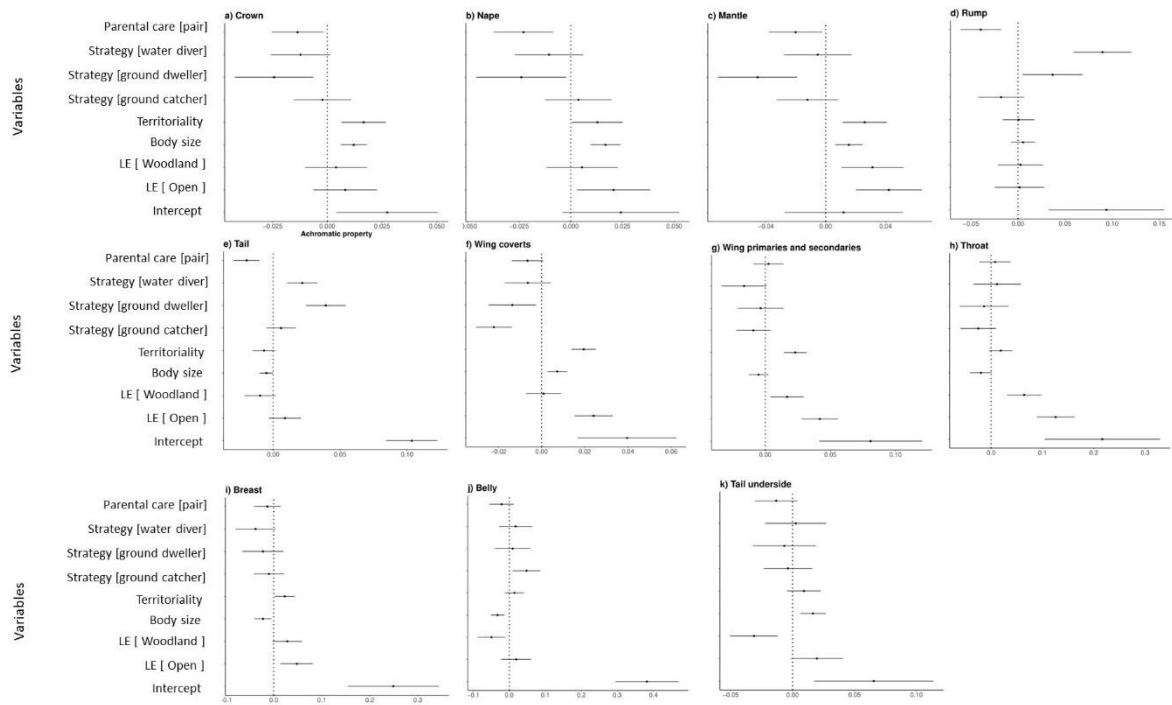


Figure S5. Predictors of the achromatic colour variation of males in Coraciiformes. Every plot within the figure represents different body part: a) crown, b) nape, c) mantle, d) rump, e) tail, f) wing coverts, g) wing primaries and secondaries, h) throat, i) breast, j) belly, k) tail underside. Variables that we tested are indicated on the y-axis of the most left plot in each row. PC1 values are indicated on the x-axis of each plot separately. Within each plot, points indicate values of intercept estimate of regression of each variable and lines indicate their standard error. Within each plot variables with a significant effect do not cross the vertical line that indicates zero.

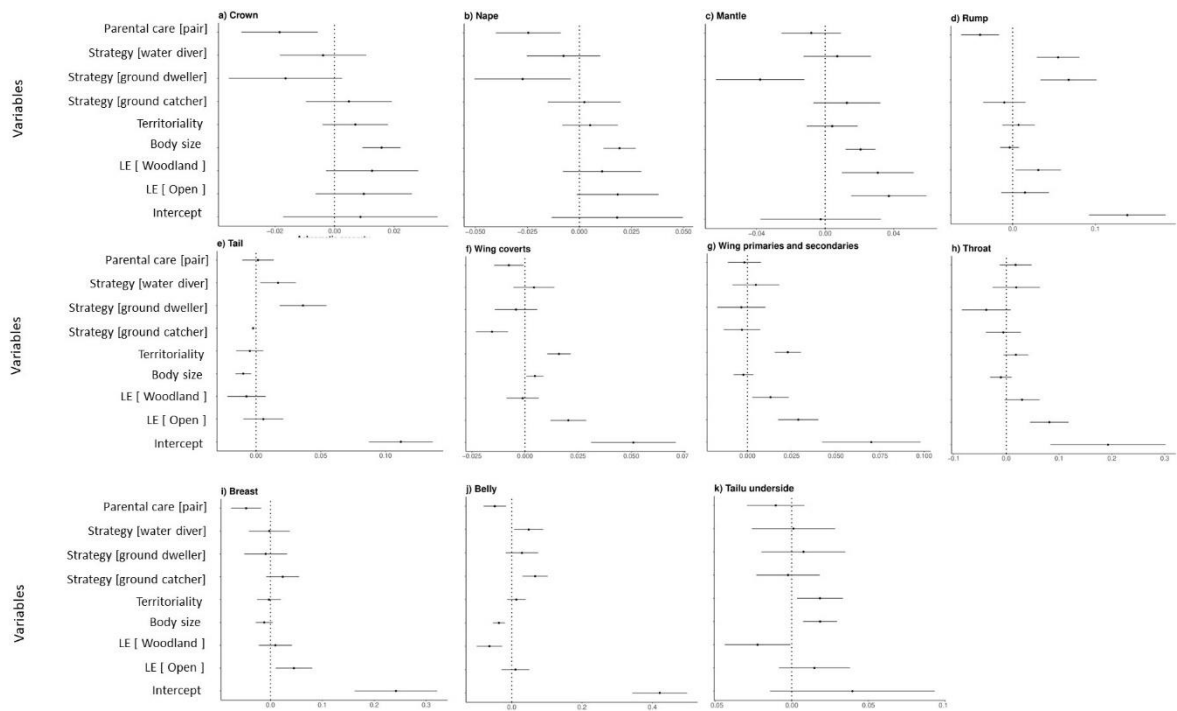


Figure S6. Predictors of the achromatic colour variation of females in Coraciiformes. Every plot within the figure represents different body part: a) crown, b) nape, c) mantle, d) rump, e) tail, f) wing coverts, g) wing primaries and secondaries, h) throat, i) breast, j) belly, k) tail underside. Variables that we tested are indicated on the y-axis of the most left plot in each row. PC1 values are indicated on the x-axis of each plot separately. Within each plot, points indicate values of intercept estimate of regression of each variable and lines indicate their standard error. Within each plot variables with a significant effect do not cross the vertical line that indicates zero.

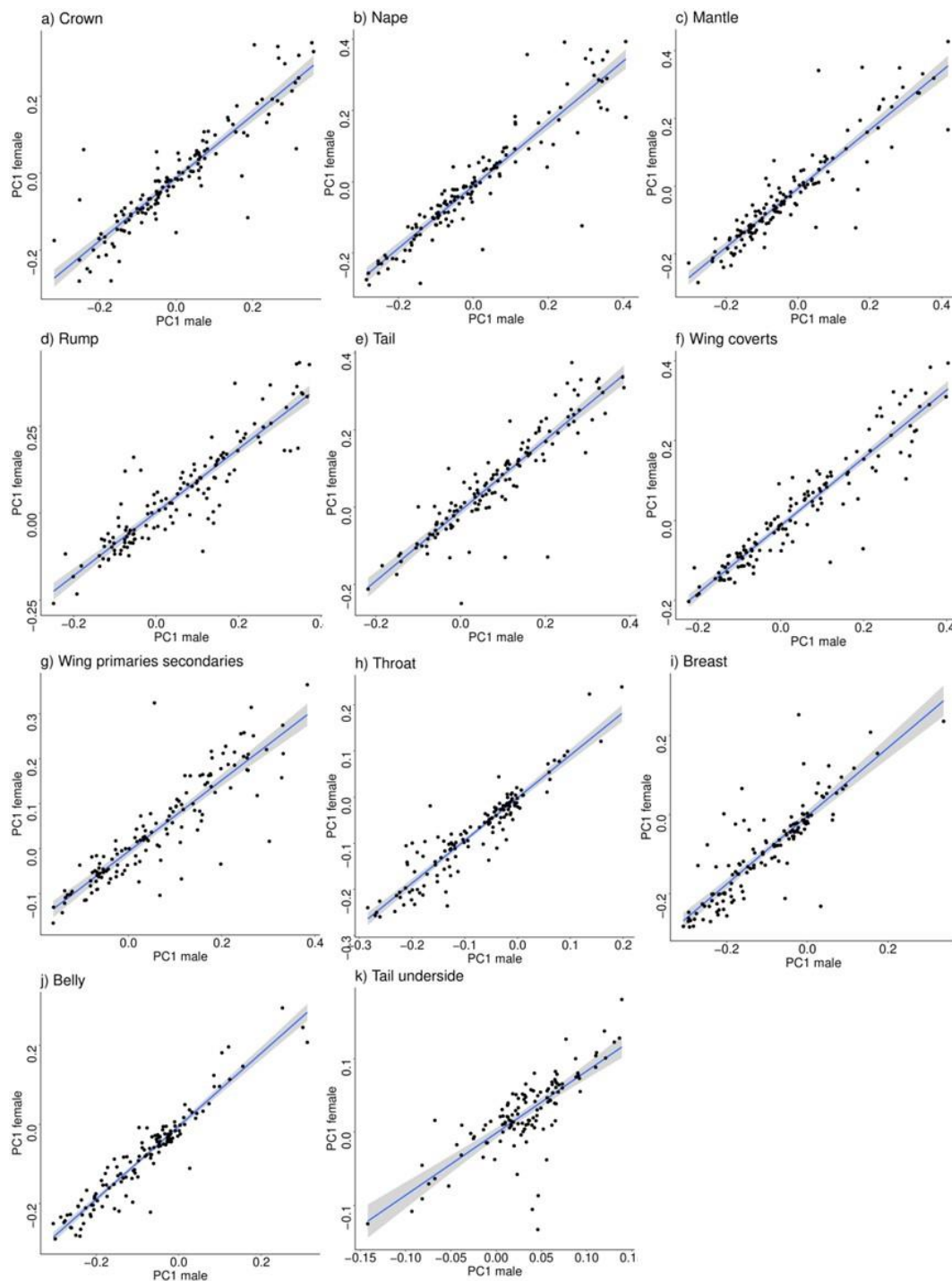


Figure S7. Scatterplot of female and male values for PC1 part of chromatic colour variation in Coraciiformes. Every plot within the figure represents different body part: a) crown, b) nape, c) mantle, d) rump, e) tail, f) wing coverts, g) wing primaries and secondaries, h) throat, i) breast, j) belly, k) tail underside. Every dot within each plot represents a species of Coraciiformes. On the y-axis, female values are represented, while on the x-axis male values are represented. On every plot, the blue line represents the regression line.

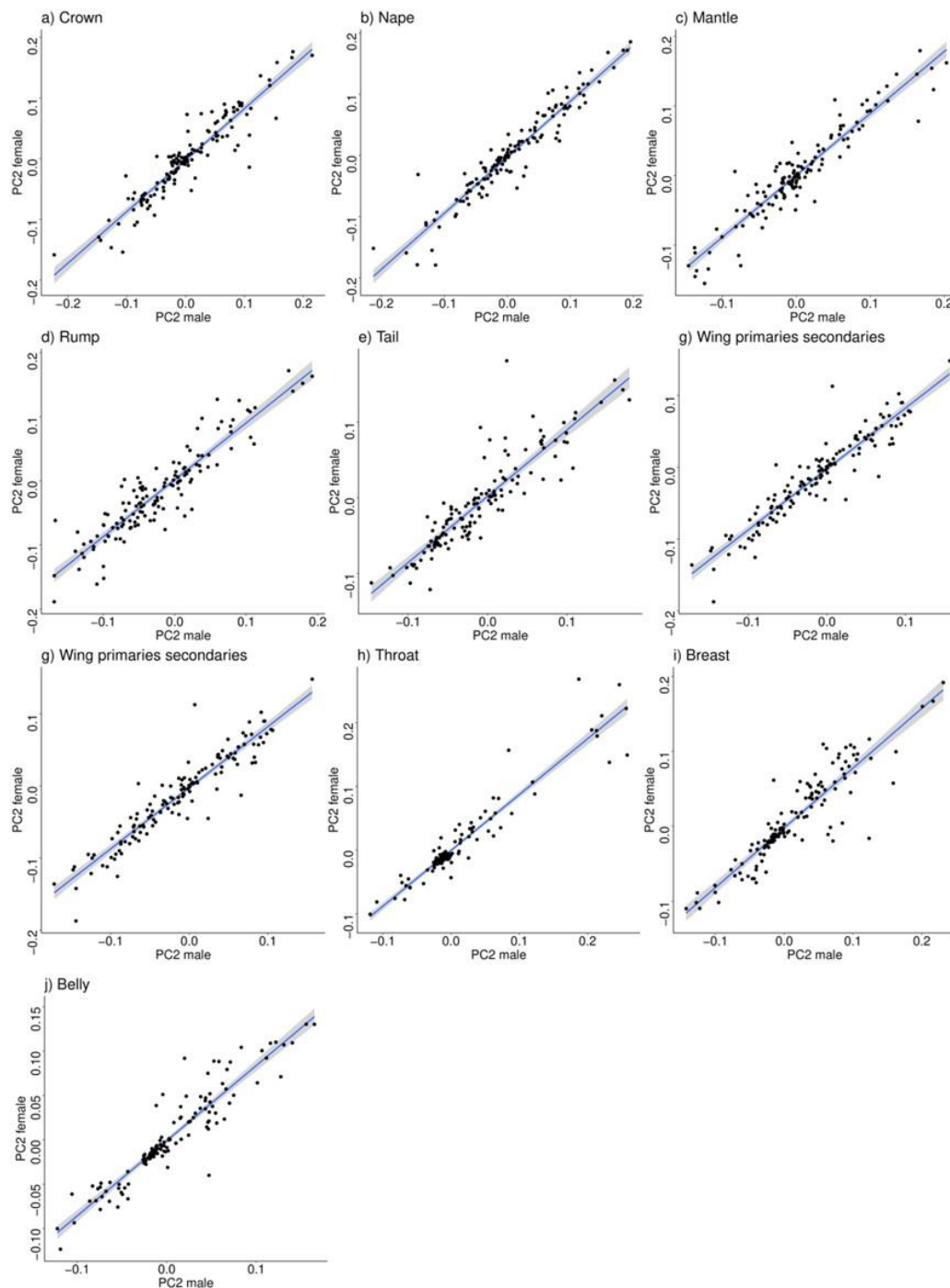


Figure S8. Scatterplot of female and male values for PC2 part of chromatic colour variation in Coraciiformes. Every plot within the figure represents different body part: a) crown, b) nape, c) mantle, d) rump, e) tail, f) wing coverts, g) wing primaries and secondaries, h) throat, i) breast, j) belly, k) tail underside. Every dot within each plot represents a species of Coraciiformes. On the y-axis, female values are represented, while on the x-axis male values are represented. On every plot, the blue line represents the regression line.

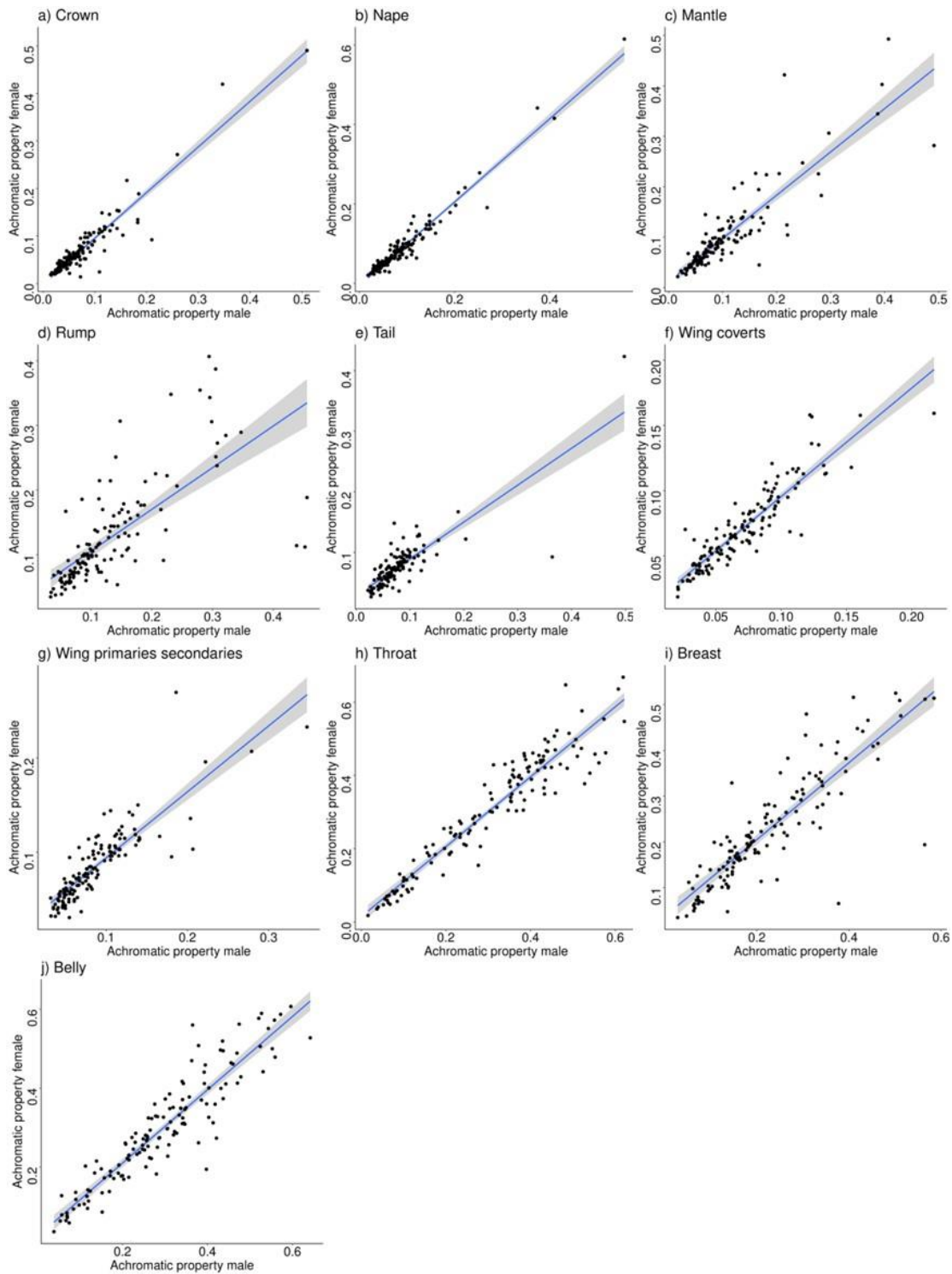


Figure S9. Scatterplot of female and male values for achromatic colour variation in Coraciiformes. Every plot within the figure represents different body part: a) crown, b) nape, c) mantle, d) rump, e) tail, f) wing coverts, g) wing primaries and secondaries, h) throat, i) breast, j) belly, k) tail underside. Every dot within each plot represents a species of Coraciiformes. On the y-axis, female values are represented, while on the x-axis male values are represented. On every plot, the blue line represents the regression line.

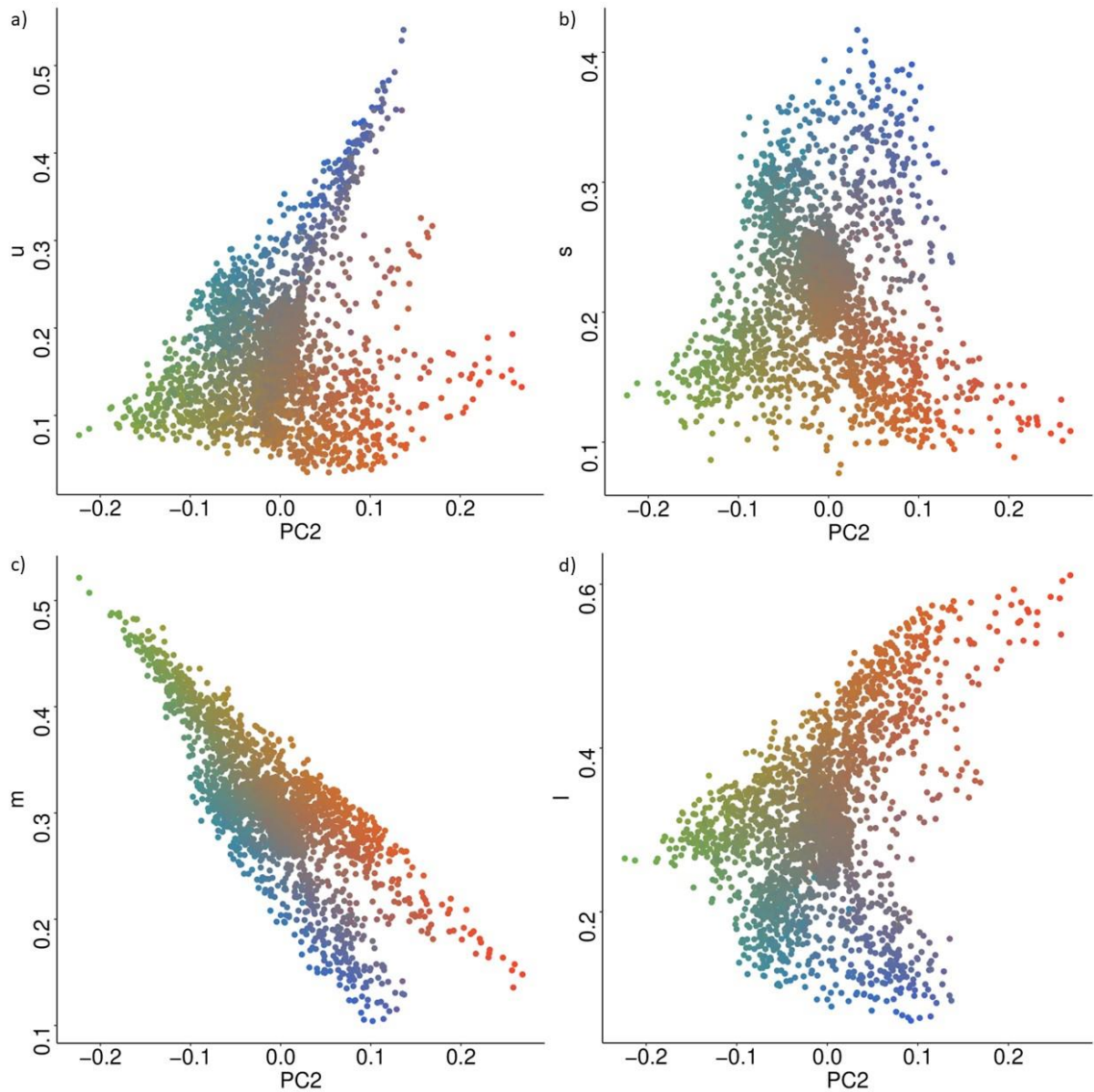


Figure S10. Scatterplots of cone catch values (u, s, m and l) extracted from digital photography and PC1 part of the chromatic variation in Coraciiformes. Principal components are obtained by principal component analysis of the morphospace constructed by cone catch values. Panel a) represents u cone against PC1, panel b) represents s cone against PC1, panel c) represents m cone against PC1, and panel d) represents l cone against PC1.

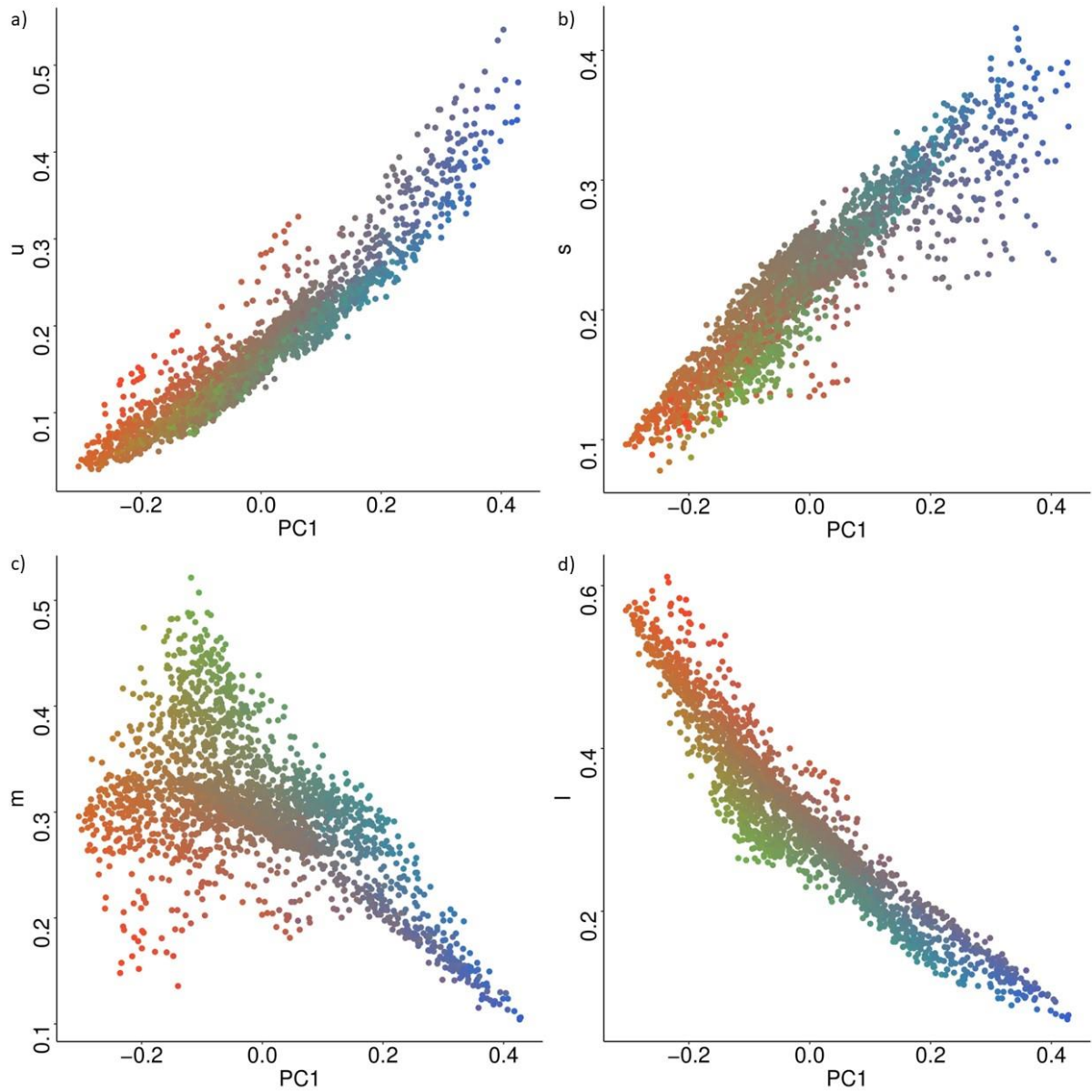


Figure S11. Scatterplots of cone catch values (u, s, m and l) extracted from digital photography and PC2 part of the chromatic variation in Coraciiformes. Principal components are obtained by principal component analysis of the morphospace constructed by cone catch values. Panel a) represents u cone against PC1, panel b) represents s cone against PC1, panel c) represents m cone against PC1, and panel d) represents l cone against PC1.

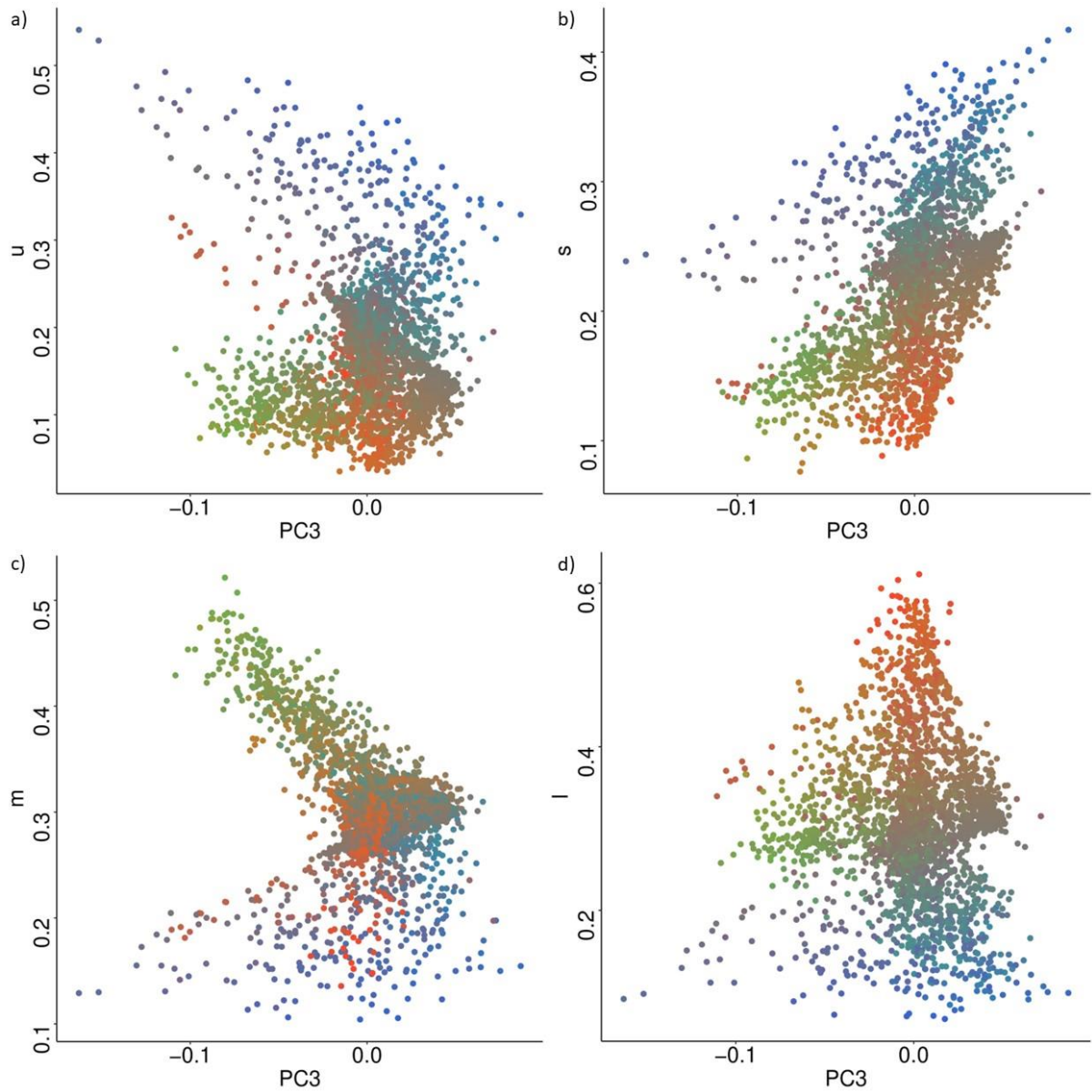


Figure S12. Scatterplots of cone catch values (u, s, m and l) extracted from digital photography and PC3 part of the chromatic variation in Coraciiformes. Principal components are obtained by principal component analysis of the morphospace constructed by cone catch values. Panel a) represents u cone against PC1, panel b) represents s cone against PC1, panel c) represents m cone against PC1, and panel d) represents l cone against PC1.

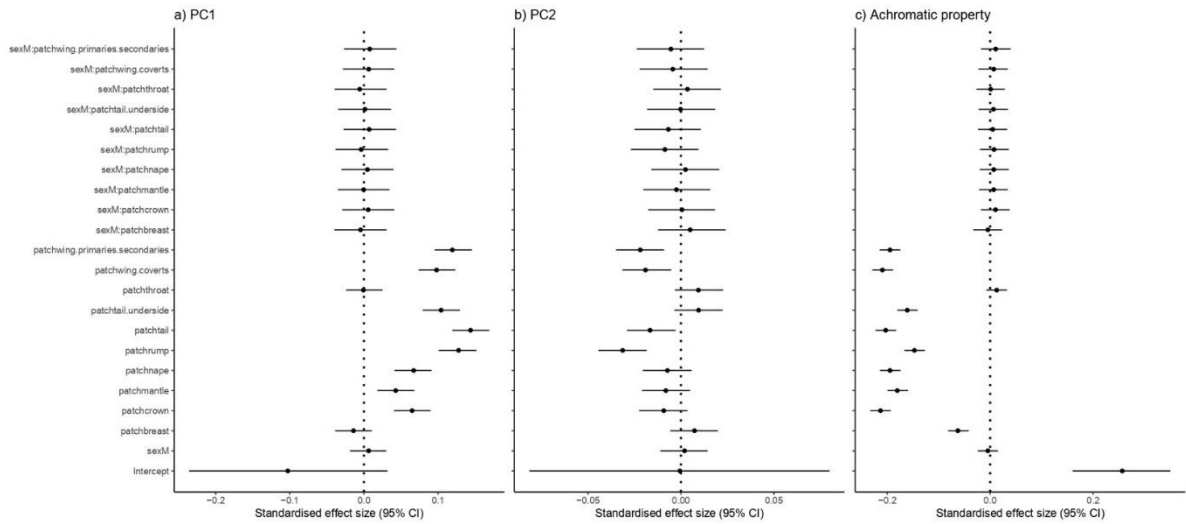


Figure S13. Results of the MCMCglmm analysis used to test for the differences between body parts with PC1, PC2 and achromatic property of plumage colour as a dependent variable and sex and patch as independent variable. Panel a) shows results for PC1, panel b) shows the results for PC2, and panel c) shows the results for the achromatic property of the colour. On each panel points indicate the mean standardised effect sizes for each of the variables and lines indicate 95% credible intervals. Predictors with the significant effect (pMCMC < 0.05) are those that do not cross the vertical line with negative effects one leaning on the left hand side and positive effect ones leaning on the right hand side.

APPENDIX 2

Supplementary materials and methods for Chapter 3: Evolutionary dynamics of pigmentary grey and non- iridescent structural blue colouration in Tanagers (family: Thraupidae)

Table S1. Table containing values of colour measurements and colour descriptions with sex, latin and english name and region of the plumage patch where the measurement was taken. Column u, s, m and l are the results of the quantification of the colour from digitally calibrated images. Column colour_HBW is the plumage colour description from the Birds of the World and colour coding column is the result of classification of the colour descriptions from HBW into the colour categories, i.e. blue, slate and grey. Finally, projection values is the column containing calculations of the projection values.

Latin name	English Name	sex	region	colour HBW	colour coding	u	s	m	l	projection values
Anisognathus lacrymosus	Lacrimose Mountain-Tanager	M	cro	slaty blue	blue	0.208	0.271	0.270	0.251	0.271
Anisognathus melanogenys	Black-cheeked Mountain-Tanager	M	cro	shining blue	blue	0.206	0.284	0.266	0.244	0.284
Buthraupis eximia	Black-chested Mountain-Tanager	M	cro	blue	blue	0.270	0.303	0.235	0.192	0.303
Conirostrum bicolor	Bicolored Conebill	M	cro	pale bluish-grey	blue	0.184	0.251	0.288	0.277	0.251
Cyanerpes caeruleus	Purple Honeycreeper	M	cro	lustrous violet-blue	blue	0.540	0.218	0.132	0.110	0.218
Cyanerpes cyaneus	Red-legged Honeycreeper	M	cro	azure / blue	blue	0.147	0.218	0.272	0.363	0.218
Cyanerpes lucidus	Shining Honeycreeper	M	cro	ultramarine blue	blue	0.411	0.300	0.169	0.120	0.300
Cyanerpes nitidus	Short-billed Honeycreeper	M	cro	purplish-blue	blue	0.350	0.373	0.163	0.114	0.373
Cyanicterus cyanicterus	Blue-backed Tanager	M	cro	bright cadet-blue	blue	0.405	0.308	0.168	0.120	0.308
Dacnis cayana	Blue Dacnis	M	cro	bright turquoise-blue	blue	0.262	0.295	0.304	0.139	0.295
Dacnis hartlaubi	Turquoise Dacnis	M	cro	turquoise	blue	0.280	0.287	0.293	0.140	0.287
Dacnis lineata	Black-faced Dacnis	M	cro	turquoise-blue	blue	0.280	0.299	0.280	0.141	0.299
Dacnis nigripes	Black-legged	M	cro	greenish blue /	blue	0.23	0.28	0.318	0.164	0.284

	Dacnis			turquoise		4	4			
Dacnis venusta	Scarlet-thighed Dacnis	M	cro	black / turquoise	blue	0.227	0.302	0.323	0.148	0.302
Dacnis viguieri	Viridian Dacnis	M	cro	green	blue	0.297	0.166	0.379	0.159	0.166
Diglossa albilatera	White-sided Flowerpiercer	M	cro	dark slate-grey	blue	0.212	0.252	0.279	0.258	0.252
Diglossa cyanea	Masked Flowerpiercer	M	cro	dark blue	blue	0.278	0.315	0.232	0.176	0.315
Diglossa glauca	Deep-blue Flowerpiercer	M	cro	deep blue	blue	0.355	0.259	0.209	0.177	0.259
Diglossa indigotica	Indigo Flowerpiercer	M	cro	indigo-blue	blue	0.305	0.355	0.199	0.141	0.355
Iridosornis analis	Yellow-throated Tanager	M	cro	deep purplish blue	blue	0.200	0.259	0.281	0.259	0.259
Iridosornis porphyrocephalus	Purplish-mantled Tanager	M	cro	dark blue	blue	0.340	0.241	0.221	0.198	0.241
Pipraeidea melanonota	Fawn-breasted Tanager	M	cro	medium blue	blue	0.298	0.349	0.205	0.147	0.349
Porphyrospiza caerulescens	Blue Finch	M	cro	bright indigo-blue	blue	0.267	0.287	0.243	0.203	0.287
Tangara cyanicollis	Blue-necked Tanager	M	cro	blue	blue	0.221	0.303	0.325	0.152	0.303
Tangara cyanocephala	Red-necked Tanager	M	cro	blue-violet	blue	0.343	0.368	0.170	0.119	0.368
Tangara nigrocincta	Masked Tanager	M	cro	pale lavender	blue	0.238	0.316	0.249	0.197	0.316
Tangara seledon	Green-headed Tanager	M	cro	turquoise-green	blue	0.078	0.275	0.446	0.201	0.275
Tangara vassorii	Blue-and-black Tanager	M	cro	dark cobalt blue	blue	0.399	0.309	0.169	0.122	0.309
Tersina viridis	Swallow Tanager	M	cro	bright turquoise-blue	blue	0.225	0.255	0.344	0.176	0.255
Thraupis abbas	Yellow-winged Tanager	M	cro	campanula-blue	blue	0.426	0.273	0.164	0.137	0.273
Thraupis bonariensis	Blue-and-yellow Tanager	M	cro	dull blue	blue	0.303	0.283	0.231	0.183	0.283
Thraupis cyanocephala	Blue-capped Tanager	M	cro	shining cornflower-blue	blue	0.429	0.273	0.169	0.129	0.273
Thraupis ornata	Golden-chevroned Tanager	M	cro	shining cadet-blue	blue	0.324	0.283	0.209	0.183	0.283
Xenodacnis parina	Tit-like Dacnis	M	cro	dark blue	blue	0.337	0.301	0.202	0.160	0.301
Anisognathus melanogenys	Black-cheeked Mountain-Tanager	M	nap	shining blue	blue	0.293	0.269	0.231	0.207	0.269
Buthraupis eximia	Black-chested Mountain-Tanager	M	nap	blue	blue	0.462	0.253	0.162	0.124	0.253
Buthraupis montana	Hooded Mountain-Tanager	M	nap	shining pale milky blue	blue	0.211	0.249	0.286	0.254	0.249
Chlorophanes spiza	Green Honeycreeper	M	nap	glossy viridian green	blue	0.051	0.267	0.460	0.221	0.267
Conirostrum bicolor	Bicolored Conebill	M	nap	pale bluish-grey	blue	0.209	0.260	0.279	0.252	0.260
Cyanerpes caeruleus	Purple Honeycreeper	M	nap	lustrous violet-blue	blue	0.640	0.196	0.154	0.011	0.196
Cyanerpes lucidus	Shining Honeycreeper	M	nap	ultramarine blue	blue	0.415	0.284	0.178	0.122	0.284
Cyanerpes nitidus	Short-billed Honeycreeper	M	nap	purplish-blue	blue	0.345	0.348	0.174	0.134	0.348
Cyanicterus cyanicterus	Blue-backed Tanager	M	nap	bright cadet-blue	blue	0.366	0.296	0.192	0.146	0.296
Dacnis cayana	Blue Dacnis	M	nap	bright turquoise-blue	blue	0.278	0.305	0.291	0.127	0.305
Dacnis nigripes	Black-legged Dacnis	M	nap	greenish blue / turquoise	blue	0.248	0.280	0.304	0.168	0.280
Dacnis venusta	Scarlet-thighed Dacnis	M	nap	turquoise	blue	0.237	0.311	0.300	0.152	0.311

Dacnis viguieri	Viridian Dacnis	M	nap	greenish blue	blue	0.27 5	0.19 6	0.378	0.151	0.196
Diglossa albilatera	White-sided Flowerpiercer	M	nap	dark slate-grey	blue	0.22 9	0.24 5	0.268	0.258	0.245
Diglossa cyanea	Masked Flowerpiercer	M	nap	dark blue	blue	0.30 6	0.31 7	0.218	0.159	0.317
Diglossa glauca	Deep-blue Flowerpiercer	M	nap	deep blue	blue	0.36 2	0.25 1	0.208	0.180	0.251
Diglossa indigotica	Indigo Flowerpiercer	M	nap	indigo-blue	blue	0.30 1	0.33 0	0.206	0.164	0.330
Iridosornis analis	Yellow-throated Tanager	M	nap	greenish turquoise	blue	0.21 9	0.26 8	0.267	0.247	0.268
Iridosornis porphyrocephalus	Purplish-mantled Tanager	M	nap	dark blue	blue	0.37 9	0.27 0	0.194	0.157	0.270
Pipraeidea melanonota	Fawn-breasted Tanager	M	nap	medium blue	blue	0.35 7	0.34 5	0.166	0.131	0.345
Porphyospiza caerulescens	Blue Finch	M	nap	bright indigo-blue	blue	0.24 0	0.26 7	0.257	0.236	0.267
Tangara cyanicollis	Blue-necked Tanager	M	nap	blue	blue	0.22 7	0.31 5	0.304	0.155	0.315
Tangara cyanocephala	Red-necked Tanager	M	nap	blue-violet	blue	0.21 9	0.22 5	0.215	0.341	0.225
Tangara nigrocincta	Masked Tanager	M	nap	pale lavender	blue	0.26 1	0.31 7	0.235	0.187	0.317
Tangara seledon	Green-headed Tanager	M	nap	turquoise-green	blue	0.09 4	0.27 3	0.435	0.198	0.273
Tangara vassorii	Blue-and-black Tanager	M	nap	dark cobalt blue	blue	0.41 4	0.31 8	0.152	0.116	0.318
Tersina viridis	Swallow Tanager	M	nap	bright turquoise-blue	blue	0.23 2	0.26 2	0.349	0.156	0.262
Thraupis abbas	Yellow-winged Tanager	M	nap	campanula-blue	blue	0.39 2	0.24 2	0.194	0.172	0.242
Thraupis bonariensis	Blue-and-yellow Tanager	M	nap	dull blue	blue	0.31 9	0.28 5	0.222	0.174	0.285
Thraupis cyanocephala	Blue-capped Tanager	M	nap	shining cornflower-blue	blue	0.45 0	0.25 6	0.164	0.129	0.256
Thraupis ornata	Golden-chevroned Tanager	M	nap	shining cadet-blue	blue	0.38 3	0.27 9	0.181	0.156	0.279
Xenodacnis parina	Tit-like Dacnis	M	nap	dark blue	blue	0.31 7	0.31 2	0.213	0.158	0.312
Anisognathus lacrymosus	Lacrimose Mountain-Tanager	M	man	slaty blue	blue	0.21 5	0.25 8	0.268	0.258	0.258
Anisognathus melanogenys	Black-cheeked Mountain-Tanager	M	man	dark grey-blue	blue	0.21 8	0.26 7	0.273	0.242	0.267
Buthraupis montana	Hooded Mountain-Tanager	M	man	shining dark blue	blue	0.60 2	0.23 3	0.131	0.035	0.233
Chlorophanes spiza	Green Honeycreeper	M	man	glossy viridian green	blue	0.05 1	0.32 2	0.431	0.197	0.322
Conirostrum bicolor	Bicolored Conebill	M	man	pale bluish-grey	blue	0.21 1	0.25 8	0.277	0.254	0.258
Cyanerpes caeruleus	Purple Honeycreeper	M	man	lustrous violet-blue	blue	0.57 5	0.25 1	0.133	0.042	0.251
Cyanerpes lucidus	Shining Honeycreeper	M	man	ultramarine blue	blue	0.40 4	0.26 6	0.186	0.144	0.266
Cyanerpes nitidus	Short-billed Honeycreeper	M	man	purplish-blue	blue	0.37 7	0.34 7	0.158	0.118	0.347
Cyanicterus cyanicterus	Blue-backed Tanager	M	man	bright cadet-blue	blue	0.31 4	0.26 6	0.240	0.180	0.266
Diglossa albilatera	White-sided Flowerpiercer	M	man	dark slate-grey	blue	0.23 5	0.24 7	0.265	0.253	0.247
Diglossa cyanea	Masked Flowerpiercer	M	man	dark blue	blue	0.29 5	0.30 5	0.227	0.172	0.305
Diglossa glauca	Deep-blue Flowerpiercer	M	man	deep blue	blue	0.40 2	0.26 4	0.188	0.145	0.264
Diglossa indigotica	Indigo Flowerpiercer	M	man	indigo-blue	blue	0.31 2	0.32 5	0.203	0.161	0.325
Dubusia taeniata	Buff-breasted Mountain-Tanager	M	man	black / dark blue	blue	0.23 3	0.26 5	0.261	0.240	0.265

Iridosornis analis	Yellow-throated Tanager	M	man	greenish turquoise	blue	0.158	0.270	0.310	0.262	0.270
Iridosornis porphyrocephalus	Purplish-mantled Tanager	M	man	dark blue	blue	0.266	0.306	0.242	0.186	0.306
Iridosornis rufivertex	Golden-crowned Tanager	M	man	purplish-blue	blue	0.244	0.257	0.254	0.245	0.257
Pipraeidea melanonota	Fawn-breasted Tanager	M	man	blackish blue	blue	0.379	0.290	0.179	0.152	0.290
Porphyrospiza caerulescens	Blue Finch	M	man	bright indigo-blue	blue	0.256	0.279	0.250	0.215	0.279
Stephanophorus diadematus	Diademed Tanager	M	man	shining dark blue	blue	0.481	0.245	0.155	0.119	0.245
Tangara vassorii	Blue-and-black Tanager	M	man	dark cobalt blue	blue	0.423	0.321	0.148	0.108	0.321
Tangara viridicollis	Silvery Tanager	M	man	pale turquoise	blue	0.043	0.284	0.365	0.307	0.284
Tangara xanthocephala	Saffron-crowned Tanager	M	man	black / turquoise green	blue	0.080	0.247	0.414	0.260	0.247
Tersina viridis	Swallow Tanager	M	man	bright turquoise-blue	blue	0.241	0.264	0.337	0.159	0.264
Thraupis glaucocolpa	Glaucous Tanager	M	man	smoky grey / greenish	blue	0.181	0.242	0.305	0.272	0.242
Xenodacnis parina	Tit-like Dacnis	M	man	dark blue	blue	0.297	0.324	0.221	0.158	0.324
Anisognathus igniventris	Scarlet-bellied Mountain-Tanager	M	rum	blue	blue	0.285	0.292	0.229	0.194	0.292
Anisognathus lacrymosus	Lacrimose Mountain-Tanager	M	rum	slaty blue	blue	0.253	0.247	0.249	0.251	0.247
Anisognathus melanogenys	Black-cheeked Mountain-Tanager	M	rum	dark grey-blue	blue	0.219	0.247	0.277	0.257	0.247
Buthraupis montana	Hooded Mountain-Tanager	M	rum	shining dark blue	blue	0.293	0.236	0.240	0.232	0.236
Chlorophanes spiza	Green Honeycreeper	M	rum	glossy viridian green	blue	0.069	0.330	0.396	0.204	0.330
Conirostrum bicolor	Bicolored Conebill	M	rum	pale bluish-grey	blue	0.211	0.248	0.274	0.266	0.248
Cyanerpes caeruleus	Purple Honeycreeper	M	rum	lustrous violet-blue	blue	0.602	0.224	0.135	0.039	0.224
Cyanerpes lucidus	Shining Honeycreeper	M	rum	ultramarine blue	blue	0.478	0.240	0.186	0.095	0.240
Cyanerpes nitidus	Short-billed Honeycreeper	M	rum	purplish-blue	blue	0.401	0.337	0.135	0.127	0.337
Cyanicterus cyanicterus	Blue-backed Tanager	M	rum	bright cadet-blue	blue	0.276	0.260	0.253	0.211	0.260
Dacnis cayana	Blue Dacnis	M	rum	turquoise blue	blue	0.212	0.272	0.257	0.259	0.272
Dacnis hartlaubi	Turquoise Dacnis	M	rum	turquoise	blue	0.237	0.291	0.254	0.218	0.291
Dacnis nigripes	Black-legged Dacnis	M	rum	light turquoise / greenish blue / black	blue	0.235	0.279	0.281	0.205	0.279
Dacnis viguieri	Viridian Dacnis	M	rum	greenish blue	blue	0.172	0.223	0.330	0.275	0.223
Diglossa albilatera	White-sided Flowerpiercer	M	rum	dark slate-grey	blue	0.223	0.239	0.265	0.273	0.239
Diglossa cyanea	Masked Flowerpiercer	M	rum	dark blue	blue	0.265	0.284	0.245	0.206	0.284
Diglossa glauca	Deep-blue Flowerpiercer	M	rum	deep blue	blue	0.424	0.266	0.178	0.132	0.266
Diglossa indigotica	Indigo Flowerpiercer	M	rum	indigo-blue	blue	0.312	0.324	0.203	0.161	0.324
Dubusia taeniata	Buff-breasted Mountain-Tanager	M	rum	dark blue	blue	0.227	0.247	0.263	0.263	0.247
Iridosornis analis	Yellow-throated Tanager	M	rum	greenish turquoise	blue	0.175	0.230	0.303	0.292	0.230
Iridosornis porphyrocephalus	Purplish-mantled Tanager	M	rum	dark blue	blue	0.191	0.217	0.279	0.313	0.217

<i>Iridosornis rufivertex</i>	Golden-crowned Tanager	M	rum	purplish-blue	blue	0.29 2	0.27 6	0.221	0.211	0.276
<i>Pipraeidea melanonota</i>	Fawn-breasted Tanager	M	rum	bright turquoise blue	blue	0.35 6	0.35 1	0.170	0.123	0.351
<i>Porphyrospiza caerulescens</i>	Blue Finch	M	rum	bright indigo-blue	blue	0.25 4	0.26 0	0.252	0.234	0.260
<i>Stephanophorus diadematus</i>	Diademed Tanager	M	rum	shining dark blue	blue	0.30 0	0.24 8	0.226	0.226	0.248
<i>Tangara labradorides</i>	Metallic-green Tanager	M	rum	opalescent blue-green	blue	0.11 0	0.24 5	0.390	0.256	0.245
<i>Tangara larvata</i>	Golden-hooded Tanager	M	rum	light blue	blue	0.20 4	0.26 8	0.281	0.247	0.268
<i>Tangara nigrocincta</i>	Masked Tanager	M	rum	light blue	blue	0.27 4	0.34 5	0.252	0.129	0.345
<i>Tangara ruficervix</i>	Golden-naped Tanager	M	rum	bright blue	blue	0.21 4	0.25 4	0.284	0.248	0.254
<i>Tangara vassorii</i>	Blue-and-black Tanager	M	rum	dark cobalt blue	blue	0.43 8	0.29 5	0.159	0.108	0.295
<i>Tangara viridicollis</i>	Silvery Tanager	M	rum	pale turquoise	blue	0.08 1	0.25 6	0.354	0.308	0.256
<i>Tangara xanthocephala</i>	Saffron-crowned Tanager	M	rum	black / turquoise green	blue	0.08 7	0.23 6	0.419	0.258	0.236
<i>Tersina viridis</i>	Swallow Tanager	M	rum	bright turquoise-blue	blue	0.23 9	0.26 6	0.320	0.175	0.266
<i>Thraupis glaucocolpa</i>	Glauous Tanager	M	rum	smoky grey / greenish	blue	0.18 8	0.24 1	0.315	0.256	0.241
<i>Xenodacnis parina</i>	Tit-like Dacnis	M	rum	dark blue	blue	0.27 7	0.29 7	0.244	0.182	0.297
<i>Chlorophanes spiza</i>	Green Honeycreeper	M	thr	glossy viridian green	blue	0.05 1	0.30 2	0.444	0.203	0.302
<i>Cyanerpes cyaneus</i>	Red-legged Honeycreeper	M	thr	purplish-blue	blue	0.52 4	0.25 6	0.140	0.080	0.256
<i>Dacnis lineata</i>	Black-faced Dacnis	M	thr	turquoise-blue	blue	0.26 7	0.27 3	0.285	0.175	0.273
<i>Dacnis viguieri</i>	Viridian Dacnis	M	thr	verditer blue/green	blue	0.27 6	0.21 7	0.334	0.173	0.217
<i>Diglossa albilatera</i>	White-sided Flowerpiercer	M	thr	dark slate-grey	blue	0.20 2	0.24 7	0.282	0.270	0.247
<i>Diglossa glauca</i>	Deep-blue Flowerpiercer	M	thr	deep blue	blue	0.41 8	0.27 3	0.179	0.130	0.273
<i>Diglossa indigotica</i>	Indigo Flowerpiercer	M	thr	indigo-blue	blue	0.28 0	0.34 9	0.218	0.153	0.349
<i>Porphyrospiza caerulescens</i>	Blue Finch	M	thr	bright indigo-blue	blue	0.27 7	0.28 3	0.234	0.207	0.283
<i>Tangara chilensis</i>	Paradise Tanager	M	thr	dark blue	blue	0.52 2	0.27 4	0.121	0.083	0.274
<i>Tangara labradorides</i>	Metallic-green Tanager	M	thr	opalescent blue-green	blue	0.11 0	0.27 0	0.348	0.271	0.270
<i>Tangara mexicana</i>	Turquoise Tanager	M	thr	dark turquoise blue	blue	0.38 5	0.29 6	0.181	0.138	0.296
<i>Tangara nigrocincta</i>	Masked Tanager	M	thr	pale lavender	blue	0.19 2	0.33 5	0.272	0.200	0.335
<i>Tangara peruviana</i>	Black-backed Tanager	M	thr	bluish-green	blue	0.09 0	0.22 5	0.388	0.297	0.225
<i>Tangara preciosa</i>	Chestnut-backed Tanager	M	thr	blue-green	blue	0.08 1	0.23 1	0.394	0.294	0.231
<i>Tangara vassorii</i>	Blue-and-black Tanager	M	thr	dark blue	blue	0.37 2	0.29 4	0.193	0.142	0.294
<i>Tangara velia</i>	Opal-rumped Tanager	M	thr	deep purplish-blue	blue	0.29 3	0.34 2	0.204	0.161	0.342
<i>Thraupis abbas</i>	Yellow-winged Tanager	M	thr	blue	blue	0.26 8	0.24 2	0.246	0.244	0.242
<i>Thraupis bonariensis</i>	Blue-and-yellow Tanager	M	thr	dull blue	blue	0.25 2	0.26 7	0.254	0.228	0.267
<i>Thraupis ornata</i>	Golden-chevroned Tanager	M	thr	shining cadet-blue	blue	0.26 4	0.24 9	0.242	0.244	0.249
<i>Xenodacnis parina</i>	Tit-like Dacnis	M	thr	dark blue	blue	0.26 4	0.29 1	0.248	0.198	0.291
<i>Chlorochrysa</i>	Orange-eared	M	bre	emerald-green	blue	0.08	0.24	0.493	0.181	0.245

calliparaea	Tanager					1	5			
Chlorophanes spiza	Green Honeycreeper	M	bre	glossy viridian green	blue	0.057	0.325	0.416	0.201	0.325
Cyanerpes caeruleus	Purple Honeycreeper	M	bre	lustrous violet-blue	blue	0.694	0.140	0.166	0.000	0.140
Cyanerpes cyaneus	Red-legged Honeycreeper	M	bre	purplish-blue	blue	0.602	0.197	0.139	0.062	0.197
Cyanerpes lucidus	Shining Honeycreeper	M	bre	ultramarine blue	blue	0.478	0.276	0.167	0.079	0.276
Cyanerpes nitidus	Short-billed Honeycreeper	M	bre	purplish-blue	blue	0.383	0.317	0.168	0.132	0.317
Dacnis cayana	Blue Dacnis	M	bre	turquoise	blue	0.206	0.285	0.269	0.241	0.285
Dacnis hartlaubi	Turquoise Dacnis	M	bre	turquoise	blue	0.279	0.273	0.281	0.168	0.273
Dacnis lineata	Black-faced Dacnis	M	bre	turquoise-blue	blue	0.253	0.285	0.291	0.171	0.285
Dacnis nigripes	Black-legged Dacnis	M	bre	light turquoise	blue	0.218	0.288	0.293	0.202	0.288
Dacnis viguieri	Viridian Dacnis	M	bre	verditer blue/green	blue	0.262	0.227	0.342	0.169	0.227
Diglossa albilatera	White-sided Flowerpiercer	M	bre	dark slate-grey / white	blue	0.229	0.252	0.266	0.253	0.252
Diglossa cyanea	Masked Flowerpiercer	M	bre	dark blue	blue	0.278	0.311	0.234	0.177	0.311
Diglossa glauca	Deep-blue Flowerpiercer	M	bre	deep blue	blue	0.388	0.258	0.194	0.160	0.258
Diglossa indigotica	Indigo Flowerpiercer	M	bre	indigo-blue	blue	0.299	0.323	0.207	0.171	0.323
Iridosornis rufivertex	Golden-crowned Tanager	M	bre	purplish-blue	blue	0.270	0.279	0.231	0.220	0.279
Stephanophorus diadematus	Diademed Tanager	M	bre	shining dark blue	blue	0.381	0.254	0.193	0.173	0.254
Tangara chilensis	Paradise Tanager	M	bre	dark blue	blue	0.164	0.252	0.181	0.403	0.252
Tangara cyanoventris	Gilt-edged Tanager	M	bre	turquoise-blue	blue	0.152	0.258	0.281	0.309	0.258
Tangara gyrola	Bay-headed Tanager	M	bre	green / light blue	blue	0.224	0.271	0.344	0.161	0.271
Tangara labradorides	Metallic-green Tanager	M	bre	opalescent blue-green	blue	0.106	0.282	0.379	0.233	0.282
Tangara mexicana	Turquoise Tanager	M	bre	dark turquoise blue	blue	0.312	0.209	0.250	0.229	0.209
Tangara peruviana	Black-backed Tanager	M	bre	bluish-green	blue	0.065	0.245	0.403	0.286	0.245
Tangara preciosa	Chestnut-backed Tanager	M	bre	blue-green	blue	0.058	0.253	0.420	0.269	0.253
Tangara ruficervix	Golden-naped Tanager	M	bre	bright blue	blue	0.218	0.267	0.307	0.207	0.267
Tangara seledon	Green-headed Tanager	M	bre	turquoise	blue	0.211	0.298	0.330	0.160	0.298
Tangara vassorii	Blue-and-black Tanager	M	bre	dark blue	blue	0.394	0.307	0.172	0.127	0.307
Tangara velia	Opal-rumped Tanager	M	bre	purplish blue	blue	0.425	0.265	0.163	0.148	0.265
Tangara xanthocephala	Saffron-crowned Tanager	M	bre	black / turquoise green	blue	0.074	0.209	0.407	0.309	0.209
Thraupis glaucocolpa	Glaucous Tanager	M	bre	grey / turquoise-blue	blue	0.170	0.263	0.309	0.257	0.263
Thraupis ornata	Golden-chevroned Tanager	M	bre	shining cadet-blue	blue	0.329	0.257	0.210	0.205	0.257
Xenodacnis parina	Tit-like Dacnis	M	bre	dark blue	blue	0.315	0.312	0.210	0.163	0.312
Chlorochrysa calliparaea	Orange-eared Tanager	M	bel	emerald-green / dark blue-green	blue	0.143	0.274	0.410	0.174	0.274
Cyanerpes caeruleus	Purple Honeycreeper	M	bel	lustrous violet-blue	blue	0.652	0.198	0.146	0.004	0.198
Cyanerpes cyaneus	Red-legged Honeycreeper	M	bel	purplish-blue	blue	0.519	0.271	0.142	0.069	0.271

Cyanerpes lucidus	Shining Honeycreeper	M	bel	ultramarine blue	blue	0.513	0.262	0.159	0.067	0.262
Dacnis cayana	Blue Dacnis	M	bel	turquoise	blue	0.235	0.285	0.285	0.195	0.285
Dacnis hartlaubi	Turquoise Dacnis	M	bel	turquoise	blue	0.270	0.279	0.280	0.172	0.279
Dacnis nigripes	Black-legged Dacnis	M	bel	light turquoise	blue	0.244	0.289	0.299	0.168	0.289
Dacnis viguieri	Viridian Dacnis	M	bel	verditer blue/ green	blue	0.243	0.224	0.345	0.188	0.224
Diglossa albilatera	White-sided Flowerpiercer	M	bel	dark slate-grey	blue	0.221	0.247	0.268	0.265	0.247
Diglossa cyanea	Masked Flowerpiercer	M	bel	dark blue	blue	0.246	0.281	0.255	0.218	0.281
Diglossa glauca	Deep-blue Flowerpiercer	M	bel	deep blue	blue	0.295	0.258	0.232	0.215	0.258
Diglossa indigotica	Indigo Flowerpiercer	M	bel	indigo-blue	blue	0.297	0.321	0.214	0.168	0.321
Iridosornis rufivertex	Golden-crowned Tanager	M	bel	purplish-blue/ chestnut	blue	0.214	0.266	0.263	0.257	0.266
Stephanophorus diadematus	Diademed Tanager	M	bel	no	blue	0.357	0.246	0.204	0.193	0.246
Tangara cyanicollis	Blue-necked Tanager	M	bel	black / deep blue	blue	0.276	0.255	0.242	0.227	0.255
Tangara gyrola	Bay-headed Tanager	M	bel	green / light blue	blue	0.215	0.220	0.381	0.184	0.220
Tangara lavinia	Rufous-winged Tanager	M	bel	blue	blue	0.229	0.269	0.348	0.154	0.269
Tangara preciosa	Chestnut-backed Tanager	M	bel	blue-green / yellowish-opal	blue	0.145	0.256	0.316	0.283	0.256
Tangara vassorii	Blue-and-black Tanager	M	bel	dark blue	blue	0.381	0.305	0.169	0.146	0.305
Thraupis ornata	Golden-chevrons Tanager	M	bel	grey / blueish-green	blue	0.218	0.244	0.264	0.273	0.244
Xenodacnis parina	Tit-like Dacnis	M	bel	dark blue	blue	0.252	0.288	0.252	0.208	0.288
Anisognathus lacrymosus	Lacrimose Mountain-Tanager	F	cro	slaty blue	blue	0.215	0.273	0.268	0.245	0.273
Anisognathus melanogenys	Black-cheeked Mountain-Tanager	F	cro	shining blue	blue	0.170	0.239	0.300	0.291	0.239
Buthraupis eximia	Black-chested Mountain-Tanager	F	cro	blue	blue	0.219	0.273	0.264	0.244	0.273
Conirostrum albigrons	Capped Conebill	F	cro	dull blue	blue	0.288	0.285	0.223	0.205	0.285
Conirostrum bicolor	Bicolored Conebill	F	cro	pale bluish-grey	blue	0.130	0.185	0.326	0.359	0.185
Cyanicterus cyanicterus	Blue-backed Tanager	F	cro	bright cadet-blue	blue	0.216	0.208	0.335	0.241	0.208
Dacnis cayana	Blue Dacnis	F	cro	blue	blue	0.218	0.245	0.329	0.209	0.245
Dacnis nigripes	Black-legged Dacnis	F	cro	brownish olive / turquoise	blue	0.175	0.235	0.308	0.283	0.235
Dacnis venusta	Scarlet-thighed Dacnis	F	cro	greenish olive / blue	blue	0.168	0.220	0.321	0.291	0.220
Diglossa cyanea	Masked Flowerpiercer	F	cro	dark blue	blue	0.214	0.275	0.271	0.240	0.275
Diglossa indigotica	Indigo Flowerpiercer	F	cro	indigo-blue	blue	0.187	0.231	0.288	0.294	0.231
Iridosornis analis	Yellow-throated Tanager	F	cro	deep purplish blue	blue	0.152	0.237	0.299	0.312	0.237
Iridosornis porphyrocephalus	Purplish-mantled Tanager	F	cro	dark blue	blue	0.212	0.238	0.267	0.283	0.238
Tangara cyanocephala	Red-necked Tanager	F	cro	blue-violet	blue	0.255	0.343	0.237	0.165	0.343
Tangara nigrocincta	Masked Tanager	F	cro	pale lavender	blue	0.228	0.323	0.255	0.194	0.323
Tangara seledon	Green-headed Tanager	F	cro	turquoise-green	blue	0.077	0.227	0.443	0.252	0.227

Tangara vassorii	Blue-and-black Tanager	F	cro	dark cobalt blue	blue	0.26 1	0.29 1	0.242	0.207	0.291
Thraupis abbas	Yellow-winged Tanager	F	cro	campanula-blue	blue	0.32 1	0.24 6	0.220	0.213	0.246
Thraupis bonariensis	Blue-and-yellow Tanager	F	cro	brownish olive / blue	blue	0.15 4	0.20 1	0.313	0.331	0.201
Thraupis cyanocephala	Blue-capped Tanager	F	cro	shining cornflower-blue	blue	0.36 2	0.27 0	0.200	0.167	0.270
Thraupis ornata	Golden-chevroned Tanager	F	cro	shining cadet-blue	blue	0.21 7	0.26 9	0.265	0.250	0.269
Anisognathus melanogenys	Black-cheeked Mountain-Tanager	F	nap	shining blue	blue	0.21 8	0.25 0	0.271	0.262	0.250
Buthraupis eximia	Black-chested Mountain-Tanager	F	nap	blue	blue	0.33 6	0.30 7	0.197	0.160	0.307
Buthraupis montana	Hooded Mountain-Tanager	F	nap	shining pale milky blue	blue	0.22 1	0.24 0	0.275	0.264	0.240
Conirostrum bicolor	Bicolored Conebill	F	nap	pale bluish-grey	blue	0.14 2	0.19 4	0.316	0.348	0.194
Cyanicterus cyanicterus	Blue-backed Tanager	F	nap	bright cadet-blue	blue	0.24 1	0.22 2	0.311	0.226	0.222
Dacnis venusta	Scarlet-thighed Dacnis	F	nap	greenish olive / blue	blue	0.17 7	0.22 6	0.338	0.259	0.226
Diglossa cyanea	Masked Flowerpiercer	F	nap	dark blue	blue	0.24 0	0.28 7	0.257	0.216	0.287
Diglossa indigotica	Indigo Flowerpiercer	F	nap	indigo-blue	blue	0.20 5	0.23 4	0.279	0.283	0.234
Iridosornis analis	Yellow-throated Tanager	F	nap	greenish turquoise	blue	0.17 1	0.26 1	0.289	0.279	0.261
Iridosornis porphyrocephalus	Purplish-mantled Tanager	F	nap	dark blue	blue	0.28 0	0.28 9	0.230	0.201	0.289
Tangara cyanocephala	Red-necked Tanager	F	nap	blue-violet	blue	0.24 3	0.23 3	0.301	0.224	0.233
Tangara nigrocincta	Masked Tanager	F	nap	pale lavender	blue	0.24 9	0.33 2	0.249	0.169	0.332
Tangara seledon	Green-headed Tanager	F	nap	turquoise-green	blue	0.09 0	0.19 4	0.455	0.260	0.194
Tangara vassorii	Blue-and-black Tanager	F	nap	dark cobalt blue	blue	0.28 8	0.30 2	0.222	0.189	0.302
Thraupis abbas	Yellow-winged Tanager	F	nap	campanula-blue	blue	0.36 0	0.24 6	0.204	0.190	0.246
Thraupis cyanocephala	Blue-capped Tanager	F	nap	shining cornflower-blue	blue	0.37 7	0.24 6	0.203	0.174	0.246
Thraupis ornata	Golden-chevroned Tanager	F	nap	shining cadet-blue	blue	0.27 0	0.27 8	0.234	0.217	0.278
Anisognathus lacrymosus	Lacrimose Mountain-Tanager	F	man	slaty blue	blue	0.19 4	0.24 7	0.281	0.279	0.247
Anisognathus melanogenys	Black-cheeked Mountain-Tanager	F	man	dark grey-blue	blue	0.19 9	0.23 6	0.281	0.284	0.236
Buthraupis montana	Hooded Mountain-Tanager	F	man	shining dark blue	blue	0.64 3	0.22 0	0.137	0.000	0.220
Conirostrum bicolor	Bicolored Conebill	F	man	pale bluish-grey	blue	0.14 6	0.20 2	0.316	0.337	0.202
Diglossa cyanea	Masked Flowerpiercer	F	man	dark blue	blue	0.22 2	0.26 2	0.266	0.250	0.262
Diglossa indigotica	Indigo Flowerpiercer	F	man	indigo-blue	blue	0.19 8	0.23 3	0.281	0.289	0.233
Dubusia taeniata	Buff-breasted Mountain-Tanager	F	man	black / dark blue	blue	0.21 5	0.25 5	0.274	0.256	0.255
Iridosornis analis	Yellow-throated Tanager	F	man	greenish turquoise	blue	0.17 5	0.23 7	0.297	0.292	0.237
Iridosornis porphyrocephalus	Purplish-mantled Tanager	F	man	dark blue	blue	0.22 4	0.24 9	0.266	0.260	0.249
Stephanophorus diadematus	Diademed Tanager	F	man	shining dark blue	blue	0.33 0	0.24 5	0.217	0.208	0.245
Tangara labradorides	Metallic-green Tanager	F	man	opalescent blue-green	blue	0.05 9	0.25 7	0.426	0.258	0.257
Tangara vassorii	Blue-and-black	F	man	dark cobalt blue	blue	0.23	0.26	0.261	0.246	0.261

	Tanager					2	1			
Tangara xanthocephala	Saffron-crowned Tanager	F	man	black / turquoise green	blue	0.170	0.227	0.313	0.289	0.227
Thraupis abbas	Yellow-winged Tanager	F	man	smoky blue-grey	blue	0.320	0.189	0.245	0.245	0.189
Thraupis glaucocolpa	Glaucous Tanager	F	man	smoky grey / greenish	blue	0.180	0.249	0.297	0.275	0.249
Anisognathus igniventris	Scarlet-bellied Mountain-Tanager	F	rum	blue	blue	0.342	0.325	0.193	0.140	0.325
Anisognathus lacrymosus	Lacrimose Mountain-Tanager	F	rum	slaty blue	blue	0.282	0.278	0.234	0.206	0.278
Anisognathus melanogenys	Black-cheeked Mountain-Tanager	F	rum	dark grey-blue	blue	0.204	0.239	0.286	0.270	0.239
Buthraupis montana	Hooded Mountain-Tanager	F	rum	shining dark blue	blue	0.407	0.230	0.201	0.162	0.230
Conirostrum bicolor	Bicolored Conebill	F	rum	pale bluish-grey	blue	0.158	0.212	0.299	0.331	0.212
Cyanicterus cyanicterus	Blue-backed Tanager	F	rum	bright cadet-blue	blue	0.234	0.219	0.296	0.252	0.219
Dacnis nigripes	Black-legged Dacnis	F	rum	brownish olive / turquoise	blue	0.181	0.242	0.315	0.262	0.242
Diglossa cyanea	Masked Flowerpiercer	F	rum	dark blue	blue	0.229	0.262	0.265	0.245	0.262
Diglossa indigotica	Indigo Flowerpiercer	F	rum	indigo-blue	blue	0.198	0.220	0.273	0.309	0.220
Dubusia taeniata	Buff-breasted Mountain-Tanager	F	rum	dark blue	blue	0.223	0.233	0.267	0.276	0.233
Iridosornis analis	Yellow-throated Tanager	F	rum	greenish turquoise	blue	0.130	0.230	0.336	0.304	0.230
Iridosornis porphyrocephalus	Purplish-mantled Tanager	F	rum	dark blue	blue	0.172	0.238	0.310	0.279	0.238
Stephanophorus diadematus	Diademed Tanager	F	rum	shining dark blue	blue	0.344	0.267	0.200	0.188	0.267
Tangara labradorides	Metallic-green Tanager	F	rum	opalescent blue-green	blue	0.058	0.221	0.458	0.263	0.221
Tangara larvata	Golden-hooded Tanager	F	rum	light blue	blue	0.211	0.278	0.311	0.200	0.278
Tangara nigrocincta	Masked Tanager	F	rum	light blue	blue	0.244	0.300	0.294	0.163	0.300
Tangara vassorii	Blue-and-black Tanager	F	rum	dark cobalt blue	blue	0.218	0.253	0.264	0.265	0.253
Tangara xanthocephala	Saffron-crowned Tanager	F	rum	black / turquoise green	blue	0.138	0.216	0.352	0.294	0.216
Thraupis glaucocolpa	Glaucous Tanager	F	rum	smoky grey / greenish	blue	0.190	0.259	0.307	0.245	0.259
Diglossa indigotica	Indigo Flowerpiercer	F	thr	indigo-blue	blue	0.121	0.201	0.312	0.366	0.201
Tangara cayana	Burnished-buff Tanager	F	thr	blue-violet	blue	0.105	0.250	0.326	0.319	0.250
Tangara chilensis	Paradise Tanager	F	thr	dark blue	blue	0.463	0.276	0.159	0.102	0.276
Tangara labradorides	Metallic-green Tanager	F	thr	opalescent blue-green	blue	0.133	0.245	0.338	0.284	0.245
Tangara mexicana	Turquoise Tanager	F	thr	dark turquoise blue	blue	0.402	0.272	0.180	0.145	0.272
Tangara nigrocincta	Masked Tanager	F	thr	pale lavender	blue	0.122	0.279	0.344	0.254	0.279
Tangara vassorii	Blue-and-black Tanager	F	thr	dark blue	blue	0.219	0.268	0.261	0.253	0.268
Tangara velia	Opal-rumped Tanager	F	thr	deep purplish-blue	blue	0.232	0.391	0.224	0.153	0.391
Tangara xanthocephala	Saffron-crowned Tanager	F	thr	black / turquoise green	blue	0.138	0.212	0.317	0.333	0.212
Thraupis abbas	Yellow-winged Tanager	F	thr	blue	blue	0.235	0.240	0.261	0.264	0.240
Thraupis ornata	Golden-chevroned Tanager	F	thr	shining cadet-blue	blue	0.180	0.240	0.287	0.292	0.240

Diglossa cyanea	Masked Flowerpiercer	F	bre	dark blue	blue	0.187	0.247	0.282	0.283	0.247
Diglossa indigotica	Indigo Flowerpiercer	F	bre	indigo-blue	blue	0.178	0.216	0.281	0.324	0.216
Stephanophorus diadematus	Diademed Tanager	F	bre	shining dark blue	blue	0.288	0.254	0.234	0.224	0.254
Tangara chilensis	Paradise Tanager	F	bre	dark blue	blue	0.125	0.230	0.210	0.435	0.230
Tangara cyanoventris	Gilt-edged Tanager	F	bre	turquoise-blue	blue	0.183	0.245	0.341	0.232	0.245
Tangara gyrola	Bay-headed Tanager	F	bre	green / light blue	blue	0.213	0.260	0.369	0.157	0.260
Tangara labradorides	Metallic-green Tanager	F	bre	opalescent blue-green	blue	0.124	0.240	0.349	0.287	0.240
Tangara mexicana	Turquoise Tanager	F	bre	dark turquoise blue	blue	0.287	0.199	0.261	0.253	0.199
Tangara seledon	Green-headed Tanager	F	bre	turquoise	blue	0.184	0.251	0.365	0.201	0.251
Tangara vassorii	Blue-and-black Tanager	F	bre	dark blue	blue	0.255	0.300	0.240	0.205	0.300
Tangara velia	Opal-rumped Tanager	F	bre	purplish blue	blue	0.348	0.328	0.171	0.152	0.328
Tangara xanthocephala	Saffron-crowned Tanager	F	bre	black / turquoise green	blue	0.127	0.202	0.334	0.337	0.202
Thraupis glaucocolpa	Glaucous Tanager	F	bre	grey / turquoise-blue	blue	0.184	0.279	0.309	0.228	0.279
Thraupis ornata	Golden-chevroned Tanager	F	bre	shining cadet-blue	blue	0.256	0.246	0.244	0.254	0.246
Diglossa cyanea	Masked Flowerpiercer	F	bel	dark blue	blue	0.193	0.244	0.282	0.281	0.244
Diglossa indigotica	Indigo Flowerpiercer	F	bel	indigo-blue	blue	0.191	0.222	0.275	0.312	0.222
Stephanophorus diadematus	Diademed Tanager	F	bel	no	blue	0.242	0.243	0.255	0.259	0.243
Tangara cyanicollis	Blue-necked Tanager	F	bel	black / deep blue	blue	0.263	0.290	0.232	0.214	0.290
Tangara gyrola	Bay-headed Tanager	F	bel	green / light blue	blue	0.204	0.202	0.358	0.235	0.202
Tangara lavinia	Rufous-winged Tanager	F	bel	blue	blue	0.176	0.233	0.323	0.267	0.233
Tangara vassorii	Blue-and-black Tanager	F	bel	dark blue	blue	0.271	0.306	0.229	0.194	0.306
Thraupis ornata	Golden-chevroned Tanager	F	bel	grey / blueish-green	blue	0.149	0.228	0.298	0.325	0.228
Cnemoscopus rubrirostris	Gray-hooded Bush Tanager	M	cro	medium grey	grey	0.131	0.241	0.312	0.317	0.241
Coereba flaveola	Bananaquit	M	cro	dark grey	grey	0.182	0.241	0.292	0.285	0.241
Diuca diuca	Common Diuca-Finch	M	cro	dark gray	grey	0.161	0.249	0.294	0.296	0.249
Hemispingus melanotis	Black-eared Hemispingus	M	cro	grey	grey	0.183	0.248	0.288	0.281	0.248
Hemispingus reyi	Gray-capped Hemispingus	M	cro	grey	grey	0.167	0.243	0.291	0.299	0.243
Hemispingus xanthophthalmus	Drab Hemispingus	M	cro	brownish-grey	grey	0.120	0.208	0.310	0.362	0.208
Idiopsar brachyurus	Short-tailed Finch	M	cro	leaden gray	grey	0.178	0.243	0.284	0.295	0.243
Incaspiza laeta	Buff-bridled Inca-Finch	M	cro	grey	grey	0.172	0.242	0.288	0.299	0.242
Incaspiza personata	Rufous-backed Inca-Finch	M	cro	grey	grey	0.140	0.230	0.300	0.330	0.230
Melanodera melanodera	White-bridled Finch	M	cro	grey	grey	0.190	0.250	0.283	0.277	0.250
Neothraupis fasciata	White-banded Tanager	M	cro	grey	grey	0.174	0.250	0.290	0.285	0.250
Phrygilus fruticeti	Mourning Sierra-Finch	M	cro	grey	grey	0.182	0.242	0.286	0.289	0.242

<i>Piezorhina cinerea</i>	Cinereous Finch	M	cro	pale grey	grey	0.148	0.240	0.297	0.314	0.240
<i>Poospiza alticola</i>	Plain-tailed Warbling-Finch	M	cro	gray brown	grey	0.150	0.237	0.297	0.315	0.237
<i>Poospiza cabanisi</i>	Gray-throated Warbling-Finch	M	cro	grey	grey	0.140	0.229	0.308	0.323	0.229
<i>Poospiza caesar</i>	Chestnut-breasted Mountain-Finch	M	cro	gray	grey	0.164	0.232	0.292	0.312	0.232
<i>Poospiza hispaniolensis</i>	Collared Warbling-Finch	M	cro	grey / black	grey	0.180	0.253	0.287	0.280	0.253
<i>Poospiza nigrorufa</i>	Black-and-rufous Warbling-Finch	M	cro	blackish grey	grey	0.182	0.236	0.286	0.296	0.236
<i>Poospiza thoracica</i>	Bay-chested Warbling-Finch	M	cro	grey	grey	0.122	0.250	0.315	0.313	0.250
<i>Saltator coerulescens</i>	Grayish Saltator	M	cro	greyish	grey	0.146	0.234	0.299	0.322	0.234
<i>Sporophila caerulescens</i>	Double-collared Seedeater	M	cro	lead-grey	grey	0.168	0.238	0.288	0.306	0.238
<i>Sporophila hypoxantha</i>	Tawny-bellied Seedeater	M	cro	greyish	grey	0.179	0.250	0.285	0.286	0.250
<i>Sporophila leucoptera</i>	White-bellied Seedeater	M	cro	dark grey	grey	0.163	0.239	0.293	0.305	0.239
<i>Sporophila minuta</i>	Ruddy-breasted Seedeater	M	cro	mid-grey	grey	0.128	0.233	0.311	0.328	0.233
<i>Sporophila palustris</i>	Marsh Seedeater	M	cro	grey	grey	0.163	0.245	0.291	0.301	0.245
<i>Sporophila peruviana</i>	Parrot-billed Seedeater	M	cro	greyish	grey	0.159	0.232	0.298	0.311	0.232
<i>Sporophila plumbea</i>	Plumbeous Seedeater	M	cro	lead-grey	grey	0.162	0.247	0.291	0.300	0.247
<i>Sporophila ruficollis</i>	Dark-throated Seedeater	M	cro	grey	grey	0.162	0.240	0.291	0.307	0.240
<i>Sporophila telasco</i>	Chestnut-throated Seedeater	M	cro	mid-grey / dusky	grey	0.142	0.234	0.303	0.321	0.234
<i>Tangara inornata</i>	Plain-colored Tanager	M	cro	dark gray	grey	0.175	0.250	0.282	0.293	0.250
<i>Thraupis glaucocolpa</i>	Glaucon Tanager	M	cro	smoky grey / greenish	grey	0.170	0.233	0.300	0.297	0.233
<i>Thraupis sayaca</i>	Sayaca Tanager	M	cro	dull grey / bluish	grey	0.172	0.240	0.293	0.295	0.240
<i>Coereba flaveola</i>	Bananaquit	M	nap	dark grey	grey	0.191	0.240	0.285	0.284	0.240
<i>Coryphaspiza melanotis</i>	Black-masked Finch	M	nap	greyish	grey	0.144	0.220	0.297	0.338	0.220
<i>Creurgops verticalis</i>	Rufous-crested Tanager	M	nap	leaden grey	grey	0.129	0.196	0.297	0.378	0.196
<i>Diuca diuca</i>	Common Diuca-Finch	M	nap	dark gray	grey	0.188	0.251	0.281	0.280	0.251
<i>Hemispingus melanotis</i>	Black-eared Hemispingus	M	nap	grey	grey	0.192	0.248	0.283	0.277	0.248
<i>Hemispingus xanthophthalmus</i>	Drab Hemispingus	M	nap	brownish-grey	grey	0.143	0.214	0.297	0.346	0.214
<i>Idiopsar brachyurus</i>	Short-tailed Finch	M	nap	leaden gray	grey	0.202	0.242	0.276	0.281	0.242
<i>Incaspiza laeta</i>	Buff-bridled Inca-Finch	M	nap	grey	grey	0.172	0.246	0.288	0.294	0.246
<i>Melanoderes xanthogramma</i>	Yellow-bridled Finch	M	nap	grey	grey	0.234	0.231	0.273	0.263	0.231
<i>Neothraupis fasciata</i>	White-banded Tanager	M	nap	grey	grey	0.191	0.250	0.279	0.279	0.250
<i>Phrygilus fruticeti</i>	Mourning Sierra-Finch	M	nap	grey	grey	0.171	0.241	0.291	0.297	0.241
<i>Piezorhina cinerea</i>	Cinereous Finch	M	nap	pale grey	grey	0.162	0.244	0.290	0.305	0.244
<i>Poospiza alticola</i>	Plain-tailed Warbling-Finch	M	nap	gray brown	grey	0.163	0.233	0.291	0.313	0.233
<i>Poospiza cabanisi</i>	Gray-throated Warbling-Finch	M	nap	grey	grey	0.122	0.197	0.318	0.363	0.197

Poospiza caesar	Chestnut-breasted Mountain-Finch	M	nap	gray	grey	0.174	0.237	0.285	0.303	0.237
Poospiza hispaniolensis	Collared Warbling-Finch	M	nap	grey	grey	0.198	0.251	0.280	0.271	0.251
Poospiza nigrorufa	Black-and-rufous Warbling-Finch	M	nap	no	grey	0.171	0.231	0.288	0.310	0.231
Poospiza thoracica	Bay-chested Warbling-Finch	M	nap	grey	grey	0.142	0.251	0.303	0.304	0.251
Saltator coerulescens	Grayish Saltator	M	nap	greyish	grey	0.133	0.222	0.303	0.342	0.222
Schistochlamys melanopsis	Black-faced Tanager	M	nap	grey	grey	0.201	0.258	0.278	0.263	0.258
Sporophila albogularis	White-throated Seedeater	M	nap	no	grey	0.183	0.242	0.281	0.294	0.242
Sporophila caerulescens	Double-collared Seedeater	M	nap	olive-brown	grey	0.165	0.239	0.289	0.308	0.239
Sporophila hypoxantha	Tawny-bellied Seedeater	M	nap	greyish	grey	0.178	0.249	0.284	0.290	0.249
Sporophila leucoptera	White-bellied Seedeater	M	nap	dark grey	grey	0.201	0.245	0.276	0.277	0.245
Sporophila minuta	Ruddy-breasted Seedeater	M	nap	mid-grey	grey	0.143	0.233	0.301	0.323	0.233
Sporophila palustris	Marsh Seedeater	M	nap	grey	grey	0.180	0.239	0.282	0.299	0.239
Sporophila peruviana	Parrot-billed Seedeater	M	nap	greyish-brown	grey	0.171	0.232	0.289	0.308	0.232
Sporophila plumbea	Plumbeous Seedeater	M	nap	lead-grey	grey	0.163	0.247	0.288	0.301	0.247
Sporophila ruficollis	Dark-throated Seedeater	M	nap	grey	grey	0.185	0.247	0.281	0.287	0.247
Sporophila telasco	Chestnut-throated Seedeater	M	nap	greyish / dusky	grey	0.144	0.238	0.301	0.318	0.238
Tangara inornata	Plain-colored Tanager	M	nap	dark gray	grey	0.194	0.249	0.279	0.278	0.249
Thraupis glaucocolpa	Glaucous Tanager	M	nap	smoky grey / greenish	grey	0.194	0.228	0.298	0.280	0.228
Thraupis sayaca	Sayaca Tanager	M	nap	dull grey / bluish	grey	0.186	0.238	0.294	0.282	0.238
Charitospiza eucosma	Coal-crested Finch	M	man	silvery gray	grey	0.186	0.249	0.280	0.286	0.249
Coereba flaveola	Bananaquit	M	man	dark grey	grey	0.198	0.239	0.281	0.282	0.239
Coryphospingus pileatus	Pileated Finch	M	man	greyish	grey	0.213	0.237	0.271	0.280	0.237
Creurgops verticalis	Rufous-crested Tanager	M	man	leaden grey	grey	0.181	0.243	0.284	0.292	0.243
Diuca diuca	Common Diuca-Finch	M	man	dark gray	grey	0.197	0.240	0.276	0.286	0.240
Hemispingus verticalis	Black-headed Hemispingus	M	man	dark grey	grey	0.169	0.242	0.289	0.300	0.242
Hemispingus xanthophthalmus	Drab Hemispingus	M	man	brownish-grey	grey	0.135	0.211	0.304	0.349	0.211
Idiopsar brachyurus	Short-tailed Finch	M	man	leaden gray	grey	0.173	0.239	0.286	0.302	0.239
Melanodera xanthogramma	Yellow-bridled Finch	M	man	grey	grey	0.221	0.213	0.284	0.282	0.213
Neothraupis fasciata	White-banded Tanager	M	man	grey	grey	0.184	0.249	0.282	0.284	0.249
Paroaria coronata	Red-crested Cardinal	M	man	grey	grey	0.196	0.253	0.276	0.275	0.253
Phrygilus fruticeti	Mourning Sierra-Finch	M	man	grey	grey	0.187	0.244	0.284	0.284	0.244
Piezorhina cinerea	Cinereous Finch	M	man	pale grey	grey	0.170	0.247	0.286	0.298	0.247
Poospiza alticola	Plain-tailed Warbling-Finch	M	man	gray brown	grey	0.177	0.242	0.285	0.297	0.242
Poospiza caesar	Chestnut-breasted Mountain-Finch	M	man	gray	grey	0.203	0.241	0.274	0.282	0.241

Poospiza melanoleuca	Black-capped Warbling-Finch	M	man	grey	grey	0.176	0.251	0.289	0.285	0.251
Poospiza nigrorufa	Black-and-rufous Warbling-Finch	M	man	blue-grey	grey	0.187	0.228	0.281	0.304	0.228
Poospiza thoracica	Bay-chested Warbling-Finch	M	man	grey	grey	0.131	0.231	0.309	0.329	0.231
Poospiza torquata	Ringed Warbling-Finch	M	man	grey	grey	0.207	0.248	0.275	0.271	0.248
Saltator aurantirostris	Golden-billed Saltator	M	man	grey	grey	0.160	0.238	0.295	0.307	0.238
Saltator coerulescens	Grayish Saltator	M	man	greyish	grey	0.141	0.227	0.302	0.330	0.227
Saltator nigriceps	Black-cowled Saltator	M	man	deep gray	grey	0.173	0.248	0.287	0.291	0.248
Schistochlamys melanopis	Black-faced Tanager	M	man	grey	grey	0.210	0.257	0.274	0.259	0.257
Sicalis taczanowskii	Sulphur-throated Finch	M	man	no	grey	0.143	0.229	0.298	0.330	0.229
Sporophila albogularis	White-throated Seedeater	M	man	dark greyish	grey	0.199	0.247	0.276	0.279	0.247
Sporophila caerulescens	Double-collared Seedeater	M	man	olive-brown	grey	0.150	0.232	0.295	0.322	0.232
Sporophila hypoxantha	Tawny-bellied Seedeater	M	man	greyish	grey	0.184	0.246	0.280	0.289	0.246
Sporophila minuta	Ruddy-breasted Seedeater	M	man	mid-grey	grey	0.140	0.227	0.303	0.330	0.227
Sporophila palustris	Marsh Seedeater	M	man	grey	grey	0.174	0.244	0.284	0.298	0.244
Sporophila plumbea	Plumbeous Seedeater	M	man	lead-grey	grey	0.179	0.245	0.282	0.294	0.245
Tangara inornata	Plain-colored Tanager	M	man	dark gray	grey	0.188	0.257	0.282	0.274	0.257
Thlypopsis fulviceps	Fulvous-headed Tanager	M	man	grey	grey	0.191	0.240	0.282	0.287	0.240
Thlypopsis inornata	Buff-bellied Tanager	M	man	olive-grey	grey	0.161	0.244	0.291	0.305	0.244
Thlypopsis pectoralis	Brown-flanked Tanager	M	man	brownish-grey	grey	0.194	0.241	0.281	0.284	0.241
Thlypopsis sordida	Orange-headed Tanager	M	man	sandy-grey	grey	0.104	0.214	0.321	0.361	0.214
Thraupis sayaca	Sayaca Tanager	M	man	dull grey / bluish	grey	0.177	0.242	0.297	0.284	0.242
Charitospiza eucosma	Coal-crested Finch	M	rum	silvery gray	grey	0.157	0.243	0.291	0.309	0.243
Conothraupis speculigera	Black-and-white Tanager	M	rum	grey	grey	0.214	0.233	0.269	0.284	0.233
Coryphaspiza melanotis	Black-masked Finch	M	rum	greyish	grey	0.165	0.215	0.284	0.337	0.215
Coryphospingus pileatus	Pileated Finch	M	rum	greyish	grey	0.187	0.222	0.277	0.314	0.222
Creurgops verticalis	Rufous-crested Tanager	M	rum	leaden grey	grey	0.192	0.237	0.279	0.292	0.237
Diglossa brunneiventris	Black-throated Flowerpiercer	M	rum	grey	grey	0.230	0.243	0.267	0.261	0.243
Diglossa carbonaria	Gray-bellied Flowerpiercer	M	rum	dark grey	grey	0.212	0.251	0.273	0.263	0.251
Diuca diuca	Common Diuca-Finch	M	rum	blue gray	grey	0.193	0.244	0.277	0.286	0.244
Hemispingus verticalis	Black-headed Hemispingus	M	rum	dark grey	grey	0.178	0.223	0.281	0.318	0.223
Hemispingus xanthophthalmus	Drab Hemispingus	M	rum	brownish-grey	grey	0.166	0.210	0.284	0.340	0.210
Idiopsar brachyurus	Short-tailed Finch	M	rum	leaden gray	grey	0.206	0.242	0.273	0.280	0.242
Melanodera xanthogramma	Yellow-bridled Finch	M	rum	grey	grey	0.211	0.205	0.293	0.290	0.205
Neothraupis fasciata	White-banded Tanager	M	rum	grey	grey	0.187	0.244	0.279	0.290	0.244

<i>Paroaria coronata</i>	Red-crested Cardinal	M	rum	grey	grey	0.215	0.250	0.268	0.267	0.250
<i>Piezorhina cinerea</i>	Cinereous Finch	M	rum	pale grey	grey	0.170	0.234	0.283	0.312	0.234
<i>Poospiza alticola</i>	Plain-tailed Warbling-Finch	M	rum	gray brown	grey	0.179	0.241	0.284	0.296	0.241
<i>Poospiza caesar</i>	Chestnut-breasted Mountain-Finch	M	rum	gray	grey	0.176	0.238	0.284	0.303	0.238
<i>Poospiza hispaniolensis</i>	Collared Warbling-Finch	M	rum	brownish-grey	grey	0.195	0.254	0.279	0.272	0.254
<i>Poospiza melanoleuca</i>	Black-capped Warbling-Finch	M	rum	no	grey	0.188	0.244	0.282	0.286	0.244
<i>Poospiza nigrorufa</i>	Black-and-rufous Warbling-Finch	M	rum	blue-grey	grey	0.196	0.234	0.278	0.291	0.234
<i>Poospiza torquata</i>	Ringed Warbling-Finch	M	rum	grey	grey	0.192	0.256	0.280	0.272	0.256
<i>Saltator aurantirostris</i>	Golden-billed Saltator	M	rum	grey	grey	0.176	0.228	0.287	0.308	0.228
<i>Saltator coerulescens</i>	Grayish Saltator	M	rum	greyish	grey	0.159	0.215	0.289	0.336	0.215
<i>Saltator nigriceps</i>	Black-cowled Saltator	M	rum	deep gray / olive	grey	0.203	0.245	0.275	0.277	0.245
<i>Saltator similis</i>	Green-winged Saltator	M	rum	grey	grey	0.171	0.208	0.293	0.328	0.208
<i>Schistochlamys melanopsis</i>	Black-faced Tanager	M	rum	grey	grey	0.207	0.251	0.274	0.267	0.251
<i>Sporophila albogularis</i>	White-throated Seedeater	M	rum	dark greyish	grey	0.199	0.250	0.276	0.276	0.250
<i>Sporophila plumbea</i>	Plumbeous Seedeater	M	rum	lead-grey	grey	0.173	0.234	0.283	0.311	0.234
<i>Tangara inornata</i>	Plain-colored Tanager	M	rum	dark gray	grey	0.204	0.256	0.274	0.266	0.256
<i>Thlypopsis fulviceps</i>	Fulvous-headed Tanager	M	rum	grey	grey	0.155	0.226	0.298	0.321	0.226
<i>Thlypopsis inornata</i>	Buff-bellied Tanager	M	rum	olive-grey	grey	0.146	0.229	0.296	0.329	0.229
<i>Thlypopsis pectoralis</i>	Brown-flanked Tanager	M	rum	brownish-grey	grey	0.174	0.219	0.283	0.324	0.219
<i>Thlypopsis sordida</i>	Orange-headed Tanager	M	rum	sandy-grey	grey	0.137	0.218	0.305	0.340	0.218
<i>Thraupis sayaca</i>	Sayaca Tanager	M	rum	dull grey / bluish	grey	0.195	0.240	0.295	0.269	0.240
<i>Cnemoscopus rubrirostris</i>	Gray-hooded Bush Tanager	M	thr	medium grey	grey	0.124	0.240	0.309	0.326	0.240
<i>Embernagra platensis</i>	Great Pampa-Finch	M	thr	grey	grey	0.145	0.248	0.297	0.310	0.248
<i>Phrygilus plebejus</i>	Ash-breasted Sierra-Finch	M	thr	greyish-white	grey	0.180	0.252	0.281	0.286	0.252
<i>Tangara inornata</i>	Plain-colored Tanager	M	thr	dark gray	grey	0.176	0.249	0.285	0.290	0.249
<i>Thraupis glaucocolpa</i>	Glaucous Tanager	M	thr	smoky grey	grey	0.167	0.251	0.290	0.292	0.251
<i>Thraupis sayaca</i>	Sayaca Tanager	M	thr	light grey / bluish	grey	0.165	0.250	0.289	0.296	0.250
<i>Xenospingus concolor</i>	Slender-billed Finch	M	thr	paler grey	grey	0.159	0.251	0.291	0.298	0.251
<i>Cnemoscopus rubrirostris</i>	Gray-hooded Bush Tanager	M	bre	medium grey	grey	0.124	0.149	0.344	0.382	0.149
<i>Conirostrum bicolor</i>	Bicolored Conebill	M	bre	pale greyish-buff	grey	0.100	0.225	0.320	0.355	0.225
<i>Embernagra platensis</i>	Great Pampa-Finch	M	bre	grey	grey	0.108	0.242	0.313	0.337	0.242
<i>Hemispingus verticalis</i>	Black-headed Hemispingus	M	bre	pale grey	grey	0.176	0.248	0.285	0.290	0.248
<i>Idiopsar brachyurus</i>	Short-tailed Finch	M	bre	leaden gray	grey	0.171	0.249	0.283	0.296	0.249
<i>Incaspiza laeta</i>	Buff-bridled Inca-Finch	M	bre	grey	grey	0.144	0.244	0.297	0.315	0.244
<i>Incaspiza</i>	Rufous-backed	M	bre	grey	grey	0.13	0.24	0.300	0.322	0.243

personata	Inca-Finch					5	3			
Incaspiza pulchra	Great Inca-Finch	M	bre	grey	grey	0.16 8	0.25 4	0.286	0.292	0.254
Neothraupis fasciata	White-banded Tanager	M	bre	grey	grey	0.14 8	0.25 1	0.294	0.308	0.251
Phrygilus plebejus	Ash-breasted Sierra-Finch	M	bre	greyish-white	grey	0.15 5	0.24 5	0.290	0.310	0.245
Piezorhina cinerea	Cinereous Finch	M	bre	pale grey	grey	0.13 3	0.24 4	0.301	0.322	0.244
Poospiza hypochondria	Rufous-sided Warbling-Finch	M	bre	grey	grey	0.11 3	0.23 1	0.310	0.346	0.231
Saltator atriceps	Black-headed Saltator	M	bre	gray	grey	0.16 2	0.25 4	0.288	0.295	0.254
Saltator atripennis	Black-winged Saltator	M	bre	dove-grey	grey	0.15 6	0.25 4	0.290	0.299	0.254
Saltator aurantirostris	Golden-billed Saltator	M	bre	grey	grey	0.08 1	0.20 0	0.325	0.394	0.200
Saltator coerulescens	Grayish Saltator	M	bre	greyish	grey	0.08 6	0.20 5	0.321	0.388	0.205
Saltator maximus	Buff-throated Saltator	M	bre	grayish	grey	0.09 4	0.21 5	0.320	0.371	0.215
Saltator nigriceps	Black-cowled Saltator	M	bre	gray	grey	0.19 1	0.25 2	0.278	0.279	0.252
Sporophila plumbea	Plumbeous Seedeater	M	bre	pale grey	grey	0.15 7	0.24 9	0.288	0.306	0.249
Thlypopsis fulviceps	Fulvous-headed Tanager	M	bre	grey	grey	0.13 1	0.24 6	0.303	0.320	0.246
Thraupis sayaca	Sayaca Tanager	M	bre	light grey / bluish	grey	0.17 0	0.25 1	0.295	0.285	0.251
Xenospingus concolor	Slender-billed Finch	M	bre	paler grey	grey	0.14 4	0.24 8	0.296	0.312	0.248
Diglossa carbonaria	Gray-bellied Flowerpiercer	M	bel	grey	grey	0.18 1	0.25 0	0.283	0.285	0.250
Idiopsar brachyurus	Short-tailed Finch	M	bel	leaden gray	grey	0.16 4	0.24 4	0.289	0.303	0.244
Neothraupis fasciata	White-banded Tanager	M	bel	grey	grey	0.13 9	0.24 6	0.300	0.315	0.246
Phrygilus plebejus	Ash-breasted Sierra-Finch	M	bel	greyish-white	grey	0.15 4	0.24 9	0.292	0.305	0.249
Piezorhina cinerea	Cinereous Finch	M	bel	pale grey / white	grey	0.13 5	0.24 8	0.300	0.317	0.248
Saltator atriceps	Black-headed Saltator	M	bel	gray	grey	0.16 3	0.25 0	0.288	0.298	0.250
Saltator atripennis	Black-winged Saltator	M	bel	grey-white	grey	0.14 5	0.25 4	0.295	0.306	0.254
Saltator maximus	Buff-throated Saltator	M	bel	grayish	grey	0.11 8	0.22 5	0.309	0.348	0.225
Saltator nigriceps	Black-cowled Saltator	M	bel	gray / buffy	grey	0.12 6	0.23 2	0.306	0.336	0.232
Schistochlamys melanopis	Black-faced Tanager	M	bel	grey	grey	0.17 3	0.25 7	0.283	0.286	0.257
Sporophila plumbea	Plumbeous Seedeater	M	bel	lead-grey	grey	0.14 8	0.25 8	0.294	0.300	0.258
Thraupis glaucocolpa	Glaucous Tanager	M	bel	white	grey	0.14 6	0.25 2	0.307	0.294	0.252
Urothraupis stolzmanni	Black-backed Bush Tanager	M	bel	gray	grey	0.16 8	0.24 6	0.290	0.296	0.246
Xenospingus concolor	Slender-billed Finch	M	bel	paler grey	grey	0.15 0	0.24 6	0.296	0.308	0.246
Acanthidops bairdii	Peg-billed Finch	F	cro	brownish-olive	grey	0.13 0	0.20 9	0.313	0.347	0.209
Camarhynchus parvulus	Small Tree-Finch	F	cro	greyish-brown	grey	0.14 6	0.22 5	0.299	0.330	0.225
Cnemoscopus rubrirostris	Gray-hooded Bush Tanager	F	cro	medium grey	grey	0.13 2	0.24 6	0.311	0.312	0.246
Coereba flaveola	Bananaquit	F	cro	dark grey	grey	0.18 6	0.24 2	0.289	0.282	0.242
Creurgops verticalis	Rufous-crested Tanager	F	cro	leaden grey	grey	0.17 3	0.24 4	0.290	0.293	0.244

<i>Diuca diuca</i>	Common Diuca-Finch	F	cro	dark gray	grey	0.12 1	0.20 6	0.308	0.364	0.206
<i>Hemispingus melanotis</i>	Black-eared Hemispingus	F	cro	grey	grey	0.19 3	0.21 7	0.294	0.296	0.217
<i>Heterospingus xanthopygius</i>	Scarlet-browed Tanager	F	cro	dark leaden grey	grey	0.16 3	0.23 5	0.298	0.304	0.235
<i>Incaspiza personata</i>	Rufous-backed Inca-Finch	F	cro	grey	grey	0.14 4	0.22 4	0.301	0.331	0.224
<i>Lophospingus griseocristatus</i>	Gray-crested Finch	F	cro	gray	grey	0.16 0	0.24 7	0.292	0.301	0.247
<i>Neothraupis fasciata</i>	White-banded Tanager	F	cro	grey	grey	0.13 0	0.22 4	0.306	0.339	0.224
<i>Phrygilus atriceps</i>	Black-hooded Sierra-Finch	F	cro	black	grey	0.16 2	0.23 2	0.294	0.312	0.232
<i>Piezorhina cinerea</i>	Cinereous Finch	F	cro	pale grey	grey	0.14 0	0.23 5	0.301	0.325	0.235
<i>Poospiza alticola</i>	Plain-tailed Warbling-Finch	F	cro	gray brown	grey	0.17 8	0.23 4	0.284	0.303	0.234
<i>Poospiza caesar</i>	Chestnut-breasted Mountain-Finch	F	cro	gray	grey	0.16 2	0.23 4	0.296	0.308	0.234
<i>Poospiza thoracica</i>	Bay-chested Warbling-Finch	F	cro	grey	grey	0.11 9	0.23 4	0.312	0.335	0.234
<i>Ramphocelus passerinii</i>	Scarlet-rumped Tanager	F	cro	grey	grey	0.12 7	0.20 9	0.304	0.360	0.209
<i>Saltator coerulescens</i>	Grayish Saltator	F	cro	greyish	grey	0.15 8	0.22 6	0.293	0.322	0.226
<i>Tachyphonus luctuosus</i>	White-shouldered Tanager	F	cro	grey	grey	0.13 8	0.20 6	0.325	0.332	0.206
<i>Tachyphonus phoenicius</i>	Red-shouldered Tanager	F	cro	brownish-grey	grey	0.15 3	0.23 6	0.299	0.312	0.236
<i>Tachyphonus rufiventer</i>	Yellow-crested Tanager	F	cro	grey	grey	0.11 5	0.16 5	0.335	0.385	0.165
<i>Tangara inornata</i>	Plain-colored Tanager	F	cro	dark gray	grey	0.16 4	0.24 2	0.292	0.302	0.242
<i>Thraupis glaucocolpa</i>	Glaucous Tanager	F	cro	smoky grey / greenish	grey	0.17 7	0.24 1	0.291	0.291	0.241
<i>Thraupis sayaca</i>	Sayaca Tanager	F	cro	dull grey / bluish	grey	0.16 5	0.23 7	0.297	0.301	0.237
<i>Tiaris canorus</i>	Cuban Grassquit	F	cro	grey / greenish	grey	0.14 2	0.21 7	0.294	0.346	0.217
<i>Acanthidops bairdii</i>	Peg-billed Finch	F	nap	brownish-olive	grey	0.14 7	0.21 4	0.303	0.336	0.214
<i>Camarhynchus parvulus</i>	Small Tree-Finch	F	nap	greyish-brown	grey	0.15 4	0.22 5	0.295	0.327	0.225
<i>Coereba flaveola</i>	Bananaquit	F	nap	dark grey	grey	0.18 0	0.24 2	0.291	0.287	0.242
<i>Compsospiza garleppi</i>	Cochabamba Mountain-Finch	F	nap	leaden grey	grey	0.16 5	0.25 2	0.293	0.290	0.252
<i>Conirostrum albifrons</i>	Capped Conebill	F	nap	blue-tinged greyish	grey	0.20 7	0.25 0	0.268	0.275	0.250
<i>Coryphospingus pileatus</i>	Pileated Finch	F	nap	greyish-brown	grey	0.16 2	0.22 0	0.291	0.327	0.220
<i>Creurgops verticalis</i>	Rufous-crested Tanager	F	nap	leaden grey	grey	0.18 7	0.24 2	0.282	0.289	0.242
<i>Diuca diuca</i>	Common Diuca-Finch	F	nap	dark gray	grey	0.16 8	0.22 0	0.290	0.323	0.220
<i>Hemispingus melanotis</i>	Black-eared Hemispingus	F	nap	grey	grey	0.20 5	0.22 9	0.279	0.287	0.229
<i>Heterospingus xanthopygius</i>	Scarlet-browed Tanager	F	nap	dark leaden grey	grey	0.17 5	0.23 0	0.289	0.306	0.230
<i>Lophospingus griseocristatus</i>	Gray-crested Finch	F	nap	gray	grey	0.17 6	0.24 1	0.285	0.299	0.241
<i>Neothraupis fasciata</i>	White-banded Tanager	F	nap	grey	grey	0.14 4	0.22 6	0.298	0.332	0.226
<i>Piezorhina cinerea</i>	Cinereous Finch	F	nap	pale grey	grey	0.14 9	0.24 4	0.296	0.312	0.244
<i>Poospiza alticola</i>	Plain-tailed Warbling-Finch	F	nap	gray brown	grey	0.17 0	0.22 5	0.284	0.321	0.225
<i>Poospiza caesar</i>	Chestnut-breasted	F	nap	gray	grey	0.17	0.23	0.287	0.309	0.235

	Mountain-Finch					0	5			
Poospiza melanoleuca	Black-capped Warbling-Finch	F	nap	blue-grey	grey	0.209	0.241	0.274	0.276	0.241
Poospiza thoracica	Bay-chested Warbling-Finch	F	nap	grey	grey	0.150	0.240	0.294	0.316	0.240
Poospiza torquata	Ringed Warbling-Finch	F	nap	grey	grey	0.165	0.242	0.292	0.301	0.242
Saltator coerulescens	Grayish Saltator	F	nap	greyish	grey	0.157	0.220	0.300	0.323	0.220
Schistochlamys melanopis	Black-faced Tanager	F	nap	grey	grey	0.184	0.258	0.285	0.273	0.258
Tachyphonus luctuosus	White-shouldered Tanager	F	nap	grey	grey	0.160	0.200	0.312	0.328	0.200
Tachyphonus phoenicius	Red-shouldered Tanager	F	nap	brownish-grey	grey	0.183	0.234	0.283	0.299	0.234
Tangara inornata	Plain-colored Tanager	F	nap	dark gray	grey	0.177	0.242	0.285	0.296	0.242
Thraupis glaucocolpa	Glaucous Tanager	F	nap	smoky grey / greenish	grey	0.179	0.243	0.296	0.282	0.243
Thraupis sayaca	Sayaca Tanager	F	nap	dull grey / bluish	grey	0.171	0.232	0.300	0.297	0.232
Acanthidops bairdii	Peg-billed Finch	F	man	brownish-olive	grey	0.188	0.229	0.283	0.300	0.229
Camarhynchus parvulus	Small Tree-Finch	F	man	greyish-brown	grey	0.147	0.230	0.297	0.326	0.230
Coereba flaveola	Bananaquit	F	man	dark grey	grey	0.204	0.237	0.279	0.280	0.237
Compsospiza garleppi	Cochabamba Mountain-Finch	F	man	leaden grey	grey	0.163	0.251	0.295	0.292	0.251
Coryphospingus pileatus	Pileated Finch	F	man	greyish-brown	grey	0.183	0.230	0.283	0.305	0.230
Creurgops verticalis	Rufous-crested Tanager	F	man	leaden grey	grey	0.200	0.244	0.277	0.278	0.244
Diuca diuca	Common Diuca-Finch	F	man	dark gray	grey	0.167	0.225	0.288	0.320	0.225
Heterospingus xanthopygius	Scarlet-browed Tanager	F	man	dark leaden grey	grey	0.186	0.227	0.282	0.305	0.227
Lophospingus griseocristatus	Gray-crested Finch	F	man	gray / olive	grey	0.168	0.242	0.287	0.303	0.242
Neothraupis fasciata	White-banded Tanager	F	man	grey	grey	0.181	0.238	0.284	0.298	0.238
Paroaria coronata	Red-crested Cardinal	F	man	grey	grey	0.190	0.244	0.278	0.288	0.244
Piezorhina cinerea	Cinereous Finch	F	man	pale grey	grey	0.190	0.247	0.280	0.284	0.247
Poospiza alticola	Plain-tailed Warbling-Finch	F	man	gray brown	grey	0.147	0.225	0.298	0.330	0.225
Poospiza caesar	Chestnut-breasted Mountain-Finch	F	man	gray	grey	0.185	0.242	0.282	0.291	0.242
Poospiza melanoleuca	Black-capped Warbling-Finch	F	man	blue-grey	grey	0.194	0.254	0.280	0.272	0.254
Poospiza thoracica	Bay-chested Warbling-Finch	F	man	grey	grey	0.152	0.229	0.297	0.323	0.229
Poospiza torquata	Ringed Warbling-Finch	F	man	grey	grey	0.137	0.236	0.302	0.325	0.236
Saltator aurantirostris	Golden-billed Saltator	F	man	grey	grey	0.164	0.233	0.293	0.309	0.233
Saltator coerulescens	Grayish Saltator	F	man	greyish	grey	0.151	0.212	0.300	0.337	0.212
Schistochlamys melanopis	Black-faced Tanager	F	man	grey	grey	0.199	0.260	0.279	0.262	0.260
Tangara inornata	Plain-colored Tanager	F	man	dark gray	grey	0.185	0.246	0.281	0.288	0.246
Thlypopsis sordida	Orange-headed Tanager	F	man	sandy-grey	grey	0.101	0.217	0.323	0.359	0.217
Thraupis sayaca	Sayaca Tanager	F	man	dull grey / bluish	grey	0.179	0.235	0.297	0.289	0.235
Charitospiza eucosma	Coal-crested Finch	F	rum	gray-gold	grey	0.197	0.245	0.273	0.284	0.245

Compsospiza garleppi	Cochabamba Mountain-Finch	F	rum	leaden grey	grey	0.183	0.251	0.285	0.281	0.251
Creurgops verticalis	Rufous-crested Tanager	F	rum	leaden grey	grey	0.159	0.243	0.293	0.305	0.243
Diglossa brunneiventris	Black-throated Flowerpiercer	F	rum	grey	grey	0.211	0.247	0.273	0.268	0.247
Diuca diuca	Common Diuca-Finch	F	rum	blue gray	grey	0.159	0.224	0.292	0.324	0.224
Lophospingus griseocristatus	Gray-crested Finch	F	rum	blue gray	grey	0.191	0.243	0.278	0.287	0.243
Neothraupis fasciata	White-banded Tanager	F	rum	grey	grey	0.175	0.235	0.287	0.303	0.235
Paroaria coronata	Red-crested Cardinal	F	rum	grey	grey	0.210	0.246	0.270	0.274	0.246
Piezorhina cinerea	Cinereous Finch	F	rum	pale grey	grey	0.194	0.247	0.277	0.281	0.247
Poospiza alticola	Plain-tailed Warbling-Finch	F	rum	gray brown	grey	0.147	0.223	0.299	0.331	0.223
Poospiza caesar	Chestnut-breasted Mountain-Finch	F	rum	gray	grey	0.184	0.245	0.282	0.289	0.245
Poospiza melanoleuca	Black-capped Warbling-Finch	F	rum	blue-grey	grey	0.211	0.253	0.272	0.264	0.253
Poospiza torquata	Ringed Warbling-Finch	F	rum	grey	grey	0.167	0.243	0.288	0.302	0.243
Saltator aurantirostris	Golden-billed Saltator	F	rum	grey	grey	0.170	0.236	0.291	0.302	0.236
Saltator coerulescens	Grayish Saltator	F	rum	greyish	grey	0.136	0.217	0.306	0.341	0.217
Saltator similis	Green-winged Saltator	F	rum	grey	grey	0.160	0.212	0.300	0.328	0.212
Schistochlamys melanopis	Black-faced Tanager	F	rum	grey	grey	0.206	0.258	0.275	0.261	0.258
Tangara inornata	Plain-colored Tanager	F	rum	dark gray	grey	0.187	0.244	0.279	0.290	0.244
Thlypopsis sordida	Orange-headed Tanager	F	rum	sandy-grey	grey	0.112	0.213	0.320	0.355	0.213
Thraupis sayaca	Sayaca Tanager	F	rum	dull grey / bluish	grey	0.198	0.232	0.302	0.269	0.232
Cnemoscopus rubrirostris	Gray-hooded Bush Tanager	F	thr	medium grey	grey	0.129	0.245	0.307	0.319	0.245
Conirostrum albifrons	Capped Conebill	F	thr	pale grey / bluish	grey	0.162	0.243	0.289	0.306	0.243
Dacnis cayana	Blue Dacnis	F	thr	grey	grey	0.182	0.239	0.297	0.281	0.239
Dacnis venusta	Scarlet-thighed Dacnis	F	thr	grayish	grey	0.169	0.233	0.313	0.285	0.233
Heterospingus xanthopygius	Scarlet-browed Tanager	F	thr	paler grey	grey	0.152	0.235	0.296	0.317	0.235
Lanio aurantius	Black-throated Shrike-Tanager	F	thr	grey	grey	0.119	0.217	0.308	0.356	0.217
Lophospingus griseocristatus	Gray-crested Finch	F	thr	paler gray	grey	0.161	0.252	0.289	0.298	0.252
Loxigilla noctis	Lesser Antillean Bullfinch	F	thr	brown / greyer	grey	0.119	0.215	0.309	0.357	0.215
Loxipasser anoxanthus	Yellow-shouldered Grassquit	F	thr	grey / green	grey	0.133	0.216	0.303	0.347	0.216
Phrygilus fruticeti	Mourning Sierra-Finch	F	thr	grey	grey	0.171	0.243	0.288	0.298	0.243
Ramphocelus passerinii	Scarlet-rumped Tanager	F	thr	grey	grey	0.114	0.203	0.313	0.370	0.203
Tangara inornata	Plain-colored Tanager	F	thr	dark gray	grey	0.155	0.248	0.295	0.302	0.248
Thraupis glaucocolpa	Glaucous Tanager	F	thr	smoky grey	grey	0.170	0.251	0.286	0.292	0.251
Thraupis sayaca	Sayaca Tanager	F	thr	light grey / bluish	grey	0.148	0.248	0.297	0.307	0.248
Xenospingus concolor	Slender-billed Finch	F	thr	paler grey	grey	0.150	0.255	0.293	0.301	0.255
Cnemoscopus	Gray-hooded Bush	F	bre	medium grey	grey	0.10	0.16	0.345	0.388	0.163

rubrirostris	Tanager					5	3			
Conirostrum albifrons	Capped Conebill	F	bre	pale grey / bluish	grey	0.164	0.247	0.286	0.303	0.247
Conirostrum bicolor	Bicolored Conebill	F	bre	pale greyish-buff	grey	0.100	0.133	0.359	0.409	0.133
Heterospingus xanthopygius	Scarlet-browed Tanager	F	bre	paler grey	grey	0.183	0.236	0.283	0.298	0.236
Incaspiza laeta	Buff-bridled Inca-Finch	F	bre	grey	grey	0.120	0.235	0.306	0.339	0.235
Incaspiza personata	Rufous-backed Inca-Finch	F	bre	grey	grey	0.110	0.231	0.311	0.348	0.231
Incaspiza pulchra	Great Inca-Finch	F	bre	grey	grey	0.146	0.246	0.295	0.314	0.246
Lophospingus griseocristatus	Gray-crested Finch	F	bre	paler gray	grey	0.158	0.250	0.289	0.303	0.250
Lophospingus pusillus	Black-crested Finch	F	bre	greyish	grey	0.146	0.240	0.295	0.319	0.240
Loxipasser anoxanthus	Yellow-shouldered Grassquit	F	bre	grey / green	grey	0.134	0.215	0.308	0.343	0.215
Neothraupis fasciata	White-banded Tanager	F	bre	grey	grey	0.146	0.247	0.295	0.313	0.247
Phrygilus fruticeti	Mourning Sierra-Finch	F	bre	white	grey	0.163	0.238	0.288	0.310	0.238
Piezorhina cinerea	Cinereous Finch	F	bre	pale grey	grey	0.125	0.234	0.304	0.337	0.234
Poospiza hypochondria	Rufous-sided Warbling-Finch	F	bre	grey	grey	0.127	0.239	0.303	0.331	0.239
Saltator atriceps	Black-headed Saltator	F	bre	gray	grey	0.166	0.248	0.288	0.298	0.248
Saltator atripennis	Black-winged Saltator	F	bre	dove-grey	grey	0.165	0.253	0.288	0.294	0.253
Saltator aurantirostris	Golden-billed Saltator	F	bre	grey	grey	0.079	0.196	0.326	0.398	0.196
Saltator coerulescens	Grayish Saltator	F	bre	greyish	grey	0.100	0.203	0.320	0.377	0.203
Saltator maximus	Buff-throated Saltator	F	bre	grayish / buff	grey	0.102	0.217	0.315	0.366	0.217
Sicalis taczanowskii	Sulphur-throated Finch	F	bre	pale greyish-brown	grey	0.159	0.239	0.293	0.308	0.239
Tangara viridicollis	Silvery Tanager	F	bre	grey	grey	0.111	0.213	0.339	0.337	0.213
Thraupis sayaca	Sayaca Tanager	F	bre	light grey / bluish	grey	0.157	0.250	0.298	0.294	0.250
Tiaris canorus	Cuban Grassquit	F	bre	grey	grey	0.117	0.231	0.310	0.342	0.231
Xenospingus concolor	Slender-billed Finch	F	bre	paler grey	grey	0.151	0.253	0.292	0.304	0.253
Heterospingus xanthopygius	Scarlet-browed Tanager	F	bel	paler grey	grey	0.157	0.225	0.295	0.323	0.225
Lophospingus griseocristatus	Gray-crested Finch	F	bel	paler gray	grey	0.149	0.252	0.293	0.306	0.252
Lophospingus pusillus	Black-crested Finch	F	bel	greyish	grey	0.152	0.250	0.293	0.305	0.250
Loxipasser anoxanthus	Yellow-shouldered Grassquit	F	bel	greenish / yellow	grey	0.137	0.224	0.305	0.334	0.224
Neothraupis fasciata	White-banded Tanager	F	bel	grey	grey	0.141	0.241	0.300	0.318	0.241
Piezorhina cinerea	Cinereous Finch	F	bel	pale grey / white	grey	0.124	0.243	0.304	0.328	0.243
Saltator atriceps	Black-headed Saltator	F	bel	gray	grey	0.157	0.246	0.292	0.305	0.246
Saltator atripennis	Black-winged Saltator	F	bel	grey-white	grey	0.177	0.250	0.283	0.289	0.250
Saltator maximus	Buff-throated Saltator	F	bel	grayish	grey	0.099	0.206	0.317	0.378	0.206
Schistochlamys melanopis	Black-faced Tanager	F	bel	grey	grey	0.163	0.254	0.288	0.295	0.254
Sicalis taczanowskii	Sulphur-throated Finch	F	bel	pale greyish-brown	grey	0.185	0.254	0.278	0.283	0.254

Tangara viridicollis	Silvery Tanager	F	bel	grey	grey	0.138	0.251	0.311	0.300	0.251
Tiaris canorus	Cuban Grassquit	F	bel	olive-grey	grey	0.107	0.225	0.316	0.353	0.225
Urothraupis stolzmanni	Black-backed Bush Tanager	F	bel	gray	grey	0.170	0.248	0.288	0.294	0.248
Xenospingus concolor	Slender-billed Finch	F	bel	paler grey	grey	0.148	0.251	0.295	0.306	0.251
Acanthidops bairdii	Peg-billed Finch	M	cro	dark grey	slate	0.202	0.243	0.278	0.277	0.243
Bangsia arcaei	Blue-and-gold Tanager	M	cro	bright blue	slate	0.346	0.258	0.216	0.181	0.258
Catamenia analis	Band-tailed Seedeater	M	cro	grey	slate	0.190	0.265	0.284	0.261	0.265
Catamenia homochroa	Paramo Seedeater	M	cro	dark slate gray	slate	0.172	0.243	0.294	0.291	0.243
Catamenia inornata	Plain-colored Seedeater	M	cro	grey	slate	0.140	0.246	0.303	0.311	0.246
Conirostrum cinereum	Cinereous Conebill	M	cro	slate-gray	slate	0.136	0.234	0.310	0.320	0.234
Conirostrum rufum	Rufous-browed Conebill	M	cro	plumbeous grey	slate	0.139	0.249	0.311	0.302	0.249
Conirostrum speciosum	Chestnut-vented Conebill	M	cro	dark greyish-blue	slate	0.211	0.295	0.276	0.218	0.295
Delothraupis castaneiventris	Chestnut-bellied Mountain-Tanager	M	cro	silvery sky blue	slate	0.295	0.293	0.227	0.185	0.293
Diglossa baritula	Cinnamon-bellied Flowerpiercer	M	cro	slate-blackish	slate	0.239	0.262	0.265	0.233	0.262
Diglossa caerulescens	Bluish Flowerpiercer	M	cro	dull bluish-grey	slate	0.233	0.265	0.266	0.236	0.265
Diglossa duidae	Scaled Flowerpiercer	M	cro	slaty black	slate	0.210	0.249	0.284	0.258	0.249
Diglossa plumbea	Slaty Flowerpiercer	M	cro	blackish-grey / blue	slate	0.222	0.255	0.271	0.252	0.255
Eucometis penicillata	Gray-headed Tanager	M	cro	grey	slate	0.064	0.233	0.336	0.367	0.233
Euneornis campestris	Orangequit	M	cro	grey-blue	slate	0.239	0.290	0.264	0.207	0.290
Haplospiza unicolor	Uniform Finch	M	cro	blue-grey	slate	0.137	0.270	0.308	0.284	0.270
Oreomanes fraseri	Giant Conebill	M	cro	plumbeous	slate	0.154	0.245	0.299	0.302	0.245
Phrygilus alaudinus	Band-tailed Sierra-Finch	M	cro	grey	slate	0.196	0.242	0.279	0.283	0.242
Phrygilus erythronotus	White-throated Sierra-Finch	M	cro	blue-grey	slate	0.180	0.249	0.284	0.287	0.249
Phrygilus gayi	Gray-hooded Sierra-Finch	M	cro	bluish-grey	slate	0.250	0.263	0.256	0.231	0.263
Phrygilus patagonicus	Patagonian Sierra-Finch	M	cro	dark blue gray	slate	0.258	0.265	0.254	0.223	0.265
Phrygilus punensis	Peruvian Sierra-Finch	M	cro	grey	slate	0.203	0.254	0.277	0.265	0.254
Phrygilus unicolor	Plumbeous Sierra-Finch	M	cro	lead-grey	slate	0.184	0.252	0.285	0.279	0.252
Poospiza cinerea	Cinereous Warbling-Finch	M	cro	grey	slate	0.143	0.253	0.303	0.300	0.253
Poospiza erythrophrys	Rusty-browed Warbling-Finch	M	cro	blue-grey	slate	0.131	0.246	0.308	0.316	0.246
Poospiza whitii	Black-and-chestnut Warbling-Finch	M	cro	slate-grey	slate	0.185	0.248	0.286	0.280	0.248
Saltator fuliginosus	Black-throated Grosbeak	M	cro	deep slate-blue	slate	0.224	0.257	0.273	0.246	0.257
Saltator grossus	Slate-colored Grosbeak	M	cro	slaty blue	slate	0.227	0.252	0.269	0.253	0.252
Sporophila castaneiventris	Chestnut-bellied Seedeater	M	cro	blue-grey	slate	0.184	0.260	0.286	0.270	0.260
Sporophila intermedia	Gray Seedeater	M	cro	medium-grey / blue	slate	0.175	0.250	0.287	0.288	0.250

<i>Thraupis episcopus</i>	Blue-gray Tanager	M	cro	pale grey / blue wash	slate	0.188	0.254	0.295	0.263	0.254
<i>Xenospingus concolor</i>	Slender-billed Finch	M	cro	slate-grey	slate	0.194	0.254	0.279	0.273	0.254
<i>Acanthidops bairdii</i>	Peg-billed Finch	M	nap	dark grey	slate	0.206	0.244	0.274	0.276	0.244
<i>Bangsia arcaei</i>	Blue-and-gold Tanager	M	nap	dark blue	slate	0.337	0.252	0.220	0.191	0.252
<i>Catamenia analis</i>	Band-tailed Seedeater	M	nap	grey	slate	0.208	0.265	0.274	0.253	0.265
<i>Catamenia homochroa</i>	Paramo Seedeater	M	nap	dark slate gray	slate	0.187	0.245	0.284	0.285	0.245
<i>Catamenia inornata</i>	Plain-colored Seedeater	M	nap	grey	slate	0.147	0.246	0.298	0.309	0.246
<i>Conirostrum cinereum</i>	Cinereous Conebill	M	nap	slate-grey	slate	0.145	0.240	0.303	0.311	0.240
<i>Conirostrum rufum</i>	Rufous-browed Conebill	M	nap	plumbeous grey	slate	0.180	0.249	0.288	0.284	0.249
<i>Conirostrum sitticolor</i>	Blue-backed Conebill	M	nap	blue	slate	0.233	0.256	0.273	0.239	0.256
<i>Conirostrum speciosum</i>	Chestnut-vented Conebill	M	nap	dark greyish-blue	slate	0.230	0.279	0.265	0.226	0.279
<i>Delothraupis castaneiventris</i>	Chestnut-bellied Mountain-Tanager	M	nap	dark blue	slate	0.283	0.289	0.233	0.196	0.289
<i>Diglossa baritula</i>	Cinnamon-bellied Flowerpiercer	M	nap	slate-blackish	slate	0.253	0.261	0.258	0.228	0.261
<i>Diglossa caerulescens</i>	Bluish Flowerpiercer	M	nap	dull bluish-grey	slate	0.234	0.265	0.265	0.237	0.265
<i>Diglossa duidae</i>	Scaled Flowerpiercer	M	nap	slaty black	slate	0.228	0.245	0.267	0.260	0.245
<i>Diglossa plumbea</i>	Slaty Flowerpiercer	M	nap	blackish-grey / blue	slate	0.217	0.248	0.272	0.263	0.248
<i>Eucometis penicillata</i>	Gray-headed Tanager	M	nap	grey	slate	0.058	0.230	0.341	0.371	0.230
<i>Euneornis campestris</i>	Orangequit	M	nap	grey-blue	slate	0.252	0.288	0.254	0.205	0.288
<i>Haplospiza unicolor</i>	Uniform Finch	M	nap	blue-grey	slate	0.167	0.267	0.294	0.273	0.267
<i>Nemosia pileata</i>	Hooded Tanager	M	nap	light blue	slate	0.214	0.271	0.275	0.240	0.271
<i>Oreomanes fraseri</i>	Giant Conebill	M	nap	plumbeous	slate	0.187	0.243	0.283	0.286	0.243
<i>Phrygilus alaudinus</i>	Band-tailed Sierra-Finch	M	nap	lead-grey	slate	0.169	0.240	0.288	0.303	0.240
<i>Phrygilus erythronotus</i>	White-throated Sierra-Finch	M	nap	dark gray	slate	0.189	0.250	0.280	0.281	0.250
<i>Phrygilus gayi</i>	Gray-hooded Sierra-Finch	M	nap	bluish-grey	slate	0.215	0.217	0.284	0.285	0.217
<i>Phrygilus patagonicus</i>	Patagonian Sierra-Finch	M	nap	dark blue gray	slate	0.244	0.245	0.263	0.247	0.245
<i>Phrygilus unicolor</i>	Plumbeous Sierra-Finch	M	nap	lead-grey	slate	0.200	0.254	0.276	0.270	0.254
<i>Poospiza cinerea</i>	Cinereous Warbling-Finch	M	nap	grey	slate	0.174	0.251	0.288	0.287	0.251
<i>Poospiza whittii</i>	Black-and-chestnut Warbling-Finch	M	nap	slate-grey	slate	0.201	0.248	0.278	0.274	0.248
<i>Saltator fuliginosus</i>	Black-throated Grosbeak	M	nap	deep slate-blue	slate	0.224	0.247	0.268	0.260	0.247
<i>Saltator grossus</i>	Slate-colored Grosbeak	M	nap	slaty blue	slate	0.238	0.253	0.263	0.245	0.253
<i>Sporophila castaneiventris</i>	Chestnut-bellied Seedeater	M	nap	blue-grey	slate	0.196	0.260	0.280	0.265	0.260
<i>Sporophila intermedia</i>	Gray Seedeater	M	nap	medium-grey / blue	slate	0.184	0.252	0.284	0.280	0.252
<i>Thraupis episcopus</i>	Blue-gray Tanager	M	nap	pale grey / blue wash	slate	0.199	0.264	0.286	0.251	0.264
<i>Xenospingus concolor</i>	Slender-billed Finch	M	nap	slate-grey	slate	0.189	0.250	0.282	0.279	0.250

Acanthidops bairdii	Peg-billed Finch	M	man	dark grey	slate	0.20 2	0.24 6	0.279	0.273	0.246
Bangsia arcaei	Blue-and-gold Tanager	M	man	dark blue	slate	0.32 2	0.25 5	0.227	0.196	0.255
Catamblyrhynchus diadema	Plushcap	M	man	blue gray	slate	0.21 9	0.25 3	0.271	0.257	0.253
Catamenia analis	Band-tailed Seedeater	M	man	grey / browner	slate	0.20 1	0.26 5	0.276	0.258	0.265
Catamenia homochroa	Paramo Seedeater	M	man	dark slate gray	slate	0.17 7	0.24 3	0.287	0.293	0.243
Catamenia inornata	Plain-colored Seedeater	M	man	grey	slate	0.12 8	0.23 0	0.308	0.334	0.230
Conirostrum cinereum	Cinereous Conebill	M	man	slate-gray	slate	0.14 4	0.23 6	0.305	0.315	0.236
Conirostrum leucogenys	White-eared Conebill	M	man	dark bluish-grey	slate	0.23 5	0.28 7	0.264	0.214	0.287
Conirostrum rufum	Rufous-browed Conebill	M	man	plumbeous grey	slate	0.19 5	0.24 8	0.281	0.275	0.248
Conirostrum sitticolor	Blue-backed Conebill	M	man	blue	slate	0.35 5	0.28 7	0.201	0.158	0.287
Conirostrum speciosum	Chestnut-vented Conebill	M	man	dark greyish-blue	slate	0.22 5	0.27 8	0.267	0.230	0.278
Delothraupis castaneiventris	Chestnut-bellied Mountain-Tanager	M	man	dark blue	slate	0.26 8	0.27 7	0.241	0.214	0.277
Diglossa baritula	Cinnamon-bellied Flowerpiercer	M	man	slate gray	slate	0.23 6	0.27 1	0.263	0.230	0.271
Diglossa caerulescens	Bluish Flowerpiercer	M	man	dull bluish-grey	slate	0.24 2	0.26 8	0.262	0.229	0.268
Diglossa duidae	Scaled Flowerpiercer	M	man	slaty black	slate	0.23 2	0.24 6	0.266	0.255	0.246
Diglossa plumbea	Slaty Flowerpiercer	M	man	blackish-grey / blue	slate	0.23 8	0.26 5	0.263	0.234	0.265
Euneornis campestris	Orangequit	M	man	grey-blue	slate	0.25 4	0.28 6	0.252	0.208	0.286
Haplospiza unicolor	Uniform Finch	M	man	blue-grey	slate	0.17 0	0.26 0	0.291	0.279	0.260
Hemispingus goeringi	Slaty-backed Hemispingus	M	man	slaty	slate	0.18 6	0.24 0	0.285	0.289	0.240
Nemosia pileata	Hooded Tanager	M	man	light blue	slate	0.21 5	0.26 9	0.273	0.242	0.269
Oreomanes fraseri	Giant Conebill	M	man	plumbeous	slate	0.21 0	0.24 2	0.274	0.274	0.242
Phrygilus erythronotus	White-throated Sierra-Finch	M	man	dark gray	slate	0.20 5	0.24 3	0.274	0.279	0.243
Phrygilus unicolor	Plumbeous Sierra-Finch	M	man	lead-grey	slate	0.20 9	0.25 1	0.273	0.267	0.251
Poospiza cinerea	Cinereous Warbling-Finch	M	man	blue-grey	slate	0.21 0	0.24 6	0.272	0.272	0.246
Poospiza whitii	Black-and-chestnut Warbling-Finch	M	man	slate-grey	slate	0.16 8	0.24 8	0.294	0.290	0.248
Pyrrhocomma ruficeps	Chestnut-headed Tanager	M	man	dark grey	slate	0.21 3	0.24 6	0.272	0.269	0.246
Saltator fuliginosus	Black-throated Grosbeak	M	man	deep slate-blue	slate	0.23 4	0.26 0	0.265	0.240	0.260
Saltator grossus	Slate-colored Grosbeak	M	man	slaty blue	slate	0.22 8	0.24 3	0.264	0.265	0.243
Schistochlamys ruficapillus	Cinnamon Tanager	M	man	grey	slate	0.19 0	0.25 3	0.282	0.275	0.253
Sporophila castaneiventris	Chestnut-bellied Seedeater	M	man	blue-grey	slate	0.19 6	0.25 5	0.279	0.269	0.255
Sporophila intermedia	Gray Seedeater	M	man	medium-grey / blue	slate	0.20 0	0.25 1	0.276	0.273	0.251
Tangara heinei	Black-capped Tanager	M	man	shining grey-blue	slate	0.05 2	0.34 8	0.339	0.261	0.348
Thraupis episcopus	Blue-gray Tanager	M	man	darker bluish-grey	slate	0.20 8	0.27 3	0.291	0.228	0.273
Xenospingus concolor	Slender-billed Finch	M	man	slate-grey	slate	0.18 7	0.25 4	0.283	0.276	0.254

Acanthidops bairdii	Peg-billed Finch	M	rum	dark grey	slate	0.21 3	0.24 7	0.273	0.267	0.247
Bangsia arcaei	Blue-and-gold Tanager	M	rum	dark blue	slate	0.24 0	0.24 3	0.259	0.258	0.243
Catamblyrhynchus diadema	Plushcap	M	rum	blue gray	slate	0.21 3	0.24 6	0.272	0.270	0.246
Catamenia analis	Band-tailed Seedeater	M	rum	blue-grey	slate	0.20 7	0.26 5	0.273	0.255	0.265
Catamenia homochroa	Paramo Seedeater	M	rum	dark slate gray	slate	0.18 3	0.23 6	0.284	0.297	0.236
Catamenia inornata	Plain-colored Seedeater	M	rum	grey	slate	0.17 3	0.24 8	0.287	0.292	0.248
Conirostrum cinereum	Cinereous Conebill	M	rum	slate-gray	slate	0.16 3	0.22 7	0.294	0.315	0.227
Conirostrum leucogenys	White-eared Conebill	M	rum	dark bluish-grey	slate	0.22 2	0.25 8	0.268	0.251	0.258
Conirostrum rufum	Rufous-browed Conebill	M	rum	plumbeous grey	slate	0.20 8	0.22 1	0.270	0.300	0.221
Conirostrum sitticolor	Blue-backed Conebill	M	rum	blue	slate	0.26 5	0.25 2	0.243	0.239	0.252
Conirostrum speciosum	Chestnut-vented Conebill	M	rum	dark greyish-blue	slate	0.23 4	0.28 8	0.264	0.214	0.288
Delothraupis castaneiventris	Chestnut-bellied Mountain-Tanager	M	rum	dark blue	slate	0.26 8	0.27 0	0.242	0.220	0.270
Diglossa baritula	Cinnamon-bellied Flowerpiercer	M	rum	slate gray	slate	0.23 7	0.26 1	0.262	0.240	0.261
Diglossa caerulescens	Bluish Flowerpiercer	M	rum	dull bluish-grey	slate	0.25 6	0.26 3	0.257	0.224	0.263
Diglossa duidae	Scaled Flowerpiercer	M	rum	slaty black	slate	0.21 9	0.24 4	0.269	0.268	0.244
Diglossa plumbea	Slaty Flowerpiercer	M	rum	blackish-grey / blue	slate	0.22 4	0.24 8	0.267	0.261	0.248
Euneornis campestris	Orangequit	M	rum	grey-blue	slate	0.26 8	0.29 5	0.246	0.191	0.295
Haplospiza unicolor	Uniform Finch	M	rum	blue-grey	slate	0.19 5	0.25 8	0.283	0.264	0.258
Hemispingus goeringi	Slaty-backed Hemispingus	M	rum	dark grey	slate	0.18 6	0.23 0	0.282	0.302	0.230
Nemosia pileata	Hooded Tanager	M	rum	light blue	slate	0.21 6	0.26 7	0.273	0.244	0.267
Oreomanes fraseri	Giant Conebill	M	rum	plumbeous	slate	0.19 1	0.23 3	0.278	0.298	0.233
Phrygilus alaudinus	Band-tailed Sierra-Finch	M	rum	grey	slate	0.17 3	0.23 1	0.286	0.311	0.231
Phrygilus erythronotus	White-throated Sierra-Finch	M	rum	dark gray	slate	0.20 4	0.25 0	0.274	0.271	0.250
Phrygilus unicolor	Plumbeous Sierra-Finch	M	rum	lead-grey	slate	0.19 5	0.25 1	0.278	0.276	0.251
Poospiza cinerea	Cinereous Warbling-Finch	M	rum	blue-grey	slate	0.18 2	0.25 9	0.284	0.275	0.259
Poospiza whitii	Black-and-chestnut Warbling-Finch	M	rum	slate-grey	slate	0.21 7	0.24 9	0.271	0.263	0.249
Pyrrhocomma ruficeps	Chestnut-headed Tanager	M	rum	dark grey	slate	0.21 1	0.25 0	0.273	0.266	0.250
Saltator fuliginosus	Black-throated Grosbeak	M	rum	deep slate-blue	slate	0.24 2	0.25 1	0.263	0.245	0.251
Saltator grossus	Slate-colored Grosbeak	M	rum	slaty blue	slate	0.22 6	0.24 4	0.266	0.264	0.244
Schistochlamys ruficapillus	Cinnamon Tanager	M	rum	grey	slate	0.19 1	0.24 3	0.278	0.288	0.243
Sporophila castaneiventris	Chestnut-bellied Seedeater	M	rum	blue-grey	slate	0.19 5	0.26 0	0.278	0.267	0.260
Sporophila intermedia	Gray Seedeater	M	rum	medium-grey / blue	slate	0.20 1	0.25 0	0.276	0.273	0.250
Tangara heinei	Black-capped Tanager	M	rum	shining grey-blue	slate	0.11 7	0.31 2	0.300	0.271	0.312
Tangara vitriolina	Scrub Tanager	M	rum	greyish blue	slate	0.07 7	0.24 6	0.350	0.327	0.246

<i>Thraupis episcopus</i>	Blue-gray Tanager	M	rum	darker bluish-grey	slate	0.22 4	0.29 5	0.265	0.217	0.295
<i>Xenospingus concolor</i>	Slender-billed Finch	M	rum	slate-grey	slate	0.20 5	0.24 5	0.273	0.276	0.245
<i>Acanthidops bairdii</i>	Peg-billed Finch	M	thr	dark grey	slate	0.19 3	0.24 7	0.280	0.280	0.247
<i>Bangsia arcaei</i>	Blue-and-gold Tanager	M	thr	dark blue	slate	0.22 9	0.23 3	0.273	0.265	0.233
<i>Catamenia analis</i>	Band-tailed Seedeater	M	thr	grey	slate	0.17 4	0.26 1	0.288	0.277	0.261
<i>Catamenia homochroa</i>	Paramo Seedeater	M	thr	dark slate gray	slate	0.15 7	0.24 6	0.298	0.299	0.246
<i>Catamenia inornata</i>	Plain-colored Seedeater	M	thr	grey	slate	0.15 2	0.25 1	0.295	0.303	0.251
<i>Conirostrum leucogenys</i>	White-eared Conebill	M	thr	pale grey / bluish	slate	0.18 9	0.25 5	0.283	0.273	0.255
<i>Diglossa baritula</i>	Cinnamon-bellied Flowerpiercer	M	thr	slate-blackish / cinnamon-rufous	slate	0.14 6	0.20 3	0.292	0.359	0.203
<i>Diglossa caerulescens</i>	Bluish Flowerpiercer	M	thr	dull bluish-grey	slate	0.21 9	0.27 0	0.273	0.237	0.270
<i>Diglossa duidae</i>	Scaled Flowerpiercer	M	thr	slate-grey	slate	0.21 2	0.24 7	0.273	0.269	0.247
<i>Diglossa plumbea</i>	Slaty Flowerpiercer	M	thr	dark slate-grey	slate	0.19 0	0.24 7	0.281	0.282	0.247
<i>Haplospiza unicolor</i>	Uniform Finch	M	thr	blue-grey	slate	0.15 9	0.25 9	0.294	0.287	0.259
<i>Phrygilus gayi</i>	Gray-hooded Sierra-Finch	M	thr	bluish-grey	slate	0.22 2	0.25 9	0.267	0.252	0.259
<i>Phrygilus patagonicus</i>	Patagonian Sierra-Finch	M	thr	dark blue gray	slate	0.23 3	0.25 6	0.262	0.249	0.256
<i>Phrygilus punensis</i>	Peruvian Sierra-Finch	M	thr	grey	slate	0.19 6	0.25 3	0.277	0.273	0.253
<i>Phrygilus unicolor</i>	Plumbeous Sierra-Finch	M	thr	lead-grey	slate	0.17 5	0.25 0	0.285	0.290	0.250
<i>Saltator fuliginosus</i>	Black-throated Grosbeak	M	thr	deep slate-blue	slate	0.20 2	0.23 5	0.287	0.277	0.235
<i>Tangara vitriolina</i>	Scrub Tanager	M	thr	pale bluish-grey	slate	0.12 1	0.24 3	0.314	0.322	0.243
<i>Thraupis cyanocephala</i>	Blue-capped Tanager	M	thr	dull bluish-grey	slate	0.17 5	0.25 5	0.286	0.284	0.255
<i>Thraupis episcopus</i>	Blue-gray Tanager	M	thr	pale grey / blue wash	slate	0.19 1	0.25 7	0.286	0.266	0.257
<i>Acanthidops bairdii</i>	Peg-billed Finch	M	bre	dark grey	slate	0.18 9	0.24 9	0.280	0.281	0.249
<i>Catamenia analis</i>	Band-tailed Seedeater	M	bre	grey	slate	0.17 5	0.26 0	0.285	0.281	0.260
<i>Catamenia homochroa</i>	Paramo Seedeater	M	bre	dark slate gray	slate	0.16 8	0.24 4	0.289	0.298	0.244
<i>Catamenia inornata</i>	Plain-colored Seedeater	M	bre	grey	slate	0.13 3	0.24 6	0.302	0.318	0.246
<i>Diglossa plumbea</i>	Slaty Flowerpiercer	M	bre	dark slate-grey	slate	0.19 4	0.25 5	0.280	0.271	0.255
<i>Euneornis campestris</i>	Orangequit	M	bre	grey-blue	slate	0.23 7	0.28 7	0.264	0.213	0.287
<i>Haplospiza unicolor</i>	Uniform Finch	M	bre	blue-grey	slate	0.19 7	0.25 8	0.276	0.269	0.258
<i>Phrygilus erythronotus</i>	White-throated Sierra-Finch	M	bre	grey	slate	0.16 6	0.25 0	0.285	0.299	0.250
<i>Phrygilus unicolor</i>	Plumbeous Sierra-Finch	M	bre	lead-grey	slate	0.19 2	0.25 5	0.276	0.277	0.255
<i>Pyrrhocomma ruficeps</i>	Chestnut-headed Tanager	M	bre	dark grey	slate	0.19 1	0.25 1	0.281	0.277	0.251
<i>Tangara vitriolina</i>	Scrub Tanager	M	bre	pale bluish-grey	slate	0.06 6	0.26 2	0.341	0.330	0.262
<i>Thraupis cyanocephala</i>	Blue-capped Tanager	M	bre	dull bluish-grey	slate	0.17 4	0.26 0	0.286	0.280	0.260
<i>Thraupis episcopus</i>	Blue-gray Tanager	M	bre	pale grey / blue wash	slate	0.20 8	0.28 1	0.269	0.243	0.281
<i>Acanthidops</i>	Peg-billed Finch	M	bel	dark grey	slate	0.17	0.25	0.284	0.286	0.251

bairdii						9	1			
Catamenia homochroa	Paramo Seedeater	M	bel	dark slate gray	slate	0.153	0.240	0.296	0.312	0.240
Diglossa plumbea	Slaty Flowerpiercer	M	bel	dark slate-grey	slate	0.173	0.248	0.286	0.293	0.248
Euneornis campestris	Orangequit	M	bel	grey-blue	slate	0.231	0.274	0.265	0.230	0.274
Haplospiza unicolor	Uniform Finch	M	bel	blue-grey	slate	0.159	0.255	0.295	0.292	0.255
Phrygilus unicolor	Plumbeous Sierra-Finch	M	bel	lead-grey	slate	0.179	0.250	0.283	0.287	0.250
Pyrrhocomma ruficeps	Chestnut-headed Tanager	M	bel	dark grey	slate	0.194	0.247	0.277	0.282	0.247
Saltator fuliginosus	Black-throated Grosbeak	M	bel	deep slate-blue	slate	0.223	0.248	0.268	0.261	0.248
Saltator grossus	Slate-colored Grosbeak	M	bel	slaty blue	slate	0.209	0.249	0.272	0.270	0.249
Tangara heinei	Black-capped Tanager	M	bel	gray-blue	slate	0.120	0.310	0.301	0.270	0.310
Tangara vitriolina	Scrub Tanager	M	bel	pale glaucous	slate	0.070	0.218	0.339	0.374	0.218
Thraupis cyanocephala	Blue-capped Tanager	M	bel	dull bluish-grey	slate	0.167	0.259	0.286	0.288	0.259
Thraupis episcopus	Blue-gray Tanager	M	bel	pale grey / blue wash	slate	0.200	0.289	0.273	0.237	0.289
Bangsia arcaei	Blue-and-gold Tanager	F	cro	bright blue	slate	0.325	0.278	0.218	0.180	0.278
Conirostrum cinereum	Cinereous Conebill	F	cro	slate-gray	slate	0.149	0.224	0.303	0.324	0.224
Conirostrum ferrugineiventris	White-browed Conebill	F	cro	slaty	slate	0.171	0.244	0.296	0.290	0.244
Conirostrum rufum	Rufous-browed Conebill	F	cro	plumbeous grey	slate	0.156	0.240	0.297	0.306	0.240
Conirostrum speciosum	Chestnut-vented Conebill	F	cro	bluish-grey	slate	0.171	0.264	0.298	0.267	0.264
Delothraupis castaneoventris	Chestnut-bellied Mountain-Tanager	F	cro	silvery sky blue	slate	0.277	0.295	0.237	0.190	0.295
Diglossa caerulescens	Bluish Flowerpiercer	F	cro	dull bluish-grey	slate	0.200	0.255	0.279	0.266	0.255
Diglossa duidae	Scaled Flowerpiercer	F	cro	slaty black	slate	0.199	0.246	0.290	0.265	0.246
Eucometis penicillata	Gray-headed Tanager	F	cro	grey	slate	0.095	0.238	0.321	0.345	0.238
Euneornis campestris	Orangequit	F	cro	olive-grey	slate	0.142	0.243	0.311	0.303	0.243
Nemosia pileata	Hooded Tanager	F	cro	light blue	slate	0.166	0.262	0.299	0.272	0.262
Phrygilus erythronotus	White-throated Sierra-Finch	F	cro	dark gray	slate	0.180	0.246	0.284	0.289	0.246
Phrygilus patagonicus	Patagonian Sierra-Finch	F	cro	dark blue gray	slate	0.227	0.261	0.266	0.247	0.261
Phrygilus punensis	Peruvian Sierra-Finch	F	cro	grey	slate	0.163	0.239	0.294	0.305	0.239
Pospiza cinerea	Cinereous Warbling-Finch	F	cro	grey	slate	0.169	0.251	0.288	0.292	0.251
Pospiza erythrophrys	Rusty-browed Warbling-Finch	F	cro	blue-grey	slate	0.151	0.245	0.294	0.311	0.245
Pospiza whitii	Black-and-chestnut Warbling-Finch	F	cro	slate-grey / olive-brown	slate	0.155	0.229	0.300	0.316	0.229
Saltator fuliginosus	Black-throated Grosbeak	F	cro	deep slate-blue	slate	0.195	0.249	0.282	0.274	0.249
Saltator grossus	Slate-colored Grosbeak	F	cro	slaty blue	slate	0.194	0.251	0.285	0.270	0.251
Thraupis episcopus	Blue-gray Tanager	F	cro	pale grey / blue wash	slate	0.181	0.248	0.296	0.274	0.248
Xenospingus concolor	Slender-billed Finch	F	cro	slate-grey	slate	0.165	0.257	0.291	0.287	0.257

Bangsia arcaei	Blue-and-gold Tanager	F	nap	dark blue	slate	0.321	0.266	0.221	0.192	0.266
Conirostrum cinereum	Cinereous Conebill	F	nap	slate-gray	slate	0.146	0.225	0.302	0.326	0.225
Conirostrum ferrugineiventris	White-browed Conebill	F	nap	blue gray	slate	0.188	0.250	0.285	0.277	0.250
Conirostrum rufum	Rufous-browed Conebill	F	nap	plumbeous grey	slate	0.166	0.243	0.293	0.297	0.243
Conirostrum sitticolor	Blue-backed Conebill	F	nap	blue	slate	0.200	0.245	0.282	0.274	0.245
Conirostrum speciosum	Chestnut-vented Conebill	F	nap	bluish-grey	slate	0.194	0.267	0.285	0.254	0.267
Delothraupis castaneiventris	Chestnut-bellied Mountain-Tanager	F	nap	dark blue	slate	0.265	0.273	0.244	0.218	0.273
Diglossa caerulescens	Bluish Flowerpiercer	F	nap	dull bluish-grey	slate	0.213	0.248	0.272	0.267	0.248
Diglossa duidae	Scaled Flowerpiercer	F	nap	slaty black	slate	0.243	0.253	0.265	0.238	0.253
Eucometis penicillata	Gray-headed Tanager	F	nap	grey / green	slate	0.064	0.233	0.338	0.365	0.233
Euneornis campestris	Orangequit	F	nap	olive-grey	slate	0.148	0.239	0.306	0.306	0.239
Nemosia pileata	Hooded Tanager	F	nap	light blue	slate	0.196	0.262	0.282	0.261	0.262
Phrygilus erythronotus	White-throated Sierra-Finch	F	nap	dark gray	slate	0.176	0.249	0.286	0.288	0.249
Phrygilus patagonicus	Patagonian Sierra-Finch	F	nap	dark blue gray	slate	0.217	0.249	0.271	0.263	0.249
Phrygilus punensis	Peruvian Sierra-Finch	F	nap	grey	slate	0.178	0.240	0.286	0.296	0.240
Poospiza cinerea	Cinereous Warbling-Finch	F	nap	grey	slate	0.137	0.256	0.302	0.305	0.256
Poospiza whitii	Black-and-chestnut Warbling-Finch	F	nap	slate-grey / olive-brown	slate	0.155	0.222	0.299	0.324	0.222
Saltator fuliginosus	Black-throated Grosbeak	F	nap	deep slate-blue	slate	0.217	0.251	0.272	0.261	0.251
Saltator grossus	Slate-colored Grosbeak	F	nap	slaty blue	slate	0.217	0.251	0.272	0.259	0.251
Thraupis episcopus	Blue-gray Tanager	F	nap	pale grey / blue wash	slate	0.190	0.251	0.293	0.265	0.251
Xenospingus concolor	Slender-billed Finch	F	nap	slate-grey	slate	0.182	0.255	0.283	0.279	0.255
Bangsia arcaei	Blue-and-gold Tanager	F	man	dark blue	slate	0.268	0.248	0.247	0.238	0.248
Catamblyrhynchus diadema	Plushcap	F	man	blue gray	slate	0.218	0.252	0.270	0.261	0.252
Conirostrum cinereum	Cinereous Conebill	F	man	slate-gray	slate	0.164	0.224	0.294	0.319	0.224
Conirostrum ferrugineiventris	White-browed Conebill	F	man	blue gray	slate	0.185	0.263	0.286	0.265	0.263
Conirostrum rufum	Rufous-browed Conebill	F	man	plumbeous grey	slate	0.166	0.241	0.294	0.299	0.241
Conirostrum sitticolor	Blue-backed Conebill	F	man	blue	slate	0.269	0.259	0.243	0.229	0.259
Delothraupis castaneiventris	Chestnut-bellied Mountain-Tanager	F	man	dark blue	slate	0.265	0.288	0.242	0.205	0.288
Diglossa caerulescens	Bluish Flowerpiercer	F	man	dull bluish-grey	slate	0.226	0.270	0.268	0.236	0.270
Diglossa duidae	Scaled Flowerpiercer	F	man	slaty black	slate	0.246	0.246	0.261	0.247	0.246
Hemispingus goeringi	Slaty-backed Hemispingus	F	man	slaty	slate	0.193	0.238	0.282	0.287	0.238
Nemosia pileata	Hooded Tanager	F	man	light blue	slate	0.191	0.262	0.283	0.264	0.262
Phrygilus erythronotus	White-throated Sierra-Finch	F	man	dark gray	slate	0.186	0.247	0.282	0.285	0.247
Poospiza cinerea	Cinereous Warbling-Finch	F	man	blue-grey	slate	0.145	0.258	0.300	0.297	0.258

Poospiza whitii	Black-and-chestnut Warbling-Finch	F	man	slate-grey / olive-brown	slate	0.153	0.229	0.300	0.318	0.229
Saltator fuliginosus	Black-throated Grosbeak	F	man	deep slate-blue	slate	0.220	0.251	0.271	0.257	0.251
Saltator grossus	Slate-colored Grosbeak	F	man	slaty blue	slate	0.216	0.254	0.273	0.256	0.254
Schistochlamys ruficapillus	Cinnamon Tanager	F	man	grey	slate	0.172	0.228	0.293	0.307	0.228
Thraupis episcopus	Blue-gray Tanager	F	man	darker bluish-grey	slate	0.188	0.253	0.295	0.264	0.253
Xenospingus concolor	Slender-billed Finch	F	man	slate-grey	slate	0.185	0.253	0.282	0.281	0.253
Bangsia arcaei	Blue-and-gold Tanager	F	rum	dark blue	slate	0.324	0.267	0.220	0.188	0.267
Catamblyrhynchus diadema	Plushcap	F	rum	blue gray	slate	0.204	0.237	0.273	0.287	0.237
Catamenia analis	Band-tailed Seedeater	F	rum	brown / dark brown	slate	0.172	0.231	0.289	0.308	0.231
Conirostrum cinereum	Cinereous Conebill	F	rum	slate-gray	slate	0.159	0.218	0.293	0.330	0.218
Conirostrum ferrugineiventris	White-browed Conebill	F	rum	blue gray	slate	0.197	0.260	0.281	0.262	0.260
Conirostrum rufum	Rufous-browed Conebill	F	rum	plumbeous grey	slate	0.173	0.236	0.286	0.305	0.236
Conirostrum sitticolor	Blue-backed Conebill	F	rum	blue	slate	0.221	0.242	0.262	0.275	0.242
Delothraupis castaneiventris	Chestnut-bellied Mountain-Tanager	F	rum	dark blue	slate	0.229	0.252	0.259	0.260	0.252
Diglossa caerulescens	Bluish Flowerpiercer	F	rum	dull bluish-grey	slate	0.245	0.261	0.260	0.234	0.261
Diglossa duidae	Scaled Flowerpiercer	F	rum	slaty black	slate	0.241	0.244	0.263	0.252	0.244
Hemispingus goeringi	Slaty-backed Hemispingus	F	rum	dark grey	slate	0.189	0.231	0.281	0.299	0.231
Nemosia pileata	Hooded Tanager	F	rum	light blue	slate	0.202	0.259	0.278	0.260	0.259
Phrygilus erythronotus	White-throated Sierra-Finch	F	rum	dark gray	slate	0.226	0.249	0.266	0.258	0.249
Poospiza cinerea	Cinereous Warbling-Finch	F	rum	blue-grey	slate	0.166	0.260	0.292	0.281	0.260
Poospiza whitii	Black-and-chestnut Warbling-Finch	F	rum	slate-grey / olive-brown	slate	0.195	0.236	0.281	0.287	0.236
Saltator fuliginosus	Black-throated Grosbeak	F	rum	deep slate-blue	slate	0.207	0.250	0.276	0.267	0.250
Saltator grossus	Slate-colored Grosbeak	F	rum	slaty blue	slate	0.210	0.246	0.275	0.270	0.246
Schistochlamys ruficapillus	Cinnamon Tanager	F	rum	grey	slate	0.191	0.232	0.279	0.298	0.232
Tangara vitriolina	Scrub Tanager	F	rum	greyish blue	slate	0.111	0.231	0.335	0.322	0.231
Thraupis episcopus	Blue-gray Tanager	F	rum	darker bluish-grey	slate	0.224	0.266	0.286	0.224	0.266
Xenospingus concolor	Slender-billed Finch	F	rum	slate-grey	slate	0.195	0.254	0.277	0.274	0.254
Bangsia arcaei	Blue-and-gold Tanager	F	thr	dark blue	slate	0.234	0.220	0.273	0.273	0.220
Diglossa caerulescens	Bluish Flowerpiercer	F	thr	dull bluish-grey	slate	0.162	0.220	0.288	0.329	0.220
Diglossa duidae	Scaled Flowerpiercer	F	thr	slate-grey	slate	0.223	0.252	0.272	0.254	0.252
Embernagra platensis	Great Pampa-Finch	F	thr	grey	slate	0.121	0.234	0.304	0.341	0.234
Phrygilus patagonicus	Patagonian Sierra-Finch	F	thr	dark blue gray	slate	0.220	0.252	0.268	0.260	0.252
Saltator fuliginosus	Black-throated Grosbeak	F	thr	deep slate-blue	slate	0.170	0.223	0.294	0.313	0.223
Tangara	Scrub Tanager	F	thr	pale bluish-grey	slate	0.12	0.23	0.316	0.323	0.236

vitriolina						5	6			
<i>Thraupis cyanocephala</i>	Blue-capped Tanager	F	thr	dull bluish-grey	slate	0.154	0.252	0.295	0.300	0.252
<i>Thraupis episcopus</i>	Blue-gray Tanager	F	thr	pale grey / blue wash	slate	0.164	0.250	0.292	0.293	0.250
<i>Diglossa caerulescens</i>	Bluish Flowerpiercer	F	bre	dull bluish-grey	slate	0.221	0.269	0.267	0.242	0.269
<i>Diglossa duidae</i>	Scaled Flowerpiercer	F	bre	slate-grey	slate	0.230	0.253	0.267	0.250	0.253
<i>Embernagra platensis</i>	Great Pampa-Finch	F	bre	grey	slate	0.109	0.238	0.310	0.343	0.238
<i>Phrygilus erythronotus</i>	White-throated Sierra-Finch	F	bre	grey	slate	0.173	0.251	0.283	0.293	0.251
<i>Saltator fuliginosus</i>	Black-throated Grosbeak	F	bre	deep slate-blue	slate	0.203	0.237	0.280	0.280	0.237
<i>Saltator grossus</i>	Slate-colored Grosbeak	F	bre	slaty blue	slate	0.144	0.226	0.301	0.330	0.226
<i>Thraupis cyanocephala</i>	Blue-capped Tanager	F	bre	dull bluish-grey	slate	0.163	0.261	0.289	0.286	0.261
<i>Thraupis episcopus</i>	Blue-gray Tanager	F	bre	pale grey / blue wash	slate	0.186	0.277	0.289	0.248	0.277
<i>Saltator fuliginosus</i>	Black-throated Grosbeak	F	bel	deep slate-blue	slate	0.200	0.244	0.278	0.277	0.244
<i>Saltator grossus</i>	Slate-colored Grosbeak	F	bel	slaty blue	slate	0.165	0.234	0.290	0.311	0.234
<i>Tangara vitriolina</i>	Scrub Tanager	F	bel	pale glaucous	slate	0.089	0.238	0.329	0.344	0.238
<i>Thraupis cyanocephala</i>	Blue-capped Tanager	F	bel	dull bluish-grey	slate	0.164	0.256	0.289	0.291	0.256
<i>Thraupis episcopus</i>	Blue-gray Tanager	F	bel	pale grey / blue wash	slate	0.179	0.263	0.289	0.269	0.263

Table S2. Scoring of the plumage colour measurements for males of each species with double scoring species involved. Species with double scoring are marked in red and excluded from the second analysis.

Latin name	coding	Latin name	coding	Latin name	coding	Latin name	coding	Latin name	coding	Latin name	coding
<i>Acanthidops bairdii</i>	2	<i>Dacnis nigripes</i>	3	<i>Incapiza pulchra</i>	1	<i>Poospiza caesar</i>	1	<i>Sporophila albogularis</i>	1	<i>Tangara icterocephala</i>	0
<i>Anisognathus igniventris</i>	3	<i>Dacnis venusta</i>	3	<i>Iridophanes pulcherrimus</i>	3	<i>Poospiza cinerea</i>	2	<i>Sporophila americana</i>	0	<i>Tangara inornata</i>	3
<i>Anisognathus lacrymosus</i>	3	<i>Dacnis viguieri</i>	3	<i>Iridosornis analis</i>	3	<i>Poospiza erythroprys</i>	2	<i>Sporophila bouvreuil</i>	0	<i>Tangara johannae</i>	3
<i>Anisognathus melanogenys</i>	3	<i>Delothraupis castaneiventris</i>	2	<i>Iridosornis jelskii</i>	3	<i>Poospiza hispaniolensis</i>	1	<i>Sporophila bouvionides</i>	0	<i>Tangara labradorides</i>	3
<i>Anisognathus somptuosus</i>	3	<i>Diglossa albilatera</i>	3	<i>Iridosornis porphyrocephalus</i>	3	<i>Poospiza hypochondriaca</i>	1	<i>Sporophila caerulescens</i>	1	<i>Tangara larvata</i>	3
<i>Bangsia arcaei</i>	2	<i>Diglossa baritula</i>	2	<i>Iridosornis rufivertex</i>	3	<i>Poospiza lateralis</i>	2	<i>Sporophila castaneiventris</i>	2	<i>Tangara lavinia</i>	3
<i>Bangsia edwardsi</i>	3	<i>Diglossa brunneiventris</i>	1	<i>Lanio aurantius</i>	0	<i>Poospiza melanoleuca</i>	1	<i>Sporophila cinnamomea</i>	1	<i>Tangara mexicana</i>	3
<i>Buthraupis eximia</i>	3	<i>Diglossa caerulescens</i>	2	<i>Lanio fulvus</i>	0	<i>Poospiza nigrorufa</i>	1	<i>Sporophila collaris</i>	1	<i>Tangara nigrocincta</i>	3
<i>Buthraupis montana</i>	3	<i>Diglossa carbonaria</i>	1	<i>Lanio leucothorax</i>	0	<i>Poospiza ornata</i>	1	<i>Sporophila corvina</i>	0	<i>Tangara nigroviridis</i>	3
<i>Calochaetes</i>	0	<i>Diglossa</i>	3	<i>Lanio</i>	0	<i>Poospiza</i>	1	<i>Sporophila</i>	1	<i>Tangara</i>	3

coccineus		cyanea		versicolor		thoracica		frontalis		parzudakii	
Camarhynchus pallidus	0	Diglossa duidae	2	Lophospingus griseocristatus	1	Poospiza torquata	1	Sporophila hypoxantha	1	Tangara peruviana	3
Camarhynchus parvulus	0	Diglossa glauca	3	Lophospingus pusillus	1	Poospiza whitii	2	Sporophila intermedia	2	Tangara preciosa	3
Camarhynchus psittacula	0	Diglossa gloriosa	1	Loxigilla barbadensis	1	Porphyrospiza caerulescens	3	Sporophila leucoptera	1	Tangara punctata	3
Catamblyrhnchus diadema	2	Diglossa gloriosissima	2	Loxigilla noctis	1	Pyrrhocoma ruficeps	2	Sporophila lineola	0	Tangara ruficervix	3
Catamenia analis	2	Diglossa humeralis	1	Loxigilla portoricensis	0	Ramphocelus bresilius	0	Sporophila luctuosa	0	Tangara rufigenis	3
Catamenia homochroa	2	Diglossa indigotica	3	Loxigilla violacea	0	Ramphocelus carbo	0	Sporophila minuta	1	Tangara rufigula	0
Catamenia inornata	2	Diglossa lafresnayii	2	Loxipasser anoxanthus	0	Ramphocelus dimidiatus	0	Sporophila murallae	0	Tangara schrankii	3
Certhidea olivacea	0	Diglossa major	2	Melanodera melanodera	2	Ramphocelus flammigerus	0	Sporophila nigricollis	0	Tangara seledon	3
Charitospiza eucosma	1	Diglossa mystacalis	2	Melanodera xanthogramma	1	Ramphocelus melanogaster	0	Sporophila nigrorufa	0	Tangara varia	3
Chlorochrysa calliparaea	3	Diglossa plumbea	2	Melanospiza richardsoni	0	Ramphocelus nigrogularis	0	Sporophila palustris	1	Tangara vassorii	3
Chlorochrysa phoenicotis	0	Diglossa sittoides	2	Melopyrrha nigra	0	Ramphocelus passerinii	0	Sporophila peruviana	1	Tangara velia	3
Chlorophanes spiza	3	Diglossa venezuelensis	0	Nemosia pileata	2	Ramphocelus sanguinolentus	0	Sporophila plumbea	1	Tangara viridicollis	3
Chlorornis riefferii	0	Diuca diuca	1	Neothraupis fasciata	1	Rhodospingus cruentus	0	Sporophila ruficollis	1	Tangara vitriolina	3
Chrysothlypis chrysomelas	0	Donacospiza albifrons	1	Nesospiza acunhae	0	Rowettia goughensis	0	Sporophila simplex	1	Tangara xanthocephala	3
Chrysothlypis salmonei	0	Dubusia taeniata	3	Nesospiza questi	0	Saltator albicollis	0	Sporophila telasco	1	Tangara xanthogastrea	0
Cissopis leverianus	0	Emberizoides herbicola	1	Nesospiza wilkinsi	0	Saltator atriceps	1	Sporophila torqueola	0	Tersina viridis	3
Cnemoscopus rubrirostris	1	Embernagra platensis	2	Orchesticus abeillei	0	Saltator atricollis	0	Stephanophorus diadematus	3	Thlypopsis fulviceps	1
Coereba flaveola	1	Eucometis penicillata	2	Oreomanes fraseri	2	Saltator atripennis	1	Tachyphonus coronatus	0	Thlypopsis inornata	1
Compsospiza garleppi	1	Euneornis campestris	2	Oryzoborus angolensis	0	Saltator aurantiirostris	1	Tachyphonus cristatus	0	Thlypopsis ornata	1
Conirostrum albifrons	3	Geospiza conirostris	0	Oryzoborus crassirostris	0	Saltator coerulescens	1	Tachyphonus delatrii	0	Thlypopsis pectoralis	1
Conirostrum bicolor	3	Geospiza difficilis	0	Oryzoborus maximiliani	0	Saltator fuliginosus	2	Tachyphonus luctuosus	0	Thlypopsis ruficeps	0
Conirostrum cinereum	2	Geospiza fortis	0	Oryzoborus nuttingi	0	Saltator grossus	2	Tachyphonus phoenicius	0	Thlypopsis sordida	1
Conirostrum ferrugineiventre	2	Geospiza fuliginosa	0	Parkerthraustes humeralis	2	Saltator maxillosus	1	Tachyphonus rufiventer	0	Thraupis abbas	3
Conirostrum leucogenys	2	Geospiza magnirostris	0	Paroaria capitata	0	Saltator maximus	1	Tachyphonus rufus	0	Thraupis bonariensis	3
Conirostrum margaritae	2	Geospiza scandens	0	Paroaria coronata	1	Saltator nigriceps	1	Tachyphonus surinamus	0	Thraupis cyanocephala	3
Conirostrum	2	Gubernatrix	0	Paroaria	1	Saltator	1	Tangara	3	Thraupis	3

rufum		cristata		dominicana		orenocensis		argyrofenges		episcopus	
Conirostrum sitticolor	2	Haplospiza unicolor	2	Paroaria gularis	0	Saltator similis	1	Tangara arthus	0	Thraupis glaucocolpa	3
Conirostrum speciosum	2	Hemispingus atropileus	0	Phrygilus alaudinus	2	Saltator striatipectus	1	Tangara callophrys	3	Thraupis ornata	3
Conothraupis speculigera	1	Hemispingus calophrys	0	Phrygilus atriceps	1	Saltatricula multicolor	1	Tangara cayana	3	Thraupis sayaca	3
Coryphaspiza melanotis	1	Hemispingus frontalis	0	Phrygilus dorsalis	2	Schistochlamys melanopis	1	Tangara chilensis	3	Tiaris bicolor	1
Coryphospingus cucullatus	0	Hemispingus goeringi	2	Phrygilus erythronotus	2	Schistochlamys ruficapillus	2	Tangara chrysotis	0	Tiaris canorus	1
Coryphospingus pileatus	1	Hemispingus melanotis	1	Phrygilus fruticeti	1	Sericossypha albocristata	0	Tangara cucullata	3	Tiaris fuliginosus	0
Creurgops dentatus	2	Hemispingus reyi	1	Phrygilus gayi	2	Sicalis auriventris	0	Tangara cyanicollis	3	Tiaris obscurus	1
Creurgops verticalis	1	Hemispingus superciliaris	0	Phrygilus patagonicus	2	Sicalis citrina	0	Tangara cyanocephala	3	Tiaris olivaceus	0
Cyanerpes caeruleus	3	Hemispingus verticalis	1	Phrygilus plebejus	1	Sicalis columbiana	0	Tangara cyanoptera	3	Trichothraupis melanops	0
Cyanerpes cyaneus	3	Hemispingus xanthophthalmus	1	Phrygilus punensis	2	Sicalis flaveola	0	Tangara cyanotis	3	Urothraupis stolzmanni	1
Cyanerpes lucidus	3	Hemithraupis flavicollis	0	Phrygilus unicolor	2	Sicalis lebruni	1	Tangara cyanoventris	3	Volatinia jacarina	0
Cyanerpes nitidus	3	Hemithraupis guira	0	Piezorhina cinerea	1	Sicalis lutea	0	Tangara desmaresti	0	Xenodacnis parina	3
Cyanicterus cyanicterus	3	Hemithraupis ruficapilla	0	Pinaroloxias inornata	0	Sicalis luteocephala	1	Tangara dowii	3	Xenospingus concolor	2
Cypsnagra hirundinacea	0	Heterospingus rubrifrons	1	Pipraeidea melanonota	3	Sicalis luteola	0	Tangara fastuosa	3		
Dacnis cayana	3	Heterospingus xanthopygius	0	Platyspiza crassirostris	0	Sicalis olivascens	0	Tangara florida	0		
Dacnis flaviventer	0	Idiopsar brachyurus	1	Poospiza alticola	1	Sicalis raimondii	1	Tangara guttata	3		
Dacnis hartlaubi	3	Incaspiza laeta	1	Poospiza boliviana	1	Sicalis taczanowskii	1	Tangara gyrola	3		
Dacnis lineata	3	Incaspiza personata	1	Poospiza cabanisi	1	Sicalis uropygialis	1	Tangara heinei	3		

Table S3. Scoring of the plumage colour measurements for females of each species with double scoring species involved. Species with double scoring are marked in red and excluded from the second analysis.

Latin name	coding	Latin name	coding	Latin name	coding	Latin name	coding	Latin name	coding	Latin name	coding
Acanthidops bairdii	1	Dacnis nigripes	3	Incaspiza pulchra	1	Poospiza caesar	1	Sporophila albogularis	0	Tangara icterocephala	0
Anisognathus igniventris	3	Dacnis venusta	3	Iridophanes pulcherrimus	3	Poospiza cinerea	2	Sporophila americana	0	Tangara inornata	3
Anisognathus lacrymosus	3	Dacnis viguieri	0	Iridosornis analis	3	Poospiza erythrochrys	2	Sporophila bouvreuil	0	Tangara johannae	3
Anisognathus melanogenys	3	Delothraupis castaneoventris	2	Iridosornis jelskii	3	Poospiza hispaniolensis	0	Sporophila bouvronides	0	Tangara labradorides	3
Anisognathus somptuosus	3	Diglossa albilatera	0	Iridosornis porphyrocephalus	3	Poospiza hypochondriaca	1	Sporophila caerulescens	0	Tangara larvata	3

Bangsia arcaei	2	Diglossa baritula	0	Iridosornis rufivertex	3	Poospiza lateralis	2	Sporophila castaneiventris	0	Tangara lavinia	3
Bangsia edwardsi	3	Diglossa brunneiventris	1	Lanio aurantius	1	Poospiza melanoleuca	1	Sporophila cinnamomea	0	Tangara mexicana	3
Buthraupis eximia	3	Diglossa caerulescens	2	Lanio fulvus	0	Poospiza nigrorufa	1	Sporophila collaris	0	Tangara nigrocincta	3
Buthraupis montana	3	Diglossa carbonaria	1	Lanio leucothorax	0	Poospiza ornata	1	Sporophila corvina	0	Tangara nigroviridis	3
Calochaetes coccineus	0	Diglossa cyanea	3	Lanio versicolor	0	Poospiza thoracica	1	Sporophila frontalis	0	Tangara parzudakii	3
Camarhynchus pallidus	0	Diglossa duidae	2	Lophospingus griseocristatus	1	Poospiza torquata	1	Sporophila hypoxantha	0	Tangara peruviana	0
Camarhynchus parvulus	1	Diglossa glauca	3	Lophospingus pusillus	1	Poospiza whittii	2	Sporophila intermedia	0	Tangara preciosa	0
Camarhynchus psittacula	0	Diglossa gloriosa	1	Loxigilla barbadensis	1	Porphyrospiza caerulescens	1	Sporophila leucoptera	0	Tangara punctata	3
Catamblyrhynchus diadema	2	Diglossa gloriosissima	2	Loxigilla noctis	1	Pyrrhocomma ruficeps	0	Sporophila lineola	0	Tangara ruficervix	3
Catamenia analis	2	Diglossa humeralis	1	Loxigilla portoricensis	0	Ramphocelus bresilius	0	Sporophila luctuosa	0	Tangara rufigenis	3
Catamenia homochroa	1	Diglossa indigotica	3	Loxigilla violacea	0	Ramphocelus carbo	0	Sporophila minuta	0	Tangara rufigula	0
Catamenia inornata	1	Diglossa lafresnayii	2	Loxipasser anoxanthus	1	Ramphocelus dimidiatus	0	Sporophila murallae	0	Tangara schrankii	3
Certhidea olivacea	0	Diglossa major	2	Melanodera melanodera	0	Ramphocelus flammigerus	0	Sporophila nigricollis	0	Tangara seledon	3
Charitospiza eucosma	1	Diglossa mystacalis	2	Melanodera xanthogramma	0	Ramphocelus melanogaster	0	Sporophila nigrorufa	0	Tangara varia	0
Chlorochrysa calliparaea	3	Diglossa plumbea	0	Melanospiza richardsoni	1	Ramphocelus nigrogularis	0	Sporophila palustris	0	Tangara vassorii	3
Chlorochrysa phoenicotis	0	Diglossa sittoides	0	Melopyrrha nigra	0	Ramphocelus passerinii	1	Sporophila peruviana	0	Tangara velia	3
Chlorophanes spiza	0	Diglossa venezuelensis	0	Nemosia pileata	2	Ramphocelus sanguinolentus	0	Sporophila plumbea	0	Tangara viridicollis	1
Chlorornis riefferii	0	Diuca diuca	1	Neothraupis fasciata	1	Rhodospingus cruentus	0	Sporophila ruficollis	0	Tangara vitriolina	3
Chrysothlypis chrysomelas	0	Donacospiza albifrons	1	Nesospiza acunhae	0	Rowettia goughensis	0	Sporophila simplex	0	Tangara xanthocephala	3
Chrysothlypis salmoni	0	Dubusia taeniata	3	Nesospiza questi	0	Saltator albicollis	0	Sporophila telasco	0	Tangara xanthogastrea	0
Cissopis leverianus	0	Emberizoides herbicola	1	Nesospiza wilkinsi	0	Saltator atriceps	1	Sporophila torqueola	0	Tersina viridis	0
Cnemoscopus rubrirostris	1	Embernagra platensis	2	Orchesticus abeillei	0	Saltator atricollis	0	Stephanophorus diadematus	3	Thlypopsis fulviceps	1
Coereba flaveola	1	Eucometis penicillata	2	Oreomanes fraseri	2	Saltator atripennis	1	Tachyphonus coronatus	1	Thlypopsis inornata	1
Compsospiza garleppi	1	Euneornis campestris	2	Oryzoborus angolensis	0	Saltator aurantiirostris	1	Tachyphonus cristatus	0	Thlypopsis ornata	1
Conirostrum albifrons	3	Geospiza conirostris	0	Oryzoborus crassirostris	0	Saltator coerulescens	1	Tachyphonus delatrii	0	Thlypopsis pectoralis	1
Conirostrum bicolor	3	Geospiza difficilis	0	Oryzoborus maximiliani	0	Saltator fuliginosus	2	Tachyphonus luctuosus	1	Thlypopsis ruficeps	0

Conirostrum cinereum	2	Geospiza fortis	0	Oryzoborus nuttingi	0	Saltator grossus	2	Tachyphonus phoenicius	1	Thlypopsis sordida	1
Conirostrum ferrugineiventre	2	Geospiza fuliginosa	1	Parkerthraustes humeralis	2	Saltator maxillosus	1	Tachyphonus rufiventer	1	Thraupis abbas	3
Conirostrum leucogenys	2	Geospiza magnirostris	1	Paroaria capitata	0	Saltator maximus	1	Tachyphonus rufus	0	Thraupis bonariensis	3
Conirostrum margaritae	2	Geospiza scandens	0	Paroaria coronata	1	Saltator nigriceps	1	Tachyphonus surinamus	1	Thraupis cyanocephala	3
Conirostrum rufum	2	Gubernatrix cristata	0	Paroaria dominicana	1	Saltator orenocensis	1	Tangara argyrofenges	3	Thraupis episcopus	3
Conirostrum sitticolor	2	Haplospiza unicolor	0	Paroaria gularis	0	Saltator similis	1	Tangara arthus	0	Thraupis glaucocolpa	3
Conirostrum speciosum	2	Hemispingus atopileus	0	Phrygilus alaudinus	0	Saltator striatipectus	1	Tangara callophrys	3	Thraupis ornata	3
Conothraupis speculigera	0	Hemispingus calophrys	0	Phrygilus atriceps	1	Saltatricula multicolor	1	Tangara cayana	3	Thraupis sayaca	3
Coryphospiza melanotis	1	Hemispingus frontalis	0	Phrygilus dorsalis	2	Schistochlamys melanopis	1	Tangara chilensis	3	Tiaris bicolor	1
Coryphospingus cucullatus	0	Hemispingus goeringi	2	Phrygilus erythronotus	2	Schistochlamys ruficapillus	2	Tangara chrysotis	0	Tiaris canorus	1
Coryphospingus pileatus	1	Hemispingus melanotis	1	Phrygilus fruticeti	1	Sericossypha albocristata	0	Tangara cucullata	3	Tiaris fuliginosus	0
Creurgops dentatus	2	Hemispingus reyi	1	Phrygilus gayi	2	Sicalis auriventris	0	Tangara cyanicollis	3	Tiaris obscurus	1
Creurgops verticalis	1	Hemispingus superciliaris	0	Phrygilus patagonicus	2	Sicalis citrina	0	Tangara cyanocephala	3	Tiaris olivaceus	0
Cyanerpes caeruleus	3	Hemispingus verticalis	1	Phrygilus plebejus	1	Sicalis columbiana	0	Tangara cyanoptera	3	Trichothraupis melanops	0
Cyanerpes cyaneus	0	Hemispingus xanthophthalmus	1	Phrygilus punensis	2	Sicalis flaveola	0	Tangara cyanotis	3	Urothraupis stolzmanni	1
Cyanerpes lucidus	3	Hemithraupis flavicollis	0	Phrygilus unicolor	0	Sicalis lebruni	1	Tangara cyanoventris	3	Volatinia jacarina	0
Cyanerpes nitidus	3	Hemithraupis guira	0	Piezorhina cinerea	1	Sicalis lutea	0	Tangara desmaresti	0	Xenodacnis parina	3
Cyanicterus cyanicterus	3	Hemithraupis ruficapilla	0	Pinaroloxias inornata	0	Sicalis luteocephala	1	Tangara dowii	3	Xenospingus concolor	2
Cypsnagra hirundinacea	0	Heterospingus rubrifrons	1	Pipraeidea melanonota	3	Sicalis luteola	0	Tangara fastuosa	3		
Dacnis cayana	3	Heterospingus xanthopygius	1	Platyspiza crassirostris	0	Sicalis olivascens	1	Tangara florida	0		
Dacnis flaviventer	0	Idiopsar brachyurus	1	Poospiza alticola	1	Sicalis raimondii	1	Tangara guttata	3		
Dacnis hartlaubi	1	Incaspiza laeta	1	Poospiza boliviana	1	Sicalis taczanowskii	1	Tangara gyrola	3		
Dacnis lineata	1	Incaspiza personata	1	Poospiza cabanisi	1	Sicalis uropygialis	1	Tangara heinei	3		

Table S4. Reverse Jump analysis results for male; analysis done with the table containing double scored species

	transition rate	colour transitions	ESS	Me an	Me dia n	Mo de	95% HPD	% Zero	number of zero	total number	% not zero
male_1	q01	any other colour -> grey	6579 1.80 0	0.0 44	0.0 43	0.0 42	[0.029, 0.0604]	0.000	1.000	218000.00 0	100.000
	q02	any other	1450	0.0	0.0	0.0	[0,	6.552	14284.00	218000.00	93.448

		colour -> slate	5.70 0	41	42	00	0.0573]		0	0	
	q03	any other colour -> blue	2845 3.50 0	0.0 00	0.0 00	0.0 00	[0, 0]	99.104	216047.0 00	218000.00 0	0.896
	q10	grey -> any other colour	6634 7.30 0	0.0 44	0.0 43	0.0 42	[0.029, 0.0605]	0.000	0.000	218000.00 0	100.000
	q12	grey -> slate	6510 6.50 0	0.0 44	0.0 43	0.0 42	[0.0291, 0.0604]	0.000	0.000	218000.00 0	100.000
	q13	grey -> blue	1265 47.4 00	0.0 00	0.0 00	0.0 00	[0, 0]	99.871	217718.0 00	218000.00 0	0.129
	q20	slate -> any other colour	4839 7.30 0	0.0 30	0.0 38	0.0 00	[0, 0.0561]	29.555	64430.00 0	218000.00 0	70.445
	q21	slate -> grey	6652 4.90 0	0.0 44	0.0 43	0.0 42	[0.029, 0.0604]	0.002	4.000	218000.00 0	99.998
	q23	slate -> blue	7593 0.00 0	0.0 44	0.0 43	0.0 42	[0.0293, 0.0602]	0.000	0.000	218000.00 0	100.000
	q30	blue -> any other colour	7589 4.20 0	0.0 44	0.0 43	0.0 42	[0.0293, 0.0602]	0.000	0.000	218000.00 0	100.000
	q31	blue -> grey	9985 9.70 0	0.0 00	0.0 00	0.0 00	[0, 0.0578]	99.970	217934.0 00	218000.00 0	0.030
	q32	blue -> slate	3328 .400	0.0 01	0.0 00	0.0 00	[0, 0.0818]	98.111	213882.0 00	218000.00 0	1.889
male_2	q01	any other colour -> grey	7261 6.50 0	0.0 44	0.0 43	0.0 38	[0.029, 0.0604]	0.002	4.000	218000.00 0	99.998
	q02	any other colour -> slate	1060 9.00 0	0.0 40	0.0 42	0.0 00	[0, 0.0573]	6.806	14837.00 0	218000.00 0	93.194
	q03	any other colour -> blue	2886 5.70 0	0.0 00	0.0 00	0.0 00	[0, 0]	99.106	216051.0 00	218000.00 0	0.894
	q10	grey -> any other colour	7254 5.70 0	0.0 44	0.0 43	0.0 38	[0.029, 0.0604]	0.000	0.000	218000.00 0	100.000
	q12	grey -> slate	6619 4.80 0	0.0 44	0.0 43	0.0 38	[0.0292, 0.0604]	0.000	0.000	218000.00 0	100.000
	q13	grey -> blue	1346 40.8 00	0.0 00	0.0 00	0.0 00	[0, 0]	99.874	217725.0 00	218000.00 0	0.126
	q20	slate -> any other colour	3813 3.30 0	0.0 30	0.0 38	0.0 00	[0, 0.0561]	29.513	64338.00 0	218000.00 0	70.487
	q21	slate -> grey	7260 4.40 0	0.0 44	0.0 43	0.0 38	[0.029, 0.0604]	0.003	6.000	218000.00 0	99.997
	q23	slate -> blue	7748 1.60 0	0.0 44	0.0 43	0.0 38	[0.0294, 0.0602]	0.001	3.000	218000.00 0	99.999
	q30	blue -> any other colour	7657 5.00 0	0.0 44	0.0 43	0.0 38	[0.0294, 0.0602]	0.000	0.000	218000.00 0	100.000
	q31	blue -> grey	1404 47.3 00	0.0 00	0.0 00	0.0 00	[0, 0]	99.981	217959.0 00	218000.00 0	0.019
	q32	blue -> slate	2530 .400	0.0 01	0.0 00	0.0 00	[0, 0]	97.830	213270.0 00	218000.00 0	2.170
male_3	q01	any other colour -> grey	6807 6.50 0	0.0 44	0.0 43	0.0 43	[0.0291, 0.0607]	0.002	4.000	218000.00 0	99.998

q02	any other colour -> slate	1245 9.70 0	0.0 40	0.0 42	0.0 00	[0, 0.0574]	6.757	14730.00 0	218000.00 0	93.243
q03	any other colour -> blue	2523 5.50 0	0.0 00	0.0 00	0.0 00	[0, 0]	99.094	216026.0 00	218000.00 0	0.906
q10	grey -> any other colour	6826 2.60 0	0.0 44	0.0 43	0.0 43	[0.0291, 0.0607]	0.000	0.000	218000.00 0	100.000
q12	grey -> slate	6675 6.90 0	0.0 44	0.0 43	0.0 43	[0.0291, 0.0605]	0.000	0.000	218000.00 0	100.000
q13	grey -> blue	9073 2.20 0	0.0 00	0.0 00	0.0 00	[0, 0]	99.834	217638.0 00	218000.00 0	0.166
q20	slate -> any other colour	4473 0.80 0	0.0 30	0.0 38	0.0 00	[0, 0.0561]	29.667	64675.00 0	218000.00 0	70.333
q21	slate -> grey	6837 5.80 0	0.0 44	0.0 43	0.0 43	[0.0291, 0.0607]	0.003	6.000	218000.00 0	99.997
q23	slate -> blue	7633 4.10 0	0.0 44	0.0 43	0.0 43	[0.0291, 0.0601]	0.005	10.000	218000.00 0	99.995
q30	blue -> any other colour	7624 7.60 0	0.0 44	0.0 43	0.0 43	[0.0291, 0.0601]	0.000	0.000	218000.00 0	100.000
q31	blue -> grey	1582 34.7 00	0.0 00	0.0 00	0.0 00	[0, 0]	99.978	217951.0 00	218000.00 0	0.022
q32	blue -> slate	2428 .400	0.0 01	0.0 00	0.0 00	[0, 0]	97.913	213451.0 00	218000.00 0	2.087

Table S5. Reverse Jump analysis results for female; analysis done with the table containing double scores species

	transition rate	colour transitions	ESS	Mean	Median	Mode	95% HPD	% Zero	number of zero	total number	% not zero
female_1	q01	any other colour -> grey	1033 42.20 0	0.06 5	0.06 4	0.06 4	[0.048, 0.0807]	0.00 0	0.000	218000.000	100.000
	q02	any other colour -> slate	1343 60.50 0	0.00 2	0.00 0	0.00 0	[0, 0]	96.6 78	210758.0 00	218000.000	3.322
	q03	any other colour -> blue	8683 9.800	0.00 0	0.00 0	0.00 0	[0, 0]	99.9 58	217908.0 00	218000.000	0.042
	q10	grey -> any other colour	1025 56.30 0	0.06 5	0.06 4	0.06 4	[0.0481, 0.0807]	0.00 0	0.000	218000.000	100.000
	q12	grey -> slate	1440 16.00 0	0.06 4	0.06 4	0.06 4	[0.0484, 0.0807]	0.00 1	2.000	218000.000	99.999
	q13	grey -> blue	9287 0.600	0.00 0	0.00 0	0.00 0	[0, 0]	99.9 96	217991.0 00	218000.000	0.004
	q20	slate -> any other colour	7110 5.400	0.06 4	0.06 4	0.00 0	[0.0479, 0.0807]	0.53 3	1162.000	218000.000	99.467
	q21	slate -> grey	1056 26.00 0	0.06 4	0.06 4	0.00 0	[0.048, 0.0807]	0.05 9	128.000	218000.000	99.941
	q23	slate -> blue	1370 94.20 0	0.06 4	0.06 4	0.06 4	[0.0484, 0.0807]	0.00 0	1.000	218000.000	100.000
	q30	blue -> any other colour	1355 17.90 0	0.06 4	0.06 4	0.06 4	[0.0484, 0.0807]	0.00 0	0.000	218000.000	100.000

female_ 2	q31	blue -> grey	1849 4.200	0.00 0	0.00 0	0.00 0	[0, 0]	99.8 93	217767.0 00	218000. 000	0.107
	q32	blue -> slate	1652 9.100	0.00 0	0.00 0	0.00 0	[0, 0]	99.9 13	217811.0 00	218000. 000	0.087
	q01	any other colour -> grey	1041 50.60 0	0.06 5	0.06 4	0.06 4	[0.0482, 0.0808]	0.00 0	0.000	218000. 000	100.000
	q02	any other colour -> slate	1319 91.20 0	0.00 2	0.00 0	0.00 0	[0, 0]	96.6 16	210623.0 00	218000. 000	3.384
	q03	any other colour -> blue	6737 1.700	0.00 0	0.00 0	0.00 0	[0, 0]	99.9 72	217940.0 00	218000. 000	0.028
	q10	grey -> any other colour	1037 34.70 0	0.06 5	0.06 4	0.06 4	[0.0482, 0.0807]	0.00 0	0.000	218000. 000	100.000
	q12	grey -> slate	1396 47.80 0	0.06 4	0.06 4	0.06 4	[0.0481, 0.0804]	0.00 3	6.000	218000. 000	99.997
	q13	grey -> blue	1533 73.50 0	0.00 0	0.00 0	0.00 0	[0, 0]	99.9 97	217994.0 00	218000. 000	0.003
	q20	slate -> any other colour	5874 2.400	0.06 4	0.06 4	0.00 0	[0.0481, 0.0808]	0.47 1	1026.000	218000. 000	99.529
	q21	slate -> grey	1046 05.60 0	0.06 4	0.06 4	0.00 0	[0.0482, 0.0808]	0.07 2	158.000	218000. 000	99.928
	q23	slate -> blue	1387 04.70 0	0.06 4	0.06 4	0.06 4	[0.0481, 0.0804]	0.00 0	0.000	218000. 000	100.000
	q30	blue -> any other colour	1402 20.60 0	0.06 4	0.06 4	0.06 4	[0.0482, 0.0804]	0.00 0	0.000	218000. 000	100.000
	q31	blue -> grey	8026. 400	0.00 0	0.00 0	0.00 0	[0, 0]	99.9 24	217834.0 00	218000. 000	0.076
	q32	blue -> slate	1655 4.800	0.00 0	0.00 0	0.00 0	[0, 0]	99.9 24	217835.0 00	218000. 000	0.076
female_ 3	q01	any other colour -> grey	9941 7.200	0.06 5	0.06 4	0.06 4	[0.048, 0.0808]	0.00 0	0.000	218000. 000	100.000
	q02	any other colour -> slate	1313 06.20 0	0.00 2	0.00 0	0.00 0	[0, 0]	96.6 49	210695.0 00	218000. 000	3.351
	q03	any other colour -> blue	9443 2.100	0.00 0	0.00 0	0.00 0	[0, 0]	99.9 57	217906.0 00	218000. 000	0.043
	q10	grey -> any other colour	9870 3.800	0.06 5	0.06 4	0.06 4	[0.0479, 0.0806]	0.00 0	1.000	218000. 000	100.000
	q12	grey -> slate	1437 92.40 0	0.06 4	639. 000	0.06 4	[0.0481, 0.0805]	0.00 0	1.000	218000. 000	100.000
	q13	grey -> blue	1718 2.100	0.00 0	0.00 0	0.00 0	[0, 0]	99.9 91	217981.0 00	218000. 000	0.009
	q20	slate -> any other colour	6321 0.200	0.06 4	0.06 4	0.00 0	[0.048, 0.0808]	0.48 8	1064.000	218000. 000	99.512
	q21	slate -> grey	1016 12.80 0	0.06 4	0.06 4	0.00 0	[0.0479, 0.0806]	0.06 1	132.000	218000. 000	99.939
	q23	slate -> blue	1339 40.10 0	0.06 4	0.06 4	0.06 4	[0.0479, 0.0803]	0.00 5	11.000	218000. 000	99.995
	q30	blue -> any other colour	1380 57.80 0	0.06 4	0.06 4	0.06 4	[0.0479, 0.0803]	0.00 0	0.000	218000. 000	100.000
	q31	blue -> grey	1282 2.800	0.00 0	0.00 0	0.00 0	[0, 0]	99.9 12	217809.0 00	218000. 000	0.088
	q32	blue -> slate	1569 5.900	0.00 0	0.00 0	0.00 0	[0,0]	99.9 28	217843.0 00	218000. 000	0.072

Table S6. Reverse Jump analysis results for male; analysis done with the table not containing double scored species

	transition rate	colour transitions	ESS	Mean	Median	Mode	95% HPD	% Zero	number of zero	total number	% not zero
male _1	q01	any other colour -> grey	55006.000	0.040	0.039	0.037	[0.0271, 0.0544]	0.000	0.000	218000.000	100.000
	q02	any other colour -> slate	86926.000	0.033	0.037	0.000	[0, 0.0496]	98.331	214362.000	218000.000	1.669
	q03	any other colour -> blue	43413.000	0.000	0.000	0.000	[0, 0]	99.936	217861.000	218000.000	0.064
	q10	grey -> any other colour	55016.000	0.040	0.039	0.037	[0.0272, 0.0545]	0.000	0.000	218000.000	100.000
	q12	grey -> slate	55446.000	0.040	0.039	0.037	[0.0272, 0.0544]	0.003	6.000	218000.000	99.997
	q13	grey -> blue	50429.000	0.000	0.000	0.000	[0, 0]	99.857	217688.000	218000.000	0.143
	q20	slate -> any other colour	10190.000	0.032	0.037	0.000	[0, 0.0502]	6.456	14073.000	218000.000	93.544
	q21	slate -> grey	55579.000	0.040	0.039	0.037	[0.0272, 0.0544]	1.293	2819.000	218000.000	98.707
	q23	slate -> blue	86990.000	0.040	0.039	0.000	[0.0277, 0.054]	5.425	11827.000	218000.000	94.575
	q30	blue -> any other colour	92878.000	92878.000	0.039	0.037	[0.0272, 0.0534]	0.000	20.000	218000.000	99.991
	q31	blue -> grey	15410.000	0.000	0.000	0.000	[0, 0]	94.083	205101.000	218000.000	5.917
	q32	blue -> slate	20358.000	0.000	0.000	0.000	[0, 0]	98.737	215246.000	218000.000	1.263
male _2	q01	any other colour -> grey	54079.000	0.040	0.039	0.038	[0.0274, 0.0547]	0.000	6.000	218000.000	99.997
	q02	any other colour -> slate	88908.000	0.033	0.037	0.000	[0, 0.0496]	14.919	32523.000	218000.000	85.081
	q03	any other colour -> blue	45276.000	0.000	0.000	0.000	[0, 0]	99.457	216816.000	218000.000	0.543
	q10	grey -> any other colour	54182.000	0.040	0.039	0.038	[0.0274, 0.0547]	0.000	0.000	218000.000	100.000
	q12	grey -> slate	54228.000	0.040	0.039	0.038	[0.0274, 0.0547]	0.000	0.000	218000.000	100.000
	q13	grey -> blue	29370.000	0.000	0.000	0.000	[0, 0]	99.804	217572.000	218000.000	0.196
	q20	slate -> any other colour	10270.000	0.032	0.037	0.000	[0, 0/0504]	17.820	38847.000	218000.000	82.180
	q21	slate -> grey	55315.000	0.040	0.039	0.038	[0.0274, 0.0547]	0.003	6.000	218000.000	99.997
	q23	slate -> blue	86564.000	0.040	0.039	0.000	[0.0275, 0.0538]	0.036	78.000	218000.000	99.964
	q30	blue -> any other colour	96608.000	94608.000	0.039	0.038	[0.0275, 0.0538]	0.000	0.000	218000.000	100.000
	q31	blue -> grey	88186.000	0.000	0.000	0.000	[0, 0]	99.966	217925.000	218000.000	0.034
	q32	blue -> slate	21723.000	0.000	0.000	0.000	[0, 0]	99.468	216840.000	218000.000	0.532
male _3	q01	any other colour -> grey	57759.000	0.404	0.039	0.038	[0.0273, 0.0545]	0.001	2.000	218000.000	99.999
	q02	any other colour -> slate	94523.000	0.033	0.037	0.000	[0, 0.0498]	14.813	32293.000	218000.000	85.187
	q03	any other colour -> blue	39017.000	0.000	0.000	0.000	[0, 0]	99.478	216863.000	218000.000	0.522
	q10	grey -> any other colour	57687.000	0.404	0.039	0.038	[0.0273, 0.0545]	0.001	2.000	218000.000	99.999
	q12	grey -> slate	61338.000	0.040	0.039	0.038	[0.0274, 0.0545]	0.000	1.000	218000.000	100.000
	q13	grey -> blue	45878.000	0.000	0.000	0.000	[0, 0]	99.855	217684.000	218000.000	0.145
	q20	slate -> any other	11390.000	0.032	0.030	0.000	[0, 0]	17.6	38483.000	218000.000	82.347

		colour	0.000		7	0	0.0504]	53			
q21	slate -> grey	61674 .000	0.040	0.03 9	0.03 8	[0.0273, 0.0545]	0.00 2	5.000	218000.000	99.998	
q23	slate -> blue	89305 .000	0.040	0.03 9	0.00 0	[0.0276, 0.0539]	0.02 4	53.000	218000.000	99.976	
q30	blue -> any other colour	93404 .000	0.040	0.03 9	0.03 8	[0.0276, 0.0539]	0.00 0	0.000	218000.000	100.000	
q31	blue -> grey	77073 .000	0.000	0.00 0	0.00 0	[0, 0]	99.9 60	217913.000	218000.000	0.040	
q32	blue -> slate	25317 .000	0.000	0.00 0	0.00 0	[0, 0]	99.5 73	217069.000	218000.000	0.427	

Table S7. Reverse Jump analysis results for female; analysis done with the table not containing double scores species

	transition rate	colour transitions	ESS	Mean	Median	Mode	95% HPD	% Zero	number of zero	total number	% not zero
female_1	q01	any other colour -> grey	1716 3.000	0.05 8	0.05 7	0.05 1	[0.0383, 0.078]	0.00 0	0.000	218000.00 0	100.000
	q02	any other colour -> slate	1456 00.00 0	0.00 1	0.00 0	0.00 0	[0, 0.0889]	98.3 31	214362.00 0	218000.00 0	1.669
	q03	any other colour -> blue	8061 3.000	0.00 0	0.00 0	0.00 0	[0, 0]	99.9 36	217861.00 0	218000.00 0	0.064
	q10	grey -> any other colour	1741 1.000	0.05 8	0.05 7	0.05 1	[0.0383, 0.078]	0.00 0	0.000	218000.00 0	100.000
	q12	grey -> slate	1466 9.000	0.05 8	0.05 7	0.05 1	[0.0383, 0.078]	0.00 3	6.000	218000.00 0	99.997
	q13	grey -> blue	4568 5.000	0.00 0	0.00 0	0.00 0	[0, 0]	99.8 57	217688.00 0	218000.00 0	0.143
	q20	slate -> any other colour	671.0 00	0.05 5	0.05 7	0.00 0	[0, 0.0754]	6.45 6	14073.000	218000.00 0	93.544
	q21	slate -> grey	4044. 000	0.05 7	0.05 7	0.00 0	[0.0369, 0.0795]	1.29 3	2819.000	218000.00 0	98.707
	q23	slate -> blue	801.0 00	0.05 5	0.05 7	0.00 0	[0, 0.0754]	5.42 5	11827.000	218000.00 0	94.575
	q30	blue -> any other colour	1392 9.000	0.05 8	0.05 7	0.05 1	[0.0382, 0.078]	0.00 9	20.000	218000.00 0	99.991
	q31	blue -> grey	505.0 00	0.00 3	0.00 0	0.00 0	[0, 0.0412]	94.0 83	205101.00 0	218000.00 0	5.917
	q32	blue -> slate	1493. 000	0.00 1	0.00 0	0.00 0	[0, 0]	98.7 37	215246.00 0	218000.00 0	1.263
female_2	q01	any other colour -> grey	1048 5.000	0.05 8	0.05 7	0.05 4	[0.0382, 0.0778]	0.00 0	0.000	218000.00 0	100.000
	q02	any other colour -> slate	6572 4.000	0.00 1	0.00 0	0.00 0	[0, 0]	98.3 85	214480.00 0	218000.00 0	1.615
	q03	any other colour -> blue	3950 2.000	0.00 0	0.00 0	0.00 0	[0, 0]	99.8 96	217774.00 0	218000.00 0	0.104
	q10	grey -> any other colour	1059 7.000	0.05 8	0.05 7	0.05 4	[0.0382, 0.0778]	0.00 0	0.000	218000.00 0	100.000
	q12	grey -> slate	9841. 000	0.05 8	0.05 7	0.00 0	[0.0382, 0.0778]	0.02 0	44.000	218000.00 0	99.980
	q13	grey -> blue	2142 5.000	0.00 0	0.00 0	0.00 0	[0, 0.0791]	99.8 38	217646.00 0	218000.00 0	0.162
	q20	slate -> any other colour	307.0 00	0.05 3	0.05 6	0.00 0	[0, 0.075]	8.02 0	17484.000	218000.00 0	91.980
	q21	slate -> grey	1735. 000	0.05 7	0.05 7	0.00 0	[0.0365, 0.0809]	1.58 4	3453.000	218000.00 0	98.416
	q23	slate -> blue	362.0 00	0.05 4	0.05 6	0.00 0	[0, 0.075]	6.79 0	14802.000	218000.00 0	93.210
	q30	blue -> any other colour	8623. 000	0.05 8	0.05 7	0.05 4	[0.0382, 0.0779]	0.00 0	0.000	218000.00 0	100.000
	q31	blue -> grey	250.0 00	0.00 4	0.00 0	0.00 0	[0, 0.0494]	92.6 48	201972.00 0	218000.00 0	7.352
	q32	blue -> slate	1639.	0.00	0.00	0.00	[0, 0]	98.4	214668.00	218000.00	1.528

			000	1	0	0		72	0	0	
female_3	q01	any other colour -> grey	1593 0.000	0.05 8	0.05 7	0.05 2	[0.038, 0.0776]	0.00 0	0.000	218000.00 0	100.000
	q02	any other colour -> slate	1388 00.00 0	0.00 1	0.00 0	0.00 0	[0, 0]	98.3 49	214401.00 0	218000.00 0	1.651
	q03	any other colour -> blue	6261 1.000	0.00 0	0.00 0	0.00 0	[0, 0]	99.9 05	217792.00 0	218000.00 0	0.095
	q10	grey -> any other colour	1615 8.000	0.05 8	0.05 7	0.05 2	[0.0381, 0.0776]	0.00 0	0.000	218000.00 0	100.000
	q12	grey -> slate	1154 9.000	0.05 7	0.05 8	0.05 2	[0.038, 0.0776]	0.00 0	1.000	218000.00 0	100.000
	q13	grey -> blue	3869 4.000	0.00 0	0.00 0	0.00 0	[0, 0]	99.8 15	217596.00 0	218000.00 0	0.185
	q20	slate -> any other colour	453.0 00	0.05 4	0.05 7	0.00 0	[0, 0.0751]	7.93 6	17300.000	218000.00 0	92.064
	q21	slate -> grey	2673. 000	0.05 7	0.05 7	0.00 0	[0.0371, 0.0804]	1.67 8	3659.000	218000.00 0	98.322
	q23	slate -> blue	508.0 00	0.05 4	0.05 7	0.00 0	[0, 0.0751]	6.94 9	15149.000	218000.00 0	93.051
	q30	blue -> any other colour	1042 8.000	0.05 8	0.05 7	0.00 0	[0.0379, 0.0776]	0.03 6	78.000	218000.00 0	99.964
	q31	blue -> grey	336.0 00	0.00 4	0.00 0	0.00 0	[0, 0.0472]	92.4 28	201494.00 0	218000.00 0	7.572
	q32	blue -> slate	2066. 000	0.00 1	0.00 0	0.00 0	[0, 0]	98.6 75	215112.00 0	218000.00 0	1.325

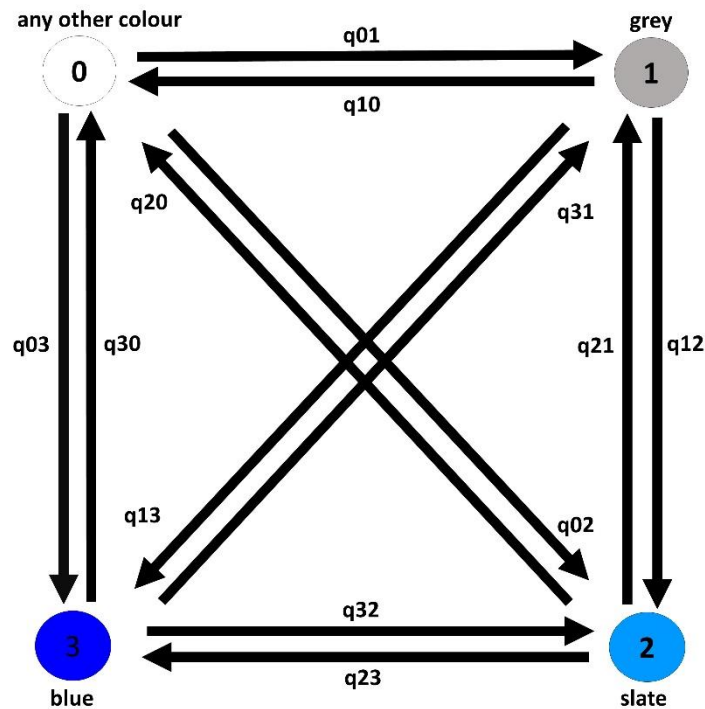


Figure S1.

(q01: any other colour -> grey, q02: any other colour -> slate, q03: any other colour -> blue, q10: grey -> any other colour, q12: grey -> slate, q13: grey -> blue, q20: slate -> any other colour, q21: slate -> grey, q23: slate -> blue, q30: blue -> any other colour, q31: blue -> grey, q32: blue -> slate)

APPENDIX 3

Supplementary materials and methods for Chapter 4: Evolutionary dynamics of pigmentary grey and non- iridescent structural blue colouration in Tanagers (family: Thraupidae)

Table S1. Sampling details of feathers from museum skins in the the Zoological Museum, Natural History Museum of Denmark, University of Copenhagen. Every row represents on feather and columns indicate details about the specimen (Species, Sex, Storage number, Tag details) and feather samples (Colour, Body part).

Species	Sex	Body part	Storage number	Tag details	Colour
<i>Tangara vitriolina</i>	Unsexed	Throat	NA	8.4.1913.220	Slate
<i>Tangara vitriolina</i>	Unsexed	Throat	NA	8.4.1913.219	Slate
<i>Tangara vitriolina</i>	Unsexed	Throat	NA	8.4.1913.221	Slate
<i>Catemina inornata</i>	Male	Mantle	105120	6.5.2010	Slate
<i>Catemina inornata</i>	Male	Mantle	105117	6.5.2010	Slate
<i>Catemina inornata</i>	Male	Mantle	105118	6.5.2010	Slate
<i>Poospiza cinera</i>	Unsexed	Mantle	20.578	NA	Slate
<i>Poospiza cinera</i>	Male	Mantle	20.576	NA	Slate
<i>Poospiza cinera</i>	Unsexed	Mantle	20.580	NA	Slate
<i>Diglossa cyanea</i>	Male	Rump	104778	20.11.1984.569	Blue
<i>Diglossa cyanea</i>	Male	Rump	104781	22.4.2010	Blue
<i>Diglossa cyanea</i>	Male	Rump	104782	22.4.2010	Blue
<i>Xenodacnis parina</i>	Male	Mantle	103020	20.3.2009-9	Blue
<i>Xenodacnis parina</i>	Male	Rump	103022	20.3.2009-11	Blue
<i>Xenodacnis parina</i>	Male	Rump	103021	20.3.2009-10	Blue
<i>Sporophila caerulescens</i>	Male	Mantle	20.468	26.4.1937.692	Grey
<i>Sporophila caerulescens</i>	Male	Mantle	20.467	26.4.1937.691	Grey
<i>Sporophila caerulescens</i>	Male	Mantle	20.462	26.4.1937.686	Grey
<i>Phygilus unicolor</i>	Male	Mantle	64080	26.8.1983-167	Grey
<i>Phygilus unicolor</i>	Male	Mantle	105109	6.5.2010	Grey
<i>Phygilus unicolor</i>	Male	Mantle	64078	26.8.1983-165	Grey
<i>Coryphospingus plieatus</i>	Male	Rump	9796	NA	Grey
<i>Coryphospingus plieatus</i>	Male	Rump	9792	NA	Grey
<i>Coryphospingus plieatus</i>	Male	Rump	9797	NA	Grey
<i>Diuca diuca</i>	Male	Breast	9720	NA	Grey

<i>Diuca diuca</i>	Male	Breast	9721	28.6.1937.7	Grey
<i>Diuca diuca</i>	Male	Breast	9717	NA	Grey
<i>Poospiza hypochondria</i>	Unsexed	Mantle	104995	3.5.2010	Grey
<i>Poospiza hypochondria</i>	Female	Mantle	104996	3.5.2010	Grey
<i>Poospiza hypochondria</i>	Male	Mantle	104998	3.5.2010	Grey
<i>Saltator albicollis</i>	Unsexed	Nape	20.274	NA	Grey
<i>Saltator albicollis</i>	Unsexed	Nape	20.260	NA	Grey
<i>Saltator albicollis</i>	Male	Nape	20.278	NA	Grey
<i>Neothraupis fasciata</i>	Male	Mantle	NA	NA	Grey
<i>Neothraupis fasciata</i>	Male	Mantle	NA	NA	Grey
<i>Neothraupis fasciata</i>	Male	Mantle	NA	NA	Grey
<i>Sporophila plumbea</i>	Male	Mantle	20.374	NA	Grey
<i>Sporophila plumbea</i>	Male	Mantle	20.370	NA	Grey
<i>Sporophila plumbea</i>	Male	Mantle	20.373	NA	Grey
<i>Thraupis sayaca</i>	Male	Throat	NA	26.4.1937.578	Grey
<i>Thraupis sayaca</i>	Male	Throat	NA	26.4.1937.579	Grey
<i>Thraupis sayaca</i>	Male	Throat	NA	26.4.1937.577	Grey
<i>Phryglius alaudinus</i>	Unsexed	Throat	9765	15.2.1915.211	Slate
<i>Phryglius alaudinus</i>	Male	Throat	67932	27.3.1979.138	Slate
<i>Phryglius alaudinus</i>	Male	Throat	9761	NA	Slate
<i>Thraupis cyanocephala</i>	Male	Breast	NA	30.1.91-41	Slate
<i>Thraupis cyanocephala</i>	Male	Breast	103009	20.9.1980.48	Slate
<i>Thraupis cyanocephala</i>	Male	Breast	NA	30.1.91-40	Slate
<i>Thraupis episcopus</i>	Male	Throat	NA	30.1.91-39	Slate
<i>Thraupis episcopus</i>	Male	Throat	NA	20.9.1980.46	Slate
<i>Thraupis episcopus</i>	Male	Mantle	NA	30.1.91-38	Slate
<i>Tangara heinei</i>	Male	Breast	NA	NA	Slate
<i>Tangara heinei</i>	Male	Breast	NA	30.1.1991-287	Slate
<i>Tangara heinei</i>	Male	Breast	NA	15.2.1915.185	Slate
<i>Catamblyrhynchus diadema</i>	Male	Mantle	104900	28.4.2010	Slate
<i>Catamblyrhynchus diadema</i>	Unsexed	Mantle	9647	8.2.1921.490	Slate
<i>Catamblyrhynchus diadema</i>	Unsexed	Mantle	64085	26.8.1983-156	Slate
<i>Catamenia analis</i>	Male	Rump	105122	6.5.2010	Slate
<i>Catamenia analis</i>	Male	Rump	105114	6.5.2010	Slate
<i>Catamenia analis</i>	Male	Rump	10515	6.5.2010	Slate
<i>Diglossa lafresnayi</i>	Unsexed	Wing covert	NA	1.6.1930.366	Slate
<i>Diglossa lafresnayi</i>	Unsexed	Wing covert	NA	NA	Slate
<i>Diglossa lafresnayi</i>	Unsexed	Wing covert	NA	8.2.1921.349	Slate
<i>Diglossa albilatera</i>	Unsexed	Breast	NA	NA	Slate
<i>Diglossa albilatera</i>	Male	Breast	104797	22.4.2010	Slate
<i>Diglossa albilatera</i>	Male	Breast	NA	NA	Slate
<i>Diglossa brunneiventris</i>	Male	Rump	104899	27.4.2010	Slate
<i>Diglossa brunneiventris</i>	Male	Rump	103034	20.3.2009-21	Slate
<i>Diglossa brunneiventris</i>	Male	Rump	103040	NA	Slate
<i>Diglossa sittoides</i>	Male	Nape	NA	8.2.1921.353	Slate
<i>Diglossa sittoides</i>	Male	Nape	NA	NA	Slate

<i>Diglossa sittoides</i>	Male	Mantle	NA	NA	Slate
<i>Diglossa caerulescens</i>	Male	Breast	104791	22.4.2010	Slate
<i>Diglossa caerulescens</i>	Male	Breast	104793	22.4.2010	Slate
<i>Diglossa caerulescens</i>	Male	Breast	NA	NA	Slate
<i>Oreomanes fraseri</i>	Male	Nape	104831	23.4.2010	Slate
<i>Oreomanes fraseri</i>	Male	Nape	104822	23.4.2010	Slate
<i>Oreomanes fraseri</i>	Male	Nape	104839	26.4.2010	Slate
<i>Conirostrum cinerum</i>	Male	Nape	104802	27.3.1979.130	Slate
<i>Conirostrum cinerum</i>	Male	Nape	104801	23.4.2010	Slate
<i>Conirostrum cinerum</i>	Male	Nape	104803	23.4.2010	Slate
<i>Conirostrum sitticolor</i>	Unsexed	Rump	104804	23-4-1985-18	Blue
<i>Conirostrum sitticolor</i>	Male	Rump	103028	20.3.2009-17	Blue
<i>Conirostrum sitticolor</i>	Male	Rump	104805	23.4.2010	Blue
<i>Dacnis cayana</i>	Male	Breast	137319	8.6.2011.20	Blue
<i>Dacnis cayana</i>	Male	Breast	NA	27.3.1979.131	Blue
<i>Dacnis cayana</i>	Male	Breast	NA	20.9.1980.38	Blue
<i>Cyanerpes cyaneus</i>	Male	Breast	59979	1.7.1971.579	Blue
<i>Cyanerpes cyaneus</i>	Male	Breast	NA	25.12.1922.99	Blue
<i>Cyanerpes cyaneus</i>	Male	Breast	59980	1.7.1971.580	Blue
<i>Chlorophanes spiza</i>	Male	Breast	NA	NA	Blue
<i>Chlorophanes spiza</i>	Male	Breast	103018	NA	Blue
<i>Chlorophanes spiza</i>	Male	Breast	NA	1.6.1930.373	Blue
<i>Anisognathus igniventris</i>	Male	Rump	102988	19.3.2009-2	Blue
<i>Anisognathus igniventris</i>	Male	Rump	NA	20.1.1982	Blue
<i>Anisognathus igniventris</i>	Male	Rump	104882	26.4.2010	Blue
<i>Pipraeidea melanota</i>	Male	Rump	NA	NA	Blue
<i>Pipraeidea melanota</i>	Male	Rump	NA	NA	Blue
<i>Pipraeidea melanota</i>	Unsexed	Rump	NA	NA	Blue
<i>Tangara chilensis</i>	Male	Throat	NA	1.6.1930.393	Blue
<i>Tangara chilensis</i>	Unsexed	Throat	NA	1.6.1930.396	Blue
<i>Tangara chilensis</i>	Unsexed	Throat	NA	1.6.1930.395	Blue
<i>Tangara nigroviridis</i>	Unsexed	Throat	NA	8.4.1913.203	Blue
<i>Tangara nigroviridis</i>	Male	Throat	92.806	18.12.1998-16	Blue
<i>Tangara nigroviridis</i>	Male	Throat	NA	30.1.91-137	Blue
<i>Poospiza schistacea</i>	Unsexed	Mantle	20.580	NA	Slate
<i>Poospiza schistacea</i>	Unsexed	Mantle	20.578	NA	Slate
<i>Poospiza schistacea</i>	Male	Mantle	20.576	NA	Slate
<i>Paroaria coronata</i>	Male	Mantle	9311	NA	Grey
<i>Paroaria coronata</i>	Male	Mantle	9310	2.4.1917.1	Grey
<i>Paroaria coronata</i>	Male	Mantle	9303	NA	Grey
<i>Thraupis bonariensis</i>	Male	Throat	NA	R 2-8-1907	Blue
<i>Thraupis bonariensis</i>	Male	Throat	103013	20.3.2009-1	Blue
<i>Thraupis bonariensis</i>	Male	Throat	92.805	18.1.1998-15	Blue
<i>Charitospiza eucoma</i>	Male	Mantle	9772	NA	Grey
<i>Charitospiza eucoma</i>	Male	Mantle	9773	NA	Grey
<i>Charitospiza eucoma</i>	Male	Mantle	9774	NA	Grey

Table S2. Colour measurements for feather samples in Tanagers. Each row represents average colour measurement per species from 3 feathers. First column shows Latin name of the species, second patch where the feathers are sampled from, third colour of the feathers, columns 4 – 7 show cone catch values, eighth column shows Projection values, column 9 – 10 show PC1 and PC2 from Principal component analysis.

Latin name	Patch	Colour	u	s	m	l	Projection_values	PC1	PC2
<i>Diglossa cyanea</i>	rump	blue	0.386	0.405	0.151	0.059	0.191	-0.275	0.037
<i>Xenodacnis parina</i>	mantle / rump	blue	0.366	0.398	0.180	0.055	0.203	-0.251	0.054
<i>Conirostrum sitticolor</i>	rump	blue	0.455	0.339	0.136	0.070	0.322	-0.303	-0.049
<i>Dacnis cayana</i>	breast	blue	0.276	0.301	0.343	0.080	0.397	-0.088	0.079
<i>Cyanerpes cyaneus</i>	breast	blue	0.465	0.445	0.070	0.021	0.110	-0.392	0.015
<i>Chlorophanes spiza</i>	breast	blue	0.010	0.453	0.420	0.118	0.095	0.101	0.312
<i>Anisognathus igniventris</i>	rump	blue	0.454	0.396	0.111	0.040	0.208	-0.345	-0.006
<i>Pipraeidea melanonota</i>	rump	blue	0.412	0.440	0.117	0.030	0.119	-0.331	0.050
<i>Tangara chilensis</i>	throat	blue	0.626	0.309	0.047	0.018	0.382	-0.473	-0.156
<i>Tangara nigroviridis</i>	throat	blue	0.060	0.526	0.311	0.103	0.052	-0.003	0.305
<i>Thraupis bonariensis</i>	crown	blue	0.437	0.348	0.144	0.071	0.305	-0.290	-0.033
<i>Sporophila caerulescens</i>	mantle	grey	0.136	0.240	0.289	0.335	0.521	0.149	-0.037
<i>Phrygilus unicolor</i>	mantle	grey	0.192	0.268	0.266	0.274	0.464	0.060	-0.023
<i>Coryphospingus pileatus</i>	rump	grey	0.172	0.225	0.264	0.339	0.551	0.122	-0.074
<i>Diuca diuca</i>	breast	grey	0.124	0.238	0.286	0.352	0.523	0.166	-0.041
<i>Poospiza hypochondria</i>	mantle	grey	0.130	0.202	0.278	0.390	0.596	0.191	-0.089
<i>Saltator albicollis</i>	nape	grey	0.089	0.153	0.319	0.438	0.693	0.275	-0.110
<i>Neothraupis fasciata</i>	mantle	grey	0.160	0.234	0.267	0.338	0.531	0.127	-0.061
<i>Sporophila plumbea</i>	mantle	grey	0.141	0.237	0.279	0.343	0.526	0.147	-0.048
<i>Thraupis sayaca</i>	throat	grey	0.175	0.258	0.281	0.287	0.485	0.087	-0.023
<i>Charitospiza eucosma</i>	nape	grey	0.167	0.247	0.278	0.309	0.507	0.106	-0.038
<i>Catamenia inornata</i>	mantle	slate	0.145	0.256	0.291	0.307	0.488	0.123	-0.016
<i>Poospiza cinerea</i>	mantle	slate	0.118	0.257	0.299	0.325	0.486	0.154	-0.009
<i>Phrygilus alaudinus</i>	throat	slate	0.184	0.258	0.270	0.288	0.483	0.077	-0.031
<i>Thraupis cyanocephala</i>	breast	slate	0.148	0.271	0.283	0.298	0.457	0.108	-0.006
<i>Thraupis episcopus</i>	throat/mantle	slate	0.225	0.262	0.315	0.198	0.476	0.014	0.011
<i>Tangara heinei</i>	breast	slate	0.048	0.392	0.342	0.218	0.216	0.120	0.179
<i>Catamblyrhynchus diadema</i>	mantle	slate	0.224	0.280	0.261	0.235	0.439	0.010	-0.014
<i>Catamenia analis</i>	rump	slate	0.226	0.277	0.256	0.241	0.447	0.012	-0.022
<i>Diglossa lafresnayii</i>	wing_covers	slate	0.332	0.304	0.208	0.155	0.392	-0.134	-0.030
<i>Diglossa albilatera</i>	breast	slate	0.212	0.268	0.263	0.257	0.464	0.036	-0.026
<i>Diglossa brunneiventris</i>	rump	slate	0.229	0.268	0.260	0.244	0.465	0.015	-0.029
<i>Diglossa sittoides</i>	nape / mantle	slate	0.206	0.271	0.266	0.257	0.457	0.039	-0.020
<i>Diglossa caerulescens</i>	breast	slate	0.231	0.299	0.259	0.210	0.401	-0.015	0.006
<i>Oreomanes fraseri</i>	nape	slate	0.135	0.200	0.281	0.384	0.599	0.185	-0.088
<i>Conirostrum cinereum</i>	nape	slate	0.159	0.249	0.288	0.304	0.501	0.112	-0.027

<i>Sporophila schistacea</i>	mantle	slate	0.143	0.263	0.291	0.303	0.474	0.120	-0.009
<i>Tangara vitriolina</i>	mantle	slate	0.041	0.240	0.416	0.303	0.521	0.242	0.068

Table S3. Measurements of variables explaining properties of spongy layer for feathers in Tanagers. Every row represents an average value of the measurement for a species.

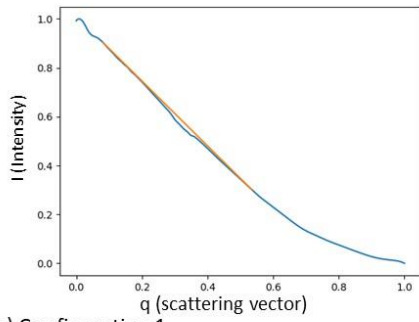
Latin name	Patch	Colour	Nanostructure complexity	Long Period	Average Hard Block Thickness	Average Soft Block Thickness	Filling fraction	l_(max)	q_(max)
<i>Diglossa cyanea</i>	rump	blue	5	1580.860	537.452	1043.408	0.340	20779.739	0.003
<i>Xenodacnis parina</i>	mantle / rump	blue	3	1772.810	570.865	1201.945	0.322	46668.925	0.003
<i>Conirostrum sitticolor</i>	rump	blue	5	1549.061	394.873	1154.188	0.255	37991.228	0.004
<i>Dacnis cayana</i>	breast	blue	11	2129.783	458.322	1671.460	0.215	208921.355	0.003
<i>Cyanerpes cyaneus</i>	breast	blue	8	1597.818	424.751	1173.067	0.266	149011.112	0.004
<i>Chlorophanes spiza</i>	breast	blue	11	1823.650	568.041	1255.609	0.311	92476.241	0.003
<i>Anisognathus igniventris</i>	rump	blue	6	1633.111	400.252	1232.859	0.245	54499.423	0.004
<i>Pipraeidea melanonota</i>	rump	blue	8	1790.954	392.479	1398.474	0.219	89431.475	0.003
<i>Tangara chilensis</i>	throat	blue	8	1528.866	389.079	1139.787	0.254	246532.322	0.004
<i>Tangara nigroviridis</i>	throat	blue	8	1887.185	472.732	1414.452	0.251	85120.934	0.003
<i>Thraupis bonariensis</i>	crown	blue	5	1715.943	387.121	1328.822	0.226	58920.096	0.003
<i>Sporophila caerulea</i>	mantle	grey	0	0.000	0.000	0.000	0.000	0.000	0.000
<i>Phrygilus unicolor</i>	mantle	grey	1	4565.184	693.784	3871.401	0.152	2749.584	0.004
<i>Coryphospingus pileatus</i>	rump	grey	0	0.000	0.000	0.000	0.000	0.000	0.000
<i>Diuca diuca</i>	breast	grey	0	0.000	0.000	0.000	0.000	0.000	0.000
<i>Poospiza hypochondria</i>	mantle	grey	0	0.000	0.000	0.000	0.000	0.000	0.000
<i>Saltator albicollis</i>	nape	grey	0	0.000	0.000	0.000	0.000	0.000	0.000
<i>Neothraupis fasciata</i>	mantle	grey	0	0.000	0.000	0.000	0.000	0.000	0.000
<i>Sporophila plumbea</i>	mantle	grey	0	0.000	0.000	0.000	0.000	0.000	0.000
<i>Thraupis sayaca</i>	throat	grey	10	2366.482	608.738	1757.744	0.257	48398.289	0.003
<i>Charitospiza eucosma</i>	nape	grey	0	0.000	0.000	0.000	0.000	0.000	0.000
<i>Catamenia inornata</i>	mantle	slate	0	0.000	0.000	0.000	0.000	0.000	0.000
<i>Poospiza cinerea</i>	mantle	slate	1	4891.576	907.524	3984.052	0.185	2906.703	0.005
<i>Phrygilus alaudinus</i>	throat	slate	1	4531.911	647.932	3883.979	0.143	5088.436	0.004
<i>Thraupis cyanocephala</i>	breast	slate	8	1890.390	472.018	1418.373	0.250	36345.311	0.003
<i>Thraupis episcopus</i>	throat/mantle	slate	13	2245.888	512.694	1733.195	0.228	93194.209	0.003
<i>Tangara heinei</i>	breast	slate	10	1920.843	522.688	1398.155	0.272	72541.883	0.003
<i>Catamblyrhynchus diadema</i>	mantle	slate	1	4681.162	714.423	3966.739	0.149	8038.068	0.004
<i>Catamenia analis</i>	rump	slate	1	4554.478	629.440	3925.037	0.139	5340.388	0.004

Diglossa_lafresnayii	wing_covers	slate	1	1551.946	438.895	1113.051	0.284	6338.845	0.004
Diglossa_albilatera	breast	slate	1	4958.444	812.630	4145.814	0.164	6487.227	0.004
Diglossa_brunneiventris	rump	slate	1	4126.726	670.502	3456.224	0.187	3838.032	0.005
Diglossa_sittoides	nape / mantle	slate	1	2704.349	797.101	1907.248	0.308	8310.673	0.002
Diglossa_caerulescens	breast	slate	3	1716.007	556.041	1159.966	0.325	36125.357	0.003
Oreomanes_fraseri	nape	slate	2	3978.629	824.841	3153.788	0.220	6779.868	0.002
Conirostrum_cinereum	nape	slate	2	2327.823	652.770	1675.053	0.280	27911.283	0.003
Sporophila_schistacea	mantle	slate	1	5113.273	953.833	4159.440	0.184	8103.644	0.004
Tangara_vitriolina	mantle	slate	10	1969.889	528.343	1441.546	0.268	67114.539	0.003

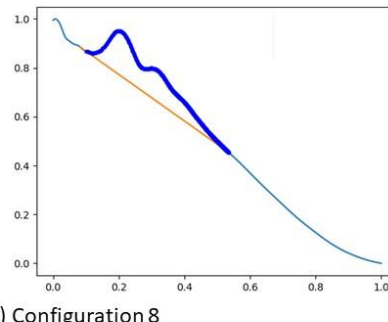
Table S4. Results of Phylogenetic generalized least square (PGLS) used to test the influence of predictor variables (nanostructure complexity, average hard block thickness, average soft block thickness, local crystallinity and I max) separately for PC1 of a) slate, b) blue and c) blue-slate-grey colours. Intercept estimates, standard error and p-values are reported.

	a) SLATE		b) BLUE		c) BLUE-SLATE-GREY	
	Estimate (+/- SE)	P [anova]	Estimate (+/- SE)	P [anova]	Estimate (+/- SE)	P [anova]
Intercept	1.1975e-01 (+/- 7.4872e-02)		5.3227e-01 (+/- 1.8853e+00)		1.5104e-01 (+/- 3.6963e-02)	
nanostructure	2.4639e-02 (+/- 1.8116e-02)	0.25916	4.0498e-02 (+/- 1.6217e-02)	0.02315 *	2.9624e-02 (+/- 7.9681e-03)	0.000895
average_hard_block_thicnkess	7.2865e-04 (+/- 2.6126e-04)	0.42831	4.7362e-03 (+/- 3.3676e-03)	0.01042 *	1.5021e-03 (+/- 3.2573e-04)	0.672532
average_soft_block_thickness	-1.0313e-04 (+/- 4.1582e-05)	0.94045	-7.5464e-04 (+/- 1.0810e-03)	0.08288	-1.939e-04 (+/- 4.938e-05)	0.294091
Local crystallinity	1.3408e+00 (+/- 4.8115e-01)	0.013	8.088e+00 (+/- 7.658e+00)	0.215	2.966e+00 (+/- 4.849e-01)	4.45E-08
I max	-1.974e-06 (+/- 2.711e-06)	0.481	-1.1499e-06 (+/- 5.225e-07)	0.079	1.938e-06 (+/- 5.059e-07)	0.0005
Multiple R2	0.503		0.883		0.714	
Adjusted R2	0.277		0.766		0.669	
Lambda	0		1		0	

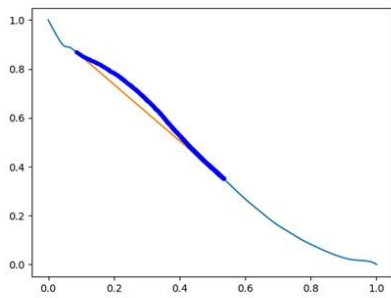
a) Configuration 0



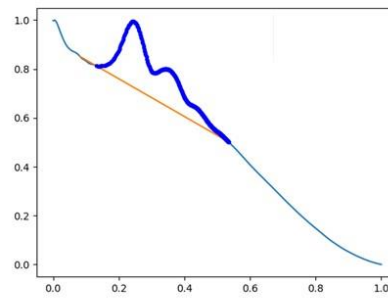
f) Configuration 6



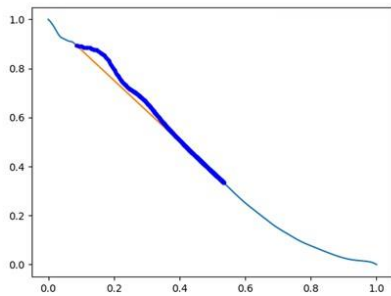
b) Configuration 1



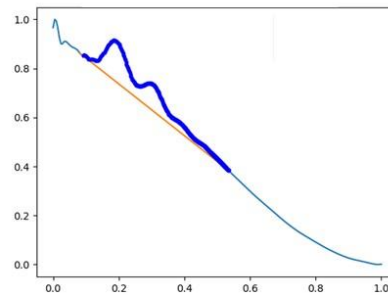
g) Configuration 8



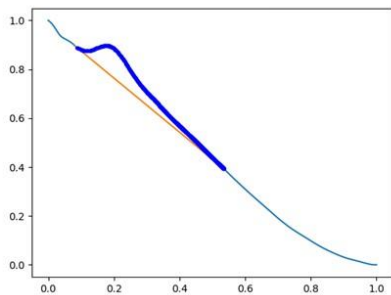
c) Configuration 2



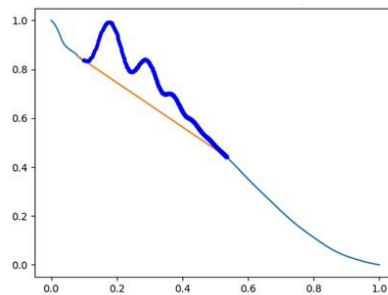
h) Configuration 10



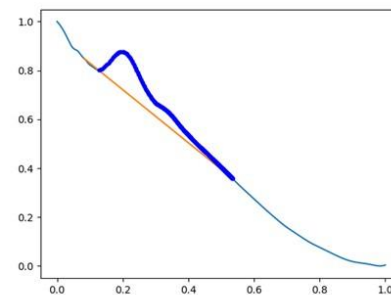
d) Configuration 3



i) Configuration 11



e) Configuration 5



j) Configuration 13

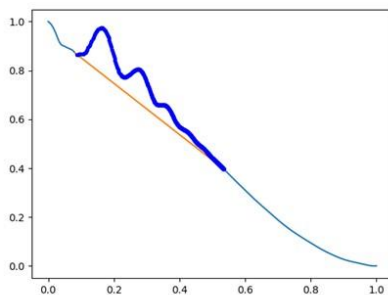


Figure S1. Examples of scattering profiles cover all possible peaks and shoulder combinations across all examined feather samples. This figure is the extension of the Figure 4.1. from the main text. The figure is a visual representation of Table 1, and the classification of combinations of features is explained in the table. In short, configuration 0 (a) indicates a lack of any structural components on the plot. Configurations 1 and 2 (b, c) have shoulder detected as the first scattering element and they are typical for the rudimentary form of the spongy nanostructure in the medullary feather cells. Configurations 3 and 5 (d, e) have peak detected as the first scattering element, and the following scattering element is either non-existing or a shoulder. Configurations 6, 8, 9, 10, 11 and 13 (f - j) have peaks detected as the first and second scattering element with any other number of elements (peaks or shoulders) detected afterwards. On each plot, an orange line represents an area that is explored for the detection of the peak and shoulders, thick blue line represents peak and shoulders detected, while a thin blue line represents all the data for each plot.